THE ENDOTHELIAL RESPONSE TO DIABETES REVEALS A PROTECTIVE ROLE FOR GALECTIN-3 IN DIABETIC VASCULOPATHY AND GLUCOSE METABOLISM

A DISSERTATION SUBMITTED TO THE GRADUATE DIVISION OF THE UNIVERSITY OF HAWAIʻI AT MĀNOA IN PARTIAL FULFILLMENT OF THE REQUIREMENTS FOR THE DEGREE OF

DOCTOR OF PHILOSOPHY

IN

CELL AND MOLECULAR BIOLOGY

May 2013

By

April L. Darrow

Dissertation Committee:

Ralph Shohet, Chairperson
Mariana Gerschenson
William Boisvert
Takashi Matsui
Qing Li

Keywords: Endothelial dysfunction, High-fat diet, Macrovasculature, Microvasculature, Transcription, Hyperglycemia

ProQuest LLC.
789 East Eisenhower Parkway
P.O. Box 1346
Ann Arbor, MI 48106 - 1346

Acknowledgements

This work was supported by National Institute of Health grants COBRE: Center for Cardiovascular Research 5P20RR016453 and University of Hawaii Research Scientist Award in Molecular Cardiology 5UH1HL-073449 (both to R.V. Shohet), Hawai'i Community Foundation Grant 20061485 (to J.G. Maresh), and American Heart Association Predoctoral Award 11PRE7720065 (to A.L. Darrow). I would also like to thank the Molecular and Cellular Immunology Core Facility supported by RCMI (5 G12 RR003061-25) and COBRE (P20RR018727) and the Genomics Core Facility and the Histology and Imaging Core Facility both supported by the Cardiovascular COBRE (5P20RR016453).

Abstract

Type II Diabetes is associated with an increased risk of cardiovascular disease primarily due to a damaged or dysfunctional endothelium. To characterize the endothelial dysfunction in diabetes, we surveyed the transcriptional responses in the vascular endothelia of mice receiving a high-fat diet. Mice were fed a 60% fat calorie diet (HFD) for up to 8 weeks to induce a state of insulin resistance; controls were fed normal chow. Transcriptional analysis of the aortic and skeletal muscle endothelium of these mice performed using whole genome microarrays identified galectin-3, a carbohydrate-binding lectin, as a highly dysregulated transcript. The mRNA for galectin-3 was 16-fold more abundant in the aortic endothelium after 4 weeks of HFD, and this same level of dysregulation was observed in the muscle endothelium after 8 weeks. LGALS3 protein was similarly upregulated in the endothelium as confirmed by immunofluorescence. The level of circulating LGALS3 in the serum of HFD mice was elevated vs. controls (91 $\pm$ 12 vs. 34 $\pm$ 3 ng/mL, $P < 0.001$) and positively correlated with the degree of insulin resistance (R^2=0.92, $P < 0.0001$), suggesting its potential for use as a biomarker for the vascular complications of diabetes. *Lgals3*-deficient mice (KO) fed a HFD for 8 weeks display impaired glucose tolerance and exacerbated hyperglycemia compared to WT (231 $\pm$ 35 vs. 185 $\pm$ 30 mg/dL, $P = 0.001$). Transcriptional analysis of the aortic and muscle endothelial response to HFD of KO mice vs. WT mice revealed differential dysregulation of transcripts involved in glucose uptake, insulin signaling, atherosclerosis, and coagulation. One highly downregulated transcript in both the macro- and microvasculture of the KO by 4- and 16-fold after high-fat feeding was the glucose transporter, *Glut4*. Immunofluorescence confirmed the decreased abundance

of GLUT4 protein in the endothelium and muscle of the diabetic KO compared to WT. Upregulated expression of coagulation factors in the aortic endothelium and decreased prothrombin time revealed increased coagulation activity occurring in the diabetic KO. This data suggests that galectin-3 is involved in regulating glucose metabolism and its upregulation in the diabetic vasculature may serve a protective role against the cardiovascular complications of diabetes.

Table of Contents

List of Tables

List of Figures

List of Abbreviations

12(S)-HETE	12(S)-hydroxyeicosatetraeonic acid
12/15-LO	12/15-lipoxygenase
15(S)-HETE	15(S)-hydroxyeicosatetraeonic acid
3T3	mouse fibroblast cell line
ANOVA	Analysis of variance
ACE	Angiotensin converting enzyme
Ac-LDL	Acetylated-low density lipoprotein
ADO	Adenosine
ADP	Adenosine diphosphate
ADRA2B	Adrenoceptor alpha 2B
AGE	Advanced glycation endproduct
AGE-R1/2/3	Advanced glycation endproduct receptor 1/2/3
AKT	v-akt murine thymoma viral oncogene homolog, or PKB
ALOX5AP	5-lipoxygenase-activating protein, or FLAP
AP-1/4	Activator Protein 1/4
APC	Allophycocyanin
APOE	Apolipoprotein E
AT-I	Angiotensin-I
AT-II	Angiotensin-II
ATP	Adenosine triphosphate
AUC	Area under the curve
Bad	Bcl-2 associated death promoter
BAEC	Bovine aortic endothelial cell
BCL-2	B-cell lymphoma 2
BH_4	Tetrahydrobiopterin
BLAST	Basic Local Alignment Search Tool
BSA	Bovine serum albumin
bZIP	Basic domain leucine-zipper
C2C12	Mouse myoblast cell line
cAMP	Cyclic adenosine monophosphate
CAV-3	Caveolin-3
CCL8	C-C chemokine 8, or MCP-2

CCL9	C-C chemokine 9
CCR-2	C-C chemokine receptor type 2
CD	Cluster of differentiation
CD115	Macrophage colony stimulating factor receptor, (MCSFR)
CD11b	Integrin alpha M (ITGAM)
CD146	Melanoma cell adhesion molecule (MCAM), or S-endo 1 antigen
CD16/32	IgG Fc receptor III (FcR III)
CD105	Endoglin
CD31	Platelet-endothelial cell adhesion molecule (PECAM)
CD45	Leukocyte common antigen
CDC	Center for Disease Control
cDNA	Copy DNA
cGMP	Cyclic guanosine monophosphate
CHO	Chinese hamster ovary cells
CHRP	Cysteine-histidine-rich protein
CMVEC	Cardiac microvascular endothelial cell
COX	Cyclooxygenase
CP	Ceruloplasmin
CP2	Alpha globin transcription factor CP2
CRD	Carbohydrate recognition domain
CREB	cAMP responsive element binding protein
CREB-L2	cAMP responsive element binding protein-like 2
cRNA	Copy RNA
C_T	Cycle threshold
CTGF	Connective tissue growth factor
CVD	Cardiovascular disease
CYP 2C	Cytochrome P450 2c
DAG	Diacylglycerol
DAPI	4',6-diamidino-2-phenylindole
DAVID	Database for Annotation, Visualization, and Integrated Discovery
DCF	Dichlorodihydrofluorescein
DIL	1,1'-dioctadecyl – 3,3,3',3'-tetramethyl-indocarbocyanine perchlorate
DNA	Deoxyribonucleic acid
EC	Endothelial cell

ECIS	Electric Cell-substrate Impedance Sensing
ECM	Extracellular matrix
EDHF	Endothelial derived hyperpolarization factor
EDTA	Ethylene diamine tetraacetic acid
EGR1	Early growth response 1
ELISA	Enzyme-linked immunosorbant assay
eNOS	Endothelial nitric oxide synthase
ET-1	Endothelin-1
ET_A	Endothelin A receptor
ET_B	Endothelin B receptor
Ets1	v-ets avian erythroblastosis virus E26 oncogene homolog 1
FACS	Fluorescence-activated cell sorting
Fas	Apoptosis stimulating fragment
FBS	Fetal bovine serum
FFA	Free fatty acid
FGF	Fibroblast growth factor
FGF-2	Fibroblast growth factor-2
FITC	Fluorescein isothiocyanate
FOXO-1	Forkhead box other-1
FSC	Forward scatter
FTL1	Ferritin light chain 1
FII	Thrombin
FI	Fibrinogen
FIII	Tissue Factor
G6PC	Glucose-6-phosphatase
GAPDH	Glyceraldehyde 3-phosphate dehydrogenase
GCH1	GTP cyclohydrolase 1
GFAT	Glutamine-fructose-6-phosphate amidotransferase
GFP	Green fluorescent protein
GLUT2	Glucose transporter 2
GLUT4	Glucose transporter 4
GO	Gene ontology
Gp90	90kD glycoprotein, or Mac-2BP
Grb2	Growth factor receptor-bound protein 2

GSK	Glycogen synthase kinase
GTP	Guanosine triphosphate
GTT	Glucose tolerance test
HA	Hyaluronic acid
HbA1c	Hemoglobin A1c
HCAEC	Human coronary artery endothelial cells
HDL	High density lipoprotein
HFD	High-fat diet
HIF-1α	Hypoxia inducible factor-1α
HOMA-IR	Homeostasis model assessment of insulin resistance
huAoEC	Human aortic endothelial cells
HUVEC	Human umbilical vein endothelial cells
ICAM	Intracellular adhesive molecule
IFG	Impaired fasting glucose
IgE	Immunoglobulin E
IGF1	Insulin-like growth factor
IGF1R	Insulin-like growth factor receptor 1
IGT	Impaired glucose tolerance
IL-1β	Interleukin 1β
IL-6	Interleukin-6
IL-8	Interleukin-8
INS2	Insulin 2
IP	Prostacyclin receptor
IPA	Ingenuity Pathway Analysis
IR	Insulin resistance
IRS-1	Insulin receptor substrate 1
ITT	Insulin tolerance test
JNK	c-Jun NH2-terminal kinase
KO	Knockout
LacZ	ß-galactosidase
LAMPS	Lysosome-associated membrane proteins
LDL	Low density lipoprotein
LDLR	Low density lipoprotein receptor
LDLRP1	Low density lipoprotein receptor-related protein 1
Lep	Leptin

Lepr	Leptin receptor
LGALS1	Galectin-1
LGALS3	Galectin-3
LOX-1	Oxidized low-density lipoprotein receptor 1
LXR/RXR	Liver X receptor/retinoic X receptor
LYVE-1	Lymphatic vessel endothelial hyaluronan receptor-1
LYZ-1	Lysozyme 1
MAPK	Mitogen-activated protein kinase
MARCO	Macrophage receptor with collagenous structure
MCP-1	Monocyte chemoattractant protein-1
MLC	Myosin light chain
MLCK	Myosin light chain kinase
mRNA	Messenger RNA
MT1	Metallothionein 1
mTOR	Mammalian target of Rapamycin
NADPH	Nicotinamide adenine dinucleotide phosphate
NF-κB	Nuclear factor κB
NG2	Neuron-glial antigen 2/Chondroitin sulfate proteoglycan 4
NIH	National Institute of Health
nNOS	Neuronal nitric oxide synthase
NO	Nitric oxide
NRF-1	Nuclear respiratory factor-1
OGTT	Oral glucose tolerance test
$ONOO^-$	Peroxynitrite
ox-LDL	Oxidized low density lipoprotein
PAD	Peripheral artery disease
PAI-1	Plasminogen activator inhibitor-1
PBMC	Peripheral blood mononuclear cell
PBS	Phosphate-buffered saline
PCR	Polymerase chain reaction
PDK1	Phosphoinositide-dependent protein-1
PE	Phycoerythrin
PEA3	Polyomavirus enhancer activator 3
PECAM	Platelet endothelial cell adhesion molecule

PEPCK	phosphoenolpyruvate carboxykinase
PerCp	Peridinin chlorophyll protein
PFA	Paraformaldehyde
PGC-1α	Peroxisome proliferator activated receptor-γ coactivator-1α
PGH2	Prostaglandin H2
PGI2	Prostacyclin
PGIS	Prostaglandin I synthase
PI3K	Phosphatidylinositol-3 kinase
PIP2	Phosphatidylinositol 4,5-bisphosphate
PIP3	Phosphatidylinositol (3,4,5)-trisphosphate
PKA/B/C/G	Protein kinase A/B/C/G
PLC	Phospholipase C
PMSF	Phenylmethanesulfonyl fluoride
PPAR-γ	Peroxisome proliferator activated receptor gamma
PT	Prothrombin time
PTEN	Phosphatase and tensin homologue deleted on chromosome 10
PTGFR	Prostaglandin F Receptor
qPCR	Quantitative PCR
RAAS	Renin-angiotensin aldosterone system
RAGE	Receptor for advanced glycation endproducts
Ras	Rat sarcoma
RBC	Red blood cell
RETNLA	Resistin-like alpha
RNA	Ribonucleic acid
ROS	Reactive oxygen species
RT	Room temperature
RT-PCR	Real-time PCR
SAPK1	Stress activated protein kinase-1
SD	Standard deviation
SDH	Sorbitol dehydrogenase
SEM	Standard error of the mean
SMC	Smooth muscle cell
SOD	Superoxide dismutase
Sos	Son of sevenless
Sp1	Specificity protein-1

SR-A	Scavenger receptor-A
SREBP	Serum response element binding protein
SSC	Side scatter
STZ	Streptozotocin
SUFU	Suppressor of Fused
SV40	Simian virus 40
T2D	Type 2 diabetes
TAC	Transverse aortic constriction
TBST	Tris-buffered saline with Tween 20
TF	Tissue factor
TGF-β	Transforming growth factor-β
THP-1	Human acute monocytic leukemia cell line
TLR4	Toll-like receptor 4
TNFα/β	Tumor necrosis factor-α/β
t-PA	Tissue type plasminogen activator
TPr	Thromboxane A2 receptor
tRNA	Transfer RNA
TTF-1	Thyroid-specific transcription factor-1
TXA2	Thromboxane A2
UTR	Untranslated region
VCAM	Vascular cell adhesion molecule
VE-cadherin	Vascular endothelial cadherin
VEGF	Vascular endothelial growth factor
VEGFR	Vascular endothelial growth factor receptor
vWF	von Willebrand Factor
WHO	World Health Organization
Wk	Week
WT	Wild-type

Chapter 1: Introduction

The endothelium is a complex organ mediating interactions between cells of the intravascular compartment and underlying stromal cells. The proper functioning of the endothelium relies upon a delicate balance of vasoactive factors, coagulation pathways, and adhesive and inflammatory molecules. Any imbalance of these factors leads to endothelial dysfunction which can promote adverse cardiovascular events. In diabetes, vascular complications are the main causes of human morbidity and mortality, and it is our goal to elucidate the endothelial responses that lead to this pathology. In order to understand the endothelial responses under pathophysiological conditions, knowledge of the basic functions and physiological responses of the endothelium is required. As background to the discussion in this chapter, the structure of the vasculature and the physiological functions of the endothelium will be reviewed. Next, type II diabetes, its associated vasculopathies, and the mechanisms implicated in the endothelial dysfunction leading to these complications will be discussed. Finally, our murine model of diabetes and our *in vivo* approach to elucidate the transcriptional changes occurring in the diabetic endothelium will be described.

1.1 The Vasculature

The circulatory system is composed of the arterial and venous circulation. The arteries carry oxygenated blood away from the heart to the tissues, and the venous system returns deoxygenated blood to the heart. All blood vessels from the largest arteries and veins to the smallest capillaries are lined by a single layer

of endothelial cells that serve as a barrier between the blood circulation and the underlying vessel wall (Figure 1.1A). The structure of the vessel depends on its function and hemodynamic stress. The largest vessels are the aorta and vena cava. Although the diameter of the vena cava is greater than that of the aorta (3cm vs. 2.5cm), the wall of the aorta is thicker, which is necessitated by its exposure to higher pressures (Burton, 1954). Figure 1.1B shows the structure of the aorta, which is also representative of other large arteries known as elastic arteries such as the pulmonary, common carotid, subclavian, and common iliac artery. The endothelial layer and the adjacent elastic lamina compose the tunica intima (Figure. 1.1B). Beneath the intima lies a thicker layer of smooth muscle cells (SMCs) known as the tunica media. The outermost layer consisting of fibroblasts, extracellular matrix (ECM) components, and fat is the advential layer, or media externa (Fig. 1.1B). When the underlying SMCs are contracted, leading to a smaller lumen, the endothelial cells are found within the folds of the elastic lamina. Muscular arteries are medium-sized arteries that distribute blood to the organs such as the femoral arteries of the thighs, the brachial arteries of the arms, and the mesenteric arteries of the abdomen. Arterioles are much smaller than muscular arteries and do not have a complete layer of SMCs. Arterioles dilate when oxygen levels are low, permitting more blood to reach the capillary beds. Capillary beds are a highly interconnected network of the smallest blood vessels. Capillaries have thin walls consisting of only endothelial cells and the basal lamina to allow for the passage of oxygen and small solutes from the blood into the interstitium. Deoxygenated blood then passes into venules, and on to

medium-sized veins with a thick tunica externa composed of elastin and collagen, and finally, to large veins. Pressure in the venous system is so low that valves are needed to ensure unidirectional flow back to the heart when movement compresses the vein.

The exchange of oxygen and nutrients between the blood circulation and the interstitial fluid occurs by diffusion through the capillaries. The capillary endothelial cells of most tissues are connected to adjacent cells through tight junctions, which permit the movement of small solutes such as glucose, water, oxygen, and CO_2, but do not allow the passage of larger plasma peptides. However, the capillary endothelium of endocrine organs is fenestrated, or contains small pores, to allow the passage of hormones and peptides.

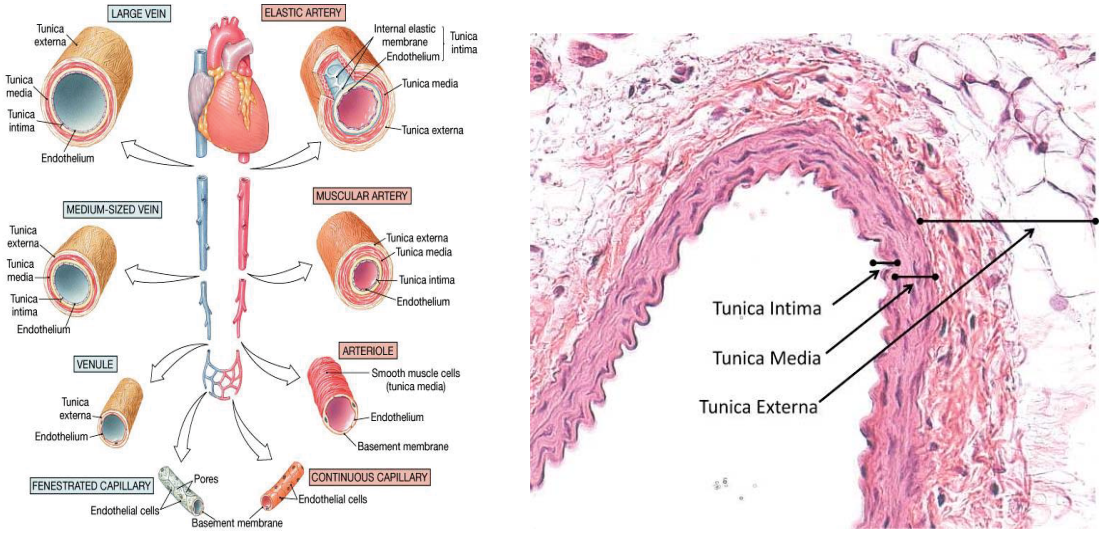

Figure 1.1. Overview of the vasculature. (Left) Schematic distinguishing the various vessel types and structures (from Martini and Nath, *Fundamentals of Anatomy and Physiology* (2009), Pearson Education, Inc.). (Right) A paraffin-embedded cross-section of a mouse aorta stained with Hematoxylin and Eosin (H&E) with the intimal, medial, and external layers indicated. The intima consists of the endothelium and basement membrane, the medial later is composed of smooth muscle cells, and the externa is comprised of the extracellular matrix and adventia.

1.2 The Endothelium

Due to its position at the interface between the blood circulation and the underlying vessel wall, the endothelium exerts effects on both underlying smooth muscle cells and cells in the bloodstream, thereby playing a crucial role in maintaining vascular tone and structure (Hadi, 2007). A healthy endothelium responds appropriately to stimuli in order to increase or decrease blood flow, and it is anti-atherogenic, inhibiting the adhesion of inflammatory cells, as well as anti-thrombotic, maintaining the proper balance of clotting and fibrinolytic factors. A dysfunctional endothelium is unable to perform these functions and favors vasoconstriction, inflammation, atherosclerosis, cell-adhesion, and coagulation (Figure 1.2).

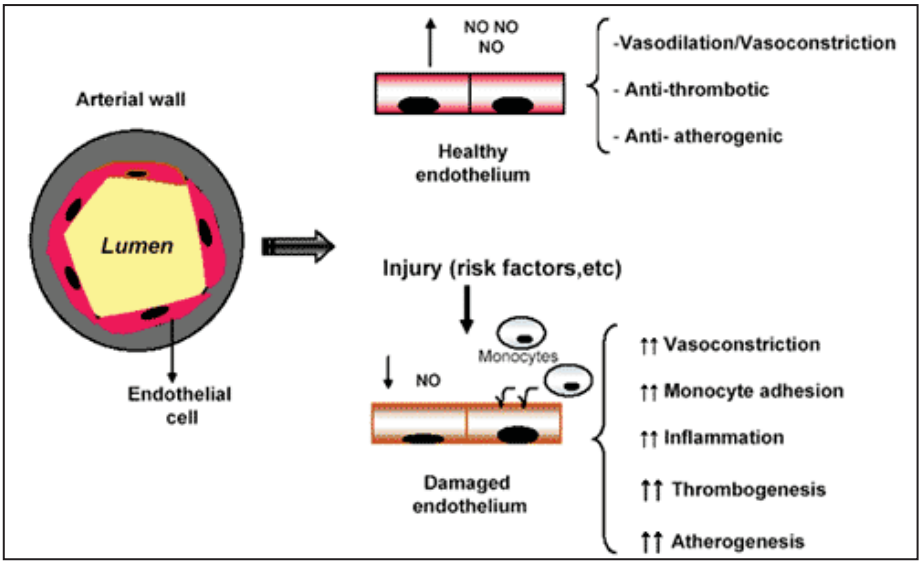

Figure 1.2. Responses of a healthy vs. damaged endothelium. A healthy endothelium responds appropriately to stimuli in order to maintain vascular homeostasis by producing vasoactive factors such as nitric oxide (NO). It is also anti-thrombotic and anti-atherogenic. A damaged or dysfunctional endothelium does not regulate blood flow properly and produces adhesion molecules and inflammatory substances that promote atherogenesis and thrombosis (from Rodriguez-Feo and Pasterkamp, 2007).

Along with the influence exerted by the endothelium on surrounding cell types, the SMCs and blood (including RBCs, platelets, and leukocytes) also, in turn, modify endothelial responses and gene expression. In addition, circulating peptides, hormones, and cytokines in the blood also direct responses from the endothelium. Pathological levels of these substances and activation of these cell types in response to injury also alter endothelial function.

1.3 Diabetes Mellitus

Diabetes is a metabolic disorder characterized by excessive blood glucose levels due to the inability of the body to produce or respond properly to insulin. Two main forms of diabetes exist- Type I diabetes affects 5% of diabetic patients and Type II accounts for 90-95% of the diabetic cases. Type I diabetes was formally referred to as juvenile diabetes because it is commonly diagnosed in children or young adults. It is also known as insulin dependent diabetes because of the failure of the body to produce adequate amounts of insulin due to the autoimmune destruction of insulin producing cells, known as β cells, in the pancreas. Type II diabetes is referred to as non-insulin dependent diabetes. Unlike patients with Type I, individuals with Type II diabetes are initially able to produce sufficient amounts of insulin, but the insulin is not able to elicit the appropriate response in the target tissues. In both types of diabetes, the lack of insulin or insulin signaling leads to reduced glucose uptake and energy substrate overload that promotes a variety of negative effects.

1.3.1 History and Epidemiology

Diabetes is an ancient disease first recorded around 1500BC (King, 2003). The term “diabetes” literally means “to flow through” referring to the unquenchable thirst and frequent urination experienced by diabetic patients (Laios, 2012). In 1675, the term “mellitus”, or honey sweet, was coined by Thomas Willis after discovering the sweetness of the urine and blood of diabetic patients, subsequently ascribed to excess sugar (Ahmed, 2002). Today, diabetes is a global epidemic, 366 million people have diabetes and 4.6 million deaths were attributed to diabetes in 2011 (Olokoba, 2012). According to the Center for Disease Control and Prevention (CDC) *National Diabetes Fact Sheet* (2011), 25.8 million people in the US were diabetic (8.3% of the population) in 2010 with 90% to 95% of them being type 2. In addition, they estimate that 79 million people over age 20 in the US have pre-diabetes, a condition in which individuals have elevated glucose or hemoglobin A1c levels but do not yet meet the criteria for diabetes.

In 2007, diabetes was the 7th leading cause of death in the US (CDC, *National Diabetes Fact Sheet*, 2011). Most of the mortality and morbidity associated with diabetes is due to cardiovascular complications. In 2004, heart disease accounted for 68% of diabetes related deaths, and diabetics have a 2-4 fold increased risk for developing cardiovascular disease (CDC, *National Diabetes Fact Sheet*, 2011). The increasing number of diabetic patients and increased expenses associated with their medical care emphasize the need to improve treatment. The importance of vascular complications in diabetes means

that we must understand the mechanisms underlying this association in order to provide better care.

1.3.2 Clinical Definition of Type II Diabetes

The diagnosis of diabetes is based on fasting plasma glucose levels, glucose levels following an oral glucose load, and more recently, the percentage of glycated hemoglobin (HbA1c) in the blood. Based upon these criteria, individuals with normoglycemia, intermediate hyperglycemia (pre-diabetes), and diabetes can be distinguished. Table 1.1 lists the current diagnostic recommendations of the World Health Organization (WHO), as published in *The Definition and Diagnosis of Diabetes Mellitus and Intermediate Hyperglycemia* (2006), as well those of the American Diabetes Association, as described in the *Report of the expert committee on the diagnosis and classification of diabetes mellitus* (2003). The WHO derives its diagnostic cut-offs based on the occurrence of diabetes-specific complications with increasing hyperglycemia as well as the population distributions of plasma glucose levels. In 2011, the WHO concluded that HbA1c can be used as a diagnostic test for diabetes and established the lower cut-off as 6.5% for diagnosing diabetes (World health Organization, 2011). The extent of hemoglobin glycosylation provides an indirect measure of glycemic control over the preceding 8-12 weeks (Nathan, 2007). The relationship between HbA1c levels and average glucose levels across a range of diabetic severities and populations has been established (Nathan, 2008).

Table 1.1. Diagnostic criteria established by the WHO for the diagnosis of diabetes and intermediate hyperglycemia. Diagnostic criteria of the American Diabetes Association are listed in parentheses where different from WHO guidelines.

Classification	Fasting Plasma Glucose (mg/dL)	HbA1c (%)	OGTT (mg/dL)*
Diabetes	≥ 126 mg/dL	≥ 6.5	≥ 200
Intermediate Hyperglycemia (Pre-diabetes)	≥ 110 (100) and < 126	(≥ 5.7 and < 6.5)	≥ 140 and <200
Normoglycemia	<110 (100)	(< 5.7)	<140

*2-hr plasma glucose following a 75g oral glucose load

Furthermore, the WHO defines two categories of intermediate hyperglycemia, impaired fasting glucose (IFG) and impaired glucose tolerance (IGT) and recommends both fasting glucose and oral glucose tolerance testing to diagnose both conditions. IFG is associated with impaired insulin secretion and impaired suppression of hepatic glucose output, and isolated IFG is defined as a fasting glucose between 110-125 mg/dL and 2h plasma glucose levels <140 mg/dL following an oral glucose load. IGT is associated with muscle insulin resistance and defective second phase insulin secretion, resulting in less efficient disposal of the glucose load during the OGTT and is defined as fasting plasma glucose levels <126 mg/dL and 2h plasma glucose of ≥ 140 and <200mg/dL (Abdul-Ghani, 2006). The relative risk for progression to diabetes in individuals with isolated IFG or IGT is 6- or 4.7-fold increased, respectively, compared to individuals with normal glucose tolerance, and having both IFG and IGT increases the risk 12-fold (Santaguida, 2005). Although intermediate hyperglycemia was initially used to describe individuals with an increased risk of developing diabetes, it is well recognized that people with intermediate glucose

levels also have an increased risk of developing cardiovascular disease and other adverse outcomes (Alzahrani, 2010). This cut-off point between intermediate and normoglycemia is based on this being the level above which first phase insulin secretion is lost in response to intravenous glucose and is associated with progressively greater risk of developing micro- and macrovascular complications (World Health Organization, 2006).

1.4 The Insulin-Glucose Pathway

During digestion, polysaccharides are broken down into monosaccharides by a series of hydrolysis steps. Glucose is a monosaccharide that is absorbed directly into the bloodstream from the small intestine and serves as the major source of fuel for the body. Circulating glucose is first monitored by pancreatic β cells located in the Islets of Langerhans in the pancreas. These cells serve as the "glucose sensors" of the body, and they secrete insulin to stimulate glucose uptake in muscle, fat, and liver cells. Once in the cells, glucose may undergo substrate-level phosphorylation during glycolysis and the Krebs cycle and oxidative phosphorylation during aerobic respiration, to produce ATP. Excess glucose may also be stored as glycogen in muscle or liver cells or converted to fatty acids and stored as triglycerides in fat. Under physiological conditions, the levels of glucose are tightly regulated to meet the energy demands of the body. However, in the presence of excessive dietary intake, disruption of these metabolic pathways occurs, eventually leading to the deregulation of glucose homeostasis and the rise in serum glucose.

1.4.1 The Glucose Sensor

Glucose enters the β cells of the pancreas through the GLUT2 transporter. Elevated levels of intracellular glucose increase glycolysis and ATP. ATP-sensitive potassium channels are inhibited, reducing K^+ efflux and leading to depolarization and the opening of voltage-gated Ca^{2+} channels. Influx of calcium is needed for exocytosis of insulin-containing granules and subsequent release of insulin. Initial release is rapid due to granules already docked at the plasma membrane. Subsequent insulin release requires the mobilization and docking of the granules to the membrane, resulting in a slower, sustained release of insulin. These processes leading to insulin secretion from β cells are summarized in Figure 1.3.

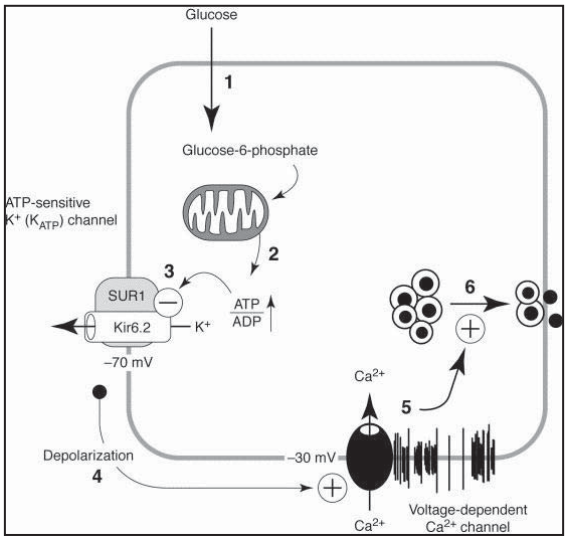

Figure 1.3. Processes leading to insulin secretion from β cells. (1) Glucose enters the β cell through the glucose transporter, GLUT2. (2) Glucose is converted to glucose-6-phosphate and ATP by glycolysis. (3) The increase in ATP levels inhibits K^+ efflux leading to (4) depolarization of the cell and the opening of voltage-gated calcium channels. (5 and 6) The influx of calcium promotes the exocytosis of insulin-containing granules resulting in the release of insulin (from Dunne, 1999).

1.4.2 Insulin Pathway

A simplified schematic of the insulin signaling pathway is provided in Figure 1.4. Binding of insulin to the insulin receptor, a receptor tyrosine kinase, causes a rearrangement of the 2 transmembrane domains bringing the kinase domains in close proximity to each other. Autophosphorylation of the cytoplasmic tails of the insulin receptor recruits insulin receptor substrate-1 (IRS-1), which also becomes phosphorylated. Membrane-bound phosphoinositide 3-kinase (PI3-kinase) is then able to bind pIRS-1 and catalyze the phosphorylation of PIP2 to create PIP3. Proteins with a Pleckstrin Homology domain such as protein kinase B (AKT) and phosphoinositide-dependent protein-1 (PDK1) are then able to bind PIP3. PDK1 phosphorylates and activates AKT, a serine-threonine kinase, which then phosphorylates many downstream substrates.

Under physiological conditions, insulin stimulation of adipocyte and muscle cells causes a rapid increase in the uptake of glucose through the glucose transporter, GLUT4. The activation of AKT is necessary for the translocation of GLUT4-containing vesicles to the plasma membrane, although the exact mechanism is not yet known. It is suggested that AKT may indirectly alter the activity of small G-proteins known as Rabs that, in their GTP-bound form, participate in vesicle movement and fusion (Miinea, 2005). AKT also phosphorylates and inactivates GSK, an inhibitor of glycogen synthase, which thereby leads to glucose storage in the form of glycogen.

In fat, adipocytes are insulin-sensitive cells that take up glucose and store energy in the form of triglycerides that are subsequently broken down into free

fatty acids (FFAs) and glycerol in times of energy need. In adipocytes, insulin promotes the uptake of fatty acids and the synthesis of lipids by increasing expression of steroid regulatory element binding protein (SREBP). AKT inhibits lipolysis, or the breakdown of fat into fatty acids, by activating a cAMP phosphodiesterase thereby reducing cAMP levels and downstream activation of lipase, the enzyme responsible for lipid hydrolysis (Belfrage, 1982).

When glucose levels are low, glucagon, released from α cells of the pancreas, binds to G-protein coupled receptors on liver cells that activate adenylate cyclase leading to PKA activation. Subsequent downstream phosphorylation of glycogen phosphorylase, the enzyme responsible for the release of glucose-1-phosphate from glycogen polymers (glycogenolysis), leads to the release of glucose into the blood. When the glycogen stores are depleted, the generation of glucose from non-carbohydrate sources such as amino- and fatty acids then occurs in the process known as gluconeogenesis. However, in the presence of excess glucose, insulin serves to regulate the expression and activity of key enzymes involved in gluconeogenesis and glycogenolysis to inhibit these pathways. For example, pAKT phosphorylates forkhead transcription factors such as forkhead box other -1 (FoxO-1), which leads to its sequestration in the cytoplasm where it is unable to activate transcription of phosphoenolpyruvate carboxykinase (PEPCK) and glucose-6-phosphate, consequently inhibiting gluconeogenesis (Li, 2007). AKT also indirectly activates mTOR, which stimulates cell growth and survival and inactivates BAD, a pro-

apoptotic member of the BCL-2 family. This leads to the release of apoptosis inhibitory proteins thereby preventing apoptosis.

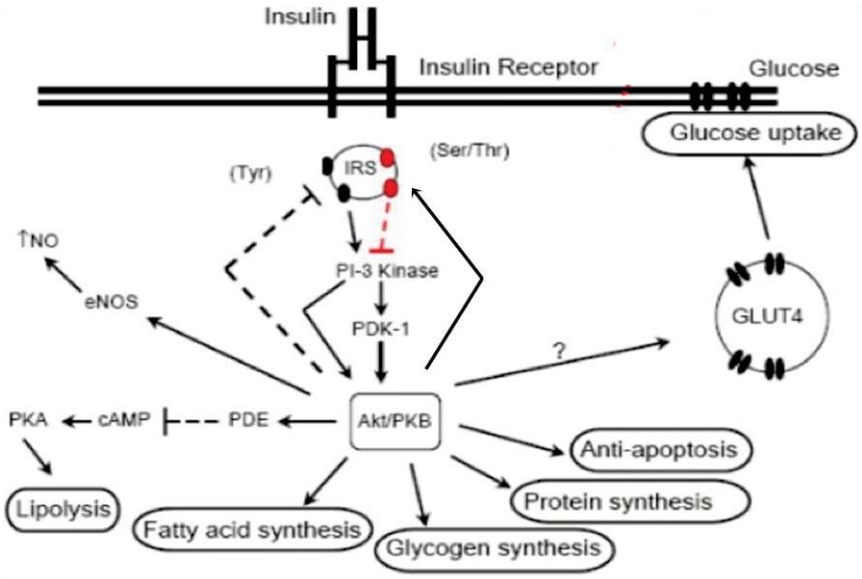

Figure 1.4 Simplified schematic of the insulin receptor signaling pathway and its downstream effects (adapted from Davidoff, 2006). Binding of insulin to the insulin receptor activates a signaling cascade leading to the phosphorylation/activation of AKT. Activation of AKT serves to promote protein, glycogen, and fatty acid synthesis and eNOS activity while inhibiting lipolysis and cell death. AKT activation also leads to the translocation of GLUT4-containing vesicles to the cell surface by an unknown mechanism to allow for cellular uptake of glucose. Prolonged insulin stimulation leads to negative feedback regulation by preventing insulin receptor substrate (IRS) interaction with the insulin receptor, decreasing tyrosine phosphorylation, and increasing the inhibitory Ser/Thr phosphorylation.

1.4.3 Insulin Resistance

Insulin resistance occurs when the target organs no longer respond to insulin appropriately. The same amount of insulin may be produced and secreted by the β cells, but it no longer has the desired effect (Figure 1.5). In adipose tissue, lipolysis is no longer inhibited increasing the amount of free fatty acids in the circulation. Glycogen and lipid synthesis is no longer activated by AKT, and hepatic glucose production is not inhibited even in the presence of high glucose levels. Defective insulin signaling reduces translocation of GLUT4 transporters to

the cell surface, reducing cellular uptake of glucose and leading to its accumulation in the blood (hyperglycemia). Excessive glucose stimulates overproduction of insulin in the pancreas which can produce hyperinsulinemia. Prolonged insulin stimulation also leads to negative feedback regulation of the insulin signaling pathway (Figure 1.4). Excessive insulin promotes serine/threonine phosphorylation of IRS-1 that disrupts its interaction with the insulin receptor leading to a reduction in IRS-1 tyrosine phosphorylation and also leads to increased proteosomal degradation of IRS-1. These inhibitory effects are mediated through activation of mTOR and the p70 S6 kinase (Harrington, 2005).

These pathophysiological increases in glucose, insulin, and free fatty acids, along with other adipokines and inflammatory factors of the diabetic milieu, create an environment that fosters cardiovascular damage. The following sections will discuss the vascular complications of diabetes and the mechanisms thought to be responsible for these complications.

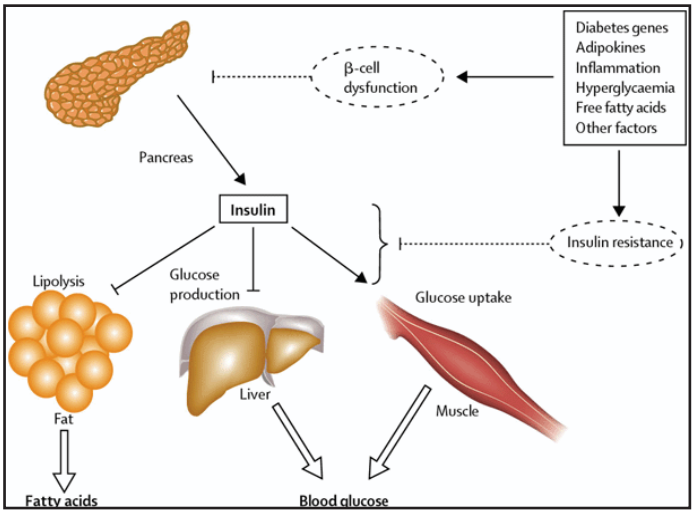

Figure 1.5. Insulin resistance impairs insulin action in target tissues. Insulin normally promotes glucose uptake and inhibits glucose production and lipolysis. In the insulin resistant state, insulin action is impaired leading to increased glucose and fatty acid production (from Stumvoll, 2005).

1.5 Vascular Complications of Diabetes

1.5.1 Microvascular Complications

Progressive degeneration of microvascular beds is a major contributing factor to many complications of diabetes: retinopathy, nephropathy, and neuropathy.

Microangiopathy has been implicated in the pathogenesis of diabetic neuropathy generally due to insufficient blood flow to the nerves resulting in nerve hypoxia and subsequent damage (Cade, 2008). Increased basement membrane thickening, endothelial cell hypertrophy and hyperplasia (Malik, 1993), and reduced luminal size have been related to the pathogenesis of neuropathy. Diabetics may also develop cardiovascular autonomic neuropathy, which increases the risk for major cardiovascular events (Vinik, 2003). This is caused by damage to the autonomic nerve fibers that innervate the heart and blood vessels and is manifested by abnormalities in heart rate control and vascular reactivity (Vinik, 2003).

Between 2005-2008, 4.2 million people with diabetes aged older than 39 had diabetic retinopathy (28.5% of these older diabetics) (CDC, *National Diabetes Fact Sheet*, 2011). In non-proliferative retinopathy, microanyeurisms of the capillaries in the back of the retina cause swelling, and the dysfunction of capillary endothelium results in the inability to regulate the exchange of oxygen and nutrients progressing toward ischemia (Fowler, 2008). In proliferative retinopathy, hypoxic conditions stimulate neovascularization by the overproduction of VEGF (Bassi, 2012), but the newly formed vessels are

abnormal and leak blood into the eye (vitreous hemorrhage), resulting in blurred vision.

Diabetic nephropathy is the leading cause of renal failure in the US, and is linked to endothelial dysfunction (Fowler, 2008). Glomerular endothelial cells play an important role in establishing the filtration barrier through which waste products leave the blood and are excreted in the urine while proteins are retained in the blood circulation. When the glomerular filtration barrier fails, increased protein passes into the urine. As albumin is one of the most abundant proteins in the plasma, it is one of the first detected in the urine with diabetic nephropathy. Markers of endothelial dysfunction are evident before the onset of microalbuminuria, indicating their potential role in the pathogenesis of nephropathy (Lim, 1999). Glomerular capillary pathology has been linked to impaired function of endothelial progenitor cells (Makino, 2009), increased vascular permeability induced by VEGF-A (Karalliede, 2011), and Ang-2-induced endothelial apoptosis (Davis, 2007). Treatment with anti-angiogenic factors (Nakagawa, 2009) and ACE inhibitors reduces progression to macroalbuminuria (Gross, 2005).

1.5.2 Macrovascular Complications

Macrovascular complications associated with diabetes include coronary heart disease, stroke, and peripheral vascular disease. All of these complications involve the narrowing or occlusion of the large blood vessels of the body thereby restricting blood flow to the target tissues. In the case of coronary heart disease, blockage of the coronary arteries supplying blood to the heart may cause angina

or a myocardial infarction in the case of severe blockage. Studies have shown that the risk of myocardial infarction (MI) in diabetics is equivalent to the risk in non-diabetic patients with a history of ischemic heart disease (Haffner, 1998). This insight has led to the recommendation by the American Diabetes Association and American Heart Association to treat people with diabetes as though they have coronary heart disease (Buse, 2007).

Patients with type 2 diabetes also have a much higher risk of stroke, with an increased risk of 150–400% (Fowler, 2008). Stroke is the result of blockage of arteries of the cerebrovasculature, which provide oxygen to the brain. Peripheral vascular disease is caused by the narrowing or obstruction of large vessels other than those of the heart or brain such as the aorta or the renal or femoral arteries. Diabetes increases the risk of developing PAD at least 2-fold (Gregg, 2004). Blockage of the leg arteries is common in diabetes and results in reduced blood flow to the lower extremities increasing the potential for lower-limb ischemia and ulceration, often requiring amputation (Prompers, 2008). Blood clots may also obstruct blood flow in the veins leading to deep vein thrombosis.

The main pathological mechanism in macrovascular disease is atherosclerosis, the development of lesions, or plaques, that narrow the arterial lumen. Plaque rupture and thrombosis can then lead to acute ischemic events such as myocardial infarction or stroke. The chronic inflammatory state in diabetes initiates atherosclerosis by activating endothelial cells, and endothelial dysfunction further exacerbates atherosclerosis progression. Enhanced expression of proinflammatory molecules in the diabetic state (TNF-α, IL-1β, and

ox-LDL) induces disruption of endothelial cell-cell junctions thereby increasing the permeability of the monolayer and leading to the presentation of P-selectin and von Willebrand factor on the endothelial cell surface (Pober, 2007). These inflammatory molecules also activate endothelial proinflammatory transcription factors, such as NF-κB, which results in the transcription of proinflammatory genes (chemokines IL8 and MCP-1 and cytokines IL-1β and TNF-α) and adhesion molecules (E-selectin, ICAM, VCAM) (Funk, 2012). Monocyte chemoattractant protein-1 (MCP-1) attracts monocytes to the area of inflammation, while the adhesion molecules allow monocytes to adhere to the endothelial cell surface and enter the sub-endothelial space by diapadesis (Ley, 2007). Subsequent uptake of ox-LDL by the differentiated macrophages in the vessel wall via scavenger receptors, such as SR-A and CD36, leads to foam cell formation and the formation of a fatty streak (Yamada, 1998).

Progression from a fatty streak to a more advanced lesion involves a chronic inflammatory state characterized by macrophage and T cell cytokine production, which further activates macrophages, endothelial cells, and SMCs. This inflammatory state promotes the migration of SMCs from the media into the intima where they also take up ox-LDL, forming foam cells, as well as proliferate and synthesize matrix components to form a fibrous cap over the lesion (Glass, 2001). The lesion, which protrudes into the lumen, may restrict blood flow to such an extent as to cause ischemic symptoms. However, most acute events are caused by rupture of the plaque and thrombosis. Diabetics have an increased propensity for thrombosis due to the increased activation of endothelial cells,

platelets, and coagulation factors, coupled with decreased fibrinolysis (Alzahrani, 2010). Under physiological conditions, the endothelium displays both anti-coagulative and anti-thrombotic properties. It inhibits platelet activation by producing nitric oxide (NO), prostacyclin (PGI_2), and endothelial ADPase, to decrease intracellular calcium and ADP stimulation of platelets. However, in diabetes, the reduced production of NO and PGI_2 accompanied by increased production of vasconstrictive molecules, such as prostaglandin and thromboxane, leads to platelet aggregation.

In addition to inducing platelet hyper-reactivity, the dysfunctional diabetic endothelium exacerbates thrombosis by the upregulation of coagulation factors and the inhibition of fibrinolysis. Tissue factor (TF) is the main initiator of the extrinsic coagulation cascade, which leads to the activation of thrombin. Thrombin cleaves soluble fibrinogen to fibrin. Fibrin monomers polymerize and cross-link with platelets, which further increases platelet aggregation, leading to thrombus formation. Normally, tissue factor expression by endothelial cells is low, but in states of inflammation such as T2D, it is more abundant. Diabetics display higher levels of circulating TF, which are influenced by the extent of hyperglycemia (Vaidyula, 2006). The formation of advanced glycation endproducts and reactive oxygen species in diabetes activates NFκB, which leads to TF production (Annex, 1995). Levels of coagulation factors produced by the liver, such as thrombin (Boden, 2007 and Ceriello, 2009), FVII (Heywood, 1996), and fibrinogen (Klein, 2003) are also enhanced in diabetes. Increased levels of fibrinogen and factor VII are associated with increased risk of

cardiovascular disease (Glass, 2001). Hepatic fibrinogen production may be related to elevated IL-6 (Wang, 2009), insulin (Barazzoni, 2003 and Tessari, 2006), and glucose (Bruno, 1996 and Ceriello, 1998) in diabetes.

The dissolution of a clot is accomplished by the activation of fibrinolytic proteins and the degradation of blood-clotting factors. Serine protease inhibitors, protein C, and protein S degrade constituents of the coagulation cascade. ECs also produce thrombolytic substances such as tissue-type plasminogen activator (t-PA), which cleaves the zymogen plasminogen into active plasmin. Plasmin is the main proteolytic enzyme in the fibrinolysis system, and its activation leads to fibrin hydrolysis and degradation. Plasminogen activator inhibitor-1 (PAI-1) is the main inhibitor of fibrinolysis and works by binding and sequestering t-PA. HbA1c positively correlates with PAI-1 levels and negatively correlates with t-PA, suggesting a role for hyperglycemia in modulating fibrinolysis (Seljeflot, 2006). Elevated levels of PAI-1 are observed in insulin-resistant subjects (Alessi, 2008), and glucose and insulin control lowers PAI-1 (Cefalu, 2002 and Stegenga, 2008). Reduced levels of t-PA have been linked to diabetic nephropathy (Hafer-Macko, 2007), whereas increased t-PA activity is found in diabetic patients with peripheral vascular disease (Sahli, 2009). Fibrinolysis rates are reduced in diabetics, partly due to decreased plasminogen binding to fibrin and impaired plasmin generation (Dunn, 2006). Also, clot structure is altered in diabetes. Clots are more compact and less permeable due to post-translational modifications of fibrinogen that occur in the diabetic state such as glycation and oxidation (Pieters, 2007 and Andrades, 2009). In summary, endothelial dysfunction in

diabetes promotes atherosclerosis and thrombosis by perpetuating inflammation, activating platelets, and altering the balance of coagulation and fibrinolytic pathways.

Vessel obstruction is further complicated by impaired arteriogenesis in diabetic patients. Arteriogenesis is the remodeling of arterioles into conductance vessels to circumvent an occluded artery and restore blood flow to downstream tissues. Many mechanisms have been suggested including alterations in the endothelial response to vasodilatory and shear stress stimuli, decreased expression of eNOS, and reduced growth factor signaling by VEGF, HIF-1α, and FGF-2, among others, which lead to impaired recruitment of endothelial progenitor cells, monocytes, and bone marrow cells that are needed for vessel remodeling (Ruiter, 2010).

1.5.3 Other Cardiovascular Complications of Diabetes

Diabetes also affects the structure and function of the heart. In diabetic patients, defects in diastolic and systolic function (Fang, 2004) as well as interstitial fibrosis (Nunoda, 1985) and increased oxidative stress (Ceylan-Isik, 2006) have been observed. Alterations in myocardial substrate utilization and energetics can occur even before the onset of diabetes, during the period of normoglycemic insulin resistance (Hseuh, 2007). There is a shift away from glucose uptake and oxidation toward increased fatty acid oxidation as well as decreased mitochondrial function (Mokuda, 1990 and Ceylan-Isik, 2006). Studies have shown that myocardial insulin resistance contributes to these metabolic changes, which eventually lead to contractile dysfunction (Abel, 2005). The

diabetic heart is also more susceptible to injury by common stressors such as ischemia (Hseuh, 2007) and hypertrophy (McQueen, 2005) due to the impaired glucose utilization which normally serves as a protective mechanism to maintain ATP concentrations (Tian, 2001).

Also, activation of the renin-angiotensin-aldosterone system (RAAS) in the diabetic heart has been shown to cause fibrosis due to increased myocyte necrosis and apoptosis (Frustaci, 2000). Activation of PKCβ and elevated expression of connective tissue growth factor (CTGF) and TGF-β have been associated with fibrosis (Way, 2002), which stiffens the heart leading to impaired relaxation and the syndrome of heart failure with preserved systolic function.

1.6 Endothelial Dysfunction in Diabetes

As the previous section demonstrates, the dysfunction of the endothelium plays a major role in both microvascular and macrovascular complications of diabetes. Endothelial dysfunction often precedes clinically significant vascular disease and is often detected before structural changes in the vascular wall (Xu, 2009). Commonly, endothelial dysfunction is characterized by reduced bioavailability of endothelial-derived relaxation factors such as nitric oxide, prostacyclin, and endothelial-derived hyperpolarizing factor (EDHF), with increased production of vasoconstricting agents, such as endothelin, prostaglandin, and angiotensin-II. Endothelial dysfunction is also mediated by oxidative and nitrositive stress. These mediators of the endothelial dysfunction observed in diabetes are discussed below.

1.6.1 Reduced eNOS Activity and Nitric Oxide Bioavailability

Under physiological conditions, the endothelium releases relaxing and contracting factors to decrease or increase blood flow depending on the needs of the body. A potent vasodilator, nitric oxide (NO), is produced by the conversion of the amino acid, L-arginine, to L-citrulline by the enzyme endothelial nitric oxide synthase (eNOS). NO has a low molecular weight and short half life of a few seconds which enables it to diffuse to the underlying SMCs and direct rapid changes in arterial diameter. In SMCs, contraction or relaxation depends on the state of phosphorylation and activity of myosin light chain (MLC). NO activates guanylate cyclase, which increases intracellular levels of cGMP. cGMP activates protein kinase G (PKG), which phosphorylates a number of substrates leading to a decrease in intracellular calcium levels (Francis, 2010) and activation of a phosphatase of myosin light chain (Wu, 1996 and Lee, 1997) leading to the inactivation of MLC and subsequent relaxation. In the presence of high intracellular calcium, there is increased formation of the Ca^{2+}/calmodulin complex, which binds and activates myosin light chain kinase (MLCK) (Kamm, 1985). In the presence of high intracellular calcium, MLCK phosphorylates smooth muscle myosin so that it is able to interact with actin filaments, ultimately leading to contraction.

In diabetes, the expression and activity of eNOS is decreased leading to impaired vasodilation. eNOS activity is altered by post-translational modifications and eNOS uncoupling. In eNOS uncoupling, the normally vasoprotective enzyme that produces NO becomes a contributor of oxidative stress by producing the

superoxide radical instead (Xu, 2009). eNOS uncoupling can occur by several mechanisms. eNOS functions as a dimer with a tetra-coordinated zinc ion held together by thiol groups. Oxidation of the zinc-thiolate cluster by anionic oxidants, such as peroxynitrite, induces loss of the zinc, leading to instability of the dimers and altered eNOS activity (Zou, 2002).

The second mechanism for eNOS uncoupling involves the reduced availability of tetrahydrobiopterin (BH_4), an essential eNOS cofactor, which enhances dimer stabilization, L-arginine binding, and electron transfer. BH_4 deficiency has been reported in diabetes, and supplementation with BH_4 has been shown to improve endothelial function in mammary artery rings from diabetic patients (Xu, 2009). BH_4 levels can be decreased either by reduced synthesis from GTP or by its oxidation to BH_2. GTP cyclohydrolase I (GCH1) is the enzyme responsible for the rate-limiting step in the conversion of GTP to BH_4, and its expression and activity is markedly reduced type 2 diabetes and insulin-resistant rat models (Alp, 2003 and Meininger, 2004). Loss of BH_4 in GCH1-deficient mice causes eNOS uncoupling, increased superoxide anion production, and inhibition of endothelial nitric oxide signaling in cerebral microvessels (Santhanam, 2012).

Under conditions of oxidant stress, the oxidation of BH_4 to BH_2 occurs. PKC activation induced by hyperglycemia leads to the generation of superoxide via increased expression of NADPH oxidase or mitochondrial uncoupling (Figure 1.6A). The superoxide anion is reduced by superoxide dismutase (SOD) resulting in hydrogen peroxide formation (H_2O_2), which can increase eNOS expression.

eNOS-derived NO can react with O_2^-, to form peroxynitrite ($ONOO^-$), which oxidizes BH_4 to BH_2. BH_2 competes with BH_4 for binding the heme oxygenase domain of eNOS (Figure 1.6B). Coupled eNOS oxidizes L-arginine to L-citrulline, producing NO, whereas uncoupled eNOS reduces molecular oxygen to O_2^-, without producing NO, leading to oxidative stress.

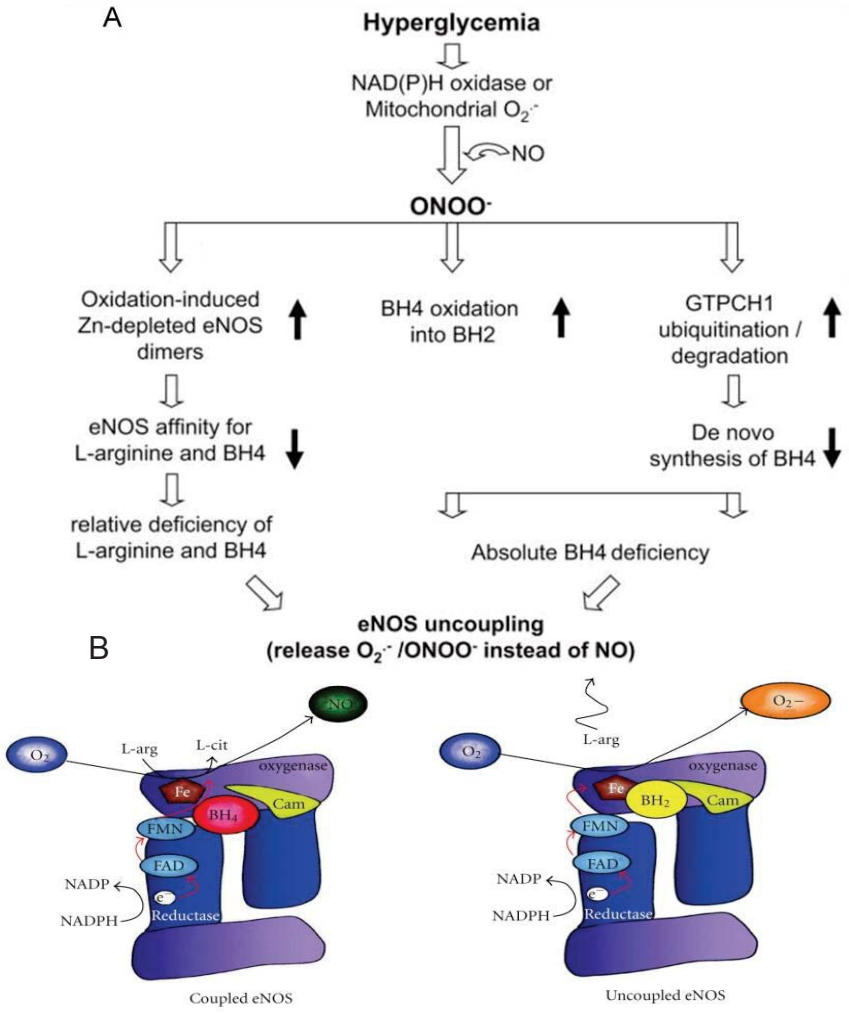

Figure 1.6. eNOS uncoupling in diabetes. (A) Superoxide anion generated by NAD(P)H oxidase or mitochondrial dysfunction reacts with nitric oxide (NO) to produce peroxynitrite ($ONOO^-$). Peroxynitrate causes eNOS uncoupling by disrupting eNOS dimerization or reducing the bioavailability of the eNOS cofactor, tetrahydrobiopterin (BH_4) (adapted from Xu, 2009). (B) Coupled eNOS (left) produces NO from the oxidation of L-arginine whereas uncoupled eNOS (Right) is unable to bind its L-arginine substrate and instead produces O_2^- (from Chen, 2010).

1.6.2 Increased Vasoconstriction in Diabetes

Arachidonic acid is released from the plasma membrane by phospholipases and is subsequently metabolized by cyclooxygenases to produce prostaglandin H_2 (PGH_2). PGH_2 is the substrate for several isomerases that can produce prostaglandins and thromboxane (Figure 1.7). Prostacyclin (PGI_2) is the predominant prostaglandin produced in endothelial cells and is an important vasodilator in vascular homeostasis. Endothelial-derived PGI_2 binds the prostacyclin I_2 receptor, a G-protein coupled receptor, and activates adenylate cyclase producing cAMP (Figure 1.7). Subsequent activation of PKA leads to increased intracellular calcium and the dephosphorylation of MLC resulting in vasodilation. Prostacyclin also binds IP receptors on the endothelial cell leading to activation of eNOS and increased NO production. In diabetes, vascular PGI_2 synthesis and release is inhibited (Johnson, 1979 and Dollery, 1979). In a type I animal model of diabetes, PGI_2 production is decreased while TXA_2 production in platelets is increased (Karpen, 1982). In diabetes, decreased levels of PGI_2 have been shown to increase platelet aggregation, adhesion, and release of PGH_2 and TXA_2 (Xu, 2009). Reduction of PGI_2 has also been proposed as a mechanism for accelerated atherosclerosis in diabetic patients (Johnson, 1979). Depletion of PGI_2 in mice results in vasculopathy and thickening of the vessel wall (Xu, 2009).

Unlike prostacyclin, PGH_2 and TXA_2 are vasoconstrictive factors that bind to the TXA2/PGH2 (TPr) receptor on SMCs to induce contraction. In the blood vessels of non-diabetic animals, PGH_2 is primarily metabolized to PGI_2 by PGI Synthase (PGIS), reducing its availability to cause vasoconstriction. However, in

diabetes, decreased activity of PGIS or increased COX activity results in increased levels of non-metabolized PGH_2. Hyperglycemia, ROS production, and decreased NO production have been implicated in the generation of PGH_2 in diabetes (Xu, 2009). In addition, peroxynitrite can nitrosylate and inactivate PGIS, leading to the accumulation of PGH_2 and increased activation of the TPr receptor (Xu, 2009). Activation of the Tpr receptor induces apoptosis and the expression of adhesion molecules, such as VCAM-1, ICAM-1, and E-selectin (Ishizuka, 1998). It also may increase ROS production, and all these effects can be prevented by Tpr antagonism or COX inhibition (Zhang, 2008b). Tpr blockade also reduces lesions in diabetic *ApoE(-/-)* mice (Xu, 2009).

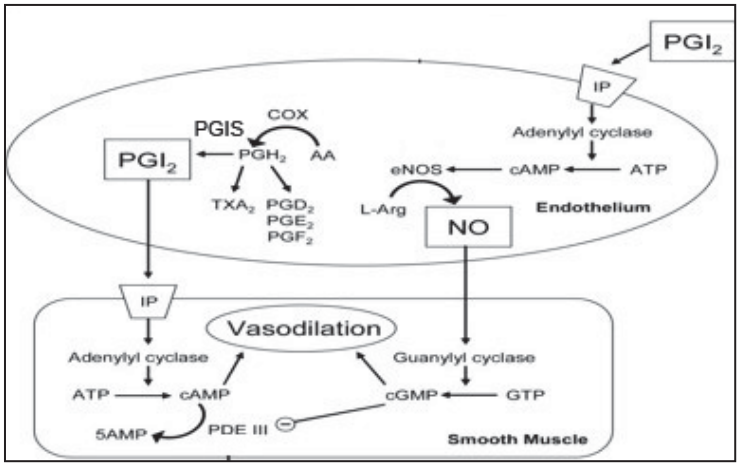

Figure 1.7. The production and vasodilatory action of prostacylin. Prostacyclin (PGI_2) is produced by the metabolism of arachidonic acid by cyclooxygenase (COX) and prostaglandin synthase (PGIS). PGI_2 promotes vasodilation by binding IP receptors resulting in cAMP production and eNOS activation. In diabetes, increased COX activity and reduced PGIS activity result in decreased abundance of PGI_2 and increased levels of non-metabolized PGH_2, which acts as a vasoconstrictor and promotes apoptosis and the expression of adhesion molecules (adapted from Lakshminrusimha, 2009).

ECs can also produce endothelin (ET) and angiotensin II, which cause contraction of the SMCs and also influence the growth, proliferation, and

differentiation of SMCs. ET_1 binds to ET_A and ET_B G-protein coupled receptors on the surface of SMCs that cause an increase in intracellular calcium levels and subsequent contraction. The renin-angiotensin-aldosterone system, important in the regulation of blood volume, initiates the production of angiotensin II by angiotensin converting enzyme (ACE) on the EC surface which then increases blood pressure, in part, by vessel constriction. Insulin-resistant patients have increased plasma levels of ET-1, and hyperinsulinemia increases ET-1 secretion. Blockade of the ET_A receptor has been shown to improve EC function in diabetics (Xu, 2009). In summary, diabetes decreases the activity of vasoprotective factors such as NO and prostacyclin while increasing the production of vasoconstrictors such as PDH_2 and ET-1 thus shifting the balance toward platelet aggregation, lesion progression, and thrombus formation.

1.6.3 Reactive Oxygen and Nitrogen Species

Many mechanisms associated with hyperglycemia such as the polyol pathway, prostanoid synthesis, glucose oxidation, and protein glycation increase the production of free radicals and oxidants. Exposure of ECs to high glucose or free fatty acids increases superoxide production and oxidant stress (Tripathy, 2003 and Inoguchi, 2000). Oxidant stress has been attributed to NAD(P)H oxidase activity through a PKCβ-dependent mechanism (Inoguchi, 2000) or mitochondrial dysfunction (Brownlee, 2001). Increased superoxide production also leads to increased production of reactive nitrogen species. NO reacts with superoxide to produce peroxynitrite ($ONOO^-$) at a faster rate than either molecule's dismutation by SOD. This reduces the bioavailability of NO as well as

generates an extremely potent oxidant. $ONOO^-$ oxidizes sulfhydral groups and thioethers and nitrates and hydroxylates aromatic groups, including those of tyrosine, tryptophan, and guanine, as well as reacts with metal centers. These modifications alter the functions of lipids and enzymes, such as eNOS and PGIS. Vascular tissues from diabetic patients and animals exhibit significantly more intense 3-nitrotyrosine staining than tissues from normal controls, especially in the endothelium (Zou, 2004 and Pacher, 2006). Peroxynitrite also impairs vasodilation and insulin sensitivity in endothelial cells by several other mechanisms including promoting the degradation of GCH1, oxidizing the zinc-thiolate center of eNOS, and inducing the formation of advanced glycation endproducts by generation of reactive *α*-oxoaldehydes from glucose (Nagai, 2002).

1.7 Mechanisms by which Diabetes Causes Endothelial Dysfunction

1.7.1 Hyperglycemia

Chronic hyperglycemia causes endothelial dysfunction by numerous mechanisms including glycosylation that degrades protein function, increased activation of protein kinase C, increased glucose flux through the polyol and hexosamine pathways, activation of the 12/15-lipoxygenase pathway, increased oxidative stress due to superoxide formation, and inflammation by the induction of cytokine secretion (Gleissner, 2007). A summary of these adverse pathways activated by hyperglycemia that result in endothelial dysfunction is shown in Figure 1.8.

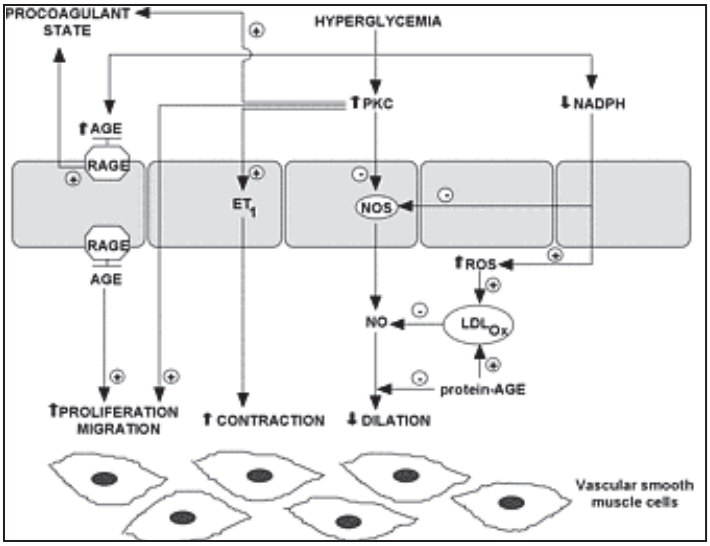

Figure 1.8. Mechanisms by which hyperglycemia induces endothelial cell dysfunction and impaired vasoregulation. Hyperglycemia results in the glycation of macromolecules to produce advanced glycation endproducts (AGEs) that may activate inflammatory pathways such as RAGE and promote reactive oxygen species (ROS) generation. Excessive glucose also activates protein kinase C and decreases NADPH availability, which alters vascular homeostasis by inhibiting eNOS activity and promoting the production of vasoconstrictors, such as endothelin (ET-1), and ROS (from Guerci, 2001).

1.7.1.2 Advanced Glycation Endproducts

Hyperglycemia leads to the non-enzymatic glycosylation of proteins and lipids through the Maillard reaction. Glucose is converted into α-oxoaldehydes such as glyoxal, methylglyoxal, and 3-deoxyglucosone, which contain reactive carbonyls that react with the amino groups of proteins to form advanced glycation endproducts (AGEs). These glycosylations may alter the functions of the proteins by disrupting molecular conformation, altering enzymatic activity, increasing stability, or interfering with receptor recognition (Xu, 2009). Furthermore, these modified proteins and lipids are able to bind AGE-specific receptors and initiate downstream signaling. Receptors for AGEs are expressed on the surface of many cell types including endothelial cells, macrophages, and vascular SMCs.

Some AGE receptors, such as the receptor for advanced glycation endproducts (RAGE), have been shown to activate inflammatory pathways and promote oxidative stress in endothelial cells (Win, 2012 and Mangalmurti, 2010). RAGE ligation leads to the nuclear translocation of NFκB and the transcriptional activation of adhesion molecules and pro-inflammatory factors (Win, 2012). Antagonism of the RAGE receptor with soluble RAGE has been shown to reduce atherosclerotic lesion size and inflammation in *ApoE(-/-)/db/db* mice (Wendt, 2006). Intracellular signaling pathways have not yet been identified for other AGE receptors such as galectin-3 and macrophage scavenger receptors, although their increased expression by AGEs has been demonstrated (Stitt, 1999 and Pugliese, 2000). AGEs also increase the permeability of the endothelium and act as chemotactic agents for macrophages (Sano, 2000). Glycosylation of certain proteins such as hemoglobin can serve as an indirect measure of glucose levels over a 2-3 month period due to the protein's long half-life of about 100 days. Hb1Ac measurements have become a useful clinical tool, along with fasting glucose levels, to determine diabetic status. Diabetics with poor glycemic control have HbA1c levels of 8-10% of total hemoglobin (compared to the normal range below 6%).

1.7.1.3 Protein Kinase C Activation

High glucose levels have also been shown to activate protein kinase C. Most isoforms of PKC are activated by diacylglycerol (DAG), which is synthesized in the presence of high glucose. PKC may also be activated indirectly by the polyol, hexosamine, 12/15-LO, and RAGE pathways. PKCδ has

been shown to upregulate adhesion molecules in human umbilical vein endothelial cells (HUVECs) (Rask-Madsen, 2005) resulting in increased adherence of monocytes to the endothelium (Manduteanu, 1999). PKCβ has been implicated in glucose-induced upregulation of the LOX-1 scavenger receptor, and PKCα mediates SMC proliferation through TGF-β. Peroxisome proliferator-activated receptor-gamma (PPAR-γ) agonists have been shown to reduce PKC activity induced by hyperglycemia in the endothelium and SMCs (Verrier, 2004).

1.7.1.4 Increased Glucose Flux through the Polyol and Hexosamine Pathways

Under physiological conditions, aldose reductase converts toxic aldehydes to alcohols. However, in hyperglycemic conditions, it acts in the polyol pathway to perform the NADPH-dependent reduction of glucose to produce sorbitol, which may accumulate in the cell causing osmotic stress. Oxidant stress is also caused by the depletion of NADPH, which is needed to regenerate the antioxidant glutathione. Sorbitol may then be converted to fructose by sorbitol dehydrogenase (SDH), which may also promote increased AGE formation. Activation of the polyol pathway is implicated in the microvascular complications of diabetes such as retinopathy (Lorenzi, 2007). The overexpression of aldose reductase in *LDLR(-/-)* mice rendered diabetic by streptozotocin injection has been shown to increase lesion size (Vikramadithyan, 2005).

The flux of excess glucose through the hexosamine pathway leads to increased O-linked glycosylation of proteins that alter their enzymatic activity (Xu, 2009). The hexosamine pathway converts fructose-6-phosphate to glucosamine-

6-phosphate through glutamine-fructose-6-phosphate amidotransferase (GFAT). Inhibitors of GFAT have been shown to reduce hyperglycemia-induced transcription of transforming growth factor β1 (TGFβ1) and PAI-1 and to restore eNOS activity in bovine aortic endothelial cells (BAECs) (Gleissner, 2007).

1.7.1.5 Increased Activation of Lipoxygenases

Hyperglycemia also increases expression of 12- and 15-lipoxygenase enzymes, which insert oxygen at the 12 or 15 carbon positions of arachidonic acid to produce 12(S)- and 15(S)-hydroxyeicosatetraeonic acid (12(S)- or 15(S)-HETE). 12(S)-HETE has been shown to promote monocyte adhesion to ECs by increased expression of VCAM-1 (Natarajan, 2004). 12-LO deficient mice are resistant to the development of type I diabetes induced by STZ (Bleich, 1999). In models of type II diabetes, LO inhibitors restore insulin sensitivity, suggesting a role for lipoxygenases in the pathogenesis of diabetes. Also, lipoxygenase activity has been linked to pro-atherogenic mechanisms. 15-LO activity has been detected in human atherosclerotic lesions, and lipoxygenases oxidize LDL to create the atherogenic oxidized LDL (Kuhn, 1997). The deletion of 12-LO and 15-LO on the apolipoprotein E (ApoE) or low-density lipoprotein receptor (LDLR) knockout strains reduces lesion size (Cyrus, 2001 and George, 2001). Thus, these enzymes also play a role in the cardiovascular complications of diabetes.

Reduction of hyperglycemia has been shown to reduce the microvascular complications of diabetes (Gleissner, 2007)). However, increased risk for developing macrovascular complications such as atherosclerosis is still present in diabetics when glucose levels are normalized, suggesting the involvement of

other mechanisms. Furthermore, endothelial dysfunction may precede the development of hyperglycemia in T2D and prediabetic states (Xu, 2009) suggesting that other factors contribute to the endothelial dysfunction observed in diabetes.

1.7.2 Insulin Resistance and Hyperinsulinemia

In humans, insulin resistance has been related to lower insulin receptor substrate-1 (IRS-1) expression. Individuals with lower IRS-1 have also been shown to have increased intimal thickening of their carotid arteries, which is used in clinical studies as a proxy for atherosclerosis in other vascular beds (Jansson, 2003). In mice, deletion of the insulin receptor and IRS-1 on the *ApoE(-/-)* background, has been shown to lead to increased atherosclerosis (Gleissner, 2007).

Insulin levels in the physiological range can enhance eNOS mRNA and protein activity by increasing serine 1177 phosphorylation by AKT, thus favoring vasodilation (Shahab, 2006). Insulin also activates Ras/mitogen-activated protein kinase (MAPK)–dependent pathways, leading to ET-1 production and the expression of adhesion molecules (Figure 1.9). In insulin resistant states, the PI3K-AKT arm of insulin-receptor signaling is impaired, but the MAPK signaling is not. Pathologically increased levels of insulin (hyperinsulinemia) over-activate the MAPK pathway thus shifting the balance toward vasoconstriction and monocyte adhesion (Figure 1.9). Insulin also activates the RAAS system by increasing the number of AT-I receptors, resulting in increased production of AT-II and further enhancing vasoconstriction (Shahab, 2006). Also, when increased levels of

insulin are being produced in efforts to overcome IR, increased levels of C peptide, a decomposition product of proinsulin, are produced. *In vitro* studies have shown that C-peptide is a chemoattractant for monocytes via a G-protein coupled receptor and phosphatidylinositol-3 kinase-dependent mechanism (Marx, 2004). It also induces SMC proliferation (Walcher, 2006) and colocalizes with macrophages in atherosclerotic lesions from diabetic patients (Marx, 2004).

Furthermore, $ONOO^-$ produced in the diabetic state inhibits AKT signaling in endothelial cells. $ONOO^-$ nitrosylates a critical tyrosine residue in the p85 regulatory subunit of PI3K, preventing its association with the catalytic p110 subunit and subsequent PI3K activation (Xu, 2009). $ONOO^-$ causes the nitrosylation of tyrosine residues in IRS-1, including Tyr939, a critical site needed for interaction with the p85 subunit of PI3K. Thus, $ONOO^-$ inhibits insulin receptor substrate-1 and PI3K activity which reduces downstream AKT activity (Nomiyama, 2004). It has also been proposed that $ONOO^-$ inhibits insulin signaling through the enhanced phosphorylation of phosphatase and tensin homologue deleted on chromosome 10 (PTEN), which inactivates pAKT (Song, 2007).

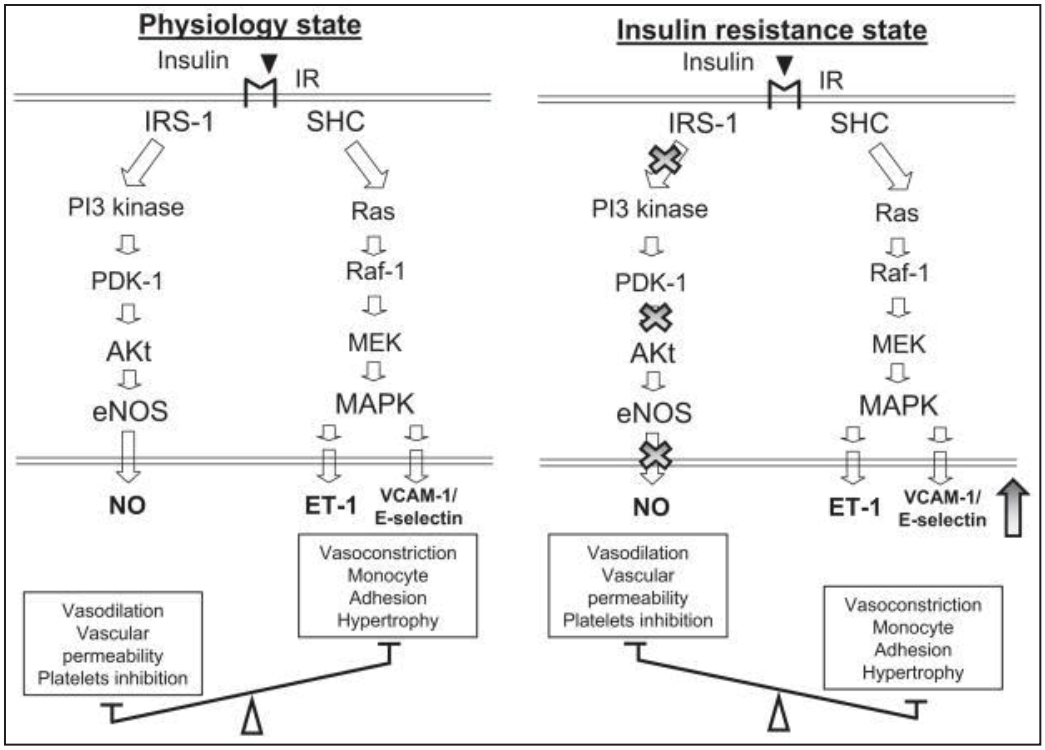

Figure 1.9. Endothelial insulin signaling in physiological and insulin resistant states. (Left) Insulin normally activates both PI3K/AKT and Ras/MAPK-dependent pathways favoring vasodilation and platelet inhibition. (Right) Insulin resistance leads to decreased activation of the PI3K/Akt pathway, while Ras/MAPK pathway signalling is unaffected. Hyperinsulinemia results in the over-activation of the Ras/MAPK pathway leading to enhanced vasoconstriction and pro-atherogenic mechanisms (from Xu, 2009)

1.7.3 Obesity

Roughly 80-85% of patients with T2D are overweight or obese (Gebel, 2012). Insulin resistance is closely linked to visceral adiposity. It was originally thought that the relationship between insulin resistance and obesity was due to the increase in circulating free fatty acids in the insulin resistant state. However, it is now also recognized that adipose tissue has important endocrine functions and produces adipokines, or adipose-specific cytokines, that influence other cell types and contribute to systemic IR. Mice with an adipocyte-specific knockout of GLUT4 develop insulin resistance in the liver and skeletal muscle suggesting that

adipocytes secrete factors that are capable of inducing insulin resistance in other organs (Kanda, 2006). Increased body fat leads to increased serum levels of TNF-α, interleukin-6, plasminogen activator inhibitor, resistin, and reduced expression of adiponectin (Hadi, 2007). In addition, adipokines released from fat may activate cytokines and transcription factors such as NFκB and JNK that lead to IR. Obese mice have increased adipocyte expression and secretion of MCP-1 and increased macrophage infiltration, suggesting a state of inflammation (Kanda, 2006). Overexpression of MCP-1 in adipocytes has also been shown to cause increased insulin resistance and hepatic steatosis (Kanda, 2006).

Adiponectin is an adipocyte specific protein that enhances insulin mediated glucose uptake and attenuates vascular inflammation (Hadi, 2007). Its levels are inversely related to degree of IR and inflammation, and its expression and secretion are reduced as fat mass increases (Hadi, 2007). Adiponectin reduces the adhesion of THP-1 monocytes and ICAM-1 expression in human coronary artery endothelial cells (HCAECs) (Ouchi, 1999). Overexpression of adiponectin in *ApoE(-/-)* mice reduces lesion size by 30% and lowers VCAM-1 mRNA abundance (Okamoto, 2002). In summary, obesity promotes vascular insulin resistance by the release of pro-inflammatory adipokines from adipose tissue accompanied by reduced expression of protective proteins such as adiponectin.

Normal insulin signaling in adipose tissue prevents the breakdown of fat into to free fatty acids. However, in insulin resistant states, lipolysis is not inhibited and increased free fatty acids are released into the circulation. FFAs

impair endothelial-mediated NO production and vasodilation by increasing oxidant stress and inflammation (Tripathy, 2003). In diabetes, the decrease in PI3K activation or the increase in reactive oxygen species due to FFA oxidation may impair NO bioavailability (Xu, 2009). There is increasing evidence that FFAs can activate receptors of inflammatory pathways in the vasculature such as the TLR4 receptor involved in innate immunity. In thoracic aorta lysates from mice with diet-induced obesity, NFκB activation and subsequent induction of inflammatory markers IL-6 and ICAM was observed, as well as reduced vascular insulin signaling (Kim, 2007). However, these effects were attenuated in TLR4 deficient mice. Similarly, *ex vivo* treatment of thoracic aorta and *in vitro* treatment of cultured cardiac microvascular ECs with palmitate mimicked the effects of HFD and activated inflammatory pathways, impaired insulin signaling, and reduced NO production, all of which were reduced in the absence of TLR4 (Kim, 2007). In addition to their effects on the vasculature, FFAs can induce islet cell apoptosis and enhance gluconeogenesis contributing to increased glucose levels and IR (Hadi, 2007).

Obesity also results in hyperlipidemia and an altered lipid profile that often precedes the onset of diabetes suggesting that dyslipidemia contributes to the pathogenesis of type II diabetes. Increased triglycerides and LDL cholesterol accompanied by reduced HDL cholesterol are characteristic of the atherogenic profile associated with diabetes. People with high levels of HDL cholesterol also display increased glucose tolerance (Kraus, 2002), and drugs that raise HDL cholesterol while lowering LDL cholesterol have been shown to reduce diabetes

among patients with coronary artery disease (Tenenbaum, 2004). Lipoproteins may be modified by oxidation, glycosylation, and glycoxidation resulting in increased oxidative stress and reactive oxygen species production that contribute to the inflammatory state of diabetes and promote endothelial dysfunction as previously described. Furthermore, oxidized LDL displaces eNOS from caveolae (invaginations of the endothelial cell membrane), which reduces eNOS activity (Blair, 1999). HDL reverses the ox-LDL-induced translocation of eNOS from caveolae and restores eNOS activity (Uittenbogaard, 2000).

Other hormones and peptides derived from adipose tissue such as leptin and apelin are implicated in the cardiovascular pathology of diabetes. Leptin is produced incrementally by adipose tissue, such that individuals with greater fat mass have higher leptin levels but are also more resistant to the satiety effects of leptin. Whether leptin plays a role in insulin resistance or is just an adaptation to increased fat mass is not known. The role of apelin in vascular pathology is also ambiguous. Smaller lesion size and reduced oxidative stress have been observed in *ApoE*(-/-) mice with inactive apelin receptors, implicating the involvement of apelin in atherogenesis (Hashimoto, 2007). The apelin receptor is expressed on a variety of cell types including endothelial cells, and its activation increases NO production by ECs and subsequent relaxation (Tatemoto, 2001). Apelin may also contribute to endothelial cell proliferation in angiogenesis (Masri, 2004).

1.7.4 Mitochondrial Dysfunction

Type II diabetic patients have decreased mitochondrial function. Mitochondrial number (Song, 2001) and Complex I activity correlate with decreased insulin-stimulated glucose disposal (Kelley, 2002). Furthermore, reduced expression of genes encoding enzymes with roles in oxidative metabolism and mitochondrial function has been detected in the skeletal muscle of diabetic patients (Patti, 2003). Interestingly, rates of substrate oxidation in the muscle of insulin-resistant offspring of type II diabetic patients has been shown to be reduced by 30% compared to control subjects (Befroy, 2007). Impaired mitochondrial activity causes impaired fatty acid metabolism leading to increased intracellular fatty acids. These fatty acids are converted to DAG, which activates PKCβ and δ and subsequently leads to the inhibitory serine phosphorylation of IRS-1, resulting in reduced glucose transport (Gleissner, 2007). In addition, mitochondrial dysfunction has been linked to eNOS uncoupling via proteosomal degradation of GTP cyclohydrolase I (GCH1, Sharma, 2012) and the generation of superoxide.

1.7.5 Inflammation

Diabetes has been described as an inflammatory condition marked by increased expression of C-reactive protein, TNF-α, IL-6, and PAI-1. Increased substrate overload promotes the inflammatory state by the increase in oxidative stress (Dandona, 2004). TNFα and IL-6 might also interfere with insulin action by suppressing insulin signal transduction and thus the anti-inflammatory effect of insulin (Dandona, 2004).

This chronic state of inflammation occurring in diabetes serves to activate endothelial cells to express adhesion molecules on their cell surface. Such adhesion molecules promote the adherence of circulating leukocytes to the vascular wall and include intracellular adhesion molecule (ICAM), vascular cell adhesion molecule (VCAM), platelet-endothelial cell adhesion molecule (PECAM), and P- and E-selectin. Lesion prone areas have been shown to display increased levels of VCAM-1 (Cybulsky, 1991). The absence of E- and P-selectins decrease atherosclerosis in *ApoE(-/-)* mice (Dong, 1998), while the deletion of ICAM has been shown to reduce monocyte recruitment. Inflammatory stimuli also induce the production of chemotactic molecules by the endothelial cells, such as monocyte chemotactic protein 1 (MCP-1), which recruits monocytes to the area via binding to the CCR-2 receptor (Glass, 2001).

1.8 Murine Models of Diabetes

Overgrowth of co-isolated, contaminating cell types has made long-term cultures of primary EC isolates a difficult task. For this reason, cloned, immortalized cell lines have been developed. However, transformed cells often loose expression of surface receptors and display altered cellular functions (Marelli-Berg, 2000). We have also found that primary endothelial cells isolated by FACS from mice display altered expression of endothelial markers such as vascular endothelial (VE)-cadherin, claudin-5, VEGF receptor 2, and PECAM. Most importantly, mono-culture of endothelial cells is a terrifically artificial environment lacking the hemodynamic stimuli, inter-cellular interactions, and hormonal influences of the intact, perfused, *in vivo* blood vessel. Responses of

ECs to cytokines such as TNF-α and IL-1β depends on whether they are grown in static or flow conditions (Luu, 2010). ECs cultured in static conditions display a different gene expression profile compared to cells freshly isolated from the vessel, and this differential expression is only partially reversed by exposure to flow, indicating that other locally derived factors contribute to EC phenotype (Luu, 2010). Furthermore, the choice of culture medium has been shown to influence inflammatory responses of the ECs. Therefore, we have chosen to perform our assessment of the endothelial response to diabetes using an *in vivo* murine model wherein diabetes is induced by a high-fat diet.

Several mouse models of diabetes created from genetic, chemical, or nutritional alterations exist, each with their advantages and limitations. Lep^{ob} and $Lepr^{db}$, mice have mutations in leptin or the leptin receptor, respectively, which are responsible for modulating satiety and energy expenditure. Such monogenic models of diabetes, while simulating many of the attributes of type II diabetes, are somewhat unrealistic as they do not address the heterogeneity observed in humans where polygenic mutations as well as environmental factors combine to cause diabetes (Ikegami, 2004). Although mutations in the leptin gene have been found to cause diabetes in humans, these instances are exceptionally rare.

Other spontaneous type 2 diabetic mouse models such as the Akita mouse, which has a mutation in the *Ins2* gene and therefore produces little mature insulin, develop characteristics of diabetes without becoming obese. Such models are useful for distinguishing those effects due to insulin resistance from those due to increased fat. However, weight gain is characteristic of T2D in

human patients, and adipose tissue is a major contributor of adipokines and hormones that contribute to metabolic derangement and insulin resistance. Other models that promote hyperlipidemia, such as apolipoprotein E and low-density liproprotein receptor deficient mice, are useful for studying the development and progression of atherosclerosis as these mice develop lesions upon high-fat feeding (Figure 1.10).

Although mostly used to generate type I diabetic models, chemical methods such as streptozotocin administration destroy beta cells and can be modulated to impair insulin production to create a type II model (Tahara, 2012 and Perez-Guiterez, 2012). However, the degree of diabetes obtained is variable, and undesired cytotoxic effects to other tissues may also occur. Knockout animal models of T2D target the insulin signaling pathway, insulin secretion, or hepatic glucose production. These knockout models are valuable for studying the effect of these specific genes on insulin resistance and insulin signaling pathways.

Finally, nutritional models of type II diabetes induced by feeding a high-fat diet provide a more authentic model of the pathophysiological response observed in the human population. These mice exhibit the characteristics of a patient developing metabolic syndrome, including increased weight gain, hyperglycemia, hyperinsulinemia, impaired glucose tolerance, and impaired response to insulin challenge. Since we are interested in the overall transcriptomic changes occurring in the endothelium as IR develops, we chose to use a high-fat diet model. This way, we are not selecting for particular attributes of diabetes; rather, we are assessing the endothelial response to the diabetic milieu as a whole.

However, this also means that individual responses of the endothelium cannot be definitively ascribed to one aspect of diabetes or another, such as those changes due to insulin resistance vs. hyperglycemia vs. weight gain, etc. However, we may be able to appropriately assign such changes based on our current understanding of endothelial cell biology and the effects of diabetes in other cell types.

1.8.1 Our Diabetic Mouse Model

We have chosen to use a high-fat diet to induce insulin resistance in our mice as previously described by Surwit et al. A high-fat diet has been shown to cause hyperglycemia, hyperinsulinemia, and obesity in C57BL/6 mice (Surwit, 1988) and these effects were not observed in mice fed high sucrose/low-fat diets (Surwit, 1995). The composition of the diet is presented in Table 1.2. The high-fat diet contains nearly 60% of its calories from fat, while the normal chow diet derives 60% of its calories from carbohydrates and only 12% of its calories from fat. In humans, dietary fat intake has been linked to diabetes. High fat diets also raise LDL cholesterol and increase LDL particle size compared to low-fat diets in human subjects (Guay, 2012).

Furthermore, the overall kilocalorie per gram of the HFD is 5.5 kcal/gm while the chow diet is 3.34 kcal/gm. Therefore, mice consuming equal quantities of the diet would receive more calories from the HFD than the chow diet, and this is further exacerbated by the fact that a high-fat diet induces hyperphagia in C57/BL6 mice (Surwit, 1995). Mice on a restrictive HFD where they consume an equal number of calories as mice fed a low-fat diet also develop obesity and

increased glucose levels, although these metabolic derangements were less extreme than the group fed HFD ad libitum (Petro, 2004). This intriguingly suggests that calories derived from fat are more diabetogenic than the same caloric intake from carbohydrates. While the oxidation of carbohydrates and protein is increased proportional to their intake, fat oxidation is decreased by increased energy intake vs. expenditure (Flatt, 1987), thereby leading to adipocyte hypertrophy and hyperplasia in C57BL/6 mice (Surwit, 1995).

Table 1.2 Composition of high-fat diet vs. chow diet.

Diet	Nutritional Component	Composition by Weight (%)	Calories (kcal/gm)	% Calories
High-Fat	Fat	36	3.2	59
	Carbohydrate	35.7	1.4	26
	Protein	20.5	0.8	15
	Total		5.5	
Chow	Fat	4.5	0.40	12
	Carbohydrate	49.9	2.0	60
	Protein	23.4	0.94	28
	Total		3.34	

Our model allows us to assess the transcriptional changes occurring in the endothelium as insulin resistance develops, and thus to determine the earliest responses of the vasculature to the diabetic milieu. We expect that these changes set the stage for further cardiovascular complications. When fed a high-

fat diet for periods of 8 weeks, these mice do not show staining with Oil Red O (Figure 1.10), which identifies esterified lipids in atherosclerotic plaques, particularly cholesterol ester (Hsueh, 2007). The ratio of heart weight to tibia length is not different between chow and HFD-fed mice nor are there any visible signs of fibrosis of the ventricular tissue when stained for collagen deposition. Thus, we are examining the cardiovascular system before any detectable evidence of the structural changes that accompany heart disease or vascular pathology.

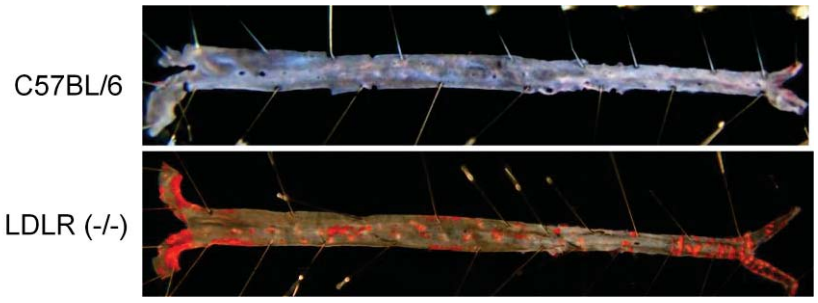

Figure 1.10. Wild-type mice fed a high-fat diet for 8 weeks do not develop atherosclerotic lesions. Aortae fixed in 4% paraformaldehyde were excised and freed of adherent fat. Lipids were stained with Oil Red O. For comparision, a hyperlipidemic *LDLR(-/-)* mouse fed a HFD for 12 weeks develop significant lesions (image from Y.Baumer).

1.8.2 Limitations of Using Mouse Models to Recapitulate Human Disease

The use of murine models has many advantages. The mouse genome was sequenced in 2002, and it revealed that approximately 99% of mouse genes have homologues in the human genome (Waterston, 2002). The sequence and function of many gene products are also highly conserved among the two

species and the disruption of a particular gene often causes similar pathologies in both species. These similarities, and our ability to introduce or remove genes of interest, make the mouse an excellent organism for studying human diseases. The genetic homogeneity of mouse models and their rapid reproduction and relatively inexpensive maintenance are also advantages. However, there are certain limitations when using mouse models to recapitulate human disease. There are some inherent differences between the metabolism and the pathology of diabetes in mice compared to humans. For example, humans and mice differ in their production of apolipoproteins B100 and B48, which causes differences in their circulating lipoprotein (Hinsdale, 2002). Humans carry 75% of their plasma cholesterol in the atherogenic LDL, while mice carry their cholesterol mostly on anti-atherogenic HDL (Meyrelles, 2011). Normal mice are resistant to atherogenesis (Meyerelles, 2011). Furthermore, glucose uptake in humans occurs mostly through the skeletal muscle, while in mice, glucose removal from the circulation occurs mostly through the liver. In addition, some genes found to be important in glucose uptake in humans are absent in mice.

Furthermore, the background mouse strain can influence phenotypes (Berglund, 2008). Indeed differences in the severity of insulin resistance have been observed in the *ob/ob* mouse on C57BL/6J background compared to FVB/N (Haluzik, 2004). *ApoE(-/-)* mice on the BALB/c background have higher levels of HDL cholesterol and lower levels of circulating inflammatory factors than *ApoE(-/-)* mice on the B6 background (Li, 2011). When fed a high-fat diet, *B6.ApoE(-/-)* mice display hyperglycemia and impaired glucose tolerance, while

BALB/c.ApoE(-/-) mice display increased islet area and a compensatory increase in insulin production that maintains normoglycemia (Li, 2011). Other studies have shown that the size and structure of the endocrine pancreas is dependent on genetic background (Li, 2011).

1.9 EC Heterogeneity

The structure and phenotype of the endothelial cell varies with vessel type. It is also influenced by the local environment created by other constituents of the vessel wall such as smooth muscle cells, fibroblasts, and matrix components. Growth factors and cytokines released from SMCs and fibroblasts have been shown to modulate inflammatory responses of the ECs (Luu, 2009). Different types of fibroblasts have been shown to elicit disparate effects on the ability of ECs to recruit lymphocytes (McGettrick, 2009). Various matrix proteins have been shown to be a determinant of endothelial response to the frictional forces of blood flow, known as shear stress (Orr, 2005). Finally, shear stress may also influence the interaction of ECs with the stromal cells as well as influence the phenotype and gene expression profile of endothelial cells (Chiu, 2003). The immediate endothelial response to shear stress is to increase intracellular Ca^{2+}, which enhances prostanoid synthesis and NO production leading to "flow-mediated" dilation (Cllifford, 2004). Diabetes reduces shear stress-induced dilation, in part by reducing eNOS phosphorylation and increasing its inhibitory nitrosylation (Huang, 2012). This reduced sensing alters arteriogenesis (Ruiter, 2010), and increased AGEs and ROS in diabetes contribute to decreased endothelium-mediated dilation in remodeled vessels (Vessieres, 2012). Shear

stress under high glucose conditions increases RAGE and inflammatory gene expression in human aortic endothelial cells in culture (Deverse, 2012). Hyperglycemia enhances shear-stress induced platelet activation in patients with type II diabetes (Gresele, 2003).

1.9.1 Macrovascular vs. Microvascular Responses

In the past, it was thought that microangiopathy, or damage of the microvessels, was a consequence of large vessel pathology. Today, we know that primary dysfunction of the microvasculature can be the source of many of the morbidities of cardiovascular and metabolic disorders (Weinspergner, 2012). Endothelial-dependent vasodilation in the microvasculature has been shown to be independent from endothelial-dependent dilation in the macrovasculature of rheumatoid arthritis patients (Sandoo, 2011). *In vitro* stimulation of different endothelial populations to the same stimulus have been shown to elicit heterogeneous responses (Luu, 2010). The heterogeneity of endothelial populations among the different vascular beds and even within the same vascular bed suggests that the responses of any one vascular bed may not be reflective of those of the entire circulatory system. In order to assess both the specific and common responses of both large vessels and the microvasculature to the diabetic state, we have performed gene expression analyses on the endothelium derived from two vascular beds, the aorta and the skeletal muscle.

We isolated ECs of the hind limb skeletal muscle in order to assess the response of the microvasculature to diabetes and to compare this response to that of the macrovasculature. Specifically, we isolated the calf muscles consisting

of the gastronemious, plantaris, soleus, and the rear thigh muscles collectively known as the biceps femoris (Fig. 1.11A). These muscles can be easily collected by gross dissection. The vasculature of the skeletal muscle is mostly composed of small arterioles and venules of capillary beds where oxygen and nutrient exchange between the blood and interstitial fluid occurs (Fig. 1.11B). However, feeding into these capillaries are larger arteries and veins as well. Therefore, the ECs isolated from the muscle are a heterogeneous mixture of arterial, venular, or lymphatic EC populations mostly derived from microvessels. To date, there are no acceptable antibodies to specifically isolate these EC subtypes, although the differential expression of a few genes have been identified (Ieronimakis, 2008).

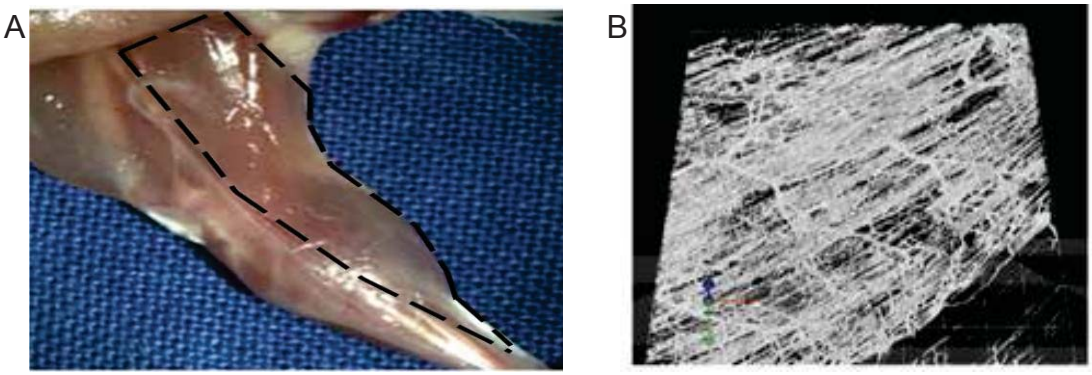

Figure 1.11 The skeletal muscle and its vasculature. (A) Grouping of gastronemious, plantaris, soleus, and biceps femoris muscles collected for analysis of skeletal muscle endothelium (adapted from Limbourg, 2009). (B) Vascular density of the gastronemius muscle revealed by imaging with the lipophilic carbocyanine dye DiI. Endothelial cells isolated from the skeletal muscle are mostly derived from capillary microvasculature (from Boden, 2012).

1.9.2 Unique Interactions of ECs within Skeletal Muscle

The endothelium of the skeletal muscle differs from that of the aorta because there is the added component of interaction with the skeletal muscle cells themselves. Skeletal muscle cells are capable of generating vasodilatory

substances such as prostaglandins, adenosine, and NO, which act in a paracrine manner with nearby ECs and SMCs (Figure 1.12). *In vitro* studies show that adenosine can enhance endothelial NO production by eNOS and it is also speculated to increase production of vasodilator prostaglandins in ECs (Clifford, 2004). NO produced by nNOS of the skeletal muscle may also indirectly enhance vasodilation by stimulating the release of vasodilatory prostaglandins from ECs via cyclooxygenase activation. In skeletal muscle endothelium, endotheial derived hyperpolarization factor (EDHF) is a metabolite of Cyp 2C, and it induces hyperpolarization of SMCs leading to the dilation of microvessels even in the presence of eNOS and COX inhibitors (Clifford, 2004).

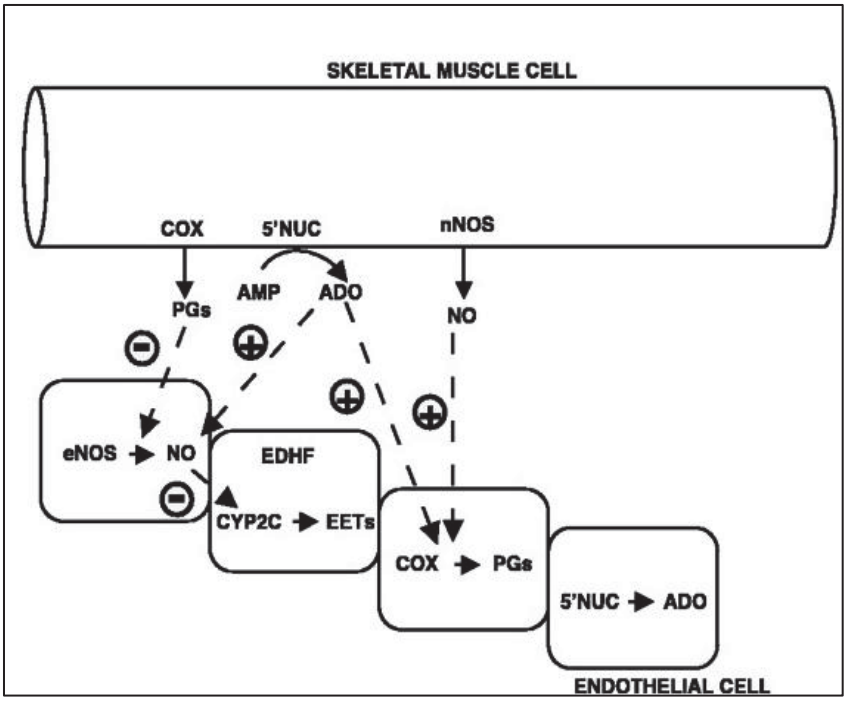

Figure 1.12. The influence of skeletal muscle on endothelial function. Adenosine (ADO), prostaglandins (PG), and nitric oxide (NO) produced by skeletal muscle cells induce vasoactive responses from endothelial cells (from Clifford, 2004).

Another consideration when dealing with capillary beds is the effect that the different endothelial populations may have on each other. For example, during exercise, the arteriolar oxygen saturation does not change but the venous pO_2 may decrease causing venular ECs to release substances that dilate nearby arterioles (Clifford, 2004). Furthermore, RBCs experiencing hemoglobin deoxygenation or mechanical deformation as they pass through the capillaries may release ATP into the circulation. ATP activates P_{2Y} purinergic receptors on the EC surface leading to the production of NO, prostaglandins, and EDHF vasodilators (Clifford, 2004). RBCs may also release NO when it binds to hemoglobin to form nitrosohemoglobin and is then released in the off-loading of oxygen. NO may also be produced by the reduction of nitrite in the blood by deoxygenated hemoglobin. These unique interactions of the capillary endothelium may lead to different responses of the microvasculature to diabetic stimuli compared to that of the macrovasculature. We therefore arranged to study the responses of both endothelial cell populations in order to gain understanding of the commonly and differentially regulated pathways occurring in the diabetic macro- and microvasculature.

1.10 Summary

The endothelium is a complex organ that responds to signals from the blood compartment and the underlying vessel wall. Under physiological conditions, the endothelium is anti-atherogenic, anti-inflammatory, and maintains proper perfusion of the tissues by balancing vasodilatory and vasoconstrictive factors. However, when the endothelium becomes damaged due to injury or

exposure to pathophysiological conditions, such as diabetes, it becomes dysfunctional, shifting the balance toward vasoconstriction, atherogenesis, thrombosis, and inflammation. In diabetes, metabolic derangement results in the activation of pathways that adversely affect endothelial cell function. This leads to an increased frequency of cardiovascular complications in diabetic patients.

To better understand the response of the endothelium to the diabetic state we have compared the transcriptional profiles of two vascular endothelial cell populations in diabetic and normal mice. The changes that occur in the endothelium are difficult to assess in cell culture. This is compounded by the heterogeneity that exists across vascular beds and even within the same vascular bed. Therefore, these studies have been carried out using an *in vivo* model created by a high-fat diet, which recapitulates the endocrine responses observed in diabetic humans. In Chapter 2, we report our comparison of mRNA abundance in diabetic vs. control endothelium to develop potential mechanisms for the enhanced susceptibility of diabetic endothelium to atherosclerosis. We also compare the responses of the aortic endothelium to skeletal muscle endothelium to gain insight into the pathogenesis of macrovascular vs. microvascular disease.

From these analyses we have identified a number of differentially regulated transcripts with roles in inflammation, insulin sensitivity, oxidative stress, and atherosclerosis. One such transcript, galectin-3, was found dysregulated in both vascular beds indicating its potential as a universal marker of the diabetic vascular response. The LGALS3 protein was also dysregulated in

both endothelial cells and the serum of diabetic mice. The exploration of the role of galectin-3 is the focus of Chapter 3, where similar studies were carried out comparing the endocrine responses and endothelial transcriptional responses of galectin-3 deficient mice to that of wild-type mice. These studies were performed in order to identify possible mechanisms for the involvement of galectin-3 in diabetic vasculopathy.

Chapter 2: Transcriptional Analysis of the Endothelial Response to Diabetes Reveals a Role for Galectin-3

2.1 Abstract

To characterize the endothelial dysfunction associated with type II diabetes, we surveyed transcriptional responses in the vascular endothelia of mice receiving a diabetogenic, high-fat diet. Tie2-GFP mice were fed a diet containing 60% fat-calories (HFD); controls were littermates fed normal chow. Following 4, 6, and 8 weeks, aortic and leg muscle tissues were enzymatically dispersed, and endothelial cells were obtained by FACS. Relative mRNA abundance in HFD vs. control endothelia was measured with long-oligo microarrays; highly dysregulated genes were confirmed by real-time PCR and protein quantification. HFD mice were hyperglycemic by 2 weeks and displayed vascular insulin resistance and decreased glucose tolerance by 5 and 6 weeks, respectively. Endothelial transcripts upregulated by HFD include galectin-3 (*Lgals3*), 5-lipoxygenase-activating protein, and chemokine ligands 8 and 9. Increased LGALS3 protein was detected in muscle endothelium by immunohistology accompanied by elevated LGALS3 in the serum of HFD mice. Our comprehensive analysis of the endothelial transcriptional response in a model of type II diabetes reveals novel regulation of transcripts with roles in inflammation, insulin sensitivity, oxidative stress, and atherosclerosis. Increased endothelial expression and elevated humoral levels of LGALS3 supports a role

for this molecule in the vascular response to diabetes, and its potential as a direct biomarker for the inflammatory state in diabetes.

2.2 Background

Type II diabetes is associated with increased atherosclerosis, retinopathy, skin ulceration, and other vascular-related diseases, all of which may involve damaged or dysfunctional endothelium. A major consequence of diabetes is endothelial exposure to elevated glucose and fatty acids, leading to eNOS uncoupling and subsequent generation of reactive oxygen and nitrogen species (Zou, 2004) as well as the formation of advanced glycation end-products (AGEs) (Zieman, 2004). Furthermore, hyperinsulinemia and other hormonal changes can alter endothelial signaling pathways. These changes may promote inflammation, impair vasoregulation, disrupt hemostasis, and inhibit reverse cholesterol transport (Bakker, 2009 and Potenza, 2009). By examining the transcriptional changes that occur in both the micro- and macrovascular endothelium of mice exposed to a dietary model of type II diabetes, we expect to gain further insight into the underlying mechanisms of the endothelial dysfunction characteristic of diabetes and the metabolic syndrome.

Transcriptomic analysis has been used to examine the responses of cultured endothelium exposed to high glucose and insulin (Hiden, 2006 and Zhou, 2005). However, an *in vitro* analysis may only partially reflect the complex *in vivo* state, where numerous hormonal, metabolic, and cellular perturbations combine to influence the endothelial cell. *In vivo* analysis of aortic endothelium from mice exposed to a type I, insulin deficient, model of diabetes revealed

dysregulation of transcripts involved in inflammation and insulin sensitivity (Maresh, 2004). Here, we study mice rendered diabetic by a high-fat diet and comprehensively evaluate arterial as well as capillary endothelial transcriptional responses in a model of type II, insulin resistant, diabetes.

For this purpose, we utilize transgenic mice expressing GFP under the endothelial specific *Tie2* promotor (Tie2-GFP). By selecting our endothelial cell population based on GFP expression as well as CD31 surface staining, we achieve a high degree of purity of the analyzed cells, assuring that our results represent transcriptional changes specifically in the diabetic endothelium. TIE2 is the tyrosine kinase receptor for angiopoietin, and is important in the regulation of vascular network formation and remodeling, or vasculogenesis and angiogenesis. It is specifically expressed in vascular endothelial cells. TIE2 expression occurs as soon as the first ECs arrive during the late primitive streak stage of development. It is detectable in the endothelial cells of all adult organs.

The first reporter gene construct created in the lab of Thomas Sato consisted of a 2.1kb region of the *Tie2* promoter followed by the *LacZ* reporter gene and SV40 poly(A) signal sequence (Schlaeger, 1997). This construct was insufficient to promote *LacZ* expression in endothelial cells beyond late gestation thereby indicating the need for other cis acting regulatory elements. A 1.7kb fragment within the first intron of the *Tie2* gene was identified as the enhancer element that confers EC-specific expression. This region, especially the 303bp core enhancer, contained binding sites for general and tissue specific transcription factors such as ETS1, basic domain leucine-zipper (bZIP), CP2-γ,

and PEA3 as well as other transcription factors known to regulate tissue remodeling and endothelial specific genes such as eNOS and vWF (Schlaeger, 1997).

To generate Tie2-GFP transgenic mice, the promoter/enhancer elements were fused to green fluorescent protein cDNA, which is derived from the jellyfish *Aequorea victoria.* This protein consists of a beta-barrel structure surrounding a chromophoric unit formed by Ser-Tyr-Gly residues. When excited at a wavelength of 488nm, the chromophore will emit light at a peak wavelength of 508nm (Figure 2.1A). Thus, endothelial cells of any tissue of the Tie2-GFP mouse are visible under the fluorescent microscope, as shown in Figure 2.1B, and we have exploited these fluorescent properties to isolate them by FACS.

2.3 Methods

2.3.1 Animals and Diet

Mice homozygous for the Tie2-green fluorescent protein (GFP) transgene [Tg(TIE2GFP)287Sato, stock no. 003658 Jackson Laboratories (Bar Harbor, ME)] were bred for these experiments. Beginning at 8 weeks of age, male mice were allowed to feed ad libitum on a high-fat diet (HFD) containing 60% fat calories (BioServ, Frenchtown, NJ, cat. no. S3282) for a period of 4, 6, or 8 weeks. Littermates fed a normal chow diet containing 12% fat calories (LabDiet, St. Louis, MO, cat. no. 5001) served as controls. All procedures were approved by the Institutional Animal Care and Use Committee of the University of Hawaii.

2.3.2 Assessment of Metabolic Characteristics

2.3.2.1 Fasting Glucose Levels and Glucose Tolerance Test

Before the start of the study and after 2, 4, 6, and 8 weeks on their respective diets, glucose levels were determined by glucometry of the tail blood following an overnight fast (OneTouch Ultra, Lifescan, Milpitas, CA). A glucose tolerance test (GTT) was performed after 6 weeks on the diet regimen. Glucose (1 mg/g of body weight) was administered i.p. following an overnight fast. Glucometry of the tail blood was performed prior to glucose injection and every 20 minutes afterwards for 2 hrs. The area under the curve (AUC) was determined using the statistical software in Graphpad.

2.3.2.2 Determination of Serum Insulin Levels

Two hundred µL of blood was collected from the tail vein, allowed to clot, and centrifuged at 5000rpm for 10 min to separate serum. Following an overnight fast, serum insulin levels were measured at 3, 6, and 8 weeks by ELISA (Mercodia, Uppsala, Sweden, cat. no. 10-1149-01). The homeostasis model assessment of insulin resistance (HOMA-IR) was calculated using the fasting glucose and insulin concentrations using the following formula: [fasting blood glucose (mg/dL) x fasting insulin (µIU/mL)] / 405 (Akagiri, 2008), where 1mg insulin= 26IU (Bristow, 1988).

2.3.2.3 Measurement of Vascular Insulin Resistance

Following 5 weeks on the diet, 6 control and 6 high-fat fed mice received an i.p. injection of insulin (0.06 U/g body weight in 300µL of sterile saline); 2-3 animals of each group received vehicle (normal saline). Mice were sacrificed 15

minutes after injection. The thoracic aorta was excised, dissected from adherent fat, and snap frozen in liquid nitrogen. Protein was subsequently extracted from the tissue and phospho-AKT (serine 473) levels were determined by ELISA (R&D Systems, Minneapolis, MN, cat. no. DYC887-2) and normalized to total protein concentration.

2.3.3 Endothelial Cell Isolation

Following 4, 6, or 8 weeks on the diet regimen, animals were sacrificed by CO_2 asphyxiation. In each experiment, pooled cells from 3 experimental and 3 control mice were collected for each tissue. Aortae from the aortic root to the iliac bifurcation were dissected. Leg muscles consisting of the plantaris, gastronemius, and biceps femoris (which are readily dissected as a single group) were excised. Tissues were placed into ice cold PBS and freed of adherent fat. The aortic and skeletal muscle tissues from 3 animals were each pooled, minced into 1 mm fragments, and dispersed as previously described (Maresh, 2004 and Maresh, 2008). Suspensions of collagenolytically separated cells were incubated with anti-mouse CD16/32 (1:500) for 5 min and then with phycoerythrin-conjugated anti-mouse CD31 (1:200) for 25 minutes on ice (eBiosciences, San Diego, CA, cat. nos. 14-0161 and 12-0311). Ten thousand endothelial cells positive for both GFP and phycoerythrin staining were isolated with a FACSAria (Becton Dickinson, Franklin Lakes, NJ) directly into Trizol (Invitrogen, Carlsbad, CA). RNA was purified with RNeasy columns (Qiagen, Valencia, CA) and subsequently amplified using an Ambion® Amino Allyl MessageAmp kit (Life

Technologies, Carlsbad, CA) according to the manufacturer's protocol to produce approximately 100µg of amino-allyl modified cRNA.

2.3.4 Confirmation of Endothelial Cell Identity and Assessment of Monocyte Contamination

2.3.4.1 Flow Cytometry Analysis of Peripheral Blood Mononuclear Cells (PBMCs)

Approximately 200µl of blood was collected from the retro-orbital vein into EDTA-coated tubes. RBCs were lysed for 15min at RT using a 1:10 dilution of lysis buffer (BD Biosciences, San Jose, CA, cat. no. 555899) and centrifuged at 1300rpm for 5min. Lysis was repeated for an additional 5min at RT followed by centrifugation. The cell pellet was reuspended in 200 µl of Hanks complete media, transferred to a 96 well plate, and centrifuged. The pellet was stained for 20min at 4°C with 50 µl of antibody cocktail containing 0.5 µl each of PE-CD115 (eBiosciences, cat. no. 12-1152), PerCP-Cy5.5 CD11b (BD Biosciences, cat. no. 550993), APC-Cy7 CD45 (BD Biosciences, cat. no. 557659), and PE-Cy7 CD31 (eBiosciences, cat. no. 25-0311) diluted in a 1:1 solution of Hanks:FACS staining buffer (1.7% BSA, 0.02% mouse serum, 0.02% rabbit serum, and 0.02% human serum). After washing in Hanks complete, samples were fixed for 20 min at RT in a 1:1 solution of Hanks:fixation buffer (BioLegend, San Diego, CA, cat. no. 420801). Cells were then permeabilized with 0.5% saponin diluted in Hanks for 10min at RT. Samples were stained with a 1:100 dilution of Alexa Fluor®647-Lgals3 antibody (BioLegend, cat. no. 125407) for 25 min at 4°C followed by washing and resuspension in Hanks. $CD45^+$ leukocytes, $CD45^+/CD11b^+$ myeloid

cells, and $CD45^+/CD11b^+/CD115^+$ monocytes were analyzed for GFP^+ signal using FlowJo software (Tree Star, Inc., Ashland, OR).

2.3.4.2 Staining of Endothelial Populations for Monocyte Markers

Endothelial cells were isolated as previously described and stained for 25 min at 4ºC with Alexa Fluor ®647 anti-mouse CD11b (eBiosciences, cat. no. 51-0112). The sorting gates for the GFP^+ endothelial cells were applied, and the number of GFP^+ and $CD11b^+$ events within that gate were analyzed using FlowJo software.

2.3.4.3 Matrigel Tube Formation and Dil-Ac-LDL Uptake Assays

GFP^+, sorted endothelial cells from the skeletal muscle were plated in 48-well plates coated with Matrigel™ Basement Membrane Matrix (BD Biosciences, 354234), at 8,000 cells/well, in Endothelial Cell Growth Medium MV with supplement mix (PromoCell, Heidelberg, Germany, cat. no. C-22020). After 5 days, tube formation was assessed. For Dil-Ac-LDL uptake assays, the sorted ECs were plated on Nunc® Lab-Tek® 8-well chamber slides (Thermo Scientific, Bellerica, MA, cat. no. 154941) and incubated with 50µg/mL Dil-Ac-LDL (Biomedical Technologies Inc., Stoughton, MA, cat. no. BT-902) for 4 hours, washed, fixed with 2% PFA, stained with DAPI, and imaged using the Axiophot system (Zeiss, Oberkochen, Germany).

2.3.5 Gene Expression Analysis

2.3.5.1 Microarray Analysis

Microarray analyses were performed to determine the transcriptional responses in aortic and skeletal muscle endothelium from mice exposed to high-

fat diet vs. control diet for 4-, 6-, and 8-weeks. Amino-allyl modified cRNA was labeled with Cy3 and Cy5 CyDye™ Post-Labeling Reactive Dye Pack (GE Healthcare, Waukesha, WI) according to the manufacturer's instructions. Following purification, 200 pmoles of Cy3 and Cy5 dye-labeled cRNA, as measured by NanoDrop 2000c spectrophotometer (Thermo Scientific), were combined and fragmented with Ambion 10X fragmentation reagents at 70ºC for 15min. Yeast tRNA (4 µg), polyA RNA (4 µg), mouse cot-1 DNA (1 µg), and Slidehyb III hybridization buffer (Ambion) were added for a total sample volume of 35µL. In general, biological replicate experiments were performed for each time-point for both tissues. For each of the two biological replicate experiments, two array hybridizations were performed, each of which included a dye reversal. Samples were hybridized overnight to glass slides spotted with the Operon Murine V4 oligo set produced by the Duke University Microarray Core. Arrays were scanned using a Genepix 4000B® (Molecular Devices, Union City, CA) system and analyzed with Genepix® and Acuity® software.

Statistical analysis of microarray results was performed using the functions available within Acuity®. Results were normalized using the ratio of medians method and filtered to exclude any exhibiting the following characteristics: a percentage of saturated pixels >3, a signal/noise ratio <3, a (regression ratio 635/532)^2 <0.6, or a Genepix flag. Transcripts exhibiting upregulation (a $\log_2$[fold change] >0.7) or downregulation ($\log_2$[fold change] <-0.7) that were found consistently dysregulated at 4, 6, and 8 weeks were tabulated for each tissue. (A $\log_2$ fold-change of 0.7 corresponds to 1.6-fold on

the linear scale). The one sample *t*-test function within Acuity® was then applied to the results to calculate *P*-values for each experiment ($n_{biological}$= 2, $n_{microarray}$= 4).

2.3.5.2 Pathway Analysis

The gene expression data was further interrogated using Database for Annotation, Visualization and Integrated Discovery (DAVID) (Huang, 2009a and 2009b) and Ingenuity Pathway Analysis (IPA) (Ingenuity® Systems, www.ingenuity.com). Datasets consisting of all transcripts differentially expressed >0.5 log_2[fold change] with a *P*-value <0.1 were uploaded into these programs. Enriched molecular functions based on Gene Ontology (GO) terms for the aortic and muscle endothelium after 4, 6, or 8 weeks of HFD were identified by DAVID. Molecular functions enriched in the endothelium after HFD for each tissue were determined based on transcripts differentially expressed >0.5 log_2[fold change] at 4,6, and 8 weeks in aortic endothelium or at both 6 and 8 weeks in the muscle endothelium.

Transcripts displaying >0.5 log_2[fold change] dysregulation and $P < 0.1$ following 4,6, or 8 weeks of high-fat feeding in the aortic endothelium or 6 or 8 weeks of HFD in skeletal muscle endothelium were analyzed by IPA. Overrepresented Biological Functions in the endothelium of each tissue at each timepoint were identified based on weighted gene co-expression. Enriched Canonical Pathways in the aortic or skeletal muscle endothelium after 8 weeks of HFD were also identified by analysis of transcripts displaying >0.5 log_2[fold change] upregulation and $P < 0.1$ by 8 weeks of HFD.

2.3.5.3 Real-time PCR

Microarray results were confirmed by semi-quantitative real-time polymerase chain reaction (RT-PCR or qPCR) performed on 3-4 biological replicate experiments. Complementary DNA was synthesized by the reverse transcription of 1µg of amplified RNA from the sorted endothelial cells using qScript (Quanta Biosciences, Gaithersburg, MD). Oligonucleotide primers were designed to generate amplicons of length 100-200 nucleotides and to span at least one intron. Primer sequences are listed in Supplement Table SI. cDNA representing 5 ng of total RNA was amplified by PCR performed using SYBR® green fluorophore (Roche, Indianapolis, IN) in an Applied Biosystems® 7900HT fast real-time PCR system. A standard two-phase reaction (95°C 15sec, 60°C 1 min) worked for all amplifications. Dissociation curves run for each reaction verified the presence of a single amplicon peak, and a single, amplified product of the expected size was confirmed by gel electrophoresis. Amplicons were also sequenced by 3730XL DNA Analyzer (Applied Biosystems), and BLAST was used to verify the alignment of the amplicon sequence with that of the target transcript (Appendix Table 1).

The expression level for each gene was interpolated from a standard curve of serial dilutions at cycle times where C_T, the threshold intensity, was exceeded. The abundance of Cyclophilin A was assessed in parallel as a loading control to which the genes of interest were normalized. Fold changes represent the ratio of diabetic to control expression values. Statistical analyses were

performed using the one sample *t*-test function in Analyse-It® software for Microsoft Excel. A *P*-value less than 0.05 was considered significant.

2.3.6 Galectin-3 Protein Confirmation

2.3.6.1 Immunofluorescence of Endothelial Cells

GFP^+ endothelial cells from the leg muscles of 3 mice receiving HFD and 3 receiving control diet for 8 weeks were isolated by FACS and sorted into tissue culture medium. Aliquots containing 1000 cells were deposited onto lysine coated slides by centrifugation at 450 rpm for 5 minutes with a Cytospin (Shandon). Cells were fixed in 10% formalin, permeabilized with 0.1% Triton X100 and incubated with rat anti-galectin-3 (Santa Cruz Biotechnology, Santa Cruz, CA, cat. no. sc-23938) at 1:100 followed by Alexa Fluor®568 goat anti-rat IgG (Invitrogen) at 1:800. Images were collected under controlled exposure and gain settings with an Axiophot system (Zeiss).

2.3.6.2 Circulating Galectin-3 Levels in Serum

Quantification of galectin-3 in the serum of mice after 4, 6, and 8 weeks on the diet following an overnight fast was performed using the Mouse Galectin-3 Duoset ELISA Development Kit (R&D Systems, cat. no. DY1197).

2.4 Results

2.4.1 The effect of HFD on metabolic parameters

As shown in Table 2.I, controlled exposure of Tie2-GFP mice to HFD resulted in the expected metabolic changes associated with diabetes, including accelerated weight gain as well as hyperglycemia by 2 weeks. These responses

were accompanied by marked hyperinsulinemia by 3 weeks (Table 2.I) and an increased HOMA-IR index by 3 weeks (Figure 2.2A). In addition, exposure to HFD for 5 weeks resulted in a reduced vascular response to insulin as reflected in attenuation of aortic AKT phosphorylation following an *in vivo* insulin challenge (Figure 2.2B). Furthermore, glucose tolerance was impaired in mice exposed to a HFD vs. control diet (Figure 2.2C, D).

2.4.2 Endothelial Cell Isolation & Confirmation of Endothelial Identity

FACS yielded at least 10,000 $GFP^+/CD31^+$ cells from each pooled tissue sample. All GFP^+ cells also exhibited phycoerythrin staining (Fig. 2.3A). $GFP^+/CD31^+$ cell populations represented approximately 2.5% and 1.5% of the total population of cells derived from muscle and aortic tissue, respectively. The ability of the sorted cells to take up fluorescent labeled acetylated-LDL and form tubes on Matrigel^{TM} further confirmed their endothelial identity (Figure 2.3B, C).

Tie2-expressing myeloid cells have been reported to account for 2-7% of human blood mononuclear cells (Venneri, 2007). Furthermore, in diabetes, there exists a state of inflammation characterized by an increase in activated monocytes in the peripheral blood of diabetic patients (Mastej, 2006). We therefore performed flow analysis of peripheral blood mononuclear cells to determine the contribution of these Tie2-expressing myeloid cells to our sorted endothelial populations. After 8 weeks of HFD, no significant increase in the total $CD11b^+/CD115^+$ inflammatory monocyte population was observed (9 $\pm$ 2% of $CD45^+$ leukocytes in chow-fed mice vs. 11 $\pm$ 3% in HFD mice). We then went on

to investigate whether the number of monocytes appearing to have a positive signal for GFP was altered by HFD. Our analysis has shown the percentage of $CD11b^+/GFP^+$ myeloid cells after 6 weeks of HFD to be 0.19 ± 0.04% vs. 0.21 ± 0.07 % in controls, and after 8 weeks of HFD to be 0.5±0.5% vs. 0.3±.4% in controls *(n*=3, Figure 2.4B). Furthermore, analysis of the specific inflammatory monocyte population described to express TIE2, revealed that only 0.8% of this $CD45^+/CD11b^+/CD115^+$ population express TIE2 in blood cell suspensions derived from both HFD and control fed animals (0.8±0.5% vs. 0.8±0.3%, *n*=3). In addition, the intensity of the GFP signal of these monocytes is much less than that of the endothelial cell population that we are sorting and would therefore be excluded by our gating.

Most importantly, FACS of muscle tissue suspensions from 3 independent experiments following 8 weeks of diet revealed that only 0.8 ± 0.4% of GFP^+ cells derived from HFD animals also displayed the monocyte marker CD11b with similar low percentages observed in control animals (0.3 ± 0.5%, Figure 2.4A). Therefore, myeloid cells are not contributing substantially or unequally to our 2 pools of sorted cells derived from chow-fed or HFD-fed mice, and we can be confident in the purity of our sorted endothelial population.

2.4.3 Microarray Results

Microarray hybridization data are available in the Gene Expression Omnibus database under series record GSE14898. Tables 2.2A (aortic) and 2.2B (muscle) display fold-change of transcripts with $|\log_2[\text{fold change}] > 0.7$ at all timepoints in aorta or by 6 or 8 weeks of feeding in the muscle in biologically

replicate, dye-reversed hybridization experiments. Dysregulated transcripts common to both aortic and muscle endothelium are presented in Table 2.2C.

2.4.4 Pathway Analysis

Insights into the endothelial systems biology occurring in diabetes were extracted from the datasets by applying DAVID and IPA. DAVID was used to identify over-represented molecular functions based on gene ontology terms derived from the lists of differentially regulated transcripts in aortic and muscle endothelia (Table 2.3). IPA was also used to identify over-represented biological functions and canonical pathways based on weighted gene co-expression. Biological functions over-represented during the time course of the feeding and canonical pathways upregulated by 8 weeks of feeding in the aortic and muscle endothelium are shown in Figures 2.5 and 2.6, respectively. These analyses further reveal the pathways and biology that are shared between the macro- and microvasculature as well as those that are specific to each vascular bed.

2.4.5 Real-Time PCR

The expression levels of highly dysregulated transcripts were confirmed by real-time PCR. These genes include galectin-3 (*Lgals3*), C-C chemokines 8 and 9 (*Ccl8*, *Ccl9*), 5-lipoxygenase-activating protein (*Alox5ap*), and ferritin light chain 1 (*Ftl1*). The real-time PCR expression levels of the cDNA transcribed from the cRNA were found to be consistent among biological replicates and in concordance with the microarray data (Figure 2.7).

2.4.6 Increased Levels of Galectin-3 Protein Detected in Endothelia and Sera Upon HFD

In order to determine if the increase in galectin-3 mRNA levels led to elevated galectin-3 protein, immunofluorescence staining for LGALS3 was performed on endothelial cells isolated from skeletal muscle. After 8 weeks, the fluorescent signal for intracellular LGALS3 protein was greater in the muscle endothelium of mice on a HFD compared to controls. Representative images of LGALS3 staining are shown in Figure 2.8.

Galectin-3 is a secreted protein normally present in the serum; we therefore evaluated levels of circulating galectin-3. On average, mice receiving a high-fat diet had more galectin-3 in their serum than mice on the control diet (Figure 2.9A). Although there was a broad range of galectin-3 levels among high-fat-fed mice, average levels are 2 to 3-fold higher in the HFD mice after 6 weeks (104.7 $\pm$ 17.1 ng/mL vs. 38.9 $\pm$ 2.9 ng/mL, $P < 0.005$) and 8 weeks (90.7 $\pm$ 12.3 ng/mL vs. 34.4 $\pm$ 3.4 ng/mL, $P<0.001$) on the diet (Figure 2.9A). Furthermore, serum galectin-3 levels correlated well with HOMA-IR after 8 weeks of feeding, exhibiting a Pearson correlation coefficient of 0.92 ($P < 0.0001$, Figure 2.9B).

2.5 Discussion

In the study described in this chapter, we performed a controlled, comprehensive survey of the transcriptional responses of the endothelium *in vivo* to a model of Type II diabetes induced by a HFD in Tie2-GFP mice. Our mouse model recapitulates clinical diabetes, which is characterized by weight gain, hyperglycemia, hyperinsulemia, and insulin resistance. It is likely that the

endothelial dysfunction observed in diabetic patients is a result of the combinatorial effect of these metabolic and hormonal derangements. Our study was not designed to distinguish endothelial responses to any single diabetic change; rather, our analysis integrates all of the diabetic influences on the endothelium, allowing our assessment to be more physiologically relevant than *in vitro* studies looking at isolated components of the diabetic milieu.

We have confirmed the purity of our sorted endothelial populations by several methods. All of our sorted GFP^+ cells also stained positive for CD31 as determined by flow cytometry (Fig. 2.3A), and GFP fluorescence of sorted cells has been confirmed by fluorescence microscopy (Fig. 2.8). FACS analysis of the PBMCs derived from HFD- or chow- fed mice shows a negligible number of GFP positive monocytes (Fig. 2.4B). Importantly, the sorted endothelial population showed very low expression of the monocyte marker CD11b with similar low percentages observed in HFD- and chow-fed animals (Fig. 2.4A). Furthermore, these cells display the endothelial-specific ability to form tubes when plated on Matrigel™ and also take up fluorescent DiI-Ac-LDL, further confirming their endothelial identity. Furthermore, the transcriptional profiles of the sorted cells show much higher fluorescence signal for endothelial markers such as von Willebrand factor, eNOS, claudin 5, VCAM and ICAM, with much lower signal for features of leukocytes such as CD45, CD11b, and CD115, suggesting little contamination from other cell types (Appendix Figure 1). Thus, we conclude that our sorting technique achieves a highly pure population of endothelial cells,

which enhances our confidence in the gene expression data we derive from these cells.

Our assessment of the endothelial response in both aorta and skeletal muscle addressed the diversity of endothelial cell populations (Ho, 2003) and may thus reflect distinct endothelial contributions to microvascular and macrovascular disease (Cade, 2008). In the present study, we observed a greater response to diet-induced diabetes in the aortic endothelium compared to that of skeletal muscle, as evidenced by both the amount and onset of dysregulation: we identified 36 transcripts with greater than 1.5 $\log_2$ fold-change in the large vessel endothelium by 4 weeks whereas the capillary endothelium of the muscle had only 16 transcripts dysregulated to this degree, and in general, only after 8 weeks of HFD (Table 2.2B). This difference in susceptibility to transcriptional regulation may represent the foundation for the physiological findings of Kim *et al.*, who observed an earlier onset of vascular vs. peripheral insulin resistance in response to a high-fat diet (Kim, 2008).

Exploration of the enhanced biological pathways by DAVID and IPA detects commonalities and differences between the macrovascular and microvascular transcriptional response. Highly upregulated pathways in the aortic endothelium include those related to signaling, including chemokines, PLC signaling, and signaling events that precede atherosclerosis (Fig. 2.6, Table 2.3). Interestingly, by 8 weeks of HFD, the liver X receptor/retinoic X receptor (LXR/RXR) activation pathway was significantly upregulated in the aortic endothelium (Fig. 2.6). These receptors have been shown to modulate the

expression of genes involved in lipid metabolism in human endothelial cells *in vitro* (Norata, 2005). Our findings implicate this pathway in the endothelial transcriptional response to an *in vivo* model of type 2 diabetes, and suggest that LXR/RXR agonists may serve a role in modulating lipid metabolism in the macrovasculature. In the microvasculature of the muscle, we observed upregulation of pathways involved in cytoskeletal rearrangements as well as glycolysis and lipid biosynthesis (Fig. 2.6). Biological functions such as molecular transport and cellular compromise are over-represented, including molecules with roles in oxidative stress and cell damage (Fig. 2.5). Other pathways, such as glycerolipid metabolism, and biological functions such as cell-to-cell signaling and interaction and small molecule biochemistry, are shared by the two vascular beds (Figs. 2.5 and 2.6).

Our comprehensive analysis of the transcriptional response of the endothelium to diet-induced diabetes has identified the dysregulation of genes with recognized roles in atherosclerosis, hyperglycemia, insulin resistance, and inflammation, as well as novel transcripts with previously unknown associations with diabetes. Chemokine (C-C motif) ligand 9 and 8 (*Ccl9, Ccl8/Mcp-2*) were both found to be dysregulated in aortic and skeletal muscle endothelium. The chemokine CCL9 has recently been suggested as a biomarker of atherosclerosis, and serum protein levels of CCL9 have been closely correlated with gene expression (Tabibiazar, 2006). The substantial upregulation of CCL8 may be related to activation of TLR4 by circulating free fatty acids (Struyf, 2009), but in any event suggests CCL8 as another potential biomarker of inflammation

in diabetes. A catalyst of leukotriene biosynthesis (Evans, 2008), arachidonate 5-lipoxygenase-activating protein (Alox5ap/FLAP), has been implicated in both coronary restenosis and the development of atherosclerosis (Hiden, 2006 and Jawien, 2006). Endothelial upregulation of *Alox5ap* upon HFD suggests roles for this protein in vascular inflammation and insulin insensitivity similar to those of 12/15-lipoxygenase (Sears, 2009).

The upregulation of metallothionein 1 (*Mt1*), a zinc-binding molecule important in maintaining redox homeostasis (Colgan 2007), is consistent with our observed down-regulation of early growth response 1 (*Egr-1*) in the skeletal muscle endothelium; transcription of *Egr-1* is regulated by the levels of intracellular zinc (Colgan, 2007). Also, ferritin light chain 1 (*Ftl1)* was up-regulated in both muscle and aortae, possibly reflecting the presence of oxidized low-density lipoproteins in diabetic endothelium (Jang, 1999). One other transcript dysregulated in both aortic and skeletal muscle endothelium, lysozyme 1 (*Lyz1*), is involved in the modulation of AGEs (Zheng, 2001) and is a vasodilator (Mink, 2008).

The transcriptional upregulation of another AGE-binding protein, galectin-3/AGE-R3, was also observed in the endothelium of the aorta and the skeletal muscle as shown by microarray and RT-PCR (Table 2.2, Figure 2.7). Galectin-3 is a component of the AGE–receptor complex prominently expressed on the surface of renal cell types important in the binding and removal of AGEs from the circulation (Sears, 2009). Previous *in vitro* studies using cultured human umbilical vein endothelial cells (HUVEC) have demonstrated increased galectin-3 mRNA

and protein levels following exposure to AGE (Sears, 2009). Galectin-3 deficient mice have been shown to display increased glomerular accumulation of AGEs in a model of type 1 diabetes and increased ox-LDL and lipoprotein products when fed an atherogenic diet (Iacobini, 2009 and Pugliese, 2001). Therefore, the observed marked upregulation of galectin-3 in the aortic endothelia may reflect elevated AGEs and modified lipids in the diabetic milieu, and suggests a role for galectin-3 in their binding and uptake by the endothelium.

Galectin-3 has been implicated in the progression of cancer (Iurisci, 2000 and Johnson, 2007) due to its anti-apoptotic properties (Glinsky, 2009) and recent studies suggest that it may contribute to heart failure, possibly due to activation of inflammation and fibrosis (de Boer, 2011 and de Boer, 2010). A role for galectin-3 in type I diabetes has been suggested by studies on the *Lgals3(-/-)* mouse, which was found to be more resistant to diabetogenesis following streptozotocin treatment, and displayed a lower expression of inflammatory cytokines and macrophages, with a reduced ability to produce TNF-α and nitric oxide (Mensah-Brown, 2009). Expression of galectin-3 was shown to be upregulated in whole aortic lysates from both *db/db* mice and mice exposed to a high-fat diet (Mzhavia, 2008), and elevated galectin-3 mRNA and protein have been demonstrated in the atherosclerotic lesions of *ApoE(-/-)* mice (Papaspyridonos, 2008). In our study, we observed upregulation of galectin-3 expression specifically in the diabetic endothelium, which places it at the appropriate site to recruit monocytes, in concert with the other inflammatory mediators demonstrated. *In vitro* studies have shown that exogenous galectin-3

acts as a chemo-attractant for monocytes and macrophages through a G-protein-coupled pathway, and it can also induce the proliferation and migration of vascular smooth muscle cells (Papaspyridonos, 2008). Our study suggests that the increased galectin-3 observed in diabetes and cardiovascular pathologies is at least partially originating from endothelial cells and potentially contributing to vascular inflammation.

We also found that serum galectin-3 levels were substantially increased in our HFD model. A recent study has similarly reported an elevation of systemic galectin-3 in obese and type II diabetic patients compared to normal weight individuals (Weigert, 2010). Thus, our murine model is accurately recapitulating the response of diabetic patients and should be useful to study the role of galectin-3 in the vascular complications of type II diabetes. Future studies stimulated by our findings could include examining the effects of galectin-3 inhibitors, such as modified citrus pectin, and the effects of diabetic treatments on galectin-3 levels and vascular pathology (Liu, 2009b and Nangia-Makker, 2002). However, it remains a possibility that some element of circulating galectin-3 is contributed by other cell types such as monocytes and macrophages, which have also been shown to secrete LGALS3 (Papaspyridonos, 2008 and Weber 2009).

Another transcript belonging to the galectin family, galectin-1 (*Lgals1*), was observed to have increased expression in the diabetic skeletal muscle endothelium. LGALS1 may play a role in the adhesion of various cell types to the vascular wall. LGALS1 is expressed on the extracellular surface of endothelial

cells and can mediate the adhesion of lymphoma cells to endothelial cells of the liver microvasculature (Lotan, 1994). Recently, mass spectroscopy analysis of differentially expressed proteins in the plasma of type II diabetic patients revealed a 4.8-fold increase in galectin-1 protein (Liu, 2009a). Galectin-1 also binds the neuropilin-1 receptor on the surface of endothelial cells leading to the increased phosphorylation of the VEGFR-2 co-receptor which activates the stress activated protein kinase-1/c-Jun NH2-terminal kinase (SAPK1/JNK) signaling pathway (Hsieh, 2008) and could influence angiogenesis in diabetic tissues.

Our analysis of the transcriptional response of the endothelium of both aortic and skeletal muscle tissues to an *in vivo* model of type II diabetes revealed novel regulation of several transcripts with roles in inflammation, vasoregulation, redox homeostasis, and modulation of responses to advanced glycation endproducts. While a greater number of differentially regulated transcripts were observed in the macrovasculature compared to the microvasculature, commonly dysregulated transcripts were shared by the two vascular beds, suggesting robust and consistent endothelial markers of diabetes. The dysregulated transcripts identified in this study reflect the various metabolic and hormonal derangements that impinge upon the diabetic endothelium and lead to its damage and dysfunction. These findings suggest potential diagnostic biomarkers of the disease and also implicate gene products and pathways that may be targets for the treatment of vascular pathology in type II diabetes.

Tables

Table 2.1. Metabolic characteristics of Tie2-GFP mice receiving high-Fat diet (60% fat calories) vs. chow diet (12%).

	Weeks on Diet	CHOW	HIGH-FAT
Weight (g)	0	22.2 ± 0.9	23.8 + 0.7
	2	24.1 ± 0.8	30.0 ± 1.6**
	4	26.8 ± 0.8	31.1 ± 1.3**
	6	26.3 ± 0.8	33.8 ± 1.2***
	8	28.0 ± 0.9	36.5 ± 1.0***
Glucose (mg/dL)	0	130 ± 20	120 ± 7
	2	148 ± 9	190 ± 10*
	4	116 ± 8	163 ± 9***
	6	139 ± 9	210 ± 10***
	8	111 ± 4	182 ± 4***
Insulin (ng/mL)	3	0.7 ± 0.2	1.3 ± 0.3
	6	0.7 ± 0.2	2.4 ± 0.4**
	8	0.9 ± 0.2	3.3 ± 0.7**

Data are means ± SEM. Weight measurements and glucometry of the tail blood was performed before the start of the high-fat or chow diet regimen and after 2,4,6, and 8 weeks of feeding (n =6-18). Serum insulin levels were quantified by ELISA following 3, 6, and 8 weeks on the diet (n=5-9). *P < 0.05; **P < 0.01; ***P < 0.001 vs. chow-fed controls.

Table 2.2A. Average $\log_2$ fold-change of dysregulated transcripts determined by microarray analysis in aortic endothelium following 4, 6, and 8 weeks of high-fat diet. Transcripts shown are dysregulated >0.7 $\log_2$ fold at all timepoints in biologically replicate experiments. Highlighted fold changes indicate $P < 0.05$.

RefSeq	Name	4 wks	6 wks	8 wks
NM_010705	lectin, galactose binding, soluble 3	**3.6**	**1.5**	**2.3**
NM_010188	Fc receptor, IgG, low affinity III (Fcgr3)	1.8	**0.9**	1.2
NM_011338	chemokine (C-C motif) ligand 9	**2.8**	**1.4**	**2.4**
NM_021443	chemokine (C-C motif) ligand 8	**3.1**	**1.9**	1.7
NM_007572	complement component 1, q subcomponent, alpha polypeptide	**3.4**	2.0	0.7
NM_008147	glycoprotein 49 A	**2.7**	0.8	**1.9**
NM_008176	Cxcl1	2.5	1.6	**1.3**
NM_008327	Ifi202b	1.6	**1.2**	1.1
NM_008677	neutrophil cytosolic factor 4	**1.7**	**1.3**	**1.6**
NM_009140	cxcl2	**4.1**	1.5	**1.8**
NM_009285	stanniocalcin 1	1.0	**0.7**	1.0
NM_009663	arachidonate 5-lipoxygenase activating protein	**1.8**	0.7	1.5
NM_009777	complement component 1, q subcomponent, beta polypeptide	**2.4**	**1.6**	0.9
NM_009876	cyclin-dependent kinase inhibitor 1C (P57)	-0.8	-0.9	**-0.8**
NM_009898	coronin, actin binding protein 1A	**1.9**	**0.9**	**1.2**
NM_010016	CD55 antigen	1.3	1.1	**1.0**
NM_010185	Fc receptor, IgE, high affinity I, gamma polypeptide	**2.1**	**1.4**	0.9
NM_010188	Fc receptor, IgG, low affinity III	**2.8**	**1.9**	1.3
NM_010240	ferritin light chain 1	**2.3**	**1.0**	0.8
NM_010545	CD74 antigen (invariant polypeptide of major histocompatibility complex, class II antigen-associated)	**2.5**	**2.1**	0.9
-	coactosin-like 1 (Dictyostelium)	**2.2**	**1.8**	**1.2**
NM_010796	macrophage galactose N-acetyl-galactosamine specific lectin 1	**2.6**	1.0	1.4
NM_011113	plasminogen activator, urokinase receptor	**0.9**	0.9	**0.8**
NM_011584	nuclear receptor subfamily 1, group D, member 2	1.2	1.5	**0.9**
NM_013590	lysozyme	3.1	**1.7**	**1.3**
NM_013777	aldo-keto reductase family 1, member C13	2.3	1.1	**1.7**
-	cDNA sequence BC032204, fermitin family homolog 3 (Drosophila)	1.9	1.0	**1.2**
NM_022431	membrane-spanning 4-domains, subfamily A, member 6D	2.4	2.0	**2.1**
NM_029097	ATPase type 13A2	1.1	**0.8**	**0.6**
NM_053214	Myo1f	1.8	2.4	**2.4**
NM_134158	Cd300D antigen	1.7	1.9	**1.1**
NM_134158	Cd300D antigen	**2.6**	1.0	0.9
NM_183168	pyrimidinergic receptor P2Y, G-protein coupled, 6	**2.5**	1.0	**1.4**
XM_354744	MRS2-like, magnesium homeostasis factor (S. cerevisiae)	1.1	**0.9**	**0.8**
NM_010766	macrophage receptor with collagenous structure	0.7	**2.9**	**1.5**

Table 2.2B. Average $\log_2$ fold-change of dysregulated transcripts determined by microarray analysis in leg muscle endothelium following 4, 6, and 8 weeks of high-fat diet. Transcripts with both >0.70 $\log_2$ fold-change and $P < 0.1$ in biologically replicate experiments after 6 or 8 weeks of the diet are shown. Highlighted fold changes indicate $P<0.05$.

RefSeq	Name	4 wks	6 wks	8 wks
NM_009140	chemokine (C-X-C motif) ligand 2 (Cxcl2)	1.6	1.5	**2.5**
NM_011338	chemokine (C-C motif) ligand 9	1.8	**1.2**	**2.4**
NM_013590	lysozyme	0.7	0.1	**1.7**
NM_017372	lysozyme	0.5	0.1	**0.8**
NM_010188	Fc receptor, IgG, low affinity III	0.3	**0.1**	**0.9**
NM_021443	chemokine (C-C motif) ligand 8	0.3	0.4	**1.4**
NM_010240	ferritin light chain 1	2.1	**1.3**	**2.4**
NM_010705	lectin, galactose binding, soluble 3	0.1	0.3	**1.8**
NM_010185	Fc receptor, IgE, high affinity I, gamma polypeptide	0.6	**0.5**	**1.6**
NM_008327	interferon activated gene 202B (Ifi202b), variant 1	0.5	0.2	**1.2**
NM_145509	RIKEN cDNA 5430435G22 gene	0.8	0.0	**1.2**
NM_009663	arachidonate 5-lipoxygenase activating protein	0.1	0.5	**1.5**
NM_024225	sorting nexin 5	-0.6	-0.2	**1.1**
NM_130904	CD209d antigen	0.2	0.6	**1.4**
NM_011175	legumain	0.5	0.6	**1.0**
NM_013602	metallothionein 1	-0.1	0.4	**0.8**
NM_008035	folate receptor 2 (fetal)	-0.2	0.4	**1.4**
-	G protein-coupled receptor 137B	-0.1	0.0	**1.0**
NM_008495	lectin, galactose binding, soluble 1	-0.2	-0.1	**1.0**
NM_133977	Transferring	2.5	1.8	**3.3**
NM_023142	actin related protein 2/3 complex, subunit 1B	0.1	0.6	**1.9**
NM_009984	cathepsin L	0.6	0.5	**1.8**
NM_133792	lysophospholipase 3	0.5	**0.9**	**1.4**
NM_007621	carbonyl reductase 2	1.0	1.0	**1.4**
-	mannosidase 2, alpha B1	0.1	0.2	**1.1**
NM_013706	CD52 antigen	0.6	1.0	**1.3**
NM_010188	Fc receptor, IgG, low affinity III	0.6	0.5	**1.2**
-	biliverdin reductase B (flavin reductase (NADPH))	0.2	0.2	**1.1**
NM_007657	CD9 antigen	1.0	-0.1	**1.4**
NM_007599	capping protein (actin filament), gelsolin-like	-0.1	0.4	**1.1**
-	RIKEN cDNA 1810019J16 gene	0.2	0.8	**0.9**
NM_007408	adipose differentiation related protein	0.0	0.3	1.2
NM_144904	ROD1 regulator of differentiation 1 (S. pombe)	-0.1	0.6	1.0
NM_178772	arylacetamide deacetylase-like 1	-0.3	-0.1	-0.7
NM_025468	SEC11 homolog C (S. cerevisiae)	1.3	1.0	1.9
NM_153795	cDNA sequence BC032204	n.d.	0.8	1.7
NM_028351	R-spondin 3 homolog (Xenopus laevis)	0.0	0.3	1.7
NM_029295	chemokine-like factor	0.4	0.6	1.4
NM_008704	expressed in non-metastatic cells 1, protein	n.d.	1.3	1.7
NM_009930	Mus musculus collagen, type III, alpha 1 (Col3a1)	1.7	**1.9**	2.1
NM_053082	tetraspanin 4	0.9	**1.1**	1.7
NM_007913	early growth response 1	-1.5	-0.8	-0.6
NM_009777	complement component 1, q subcomponent, beta	0.0	0.3	**0.8**
NM_010422	hexosaminidase B	0.0	0.7	**1.2**
NM_026678	biliverdin reductase A	-0.2	-0.1	**1.0**
-	esterase D/formylglutathione hydrolase	0.1	0.3	**1.0**
XM_486478	ferritin light chain 2	0.0	0.3	**0.8**

Table 2.2C. Transcripts commonly dysregulated in aortic (A) and skeletal muscle (M) endothelium in response to a high-fat diet. Transcripts shown demonstrate > 0.5 $\log_2$ fold dysregulation in aortic endothelium after 4 weeks of feeding and in skeletal muscle endothelium after 6 weeks. Highlighted fold changes indicate $P < 0.05$.

RefSeq	Name	4 wks (M)	4 wks (A)	6 wks (M)	6 wks (A)	8 wks (M)	8 wks (A)
NM_009777	C1qb	0.8	**2.4**	**0.8**	**1.6**	1.4	0.9
NM_009140	Cxcl2	1.8	**4.1**	1.3	1.5	**3.3**	**1.8**
NM_009303	Syngr1	0.3	**2.2**	**0.7**	0.7	1.4	1.1
NM_009663	Alox5ap	0.9	**1.8**	**1.1**	0.7	1.7	1.5
NM_010185	Fcer1g	0.6	**2.1**	0.6	**1.4**	**1.8**	0.9
NM_144797	Metrnl	0.8	**2.3**	**1.1**	0.5	**2.3**	1.2
NM_009898	Coro1a	1.1	**1.9**	0.6	**0.9**	**1.8**	**1.2**
NM_010545	Cd74	0.6	**2.5**	0.9	**2.1**	**1.4**	0.9
NM_011338	Ccl9	2.0	**2.8**	1.5	1.4	**2.5**	**2.4**
NM_013590	Lyz1	1.8	3.1	**1.2**	**1.7**	**2.4**	**1.3**
NM_010240	Ftl1	0.1	**2.3**	0.6	**1.0**	**1.9**	0.8
NM_010188	Fcgr3	1.3	**2.8**	**1.9**	**1.9**	**2.6**	1.3
NM_010658	Mafb	0.8	**2.0**	**0.7**	0.6	1.5	1.5
NM_134158	Cd300	0.5	**2.6**	1.1	1.0	**2.1**	0.9

Table 2.3. Overrepresented Molecular Functions identified by DAVID based on Gene Ontology terms.

	Aortic Endothelia		Muscle Endothelia	
Time on Diet	Molecular Function	*P*-value	Molecular Function	*P*-value
4 weeks[a]	structural constituent of ribosome	1.20E-08		
	structural molecule activity	1.50E-03		
	growth factor activity	1.10E-02		
	lysophospholipase activity	1.70E-02		
	cytokine binding	2.60E-02		
	monosaccharide binding	2.90E-02		
	immunoglobulin binding	3.10E-02		
	calcium ion binding	4.40E-02		
	GTPase activity	4.80E-02		
6 weeks[a]	immunoglobulin binding	1.50E-03	lysozyme activity	3.70E-02
	MHC protein binding	4.20E-03	folic acid binding	4.10E-02
	protein complex binding	8.70E-03	carboxylic acid binding	4.10E-02
	peptide binding	1.10E-02		
	immunoglobulin receptor activity	2.20E-02		
	IgE binding	2.70E-02		
	IgG binding	2.70E-02		
	MHC class I protein binding	4.80E-02		
8 weeks[a]	chemokine activity	3.30E-05	carboxylesterase activity	2.10E-02
	chemokine receptor binding	3.90E-05	carbohydrate binding	3.60E-02
	cytokine activity	8.00E-04	pattern binding	3.70E-02
	lipid binding	1.20E-02	polysaccharide binding	3.70E-02
	lipase activity	1.30E-02	heparin binding	4.80E-02
	immunoglobulin binding	1.30E-02	IgE binding	4.80E-02
	cyclin-dependent protein kinase regulator activity	2.50E-02	lipase activity	4.90E-02
	aldo-keto reductase activity	3.10E-02		
	carboxylesterase activity	3.30E-02		
	protein complex binding	4.00E-02		
All Time-points[b]	chemokine activity	4.80E-05	carboxylesterase activity	3.00E-03
	chemokine receptor binding	5.30E-05	protein homodimerization activity	1.40E-02
	immunoglobulin binding	1.50E-03	identical protein binding	1.50E-02
	mannose binding	3.20E-03	biliverdin reductase activity	2.60E-02
	carbohydrate binding	6.90E-03	protein dimerization activity	3.60E-02
	monosaccharide binding	8.40E-03	GTP binding	4.50E-02
	cytokine activity	1.60E-02	monosaccharide binding	4.60E-02
	sugar binding	1.60E-02	ubiquitin-protein ligase activity	4.80E-02

[a]Molecular functions based on all transcripts differentially expressed >0.5 $\log_2$ fold change and $P < 0.1$ at each separate timepoint.

[b]Molecular functions at all timepoints were differentially expressed >0.5 $\log_2$ at 4,6,and 8 weeks in aortic endothelium or at both 6 and 8 weeks in the muscle endothelium.

A

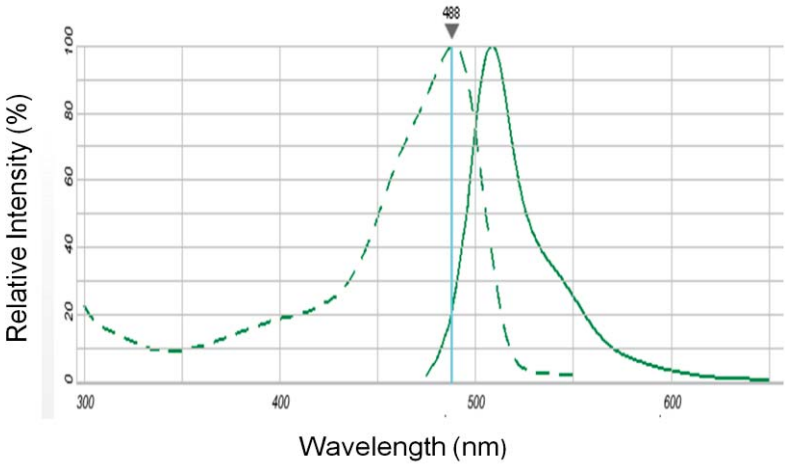

B

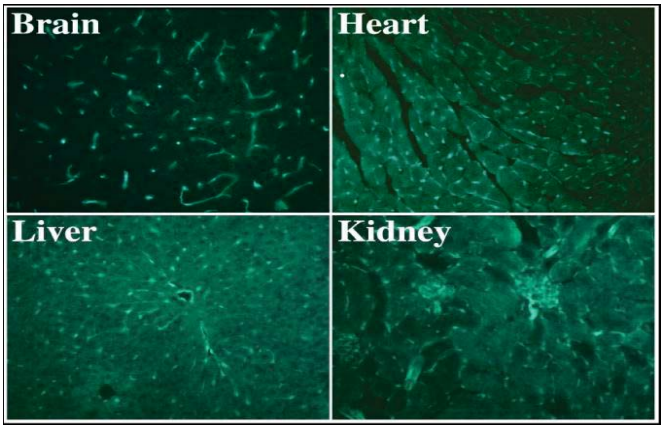

Figure 2.1. GFP fluorescence spectra and endothelial expression in Tie2-GFP mice. (A) Absorption and fluorescence emission spectra of GFP in pH 7 buffer generated using Fluorescence SpectraViewer (Invitrogen). (B) Endothelial specific GFP expression in murine tissues of the Tie2-GFP mouse (image from J.G. Maresh).

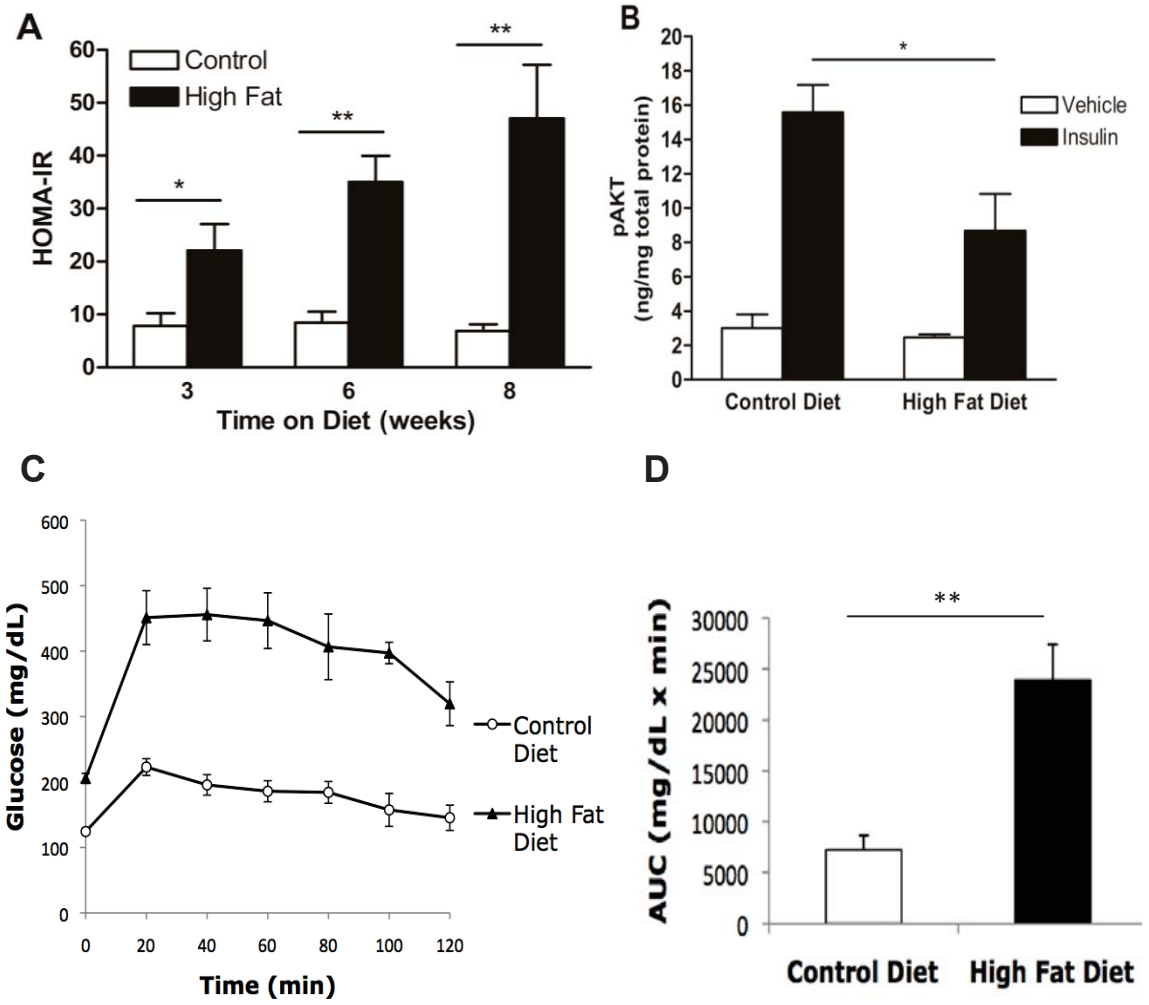

Figure 2.2. Endocrine responses of Tie2-GFP mice on high-fat diet. (A) Homeostasis model assessment of insulin resistance (HOMA-IR) calculated from measured glucose and insulin levels after 3, 6, or 8 weeks exposure to high-fat vs. control diet (*n* = 5-9). (B) Aortic AKT phosphorylation in response to insulin administration (0.06 Unit/g) vs. vehicle (i.p.) in Tie2-GFP mice after 5 weeks exposure to high-fat vs. control diet (*n* = 3-6). (C) Following 6 weeks of HFD, glucose tolerance was determined by performing glucometry over a 2hr period after an intraperitoneal injection of glucose (1mg/g) following an overnight fast (n=5). (D) Area under the curve of the glucose tolerance test. The data are presented as mean ± SEM. **P* < 0.05, ***P* < 0.01.

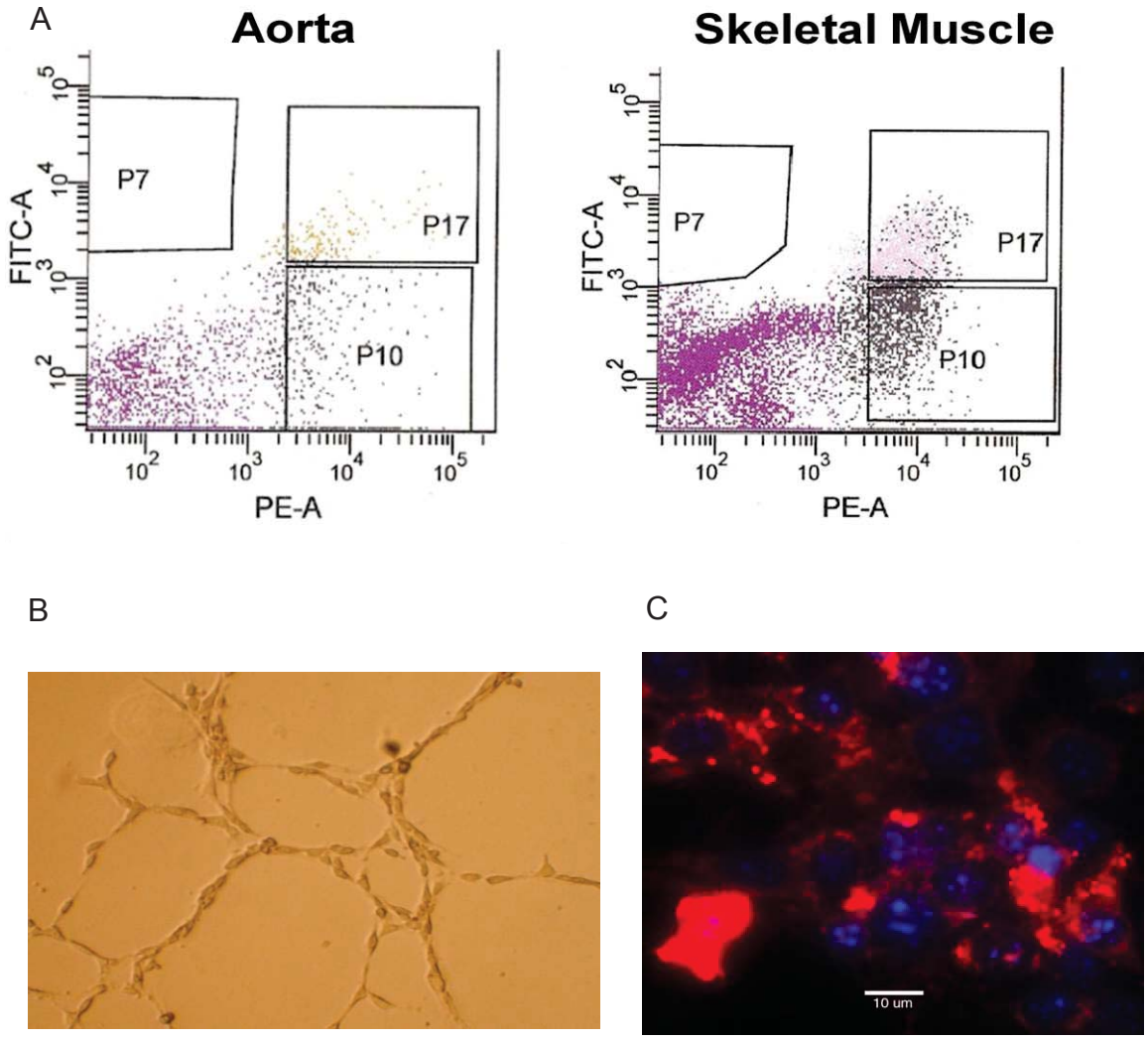

Figure 2.3. FACS isolation of endothelium. (A) Collagenolytic digests of aortae and leg muscle of Tie2-GFP mice were labeled with phycoerythrin-αCD31, and $GFP^{+}CD31^{+}$ cells were sorted on a FACSAria. Cells in the P17 gate from muscle (Right) and aortae (Left) were collected directly into TRIzol reagent. (B) Sorted cells form tubular structures after 5 days when plated on Matrigel™ and (C) Dil-Ac-LDL uptake by sorted endothelial cells after 4hr incubation.

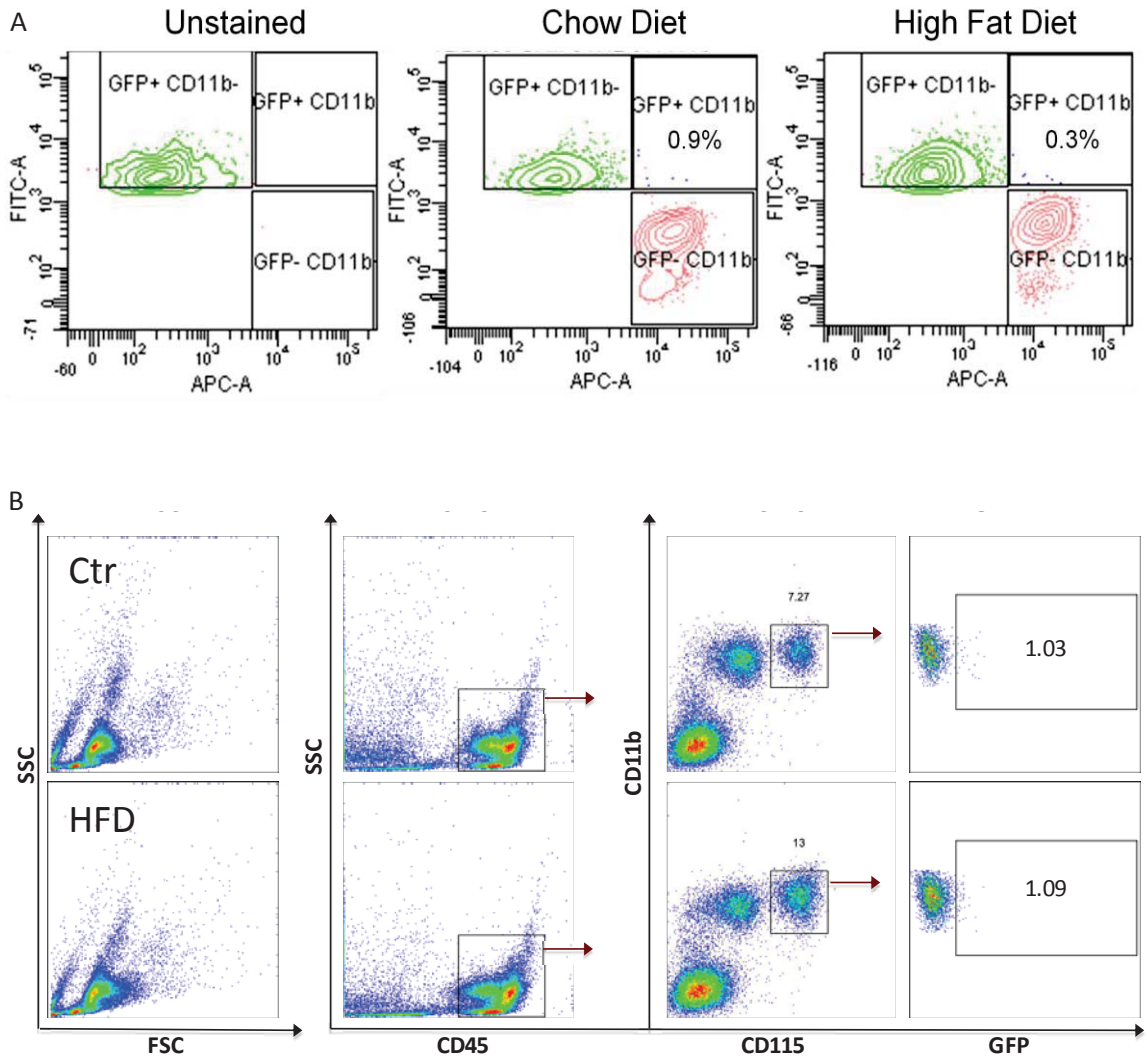

Figure 2.4. Assessment of monocyte contamination by flow cytometry. (A) Staining of GFP$^+$ endothelial cells for the monocyte marker CD11b. (B) Percentage of CD45$^+$ periphiperal blood mononuclear cells positive for CD11b, CD115, and GFP.

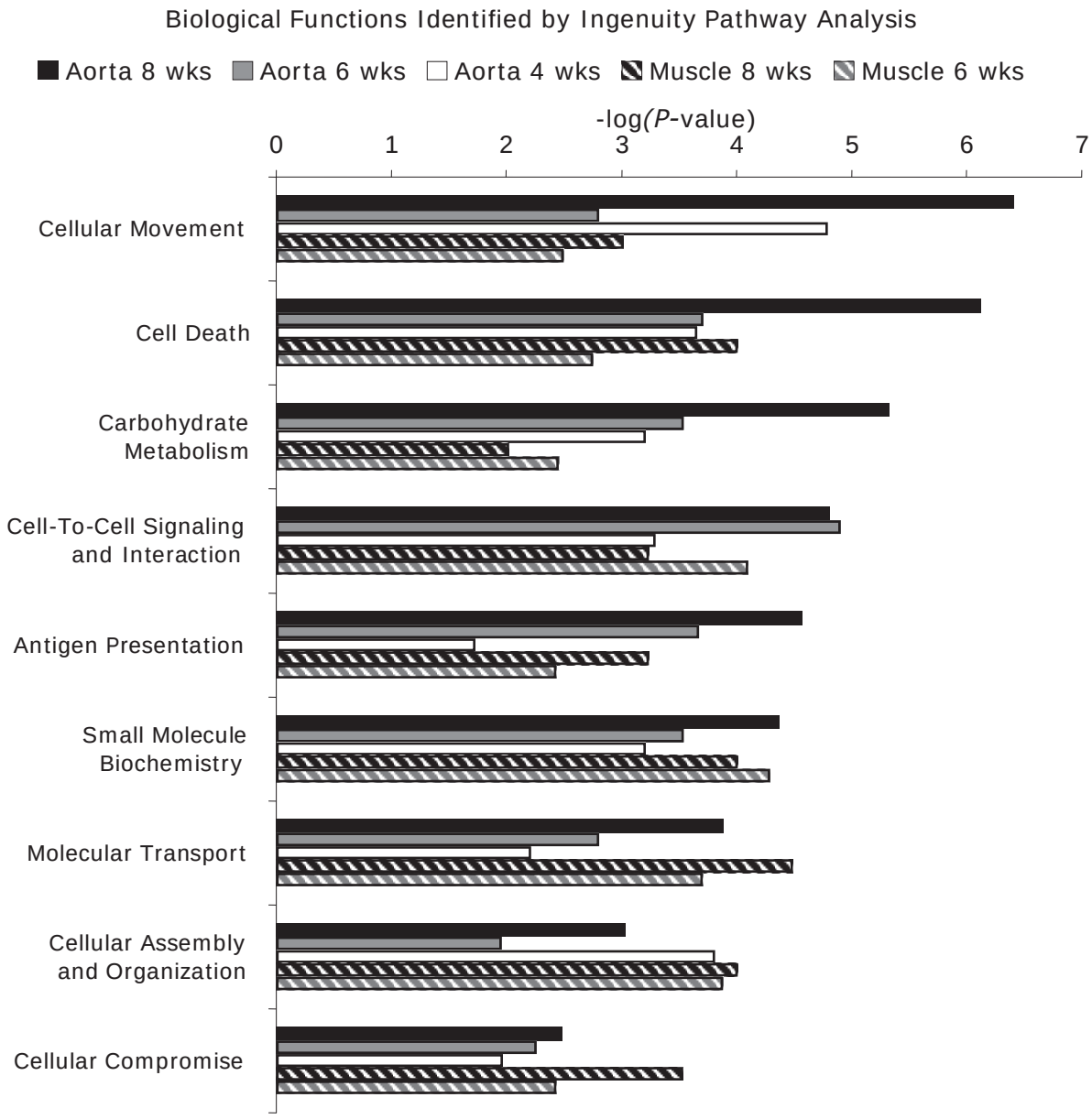

Figure 2.5. Overrepresented Biological Functions identified by Ingenuity Pathway Analysis. Transcripts displaying > 0.5 $\log_2$ [fold change] dysregulation and $P < 0.1$ following 4,6, or 8 weeks of high-fat feeding in the aortic endothelium or 6 or 8 weeks of HFD in skeletal muscle endothelium were analyzed by IPA. Shown above are the 5 most enriched biological functions after 8 weeks of feeding in the endothelium of each tissue based on weighted gene co-expression.

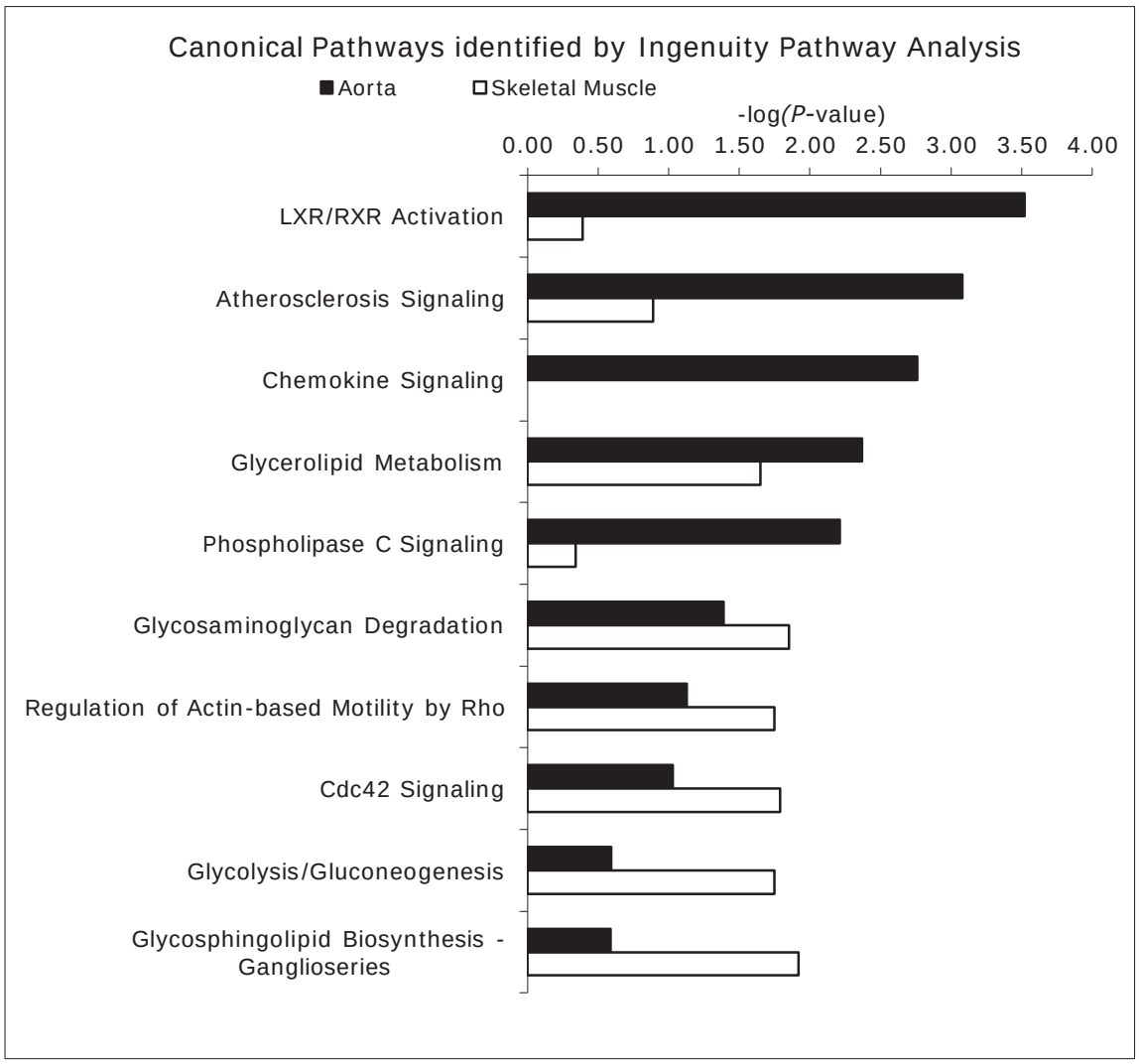

Figure 2.6. Overrepresented Canonical Pathways identified by Ingenuity Pathway Analysis. Transcripts displaying > 0.5 $\log_2$ [fold change] upregulation and $P < 0.1$ by 8 weeks of high-fat feeding in the aortic or skeletal muscle endothelium were analyzed by IPA. The 5 most enriched pathways in the endothelium of each tissue based on weighted gene co-expression are shown.

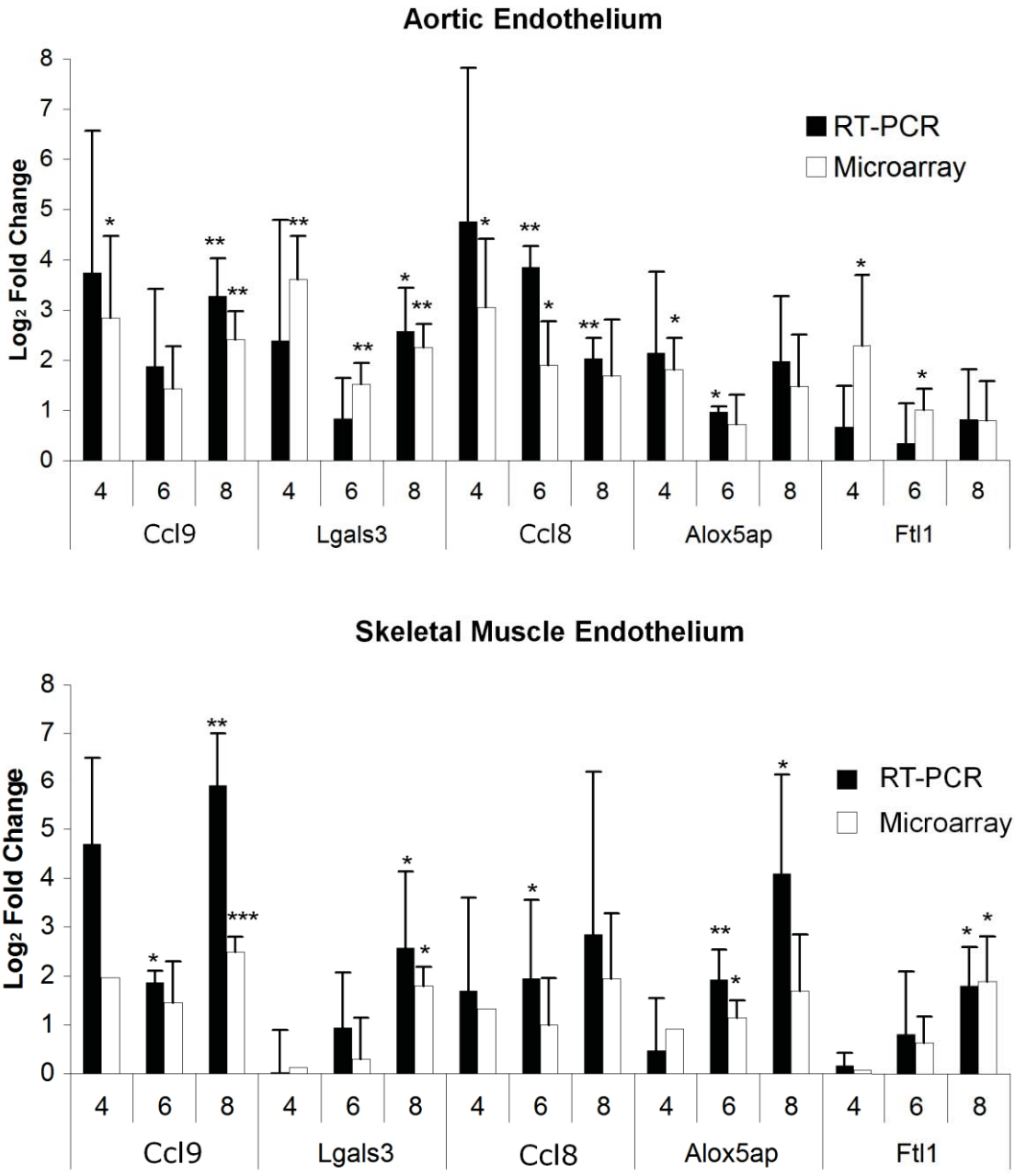

Figure 2.7. Log_2 fold change of endothelial transcripts up-regulated by high-fat diet vs. chow diet in Tie2-GFP mice after 4,6, or 8 weeks of feeding as determined by RT-PCR (*n*=3-4) and microarray analysis. Data is presented as mean + SD. **P* < 0.05, ***P* < 0.01.

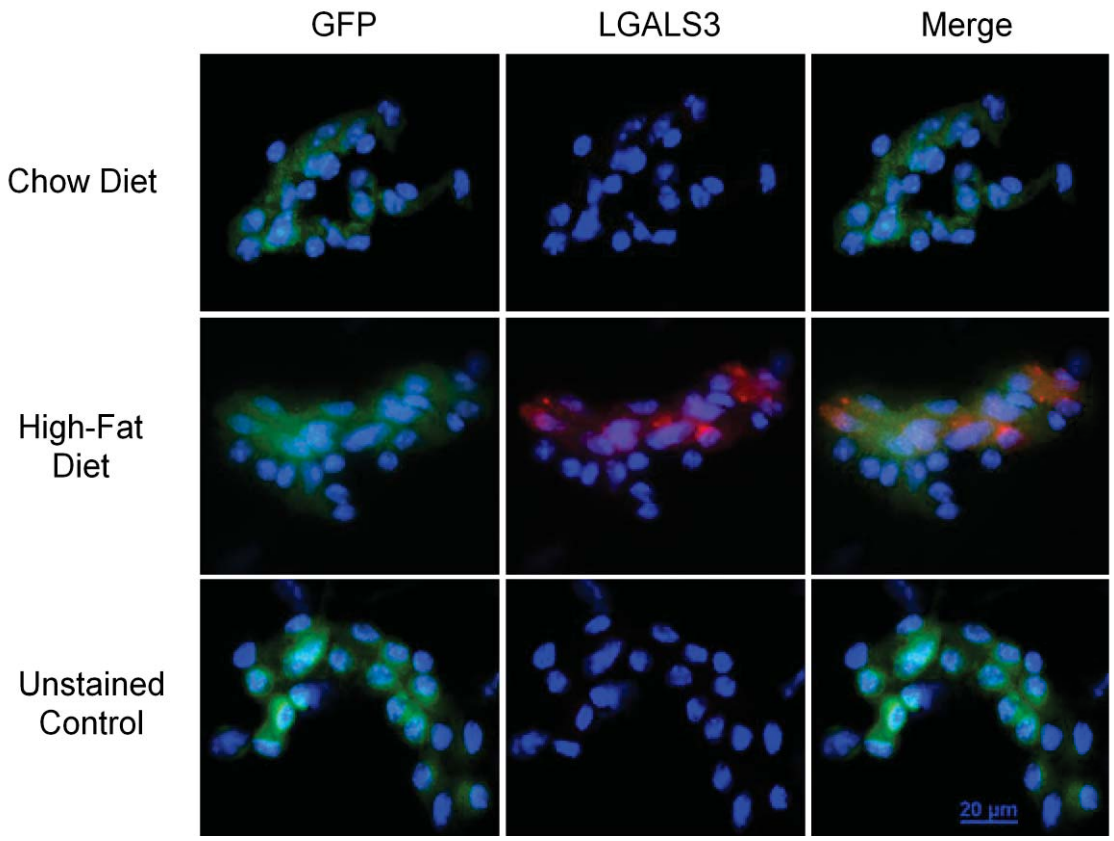

Figure 2.8. Immunofluorescence staining for galectin-3 protein in FACS sorted endothelial cells from muscle after 8 weeks of HFD or chow diet. Representative images of GFP^+ endothelial cells isolated from mice fed either chow (A) or high-fat diet (B) and stained for LGALS3 or unstained control (C).

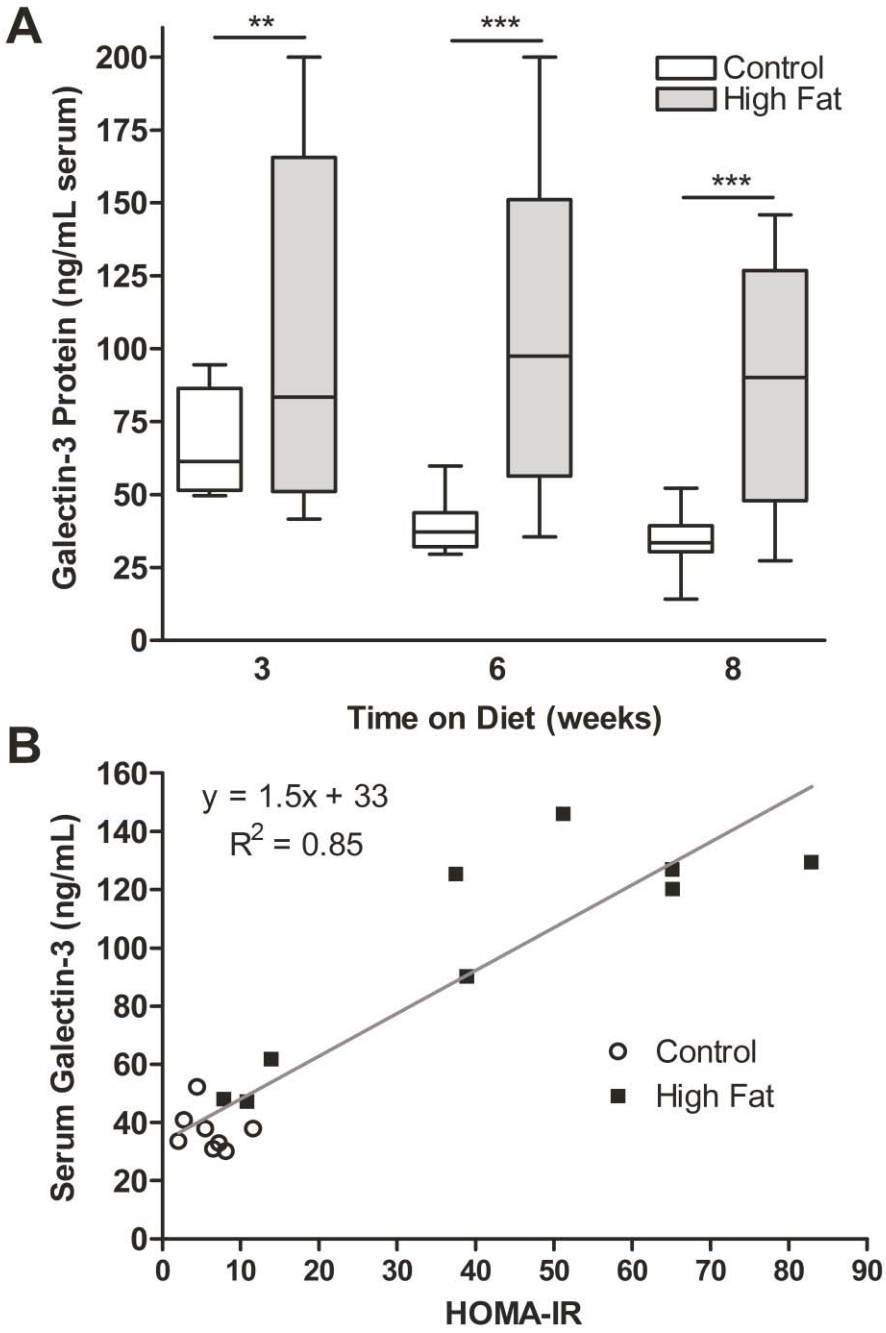

Figure 2.9. Upregulation of soluble galectin-3 by high-fat diet. (A) Galectin-3 soluble protein levels measured by ELISA in serum from mice receiving HFD vs. control diet for 3, 6, or 8 weeks. (B) Correlation of soluble LGALS3 with HOMA-IR. Data is shown as mean ± SEM (n = 5-11). $^{**}P < 0.01$, $^{***}P < 0.001$.

Chapter 3: Galectin-3 Deficiency Exacerbates Hyperglycemia and the Endothelial Response to Diabetes

3.1 Abstract

In Chapter 2, we demonstrated the upregulation of galectin-3 mRNA and protein in the endothelium of mice given a high-fat diet (HFD) compared to chow-fed controls. To assess the role of galectin-3 in the vascular pathology of diabetes we have performed similar studies with galectin-3 knockout mice (KO). KO mice were fed either chow (12% calories) or a HFD (60% fat calories) for 8 weeks and their metabolic and vascular responses were measured. KO mice exhibit increased fasting glucose levels relative to wild-type (WT) mice when fed either chow or HFD. When placed on HFD, KO mice exhibit a rapid increase in fasting glucose levels in the first 2 weeks on the diet regimen, whereas the fasting glucose levels of WT mice increase more gradually and never reach the level of KO mice. By 5 weeks on the diet, impaired response to a glucose challenge was observed in both KO and WT mice vs. chow-fed controls, with KO mice exhibiting a greater impairment in second phase insulin response. Chow-fed KO mice exhibit increased fasting glucose levels compared to WT, but no impairment of glucose tolerance. In spite of the marked hyperglycemia in the KO, these mice do not have higher insulin levels or significantly impaired response to insulin challenge compared to WT mice. Microarray analysis of the aortic and skeletal muscle endothelium revealed greater dysregulation in the KO when placed on HFD compared to WT mice. Dysregulated transcripts include those

involved in glucose uptake and insulin signaling, oxidative stress, vasoregulation, coagulation, and atherogenesis. One of the most downregulated transcripts in the aortic and skeletal muscle endothelium of the KO on HFD was the glucose transporter, *Glut4.* Immunofluorescence staining for GLUT4 in the muscle and aortic endothelium confirmed the lower abundance of GLUT4 protein compared to WT animals, possibly explaining the hyperglycemia demonstrated by the KO. Pathway analysis of transcripts dysregulated in the diabetic KO revealed "cardiovascular system development and function" as the most highly enriched molecular function with several transcripts with roles in vasoconstriction, vasculogenesis, proliferation, and migration. Direct comparison of the aortic endothelial transcriptional profiles of KO HFD and WT HFD animals identified the coagulation cascade as a highly enriched differential pathway. Blood clotting assays revealed increased coagulation occurring in the KO after 8 weeks of HFD, whereas there was no significant difference in WT mice after high-fat feeding. Exposure of cultured human aortic and cardiac microvascular endothelial cells to high glucose, ox-LDL, or advanced glycation endproducts failed to recapitulate the upregulation of galectin-3 mRNA or protein above control levels further emphasizing the relevance of our *in vivo* studies. Due to galectin-3's putative role in cardiac remodeling and the current enthusiasm for using LGALS3 as a heart failure marker, hearts from the diabetic animals were analyzed for structural signs of cardiac fibrosis and expression of connective tissue growth factor (*Ctgf*). No fibrosis was visible at this stage, however, a trend toward increased *Ctgf* in WT hearts was observed. This data shows that galectin-

3 deficiency leads to exacerbated metabolic derangement and endothelial dysfunction which contributes to the vascular pathology in diabetes.

3.2 Introduction

A high-fat diet is associated with impaired endothelial function, which precedes diabetes (Kim, 2008). The most obvious metabolic effect of diabetes is energy substrate overload that promotes production of reactive oxygen species, with a variety of negative effects on endothelial function (Avogaro, 2008). High glucose can directly affect intracellular signaling, including stimulating the synthesis of diacylglycerol, with subsequent activation of protein kinase C (Haller, 1996); high glucose levels can also cause the non-enzymatic glycation of macromolecules (advanced glycosylation end-products or AGE) that can activate specific receptors (Forbes, 2005). Previously, we have developed methods for the rapid isolation of highly purified endothelial cells from mice exposed to models of cardiovascular pathophysiology, including type I diabetes induced by streptozotocin (STZ) and type II diabetes induced by a high-fat diet (HFD) (Maresh, 2008 and Darrow, 2011). Transcriptional analysis of these diabetic endothelial cells with highly-representative microarrays revealed increased abundance of transcripts involved in insulin signaling, inflammation, and metabolic regulation. One of the most highly upregulated transcripts in the endothelium of Tie2-GFP mice exposed to a high-fat diet was galectin-3 (Lgals3), a β-galactoside-binding lectin. We therefore hypothesize that endothelial dysfunction is influenced by galectin-3, and we seek to identify its role in the vasculopathy associated with type II diabetes.

3.2.1 Galectin Family Members

Lectins are proteins with an affinity for binding specific carbohydrate structures. Lectins can be classified into 4 families based on sequence similarity and binding specificity. These groups are the C-type lectins including the selectins, the P-type lectins, pentraxins, and galectins (Barondes, 1994). Unlike the Ca^{2+}-dependent, or C-type lectins, galectins do not require divalent cations to bind their substrates. Galectins were formally known as S-type lectins because it was believed that reducing conditions were required for their binding (Woo, 1991).

The galectin family is composed of 15 members of β-galactoside specific lectins. All members, except galectin-11, possess at least one conserved carbohydrate recognition domain (CRD) of roughly 130 amino acids at their C-terminus (Elola, 2007). Galectins can be divided into 3 subgroups based on their domain structure: prototype, tandem-repeat type, and chimera type. Galectins-1, -2, -5, -7, -10, -11, -13 and -14, -15 are prototypical galectins, consisting of a short N-terminal sequence followed by a single CRD. These galectins are roughly 15 kDa and some are able to noncovalently dimerize in the presence of ligands or high concentration (Kuklinski, 1998). Galectins-4, -6, -8, -9 and -12 are tandem-repeat galectins that contain 2 CRDs in one polypeptide chain joined by a short linker peptide of about 30 residues. The tandem-repeat galectins are able to bind 2 carbohydrate epitopes (Dumic, 2006). Galectin-3 is the only known chimera type galectin consisting of a non-lectin domain of glycine/ proline repeats at its amino terminus in addition to its C-terminal CRD (de Boer, 2010).

The carbohydrate binding domain is encoded by 3 exons, with the middle exon containing all the residues that interact directly with the carbohydrate ligand. While site-directed mutagenesis of residues within the middle exon abolishes carbohydrate binding completely, deletion of other regions of the CRD not within the binding interface also reduces binding (Barondes, 1994). This region forms a series of β-strands and their connecting loops and is the most conserved region among the galectin members and among species (Fig. 3.1). The amino acid identity of the CRDs of the various galectins of the same species ranges between 20-40% similarity. While the overall amino acid homology among the galectin orthologues of different mammalian species is 65-88%, the homology of the CRD is 80-90%, making it easy to identify the homologous galectin in different species (Barondes, 1994).

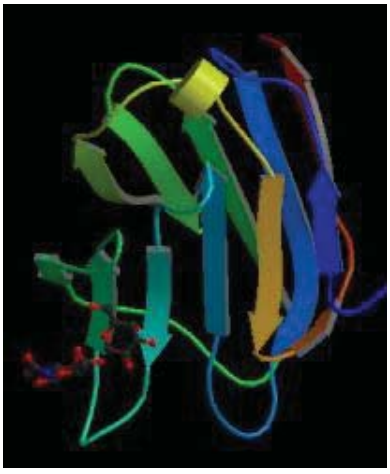

Figure 3.1 Ribbon model of the Carbohydrate Recognition Domain (CRD) of galectin-3 consisting of two anti-parallel β-sheets composed of five and 6 β-strands. (Image provided by the Consortium for Functional Glycomics grant number GM62116).

3.2.2 *Lgals3* Gene

Human *Lgals3* has been mapped to chromosome 14 at region 14q22.3 (Pricci, 2000). In both mice and humans, the gene contains 6 exons and 5 introns and spans 17kb and 10-12kb, respectively. Exon 1 encodes an untranslated

region but contains 2 transcription initiation sites just upstream of the first intron. Exon 2 contains an untranslated region followed by the translation initiation site, and the first 6 amino acids of the protein (Kuklinski, 1998). The N-terminal domain is encoded by exon 3, and the C-terminal domain is encoded by exon 5 in humans or spans across exons 4-6 in mouse. The carbohydrate binding site of mouse LGALS3 is contained in exon 5. The *Lgals3* gene structure of human and mouse origin are shown in Fig. 3.2.

In mouse, two transcription initiation sites located 27 nucleotides apart results in the use of an alternative intron 1 splice donor site and subsequently produce two distinct mRNAs that differ in their 5' UTR (Rosenberg, 1993). Several regulatory elements are contained in the human *LGALS3* promoter region including 5 SP1 binding sites, 5 cAMP-dependent response element motifs, 4 AP-1, 1 AP-4-like sites, 2 NF-kB-like sites, 1 *sis*-inducible element, and a basic-helix-loop-helix core sequence (Kadrofske, 1998). CREB, NFκB, and Jun have been shown to induce *Lgals3* expression and *sis*-inducible factors have been implicated in activation of *Lgals*3 transcription by serum (Dumic, 2006).

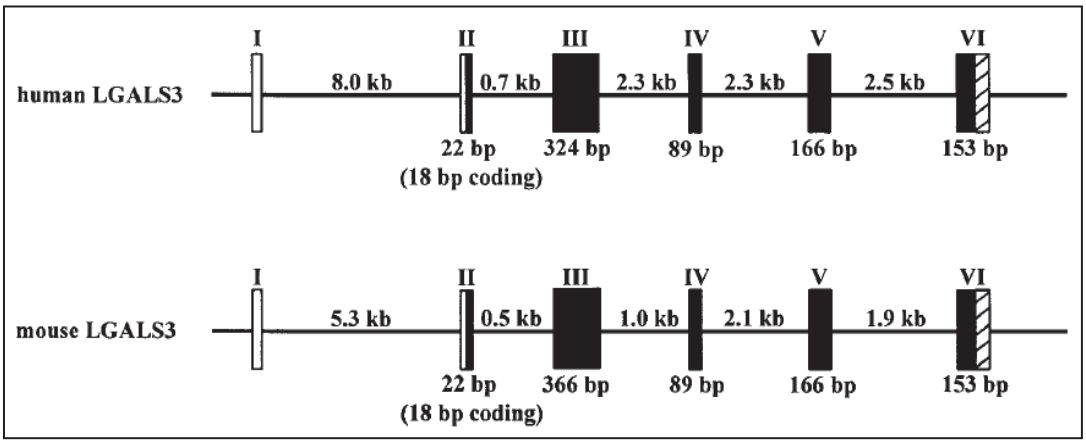

Figure 3.2. Comparison of human and murine *Lgals3* gene structure. Exons are represented by shaded boxes, introns by thin lines, and untranslated regions by open boxes (adapted from Kadrofske, 1998).

3.2.3 Amino Acid Sequence and Protein Structure

Both variants of mouse galectin-3 produce the same protein composed of 264 amino acids. Human LGALS3 protein has 2 isoforms. Variant 3 has 250 amino acids, whereas variant 1 has a shorter C-terminus and is composed of only 200 amino acids. The galectin-3 protein contains 3 domains that are highlighted in the amino acid sequence below (Figure 3.3): (1) An N-terminal domain consisting of 80 amino acids (residues 2-34), (2) an intervening domain consisting of proline, glycine, and tyrosine-rich repeats (residues 35-114, blue), and (3) the C-terminal carbohydrate recognition domain composed of 131 amino acids (residues 132-262, yellow). The repeats are a set of 7-10 conserved amino acids with the sequence $PGAYPG(X)_{1-4}$, where X is any amino acid, and this domain is homologous to proteins of the heterogeneous nuclear ribonucleoprotein particles (Kuklinski, 1998). The mouse protein contains 9 of these repeats, whereas the human homologue has 8. The variation in the number of repeat sequences among species results in a range of molecular weights from 26.2 kDa in humans to 27.5 in mouse to 30.3 kDa in dog (Barondes, 1994). LGALS3 also has a 16 amino acid nuclear export signal at the C-terminus (Figure 3.3, orange) and a 7 amino acid region in the CRD (Figure 3.3, purple) that specifically interacts with β-galactoside ligands. The N-terminal portion also demonstrates homology to the transcriptional activator, serum response factor, and deletion of the first 11 amino acids prevents secretion of LGALS3 and alters its anti-apoptotic signaling activity (Oda, 1991). Within the CRD, is a NWGR motif, which is conserved among members of the BCL-2 family

and has been shown to be responsible for the anti-apoptotic properties of BCL-2 and LGALS3 (Yang, 1996). The C and N domains have been shown to fold and function independently (Ochieng, 1993). Proteolysis of galectin-3 shows that the 2 N-terminal domains are not essential for carbohydrate binding, but they are required for multimerization (Massa, 1993).

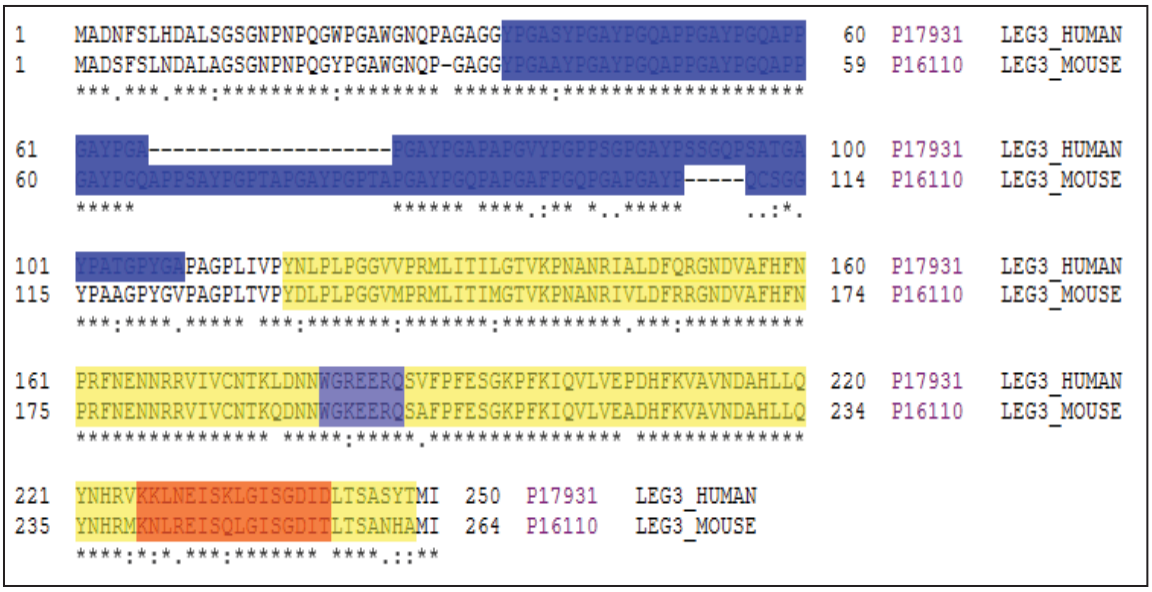

Figure 3.3. Amino acid sequences of human and mouse LGALS3 aligned using the Uniprot database. Structural features are highlighted as follows: PGY repeats = blue; Carbohydrate recognition domain = yellow; Substrate binding site = purple; Nuclear export signal motif = orange (The Uniprot Consortium, 2012).

3.2.4 Multimerization

It was initially believed that the galectins functioned solely as monomers and thus required reducing conditions to prevent dimerization and maintain sugar binding activity. However, it is now known that galectins not only maintain lectin activity upon multimerization, but many of their biological interactions are enhanced by it (Dumic, 2006). In 1991, laminin affinity chromatography was used

under non-reducing conditions to purify a 35 kDa, 67 kDa, and a 90 kDa form of galectin-3. The dimeric (67 kDa) species was shown to bind laminin with a higher affinity than the monomer alone indicating that dimers not only retain lectin activity but promote it (Woo, 1991).

The oligomerization of galectin-3 can occur in 3 ways. 1) a carbohydrate independent mechanism mediated by interactions of the N-terminal domains 2) a carbohydrate-dependent mechanism relying on the C-domain, or 3) covalent bonds formed by disulfide linkages. In solution, galectin-3 oligomerizes in the absence of ligand by the interaction of the N-terminal domains, however, this process is greatly enhanced by the presence of β-galactosides (Massa, 1993). Isolated N-terminal domains can form oligomers as well as dimers indicating that the N domain contains at least 2 binding sites involved in these interactions (Mehul, 1994). *In vitro* studies have shown that LGALS3 proteins assemble into pentamers mediated by their N-terminal domains in the presence of multivalent ligands (Ahmad, 2004). The carbohydrate-dependent oligomerization is mediated by the interaction of the C-domain with the N-domain of another monomer, and this self-association is favored in the absence of carbohydrate ligands (Kuklinski, 1998). Finally, at very high concentrations, covalently linked homodimers are formed by the oxidation of cysteine 186 residues (Woo, 1991).

3.2.5 Galectin-3 Expression

LGALS3 is ubiquitously expressed from vertebrates to insects to lower organisms such as sponges and fungi (Elola, 2007). Homologous proteins are found in plants, but not yeast (Dumic, 2006). Galectin-3 is widely distributed

among various tissue and cell types. In general, LGALS3 expression is higher in tissues with proliferating cell populations such as embryonic liver and skin, and lower in nonproliferating tissue, such as adult liver and brain (Moutsatsos, 1987). Immunohistochemical and Western analysis of normal mice reveals high expression in the lung, spleen, stomach, colon, uterus, and ovary and low to moderate levels in the cerebrum, heart, pancreas, liver, ileum, kidney, and adrenal gland (Kim, 2007). The protein is expressed by epithelial cells, fibroblasts, osteoblasts, adipocytes, leukocytes, and endothelial cells (Dumic, 2006 and Darrow, 2011).

At the cellular level, subcellular fractionation has shown that LGALS3 is localized mostly in the cytoplasm (90%), and to a much lesser degree, in the nucleus and on the cell surface (Moutsatsos, 1986). Studies in 3T3 fibroblasts have demonstrated that galectin-3 increases in the nucleus during cell proliferation where punctate, possibly nucleolar, staining is observed; whereas cytoplasmic localization is predominant in quiescent cells. In addition, nuclear localization as well as overall LGALS3 expression has been shown to be cell-cycle dependent (Moutsatsos, 1997). Import of galectin-3 into the nucleus has been shown to rely on the N-terminal 11 amino acids, as this sequence when fused to GFP has been shown to result in nuclear localization of fluorescence (Gong,1999) although involvement of the CRD has also been suggested (Davidson, 2006). Nuclear export is attributed to the leucine-rich nuclear export signal of residues 241-249 (Li, 2006).

In addition, galectin-3, which lacks the appropriate signal peptides, is secreted via ER/Golgi-independent pathways. It has been shown to spontaneously penetrate the lipid bilayer of liposomes suggesting that it may interact directly with membrane lipids in a process referred to as ectocytosis (Lukyanov, 2005). Extracellular galectin-3 can bind to ligands on the cell surface as well as to components of the ECM. Although surface-bound galectin-3 was demonstrated to account for only 5% of total cellular galectin-3, levels may increase under pathophysiological conditions such as heart failure and diabetes (de Boer, 2010 and Darrow, 2011).

3.2.6 Carbohydrate Binding Specificity

The presence of a galactose is required for all galectin binding. However, the binding affinity is greatly enhanced if the galactose monomer is attached to other saccharides, such as in polylactosamines (Dumic, 2006). Studies of the carbohydrate binding specificity of LGALS3 have shown that N-acetyllactosamine is its preferred ligand (Sato, 1992). Furthermore, X-ray crystallography studies show that LGALS3 can bind to longer oligosaccharides created by the O-linked glycosylation of a terminal galactose such as in polylactosaminoglycans (Seetharaman, 1998). Glycoproteins that contain polylactosamines, such as laminin, and polylactosamine-rich lysosome-associated membrane proteins (LAMPS) are known to bind galectin-3. Galectin-3 also binds IgE and its receptor to induce mast cell activation (Frigeri, 1993). It also binds macrophage cell surface glycoproteins such Mac-1 (CD11b), Mac-3, and CD98. LGALS3 also binds glycoconjugates of the ECM such as fibronectin, elastin, and collagen IV,

and gp90, and can bind to cell-surface integrins, such as α1β1 and α3β1 integrins, thereby preventing their interaction with the ECM (Hughes, 2001). The binding of the CRD to a ligand induces a conformational change resulting in the rearrangement of the loops near the binding site (Umemoto, 2003). In addition, the phosphorylation of Ser6 has been shown to affect binding affinity, suggesting it to be an activating switch for LGALS3 (Mazurek, 2000).

3.2.7 The Intracellular Functions of Galectin-3

Various potential functions have been described for LGALS3 including roles in adhesion, pre-mRNA splicing, proliferation, apoptosis, migration, cell growth, and inflammation (Elola, 2007). Figure 3.4 summarizes the known intracellular functions of galectin-3. In the nucleus, LGALS3 is involved in pre-mRNA splicing through its association with ribonucleoprotein complexes and involvement in spliceosome assembly (Li, 2006). LGALS3 can also associate with ssDNA and RNA indirectly via binding gemin4. Importantly, LGALS3 has been implicated in the regulation of gene transcription. Binding to the transcription factors thyroid-specific transcription factor-1 (TTF-1), CREB, and SP1 stabilizes their interaction with DNA thus enhancing transcription promoting proliferation and cell cycle regulation. LGALS3 also regulates Wnt signaling by binding B-catenin and axin (Shimura, 2005). There is also evidence that LGALS3 may also bind and regulate the nuclear export of other proteins such as Suppressor of Fused (Sufu), a negative regulator of the Hedgehog signal transduction pathway (Paces-Fessy, 2004).

In the cytoplasm, galectin-3 regulates apoptosis by binding BCL-2, Fas, and Nucling. Binding to synexin has been shown to lead to LGALS3 localization to the outer mitochondrial membrane where it can serve an anti-apoptotic role (Glinsky, 2009 and Takenaka, 2004). Other cytoplasmic binding partners include cytokeratins and CHRP, a cysteine-histidine-rich protein, although the biological function of these interactions is not known (Dumic, 2006).

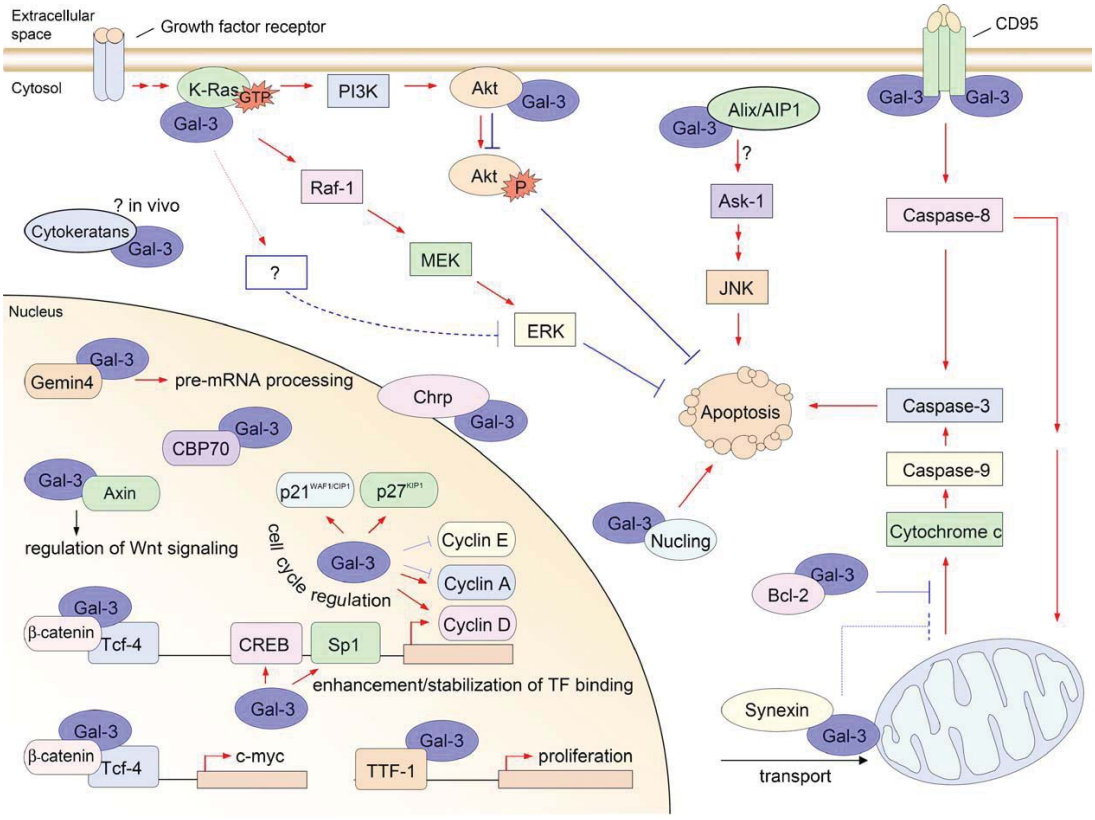

Figure 3.4. Putative intracellular binding partners and functions of galectin-3 (from Dumic, 2006).

3.2.8 The Extracellular Functions of Galectin-3

Extracellular LGALS3 can interact with components of the ECM including laminin, collagen IV, and elastin in order to modulate cell adhesion (Figure 3.5)

(de Boer, 2010). The addition of recombinant LGALS3 or the overexpression of the protein in various cancer cells types has been shown to enhance adhesion and spreading (Elola, 2007). However, the addition of soluble galectin-3 to cells already adhered to the ECM by other cell surface receptors such as integrins may also promote de-adhesion (Elola, 2007). LGALS3 also promotes cell-cell adhesion by cross-linking with carbohydrate ligands on the surface of adjacent cells (Elola, 2007). Galectin-3 expressed on the surface of endothelial cells has been shown to mediate adhesion of several carcinoma cell types, and this is inhibited by the addition of anti-LGALS3 antibodies (Khaldoyanidi, 2003 and Krishnan, 2005). Finally, LGALS3 is upregulated on the endothelial cell surface during adherence and migration of polymorphonuclear leukocytes in vitro (Gil, 2006).

This lectin also plays a role in cell migration. LGALS3 serves as a chemo-attractant for monocytes and macrophages via a G-protein-coupled pathway, and may be involved in the migration of these cells to areas of inflammation (Sano, 2000). Furthermore, galectin-3 induces the proliferation and migration of vascular smooth muscle cells (Seki, 2003). It may also be involved in mediating NG2 proteoglycan-induced motility by forming a NG2-lgals3-α3β1 integrin complex, leading to the recruitment of endothelial cells to sites of neovascularization (Fukushi, 2004).

Importantly, galectin-3 is a component of the advanced glycation endproduct (AGE)–receptor complex expressed on the surface of endothelial cells, which is linked to the binding and removal of AGEs from the circulation

(Stitt, 1999). AGEs are formed through the nonenzymatic glycation of macromolecules by reducing sugars in a process known as the Maillard reaction (Degenhardt, 2002). The AGE receptor complex consists of p60 (AGE-R1), p90 (AGE-R2), and galectin-3 (AGE-R3). AGE-R1 is involved in AGE binding and uptake while R2 and R3 are implicated in signal transduction and cell activation. The involvement of AGE-R2 in signal transduction is suggested by its increased phosphorylation after exposure to AGE-BSA (Stitt, 1999). AGE-R2 is a PKC substrate and is phosphorylated upon FGF stimulation leading to binding of Grb2 and Sos and activation of the MAPK pathway (Pricci, 2000). The role of galectin-3 in this complex is less clear. Studies in galectin-3 deficient mice have shown an increased accumulation of AGES leading to accelerated glomerularopathy (Pugliese, 2001), rather than decreased AGE-induced cell activation.

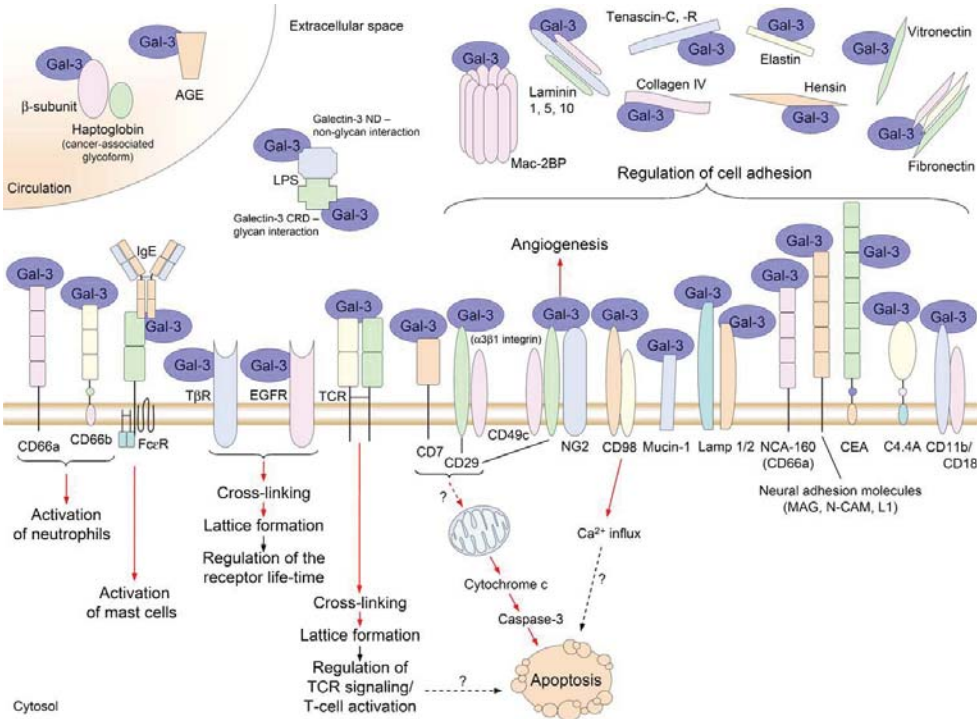

Figure 3.5. Putative extracellular binding partners and functions of galectin-3 (From Dumic, 2006).

3.2.9 Role in Diabetes

In diabetes, hyperglycemia and oxidative stress enhance the glycation reaction, leading to increased amounts of AGE-modified proteins (Forbes, 2005). Increased exposure of cultured human umbilical vein endothelial cells (HUVEC) to AGEs has been shown to upregulate galectin-3 mRNA and protein levels in a time-dependent manner (Stitt, 1999). Ablation of galectin-3 has also been shown to reduce AGE-mediated retinal ischemia and to restore the neovascular response in mice treated with AGEs (Stitt, 2005). The cellular uptake of AGEs by galectin-3 may contribute to diabetic vasculopathy *in vivo*.

The galectin-3 knockout has previously been used to study the role of galectin-3 in a murine model of type I diabetes. *Lgals3*(-/-) mice with streptozotocin-induced diabetes develops accelerated glomerulopathy and increased renal accumulation of AGEs, implying that galectin-3 protects against AGE-induced injury (Pugliese, 2001). However, another study suggests that LGALS3 is pro-diabetogenic rather than protective. Mensah-Brown et al. (2009) has shown that the galectin-3 knockout is more resistant to diabetogenesis following STZ treatment, has lower expression of inflammatory cytokines, and possesses macrophages with a reduced ability to produce TNF-α and nitric oxide. Also in the STZ model, *Lgals3(-/-)* mice display less dysfunction of the inner blood-retinal barrier due to decreased permeability of the endothelium (Canning, 2007).

Galectin-3 has also been implicated in cardiovascular disease and atherosclerosis. In mouse models of heart failure, the levels of *Lgals3* in

decompensated hearts is 5-fold upregulated compared to compensated hearts, and LGALS3 has been implicated in fibroblast activation and inflammation (de Boer, 2010). Also, galectin-3 protein expression has been shown to increase in human atherosclerotic lesions compared to the aorta of healthy controls where it was primarily localized to foam cells (Nachtigal, 1998). In addition, *Lgals3* was previously found to be highly upregulated in whole aorta of *db/db* mice and mice with diet induced obesity (Mzhavia, 2008). Galectin-3 has been shown to modulate the endocytotic uptake of modified LDL in CHO cells overexpressing LGALS3 (Zhu, 2001). In vitro, galectin-3 treatment of macrophages induced monocyte activation and chemoattraction (Papaspyridonos, 2008). *Apoe(-/-)/ Lgals3(-/-)* mice demonstrated fewer atherosclerotic lesions and plaques compared to *ApoE(-/-)* mice (Nachtigal, 1998 and Mackinnon, 2013). Administration of the galectin-3 inhibitor, modified citrus pectin, reduced plaque volume in *ApoE(-/-)* mice (Mackkinon, 2013). However, galectin-3 knockout mice fed an atherogenic diet for 8 months showed increased lesion area and length compared to wild-type mice (Iacobini, 2009).

These studies suggest an important role for galectin-3 in vascular complications. However, the conflicting reports and the lack of data regarding the role of galectin-3 in type II diabetes and its associated vasculopathy emphasize the need for further studies. In chapter 2, we have shown increased expression of galectin-3 in the aortic and muscle endothelium of a mouse model of type 2 diabetes. We also found that serum galectin-3 levels were substantially increased in our HFD model. A recent study has similarly reported an elevation

of systemic galectin-3 in obese and type II diabetic patients compared to normal weight individuals (Weigert, 2010). Thus, we hypothesize that the upregulation of galectin-3 in the endothelium contributes to the vascular pathology observed in type II diabetes. LGALS3's putative function in pre-mRNA splicing and transcription factor stabilization and the finding that galectin-3 ablation leads to altered expression of other AGE receptors, suggests that galectin-3 may regulate gene expression, which can be identified by microarray analysis. The goal of this study is to identify the role of this multifunctional lectin in the development of endothelial dysfunction induced by type II diabetes. We explore the transcriptional response of the endothelium to a high-fat diet in wild-type and galectin-3(-/-) mice. *In vitro* studies utilizing endothelial cells were also performed to extend our microarray findings, interrogate single components of the diabetic milieu, and assess endothelial function in a more controlled environment. These studies have defined the role of galectin-3 in endothelial dysfunction and insulin resistance and help to elucidate the pathogenesis of diabetic vasculopathy.

3.3 Methods

3.3.1 Animals and Diet

Mice homozygous for a targeted deletion within the galectin-3 gene (KO) [B6.Cg-*Lgals3*^{tm1Poi}/J, stock no. 006338 Jackson Laboratories (Bar Harbor, ME)] and wild-type C57BL/6J (WT) (stock no. 000664) were bred for these experiments. The galectin knockout was generated by a 3.7kb deletion of exons 2-4, including the initiating codon in exon 2 (Fig. 3.6). Genetic deletion of

galectin-3 was confirmed at the DNA level by 2% agarose gel electrophoresis and also at the RNA and protein level by real-time PCR and Western blotting, respectively, as described below.

Beginning at 8 weeks of age, male KO and WT mice were allowed to feed ad libitum on a high-fat diet (HFD) containing 60% fat calories (BioServ, Frenchtown, NJ, cat. no. S3282) or a normal chow diet containing 12% fat calories (LabDiet, St. Louis, MO, cat. no. 5001) for a period of 8 weeks. All procedures were approved by the Institutional Animal Care and Use Committee of the University of Hawaii.

3.3.2 Assessment of Metabolic Characteristics

3.3.2.1 Fasting Glucose Levels and Glucose Tolerance Test

Before the start of the diet and after 2, 4, 6, and 8 weeks on their respective diets, glucose levels were determined by glucometry of tail blood following an overnight fast (OneTouch Ultra, Lifescan, Milpitas, CA). A glucose tolerance test (GTT) was performed after 5 weeks on the diet. Glucose (1 mg/g of body weight) was administered i.p. following an overnight fast. Glucometry of the tail blood was performed prior to glucose injection and every 20 minutes afterwards for 2 hrs. The area under the curve (AUC) was determined using the statistical software in Graphpad.

3.3.2.2 Determination of Serum Insulin Levels

Two hundred µL of blood was collected from the tail vein, allowed to clot, and centrifuged at 5000rpm for 10 min to separate serum. Following an overnight fast, serum insulin levels were measured at 0, 2, 4, 6, and 8 weeks by ELISA

(Mercodia, Uppsala, Sweden, cat. no. 10-1149-01). The homeostasis model assessment of insulin resistance (HOMA-IR) was calculated using the fasting glucose and insulin concentrations at 8 weeks on the diet using the following formula: [fasting blood glucose (mg/dL) x fasting insulin (μIU/mL)] / 405 (Akagiri, 2008), where 1mg insulin= 26IU (Bristow, 1988).

3.3.2.3 Measurement of Vascular Insulin Resistance

Following 8 weeks on the diet, 3-6 control and 5-8 high-fat fed mice of each strain received an i.p. injection of insulin (0.06 U/g body weight in 300μL of sterile saline); 1-2 animals of each group received vehicle (normal saline). Mice were sacrificed 15 minutes after injection. The thoracic aorta and skeletal muscle were excised, dissected from adherent fat, and snap frozen in liquid nitrogen. Protein was subsequently extracted from the tissue and phospho-AKT (serine 473) levels were determined by Western blotting and normalized to total AKT protein as described below.

3.3.2.4 Advanced Glycation Endproduct ELISA

Following 8 weeks on the diet, blood was collected by cardiac puncture and serum was separated as previously described. Serum protein concentration was quantified by Bradford Assay and diluted to 5mg/mL. Advanced glycation endproducts in the serum were quantified by ELISA (Wuhan EIAAB Science, Co., China, cat. no. E0263m) and normalized to total protein.

3.3.3 Protein Analysis

Tissues snap-frozen in liquid nitrogen were crushed into pieces using a stainless steel mortar and pestle on dry ice. The powder was then transferred to

a tube containing cold protein lysis buffer (75mM NaCl, 40mM NaF, 10mM iodocetamide, 50mM Hepes, 1% IGEPAL 1mM Na_3VO_4, 0.25mM PMSF) containing protease inhibitors (cOmplete, Mini Protease Inhibitor Cocktail Tablets, Roche, Indianapolis, IN, cat. no. 11836153001) and disrupted using a mechanical homogenizer. Protein concentrations of the cleared supernatants resulting from centrifugation at 12,000rpm were quantified by Bradford assay. Fifty µg of denatured aorta or 30µg of skeletal muscle protein were loaded onto Bio-Rad Criterion XT, 12%Bis-Tris polyacrylamide gels (cat. no. 345-0117) and run under reducing conditions in XT MOPS Running Buffer (Bio-Rad, Hercules, CA, cat. no. 161-0788). Proteins were transferred to a Millipore Immobilon P membrane in cold Efficient Western Transfer Buffer (G Biosciences, St. Louis, MO, cat. no. 786-019) prepared as instructed and followed by blocking in 5% nonfat dried milk for 1hr. Membranes were incubated overnight in primary antibody at 4ºC with rocking. Following washes in TBST, the membrane was incubated with Alexa Fluor®568-conjugated secondary antibody (Invitrogen, Carlsbad, CA) or IRDye 800CW secondary antibody (LI-COR Biosciences, Lincoln, NE) for 1 hr at RT. Membranes were washed and imaged using a Typhoon (Amersham) or LI-COR imager. Blots were stripped and probed for GAPDH or other normalizing control. Band intensity was quantified by performing densitometry using ImageJ (Schneider, 2012). Primary antibodies include rabbit anti-mouse p-AKT and rabbit anti-mouse AKT (Cell Signaling, Beverly, MA, cat. nos. 9271 and 9272), rat anti-mouse LGALS3 monoclonal antibody (Santa Cruz

Biotechnology, Santa Cruz, CA, cat. no. sc-23938), and anti-GAPDH mouse monoclonal antibody (Calbiochem, CB1001).

3.3.4 Endothelial Cell Isolation

Following 8 weeks on the diet regimen, animals were sacrificed by CO_2 asphyxiation. In each experiment, for each diet, pooled cells from 3 KO and 3 WT mice were collected for each tissue. Aortae from the aortic root to the iliac bifurcation were dissected. Leg muscles consisting of the plantaris, gastronemius, and biceps femoris (which are readily dissected as a single group) were excised. Tissues were placed into ice cold PBS and freed of adherent fat. The aortic and skeletal muscle tissues from 3 animals were each pooled, minced into 1 mm fragments, and dispersed as previously described (Darrow, 2011). Suspensions of collagenolytically separated cells were incubated with anti-mouse CD16/32 (1:500) for 5 min and then with phycoerythrin-conjugated anti-mouse CD45 (1:800) and CD105 eFluor®450 (1:20) for 25 minutes on ice (eBiosciences, cat. nos. 14-0161, 17-0451, and 48-1051). Immediately before sorting, 5µl of Dead Cell Discriminator (Life Technologies, Carlsbad, CA, cat. no. DCD00) was added per 100µl of cell suspension. Roughly 10,000 live endothelial cells positive for CD105 staining and negative for CD45 were isolated with a FACSAria (Becton Dickinson, Franklin Lakes, NJ) directly into Trizol (Invitrogen, Carlsbad, CA). RNA was purified with RNeasy columns (Qiagen, Valencia, CA) and then amplified using an Ambion® Amino Allyl MessageAmp kit (Life Technologies, Carlsbad, CA) according to the manufacturer's protocol to produce approximately 100µg of amino-allyl modified cRNA.

3.3.5 Gene Expression Analysis

3.3.5.1 Microarray Analysis

Microarray analyses were performed to determine the transcriptional responses in aortic and skeletal muscle endothelium from KO vs. WT mice exposed to either high-fat diet or control diet for 8-weeks. Amino-allyl modified cRNA was labeled with Cy3 CyDye™ Post-Labeling Reactive Dye Pack (GE Healthcare, Waukesha, WI) according to the manufacturer's instructions. Following purification, 1.6 µg of Cy3 dye-labeled cRNA, as measured by NanoDrop 2000c spectrophotometer (Thermo Scientific, Bellerica, MA), were combined and fragmented. Biological triplicate experiments were performed for both tissues and both diets for each strain. Samples were hybridized overnight to glass slides spotted with the Whole Mouse Genome Array Kit from Agilent (Santa Clara, CA, cat. no. G4122F), which includes 44,000 murine oligonucleotides representing all known genes and transcripts of the mouse genome along with positive controls. The set of 3' biased, 60-mer oligos are synthesized *in situ* using Agilent SurePrint technology. The content is sourced from RefSeq, RIKEN, NIA, Ensembl, UCSC, Goldenpath, and Unigene databases and verified against the NCBI genome build 32. This set interrogates distinct exons of the same gene, allowing characterization of splice variants upon array hybridization and analysis. Annealed fluorescent labels were quantified with Agilent dual channel scanner, and data analysis subsequently performed with GeneSpring® and Acuity® software. For both the KO and WT strains, transcripts exhibiting upregulation (a $\log_2$[fold change] >1) or downregulation ($\log_2$[fold change] <-1) by HFD vs. chow

diet that were found consistently dysregulated in all 3 biologically replicate experiments were tabulated for each tissue. This comparison represents the endothelial response to diabetes in either strain.

3.3.5.2 Pathway Analysis

The gene expression data was further interrogated using Ingenuity Pathway Analysis (IPA) (Ingenuity® Systems, www.ingenuity.com). Datasets consisting of all transcripts differentially expressed >0.75 $\log_2$[fold change] by high-fat feeding in the WT and KO strains were uploaded into IPA. Over-represented Biological Functions in the aortic endothelium of each strain after HFD were identified based on weighted gene co-expression. IPA was also performed on differentially regulated transcripts between KO HFD and WT HFD animals. Unlike the response to HFD, this comparison also considers baseline genetic differences between the strains in addition to the response to HFD. Differential Canonical Pathways in the aortic endothelium of KO mice vs. WT mice after 8 weeks of HFD were identified.

3.3.5.3 Real-time PCR

Microarray results were confirmed by semi-quantitative real-time polymerase chain reaction (RT-PCR or qPCR) performed on 3 biological replicate experiments. Complementary DNA was synthesized by the reverse transcription of 1µg of amplified RNA from the sorted endothelial cells using qScript (Quanta Biosciences, Gaithersburg, MD). Oligonucleotide primers were designed to generate amplicons of length 100-200 nucleotides and to span at least one intron. Primer sequences are listed in Appendix Table 2. cDNA

representing 5 ng of total RNA was amplified by PCR performed using SYBR® green fluorophore (Roche, Indianapolis, IN) in an Applied Biosystems® 7900HT fast real-time PCR system. A standard two-phase reaction (95°C 15sec, 60°C 1 min) worked for all amplifications. Dissociation curves run for each reaction verified the presence of a single amplicon peak.

Fold changes represent the ratio of HFD to control diet expression values determined from the cycle times where C_T, the threshold intensity, was exceeded. The abundance of Cyclophilin A was assessed in parallel as a loading control to which the genes of interest were normalized.

3.3.6 Measurement of Prothrombin Time

After 8 weeks of high-fat diet, blood was collected by cardiac puncture following CO_2 asphyxiation into tubes containing sodium citrate anticoagulant at a ratio of 9:1. Plasma was separated by performing two centrifugation steps at 5000rpm for ten minutes each. Prothrombin time was assessed using a Diagnostica Stago STArt 4 Hemostasis Analyzer according to the manufacturer's protocol. Briefly, the time to coagulation was recorded following the addition of the calcium thromboplastin reagent Neoplastine CI Plus 5 (Diagnostica Stago, France, cat. no. 00606). Immediately before measurement, plasma was diluted 1/5 with Stago diluent buffer.

3.3.7 GLUT4 Immunofluorescence

Animals were sacrificed after 8 weeks on the diet regimen and perfused with PBS. Segments of the thoracic aorta and the entire skeletal muscle were immediately frozen in TissueTek® Optimal Cutting Temperature (O.C.T.)

Compound on dry ice. Ten micrometer sections were rehydrated in PBS, permeabilized with 0.3% Triton-X-100, and incubated overnight with rabbit anti-glucose transporter GLUT4 antibody (Abcam, Cambridge, MA, ab654) at 1:50 followed by Alexa Fluor®568 goat anti-rabbit IgG (Invitrogen) at 1:800. Stained sections were mounted in fluorescence mounting medium containing DAPI. Images were collected under controlled exposure and gain settings with an Eclipse 80i (Nikon, Tokyo, Japan) with SPOT™ software (SPOT™ Imaging Solutions, Sterling Heights, MI). Six aortic and 2 skeletal muscle sections from 3 WT and 4 KO mice per diet group were stained for GLUT4. The mean fluorescence intensity of GLUT4 staining in the skeletal muscle was determined using ImageJ to quantify the fluorescence intensity of 20 myofibers from each mouse.

3.3.8 *In vitro* Experiments

Human aortic endothelial cells (huAoECs) and human cardiac microvascular endothelial cells (CMVECs) were cultured in Endothelial Cell Growth Medium MV with supplement mix (PromoCell, Heidelberg, Germany, cat. no. C-22020) and used at passages 3-8. For high-glucose experiments, media containing 5mM glucose was supplemented with 25mM glucose or mannitol. Cells were treated with high-glucose (30mM) or the osmotic control, mannitol, for 2-10 days. For oxidized LDL experiments, HuAoECs were treated with 40µg/mL oxidized LDL (Biomedical Technologies, Inc., Stoughton, MA, cat. no. BT-910) for 24-48 hrs compared to media alone. To determine galectin-3 expression in response to advanced glycation endproducts, HuAoECs were treated with

100µg/mL glycated-BSA (AGE-BSA, BioVision, Milpitas, CA, cat. no. 2221-10), BSA alone (cat. no. 2221-BSA), or media for 4 days as previously described (Stitt, 1999). Following treatments, cells were washed and harvested in Trizol for RNA extraction or lysis buffer for protein analysis. mRNA and protein expression of galectin-3 was assessed by qPCR and Western blotting as previously described.

3.3.9 Histological Evaluation of Cardiac Fibrosis

PBS-perfused hearts obtained from 4 WT and 4 KO mice after 8 weeks of HFD or chow diet were fixed in 4% paraformaldehyde and embedded in paraffin. 5µm sections were stained with 0.1% Sirius Red in saturated picric acid (Electron Microscopy Sciences, Hatfield, PA, cat. no. 26357-02) following staining in Weigert's haematoxylin. Images were obtained using the Axioscope2 photomicroscope (Zeiss, Oberkochen, Germany) with brightfield illumination.

3.4 Results

3.4.1 Confirmation of *Lgals3* genetic deletion

Homozygous KO mice were purchased from Jackson Labs, and the genetic deletion of *Lgals3* was confirmed at the DNA, RNA, and protein level. The construct for the genetic deletion of the 3.7kb segment of the *Lgals3* gene is shown in Figure 3.6A. Agarose gel electrophoresis shows a band at 150bp for the mutant allele and 220bp for the wild-type allele (Fig. 3.6B). RT-PCR was also run on aortic and skeletal muscle endothelial RNA to confirm the absence of gene transcription, which did not amplify any product in the samples from KO

animals when using primers designed within the deleted regions (Fig. 3.6C). The absence of protein was confirmed by Western blotting for LGALS3 in aortic lysates (Fig. 3.6D).

3.4.2 Metabolic Characterization of the Galectin-3(-/-) Type II Diabetic Mouse Model

As expected, both KO and WT mice on HFD have significant weight gain compared to chow-fed controls, and this weight gain is similar between the strains (Fig. 3.7A). Before the onset of the diet regimen, it was evident that *Lgals3(-/-)* mice displayed elevated fasting glucose levels compared to WT (153$\pm$ 51 mg/dL vs. 95 $\pm$ 15 mg/dL, n = 21-32, $P < 0.0001$). After 2 weeks of high-fat feeding, KO mice display a sharp increase in fasting glucose levels, which remained high for the remainder of the study; whereas fasting glucose levels of WT mice on HFD increased at a steady rate until reaching significance at 4 weeks (wk) and then leveled off (Fig. 3.7B). By the completion of the 8wk diet regimen, fasting glucose of the KO was significantly higher than that of the WT on either chow or HFD (Fig. 3.7D). However, the percent increase in fasting glucose levels resulting from the HFD was similar between the two strains (60% vs. 59% in WT).

Although glucose levels were significantly altered in the KO mice compared to WT mice, fasting insulin levels were consistently lower in the KO over the time course of the feeding (Fig. 3.7C). By 8 weeks of feeding, insulin levels were similar between the 2 strains (Fig. 3.7E). Due to higher glucose levels and similar insulin levels, HOMA-IR is higher in KO vs. WT on chow and

HFD, but not significantly (Fig. 3.7F). After 5 weeks of HFD, both WT and KO mice have significantly impaired glucose tolerance as shown by the GTT, but this impairment is more severe in the KO (Fig. 3.7G). While the glucose of the WT begins to decline steadily after 40 min., the glucose of the KO remains elevated until 100 min. after glucose administration. Furthermore, exposure to HFD for 8 weeks did not result in a reduced response to insulin as reflected by similar levels of skeletal muscle AKT phosphorylation following an *in vivo* insulin challenge in both KO and WT mice on HFD (Fig. 3.8B). However, reduced levels of phosphorylated AKT were observed in aortic tissue lysates from both strains after HFD, indicating a state of vascular insulin resistance (Fig. 3.8A). Also, circulating levels of advanced glycation endproducts do not increase after only 8 weeks of HFD compared to chow diet, and levels are similar between the two strains (KO HFD: 1.8 $\pm$ 0.7 ng/mg protein; KO Chow: 1.7 $\pm$ 0.3 ng/mg protein; WT HFD and Chow: 1.7 $\pm$ 0.3 ng/mg protein; n=9 for HFD and n=7 for Chow).

3.4.3 Endothelial Cell Isolation

Endothelial cells were sorted by FACS based on positive expression of the endothelial cell-surface glycoprotein, endoglin (CD105). Endoglin is a component of the TGF- β receptor complex and is important in angiogenesis (Fonsatti, 2004). While predominantly expressed in endothelial cells, endoglin may also be expressed on activated monocytes and tissue macrophages (Khan, 2005). Therefore, we also stained for the common leukocyte antigen, CD45, and excluded all $CD45^+$ cells from our sorting gate. FACS sorting yielded approximately 10,000 $CD105^+/CD45^-$, live cells from each pooled sample. Figure

3.9 shows representative FACS profiles of skeletal muscle and aortic tissue digests, with the sorted endothelial cell population representing 5.7% and 6.6% of the live cell populations.

3.4.4 Microarray Results and Pathway Analysis

Tables 3.1 and 3.2 display fold-change of selected transcripts with $|\log_2[\text{fold change}]| > 1$ in all 3 distinct aortic or skeletal muscle endothelial hybridization experiments for both WT and KO strains fed a HFD compared to chow diet. These transcripts were selected based on level of dysregulation or for their roles in diabetic or cardiovascular pathophysiology or known connection to galectin-3. Venn diagrams showing the number of similarly and differentially dysregulated transcripts in KO and WT animals after HFD are shown in Figure 3.10. Transcripts dysregulated by HFD with $|\log_2[\text{fold change}]| > 1$ common to both aortic and muscle endothelium of each strain are presented in Table 3.3.

Data analysis using IPA revealed “Cardiovascular System Development and Function” as a top over-represented biological function. Transcripts involved in this function have been divided into subcategories and presented in Table 3.4. Analysis of differentially regulated aortic endothelial transcripts between KO HFD and WT HFD mice revealed the Coagulation Cascade to be a highly upregulated pathway in the KO. Log_2 fold change [diabetic KO / diabetic WT] of transcripts belonging to this canonical pathway are shown in Figure 3.11.

3.4.5 Physiological Assessment of Coagulation Pathway Activity

Due to the upregulation of transcripts involved in the coagulation pathway in the aortic endothelium from KO diabetic mice compared to WT diabetic mice,

coagulation activity was assessed in the plasma of WT and KO mice after 8 weeks of high-fat or chow diet. While no difference in prothrombin time (PT) was observed between chow-fed KO and WT animals, high-fat-fed KO animals displayed reduced PT compared to chow-fed controls and high-fat-fed WT mice (Fig. 3.12). Therefore, coagulation pathway activity is increased in diabetic KO mice after 8 weeks of HFD.

3.4.6 Real-Time PCR

The expression levels of some dysregulated transcripts were confirmed by real-time PCR. These genes include caveolin-3 (*Cav3*), insulin receptor substrate-1 *(Irs-1*), glucose-6-phosphatase (*G6pc*), ceruloplasmin (*Cp*), the glucose transporter *Glut4*, resistin-like alpha (*Retnla*), prostaglandin F receptor (*Ptgfr*), macrophage receptor with collagenous structure (*Marco*), lymphatic vessel endothelial hyaluronan receptor 1 (*Lyve1*) and insulin-like growth factor 1 (*Igf1)* and its receptor, *Igf1r*. The real-time PCR expression levels of the cDNA transcribed from the cRNA are presented in Figure 3.13 as Log_2 fold change [diabetic / control] for KO and WT strains.

3.4.7 GLUT4 Expression in Skeletal Muscle and Aortic Endothelium

Immunofluorescence staining for GLUT4 in skeletal muscle sections from chow- and HFD-fed WT and KO mice, revealed reduced protein expression in both strains after 8 weeks of high-fat feeding compared to chow-fed controls (Fig. 3.14). In chow-fed animals, intense GLUT4 fluorescence was localized to the plasma membrane with staining in the cytosol as well (Fig. 3.14A). KO mice on

either diet displayed less GLUT4 fluorescence compared to the WT strain. Diabetic KO mice had greatly reduced levels of GLUT4, especially at the membrane, compared to all other groups (Fig. 3.14A,B). Staining for GLUT4 in aortic cross-sections revealed similar trends in the smooth muscle of the tunica media as that observed in the skeletal muscle (data not shown). In the aortic endothelium, similar levels of GLUT4 were observed in chow and HFD WT animals. However, KO mice fed a high-fat diet had less endothelial GLUT4 compared to chow-fed KO mice (Fig. 3.15).

3.4.8 *In vitro* Experiments

Basal expression levels of *Lgals3* are slightly higher in HuAoECs compared to CMVECS (Fig. 3.16A). Treatment of HuAoEC or CMVECs with high-glucose (30mM) for 2 and 5 days vs. the osmotic control mannitol appeared to increase galectin-3 mRNA expression slightly. However, by 7 days of treatment, *Lgals3* expression was high under both mannitol and glucose conditions. Western blotting for LGALS3 in HuAoEC and CMVEC protein lysates revealed similar trends- an increase in LGALS3 protein expression over the time course of the experiment, and relatively similar levels between mannitol and glucose treatment (Fig. 3.16B). Blotting of the HuAoEC and CMVEC supernatants following high-glucose and mannitol treatment did not show any secreted LGALS3 protein present (data not shown).

Treatment of HuAoECs with ox-LDL for 24 or 48hrs or AGE-BSA for 4 days did not show any increase in *Lgals3* expression over media or control BSA conditions (Fig. 3.16C). Similarly, intracellular LGALS3 protein expression was

not affected by BSA or AGE-BSA treatment compared to media alone (Fig. 3.16D), nor was LGALS3 protein detected in any of the supernatants even after immunoprecipitation (data not shown).

3.4.9 Cardiac Fibrosis

Because of the putative role of LGALS3 in cardiac fibrosis and ECM synthesis, hearts of diabetic KO and WT mice were analyzed for collagen deposition following 8 weeks of high-fat diet. PicroSirius staining did not show any signs of collagen deposition beyond that of chow-fed controls (Fig. 3.17A). Expression of the pro-fibrotic cytokine, CTGF, was also assessed by real-time PCR. WT animals expressed slightly increased levels of *Ctgf* compared to KO animals on either chow or HFD, but this difference was not significant after 8 weeks of HFD (Fig. 3.17B).

3.5 Discussion

The galectin knockout mouse displays higher glucose levels before the onset of high-fat feeding at 8 weeks of age. At the end of the 8 week diet regiment, both chow- and high-fat-fed KO mice display hyperglycemia compared to WT. No other characteristics of metabolic syndrome are evident in the chow-fed KO mice as demonstrated by normal weight and insulin levels, and normal response to glucose challenge. This model of isolated hyperglycemia may be useful to elucidate pathways specifically related to increased glucose.

Mice on HFD exhibit the expected characteristics of diabetes: increased weight gain, elevated fasting glucose and insulin levels, and reduced response to glucose challenge. However, the degree of metabolic derangement is more

extreme in the KO compared to the WT on HFD. By 8 wks of high-fat feeding, KO mice display significantly increased fasting glucose levels compared to WT (Fig.3.7D). After 2 weeks of HFD, KO mice exhibit a dramatic and significant increase in fasting glucose levels vs. chow-fed controls, whereas WT levels increase more slowly over time and do not differ significantly from chow-fed controls until 4 weeks on the diet (Fig.3.7B). While the WT mouse seems to maintain lower glucose levels by compensating with increased insulin output, insulin secretion in the KO is not proportionally increased (Fig. 3.7E). This data suggests that the KO mice may be experiencing hepatic insulin resistance or impairment of insulin production/ secretion at earlier timepoints than WT mice on HFD.

By 5 weeks of HFD, both WT and KO animals display impaired glucose tolerance as demonstrated by GTT (Fig. 3.7G). While first phase insulin release is delayed in both strains, there is a prolonged second phase insulin response in diabetic KO animals vs. WT animals which is significantly different at 80 min. after glucose challenge suggesting that KO mice may be experiencing greater peripheral insulin resistance. However, even after 8 weeks of HFD, peripheral insulin resistance in the skeletal muscle is not yet observed in either KO or WT mice on HFD as demonstrated by similar levels of AKT phosphorylation compared to chow-fed controls (Fig. 3.8B). However, vascular insulin resistance is observed in diabetic KO and WT mice after this diet duration (Figure 3.8A). This is consistent with the findings of Kim *et al*., who reported that peripheral insulin resistance begins around 8 weeks of HFD whereas vascular insulin

resistance occurs earlier. Our previous studies have shown that vascular insulin resistance occurs by 5 weeks on this diet in mice of the FVB/N strain. Interestingly, circulating levels of advanced glycation endproducts (AGEs) are similar between both strains and are not elevated by 8 weeks of high-fat diet. Therefore, the differential responses we observe between the KO and WT are likely to be independent of galectin-3's role as an AGE-binding protein.

In vitro experiments were performed using human aortic endothelial cells and cardiac microvascular endothelial cells to study galectin-3 expression following treatment with isolated components of the diabetic milieu in hopes of elucidating LGALS3 pathways. Treatment with ox-LDL, AGE-BSA, or high-glucose conditions showed little upregulation of galectin-3 mRNA or protein above basal levels in either cell type (Fig. 3.16). Expression of galectin-3 seems to correlate more with the age of the culture rather than the treatment condition as demonstrated by the similar increases in intracellular LGALS3 protein in high-glucose and iso-osmolar control conditions over the 10 day treatment period (Fig. 3.16B). *In vitro* studies using mesangial cells have demonstrated increased mRNA and protein expression of galectin-3 when cultured for 4 weeks in high-glucose conditions (Pugliese, 2000). Other studies show AGE-induced increases in LGALS3 expression in human umbilical vein endothelial cells (HUVECS) (Stitt, 1999), but we could not recapitulate these results in human aortic endothelial cells.

Pugliese et al. (2000) also noticed a difference in galectin-3 expression depending on the passage number and the proliferative phase of the culture.

Other studies in 3T3 fibroblasts have shown more LGALS3 expression in sparse cell cultures compared to confluent monolayers of quiescent cells (Moutsatsos, 1987). Therefore, we also performed experiments using sub-confluent cultures, but we found even lower levels of LGALS3 expression in the sparse, proliferating cultures and the same trend in increasing expression over the time course of the treatment (data not shown). Therefore, aortic endothelial expression of galectin-3 seems highly dependent on the culture conditions and age of the culture. Further studies are required to determine whether galectin-3 levels are already elevated due to stressful culture conditions, thereby masking the effect of the treatment. Although the endothelial cells have failed to show the anticipated responses *in vitro*, these experiments emphasize the value of performing *in vivo* experiments to elucidate endothelial responses.

Our FACS technique of sorting endothelial cells based on endoglin expression identified 6-7% of live $CD45^-$ cells in our tissue digests as endothelial cells (Fig. 3.9). Using this same technique on GFP^+ endothelial cells from Tie2-GFP mice shows a large percentage of overlap between GFP and endoglin signal. Although there were some non-GFP cells that appeared to stain for endoglin, these populations were eliminated by gating for live cells, which exclude propidium iodide, and CD45 negative cells. The specificity of the endoglin antibody was also tested on C2C12 muscle cells, which showed no endoglin positive cells. This technique was much more specific and stained a greater number of GFP^+ endothelial cells than CD31, TIE2, or CD146 antibodies tested. However, we are also backcrossing *Lgals3(-/-)* mice with Tie2-GFP mice

in order to sort based on GFP^+ expression, which we have previously found to be highly effective for EC isolation.

Our assessment of the endothelial response to diabetes in KO and WT mice has shown a greater response in the aortic endothelium of KO mice compared to that of WT mice as evidenced by the number of differentially regulated transcripts. We identified 158 transcripts with greater than 2 [$\log_2$ fold-change] in the aortic endothelium of KO mice; whereas diabetic WT mice had less than half this number dysregulated to the same degree (Fig. 3.10). In the capillary endothelium of the skeletal muscle, there was less dysregulation by HFD in both strains compared to the large vessel endothelium, which we have previously observed in Tie2-GFP mice as well, and attribute to the diversity of endothelial cell populations and the later onset of muscle insulin resistance vs. vascular IR. This data may also suggest a greater role for galectin-3 in the macrovasular complications of diabetes compared to microvascular disease.

In the aortic endothelium of the diabetic KO, a number of transcripts with recognized roles in metabolic signaling, ECM synthesis, vasoconstriction, coagulation, and inflammation are differentially dysregulated compared to the diabetic WT endothelium. The glucose transporter, *Glut4*, is downregulated by HFD in both strains, but its reduction in the KO is twice as much as WT (Table 3.1). Similarly, expression of *Irs-1*, insulin-induced gene 1, *Igf1*, and glucose-6 phosphatase are dysregulated to a greater degree in the KO vs. WT on HFD (Fig. 3.13). The exacerbated response of the KO aortic endothelium to HFD

suggests a greater derangement of metabolic signaling in these cells and implicates LGALS3 in the preservation of such pathways.

Furthermore, the exacerbated upregulation of PKCα in the KO may result from their excessive glucose levels. High glucose concentration activates PKC directly by increased DAG synthesis or indirectly by the activation of the polyol, hexosamine, or 12/15-lipoxygenase pathways (Gleissner, 2007). PKCα has been shown to mediate SMC proliferation through TGF-β. Other PKC isoforms have been implicated in glucose-induced upregulation of the LOX-1 scavenger receptor and the upregulation of adhesion molecules in HUVECs resulting in increased adherence of monocytes to the endothelium (Gleissner, 2007).

In the skeletal muscle endothelium, transcripts with roles in glucose homeostasis are also differentially downregulated by HFD in the KO compared to WT animals. qPCR shows *Glut4* to be downregulated nearly 4-$\log_2$ fold in the KO after high-fat feeding, whereas it is downregulated less than 1-$\log_2$ fold in the WT (Fig. 3.13). Microarray analysis also shows the downregulation of the adenosine A2 receptor, which has been shown to be upregulated by HFD in liver, fat, and muscle after a high-fat diet and serves a protective role in glucose homeostasis as knockout mice exhibit impaired glucose tolerance and insulin signaling (Johnston-Cox, 2012). Transcripts implicated in atherosclerosis are also dysregulated in the endothelium. HDL binding protein, which is normally expressed by endothelial cells, is downregulated by HFD in the WT but not the KO. This protein was upregulated in atherosclerotic lesions in human coronary arteries (Chiu, 1997). Low density lipoprotein receptor-related protein 1

(LDLRP1) is downregulated by HFD in the KO. This protein plays a role in the inhibition of macrophage apoptosis and monocyte recruitment, and its deficiency has been associated with increased atherosclerosis (Yancey, 2011).

Also, in the skeletal muscle endothelium, multiple transcripts involved in redox homeostasis are dysregulated in the KO, suggesting a reduced ability of the KO to manage oxidative stress. Metallothionone-1, oxidative-stress responsive 1, glutathione peroxidase 3, and glutathione-5-transferase are all more downregulated in the KO than WT diabetic muscle endothelium.

The downregulation of cyclin L1 is interesting in light of the putative role of galectin-3 in enhancing CREB and SP1 transcription factor binding to induce cyclin gene expression (Dumic, 2006). Also, the KO exhibits decreased expression of cAMP responsive element binding protein-like 2 (CREB-L2), a constitutively active transcription factor involved in CREB regulation and cell cycle transcription (Thiel, 2005). Another binding partner of LGALS3, IgE, that induces mast cell activation, is upregulated by HFD in the KO, but not as much as in the WT (Frigeri, 1993).

Expression of lipocalin-2 is downregulated twice as much in the KO vs. WT after HFD compared to chow-fed controls. Levels of lipocalin-2 have been correlated to expression of adiponectin and PPARγ. Its upregulation has been reported in adipose tissue and liver of *ob/ob* mice and adipocytes from Zucker obese rats (Zhang, 2008a). Recently, lipocalin deficiency was shown to protect against endothelial dysfunction in mice and lipocalin administration induced eNOS uncoupling and COX activation in arteries (Liu, 2012). Lipocalin induces

endothelial dysfunction by inhibiting the activity cytochrome P450 2C9, which is considered to be the endothelial derived hyperpolarizing factor in muscle endothelium (Clifford, 2004). In addition, expression of endothelin and its receptor are downregulated in the diabetic KO. Endothelin is a potent vasoconstrictor. The transcriptional downregulation of lipocalin and endothelin may be a protective mechanism against endothelial dysfunction.

Prostaglandin and thromboxane receptors are upregulated in both muscle and aortic endothelium of the KO after HFD (Table 3.3). The upregulation of the prostaglandin F receptor in the aortic endothelium by greater than 2-$\log_2$ fold was confirmed by qPCR (Figure 3.13A). Prostaglandins and thromboxanes are derived from fatty acids and are produced by the conversion of DAG into arachidonic acid which is oxidized by cyclooxygenases to produce prostaglandin or thromboxane. Both substances and their receptors are involved in vasoregulation, and thromboxane also plays a major role in platelet activation and aggregation. Similarly, transcriptional upregulation of *Marco,* in the aortic endothelium of the diabetic KO by more than 4-$\log_2$ fold over chow-fed controls was observed by array and qPCR (Table 3.1, Fig. 3.13A). MARCO is a macrophage scavenger receptor, which serves a role in the binding and uptake of modified LDL. This receptor has also been shown to be constitutively expressed in endothelial cells of the lymph nodes and upregulated by LPS exposure (Ito, 1999).

Similarly, the expression of coagulation factors is dysregulated in the endothelium of both tissues of the KO after high-fat feeding, suggesting potential

alterations in blood coagulation. Direct comparison of the diabetic KO and diabetic WT transcriptional profiles shows an upregulation of the coagulation cascade in the KO (Fig. 3.11). Transcripts for the zymogens prothrombin (FII), fibrinogen (FI), and Factor Xa (FX) are all upregulated in the KO, and their activation leads to the downstream activation of fibrin, promoting clot formation. We therefore assessed coagulation activity in the plasma from diabetic and chow-fed KO mice compared to WT mice. Diabetic KO mice exhibit reduced prothrombin time compared to diabetic WT mice and chow-fed controls (Fig. 3.12). Prothrombin time specifically measures activation of the extrinsic coagulation pathway, which is activated by tissue factor and involves factors VII, V, X, II and I. Therefore, the diabetic KO displays increased activation of the extrinsic coagulation pathway, which has important implications for diabetic patients where increased activation of the coagulation cascade promotes cardiovascular complications. In atherosclerosis, repetitive cycles of plaque rupture followed by coagulation and platelet aggregation promote thrombus formation and can lead to acute, ischemic events.

The transcript for von Willebrand factor (vWF), a protein important in platelet activation and aggregation, is also highly upregulated in the endothelium of diabetic KO mice compared to diabetic WT mice (Figure 3.11). Recent studies have shown that LGALS3 and LGALS1 interact directly with vWF in endothelial cells and in plasma via the N-linked glycans of vWF (Saint-Lu, 2012). The inhibition of these galectins was associated with increased vWF-platelet string formation and more rapid thombus formation after injury (Saint-Lu, 2012). We

have found that galectin-3 deficiency promotes vWF expression in the diabetic endothelium. Therefore, LGALS3 may be protective against thrombus formation in diabetes by inhibiting vWF-induced platelet aggregation.

The expression of several collagens, elastin, tenascin, and matrix remodeling proteins is also upregulated in the diabetic KO endothelium. Conversely, transcripts for proteins Involved in the degradation of ECM components are downregulated in the KO. *Lyve1* is a receptor for hyaluronic acid (HA), a matrix component that facilitates cell migration during wound healing and inflammation. *Lyve1* is expressed in lymphatic endothelial cells and is involved in the degradation of HA (Banerji, 1999). Its downregulation by 6-$\log_2$ fold in the skeletal muscle endothelium of the diabetic KO (Fig. 3.13) suggests decreased HA turnover and reduced ability for wound repair in the diabetic KO. LGALS3 has been shown to bind to these components of the ECM to regulate cell-matrix adhesion. In the liver, galectin-3 deficiency leads to decreased procollagen mRNA expression and collagen deposition (Henderson, 2006). KO mice have been shown to display reduced hepatic fibrosis, and LGALS3 was shown to be required for TGF-β mediated fibroblast activation (Henderson, 2006). In our model, LGALS3 deficiency generally leads to increased expression of ECM components, which differs from the models of liver fibrosis, but suggests a role for galectin-3 in the modulation of ECM production by endothelial cells.

The downregulation of GLUT4 protein in the aortic endothelium and skeletal muscle tissue of galectin-3(-/-) mice after 8 weeks of HFD was confirmed by immunofluorescence (Figs. 3.14 and 3.15). GLUT4 is the glucose transporter

required for cellular uptake of glucose. The reduced levels of GLUT4 protein may be responsible for the marked hyperglycemia observed in KO mice. Although upstream insulin signaling may not differ from WT diabetic mice as demonstrated by similar levels of phosphorylated AKT (Fig. 3.8), amount of GLUT4 protein available for translocation to the plasma membrane is decreased in the KO, leading to decreased glucose uptake.

Galectin-3 is also implicated in heart failure where it is upregulated 5-fold in decompensated heart failure vs. compensated heart failure and has also been shown to play a role in streptozotocin-induced cardiomyopathy (de Boer, 2010). Specifically, expression of LGALS3 leads to fibroblast activation into matrix-secreting myofibroblasts (Henderson, 2006). A recent study showed that galectin-3 KO mice display reduced vascular fibrosis in a model of aldosterone-induced hypertension (Calvier, 2013). Therefore, we investigated whether the KO and WT displayed any differences in cardiac collagen deposition after high-fat feeding. Although collagen deposition was not observed after 8 weeks of high-fat diet, there were increased levels of *Ctgf* expression in WT mice compared to KO (Fig. 3.17). CTGF is implicated in fibrotic pathology, and its' reduced levels in KO mice suggests a role for galectin-3 in cardiac fibrosis. However, these trends do not reach significance by 8 weeks of HFD. Thus, a longer duration of high-fat feeding or HFD combined with a stress or injury model may be required to confirm any difference in cardiac fibrosis between the KO and WT strains in the diabetic state. For this purpose, diabetic KO and WT mice could undergo

transverse aortic constriction (TAC) to elicit dilated cardiomyopathy and collagen deposition (Song, 2010).

Our analysis of the transcriptional response of the endothelium to an *in vivo* model of type II diabetes in galectin deficient vs. wild-type mice has revealed differential responses in both aortic and skeletal muscle tissues. The KO displays altered expression of transcripts with roles in the glucose-insulin signaling pathway, ECM composition, vasoregulation, redox homeostasis, inflammation, coagulation, atherosclerosis, and endothelial dysfunction. While a greater number of differentially regulated transcripts were observed in the macrovasculature compared to the microvasculature, commonly dysregulated transcripts were shared by the two vascular beds, suggesting ubiquitous roles of galectin-3. Downregulation of GLUT4 mRNA and protein in the endothelium and muscle of galectin-3(-/-) mice may explain the hyperglycemia experienced by these mice, and suggests a role for galectin-3 in the regulation of glucose disposal. Transcriptional upregulation of coagulation and pro-thrombotic factors and increased blood clotting activity in the plasma from diabetic KO mice also suggests a protective role for galectin-3 in mediating coagulation and thrombosis. The differential endocrine and endothelial responses to high-fat feeding of galectin-3 deficient mice compared to WT mice are summarized in Figure 3.18. The transcriptional findings as well as the altered metabolism demonstrated by KO mice compared to WT mice suggest that galectin-3 serves a protective role against the metabolic and hormonal derangements that impinge upon the diabetic endothelium and lead to its damage and dysfunction.

Table 3.1. Aortic endothelial responses of KO and WT mice after 8 weeks of HFD vs. chow diet. Transcripts shown are dysregulated > 1$\log_2$ [fold change] in either KO or WT compared to their respective chow-fed controls.

Genbank Accession	Gene Name	WT H/C	KO H/C
NM_009605	adiponectin, C1Q and collagen domain containing	-5.47	-3.98
NM_007606	carbonic anhydrase 3	-3.65	-3.68
NM_022984	Resistin	-4.75	-4.71
NM_021282	cytochrome P450, family 2, subfamily e, polypeptide 1	-4.49	-4.67
NM_013459	complement factor D (adipsin)	-4.26	-3.90
NM_020509	resistin like alpha	-4.46	-2.32
NM_018762	glycoprotein 9 (platelet)	-0.49	-2.64
NM_007728	coagulation factor C homolog	-1.69	-2.53
NM_153526	insulin induced gene 1	-0.88	-1.76
NM_007940	epoxide hydrolase 2, cytoplasmic	-0.83	-1.29
NM_009204	solute carrier 2a4 (Glut4)	-1.06	-2.06
NM_011580	thrombospondin 1	-1.71	-0.08
NM_010570	insulin receptor substrate 1	0.52	1.47
NM_009325	thromboxane A2 receptor	1.19	1.56
NM_028784	coagulation factor XIII, A1 subunit	-2.31	-0.84
NM_010171	coagulation factor III	0.91	1.86
NM_053185	collagen, type IV, alpha 6	1.01	2.07
NM_007925	Elastin	1.07	1.92
NM_026280	matrix-remodelling associated 7	1.27	2.07
NM_007736	collagen, type IV, alpha 5	0.69	2.30
NM_178793	collagen and calcium binding EGF domains 1	-0.03	2.50
NM_009928	collagen, type XV, alpha 1	1.74	3.15
NM_010766	macrophage receptor with collagenous structure	1.08	4.27
NM_008967	prostaglandin I receptor (IP)	0.63	1.99
NM_008966	prostaglandin F receptor	0.99	2.14
NM_007617	caveolin 3	1.49	3.04
NM_011101	protein kinase C, alpha	0.76	2.52
NM_008764	tumor necrosis factor receptor superfamily, member 11b (osteoprotegerin)	1.32	4.17

Table 3.2. Skeletal muscle endothelial responses of KO and WT mice after 8 weeks of HFD vs. chow diet. Transcripts shown are dysregulated >1log_2 [fold change] in either KO or WT compared to their respective chow-fed controls.

Genbank Accession	Gene Name	WT H/C	KO H/C
NM_008491	lipocalin 2	-1.17	-2.20
NM_011784	apelin receptor	1.80	1.82
NM_009325	thromboxane A2 receptor	1.84	1.61
NM_010517	insulin-like growth factor binding protein 4	-0.09	-1.02
AK154954	metallothionein 1	-0.56	-1.08
NM_019985	C-type lectin domain family 1, member b	n.d.	-1.17
NM_133985	oxidative-stress responsive 1	0.38	-1.28
BC007177	cyclin L1	0.00	-1.29
NM_010104	endothelin 1	-0.42	-1.29
AK042211	endothelin receptor type A	-0.79	-1.58
NM_009605	adiponectin, C1Q and collagen domain containing	0.31	-1.30
NM_021896	guanylate cyclase 1, soluble, alpha 3	-1.66	-1.31
NM_009694	apolipoprotein B mRNA editing enzyme, catalytic	0.64	-1.32
NM_026672	glutathione S-transferase, mu 7	-0.69	-1.45
NM_007413	adenosine A2b receptor	-0.43	-1.49
NM_177687	cAMP responsive element binding protein-like 2	-1.17	-1.81
NM_008161	glutathione peroxidase 3	-1.79	-1.81
NM_053247	lymphatic vessel endothelial hyaluronan receptor 1	1.55	-1.83
NM_009805	CASP8 and FADD-like apoptosis regulator	0.77	-1.90
NM_013459	complement factor D (adipsin)	-1.71	-3.79
NM_009928	collagen, type XV, alpha 1	2.54	2.41
NM_011607	tenascin C	n.d.	1.82
NM_021281	cathepsin S	3.36	1.31
X70100	fatty acid binding protein 5, epidermal	1.53	0.80
L38613	glucagon receptor	1.45	0.03
J05020	Fc receptor, IgE, high affinity I	1.43	1.01
NM_011311	S100 calcium binding protein A4	1.36	1.87
NM_147776	von Willebrand factor A domain containing 1	1.35	1.07
NM_008332	interferon-induced protein with tetratricopeptide	1.25	0.57
NM_008329	interferon activated gene 204	1.20	0.68
NM_008620	guanylate binding protein 4	1.11	0.38
NM_177646	diacylglycerol kinase, delta	1.02	0.34
AK087208	endothelial PAS domain protein 1	-1.00	-0.92
NM_178020	hyaluronoglucosaminidase 3	-1.12	-0.41
AK032692	immediate early response 2	-1.12	-0.50
AK163452	aldehyde dehydrogenase 2, mitochondrial	-1.27	-0.68
NM_133808	high density lipoprotein (HDL) binding protein	-1.28	0.08
AK078273	low density lipoprotein receptor-related protein 1	n.d.	-1.06
NM_027286	Angiotensin I converting enzyme	-1.31	-0.72

Table 3.3. Commonly dysregulated responses of the aortic and muscle endothelium of KO and WT mice after 8 weeks of HFD vs. chow diet. Transcripts shown are dysregulated >1$\log_2$[fold change] by HFD in both tissues of either KO or WT mice compared to their respective chow-fed controls.

Genbank Accession	GeneName	Skeletal Muscle		Aorta	
		WT	KO	WT	KO
NM_013459	complement factor D (adipsin)	-1.71	-3.79	-4.26	-3.90
NM_009928	collagen, type XV, alpha 1	2.54	2.41	1.74	3.15
NM_016974	D site albumin promoter binding protein	1.17	2.51	1.79	2.89
NM_029568	microfibrillar-associated protein 4	1.70	3.00	0.99	1.58
NM_145434	nuclear receptor subfamily 1, group D, member 1	2.51	2.44	1.57	2.30
NM_019985	C-type lectin domain family 1, member b	n.d.	-1.17	-2.19	-1.50
NM_173385	cartilage intermediate layer protein, nucleotide pyrophosphohydrolase	2.68	2.67	0.06	1.90
AK036956	membrane protein, palmitoylated 7 (MAGUK p55 subfamily member 7)	0.72	-1.17	-1.80	-0.31
NM_013905	hairy/enhancer-of-split related with YRPW motif-like	-1.15	-1.39	2.32	1.75
NM_146162	transmembrane protein 119	2.42	1.66	1.18	1.70
NM_009605	adiponectin, C1Q and collagen domain containing	0.31	-1.30	-5.47	-3.98
NM_033037	cysteine dioxygenase 1, cytosolic	n.d.	-1.84	-3.02	-2.74
NM_178373	cell death-inducing DFFA-like effector c	-0.16	-1.56	-3.48	-3.42
NM_025626	family with sequence similarity 107, member B	n.d.	-2.27	0.71	-1.64
NM_153574	family with sequence similarity 13, member A	-2.45	-2.51	-1.13	-1.95
NM_022321	parvin, gamma	-0.74	-1.42	-1.87	-1.07
NM_009325	thromboxane A2 receptor	1.84	1.61	1.19	1.56
NM_001037724	adenylate cyclase 7	2.10	2.15	1.77	2.43

Table 3.4. Transcripts identified by Ingenuity Pathway Analysis in the Cardiovascular Function and Development category, which was the most enriched biological function in the KO data. Transcripts dysregulated >0.75log_2[fold change] in the aortic endothelium of KO and WT mice after 8 weeks of HFD vs. chow-fed controls were analyzed by IPA.

Cardiac Output	
WT	ADRA2A,ADIPOQ,AGT,DBP,IGF1,Klk1b1 (includes others),NRG1 (includes EG:112400),PDCD1,PNPLA2
KO	ABCC9,ADIPOQ,ADRA1D,ADRA2B,ARNTL,ARSB,ATP2A2,CACNB3,CACNA1G,COL4A3,DBP,EDNRA,ELN,EPHX2,FKBP1B,HLF,IGF1,IRS1,MRVI1,OXSR1,PRKCA,PTGER2,PTGES,PTGIR,SLC6A2,SNTA1,TBXA2R, WNK4
Migration	
WT	ADIPOQ,AGT,HMMR,IGF1,NRG1 (includes EG:112400),PF4,THBS1
KO	ADIPOQ,ARHGEF4,BMX,ELN,F3,FGFR1,IGF1,MMP2,PDGFRA,S100A4, S1PR2,SLIT2,SLIT3,TGFB3
CV Morphology	
WT	ADIPOQ,HEYL,MKL2,MYH10,NRG1 (includes EG:112400), NTRK3,PDCD1,PNPLA2,THBS1
KO	ADIPOQ,ADRA2B,ARSB,ATP2A2,B9D1,BCL2,CACNB3,CAV3,CNN1 (includes EG:1264),COL15A1, COL4A3, COL8A2, CYP2E1, EAF2,ECE2,EDNRA,ELN, EPHA3,F3,FGFR1, FKBP1B,GDF1, HEYL,IGF1,LEFTY1,MDK,MKL2,MMP2, NKX2-3,NTF3,NTRK3,PDGFRA,PLCE1,PRKCA,PRRX2,S1PR2,SGCD,SLC2A4, TBXA2R,TGFB3,THPO,TNFRSF11B
Growth and Proliferation	
WT	ADAMTS8,ADIPOQ,ADRA2A,AGT,ARNT,BIRC5,C5,CLEC1B,COL3A1, EPHB2,FOXS1,HEG1,HEYL,IGF1,JAM3,MKL2,NRG1 (includes EG:112400),PBX1,PF4,THBS1
KO	ADAMTS2,ADAMTS8,ADIPOQ,ADRA2B,ADRA2C,ANG,ARHGEF4,ARNTL,ATP2A2,BCL-2, BMX,C5,C6,COL15A1,COL1A1 (includes EG:1277), COL4A3,COL8A2,E2F1,EAF2,EDNRA,ELN,EPHB2,EPHB3,ESR1,F3, FGFR1,FOXS1,GPC1,HEYL,IGF1,INHBA,IRS1,LAMA2,LEFTY1,MDK,MKL2,MMP2,NKX2-3, PDGFRA,PRRX2,PTGER2,PTGES,PTGIR,PTPRF, S100A4,S1PR2,SLIT2,SLIT3,TBXA2R,TEAD4,TNFRSF11B
Vasculogenesis	
WT	ADAMTS8,ADIPOQ,ADRA2A,AGT,ARNT,BIRC5,EPHB2,HEG1,HEYL,IGF1,JAM3,MKL2,NRG1 (includes EG:112400),PBX1,PF4,THBS1
KO	ADAMTS2,ADAMTS8,ADIPOQ,ADRA2B,ADRA2C,ANG,ANGPTL2,ARHGEF4,ARNTL,B4GALNT1,BMX,C5,C6,COL15A1,COL1A1 (includes EG:1277),COL8A2,E2F1,EAF2,EDNRA,ELN,EPHB2,EPHB3,ESR1,FGFR1,GPC1HEYL,HYOU1,IGF1,INHBA,IRS1,LAMA2,LEFTY1,MDK,MKL2,MMP2,NKX2-3, PDGFRA,PRRX2,PTGER2,PTGES,PTGIR, S100A4,S1PR2,SLIT2,SLIT3,TBXA2R,TEAD4,THY1,TNFRSF11B
CV System Function	
WT	CACNA1G,JPH2,Klk1b1 (includes others),NRG1 (includes EG:112400),PDCD1,PNPLA2
KO	ADRA1D,CACNA1G,COL15A1,ELN,EPHA3,JPH2,KCNA1,MMP2,NTF3,PTGIR,SGCD,TBXA2R
Vasoconstriction	
WT	AGT
KO	ABCC9,ADRA1D,ADRA2B,EDNRA,PTGER2,TBXA2R

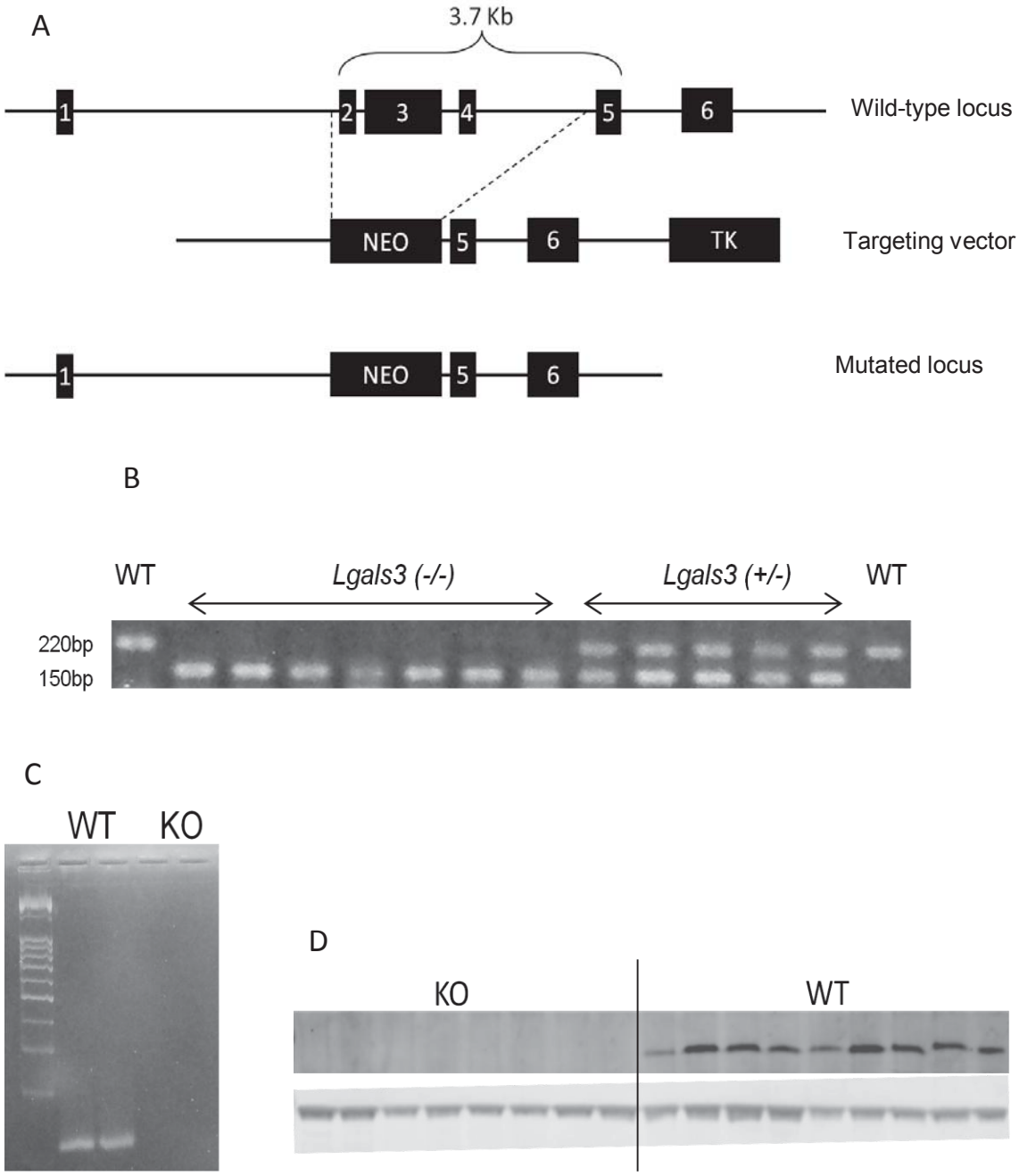

Figure 3.6. Confirmation of galectin-3 deletion in the knockout mouse at the DNA, RNA, and protein level. (A) Scheme for generating the null mutation by homologous recombination (adapted from Colnot, 1998). (B) Analysis of genomic DNA revealing fragments corresponding to the wild-type and mutated alleles at 220bp and 150bp, respectively. (C) Amplified products from qPCR using *Lgals3* primers designed within the deleted region show no amplified product in KO lanes. (D) Confirmation of galectin-3 protein loss in aortic lysates resulting from gene ablation.

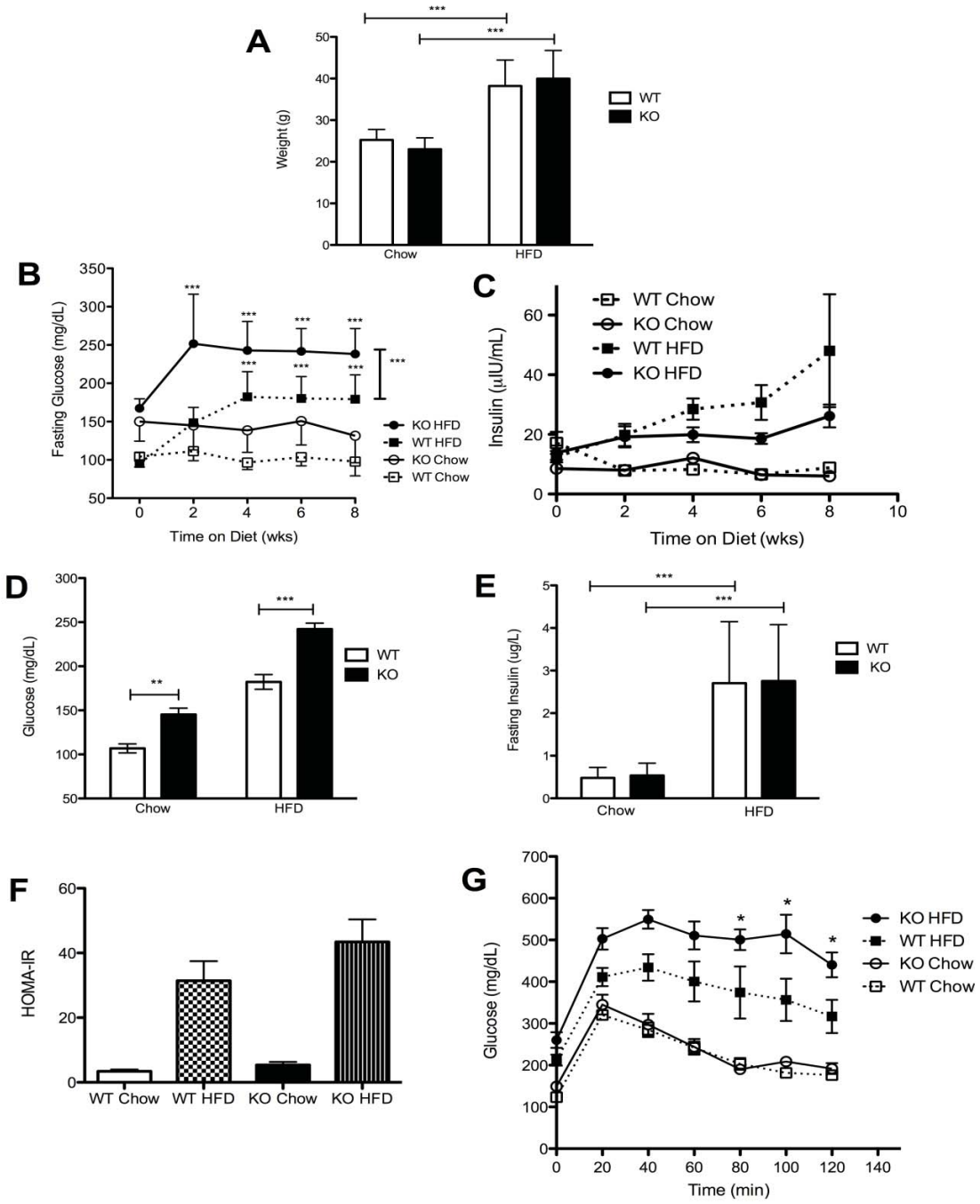

Figure 3.7. Endocrine Responses of KO vs. WT mice fed a high-fat diet. (A) Weight after 8 wks of diet (HFD *n*=19-23; Chow *n*=16-17). Increase in fasting glucose (B) and insulin (C) levels over the time course of the diet regimen (HFD *n*=7-11; Chow *n*=4-5). (D) Fasting glucose levels after 8wks of HFD *(n*=15). (E) Fasting insulin levels measured after 8wks of feeding *(n*=9-10). (F) HOMA-IR calculated from fasting glucose and insulin levels after 8wks *(n*=9-10). (G) Glucose tolerance test performed by measuring glucose levels every 20min after i.p. injection of glucose (1mg/kg, *n*=8-9). Data is shown as mean ±SD or SEM (for GTT). Statistical tests were performed using 1- or 2-way ANOVA followed by Bonferroni post-hoc tests. **P* < 0.05;***P* < 0.01; ****P* < 0.001.

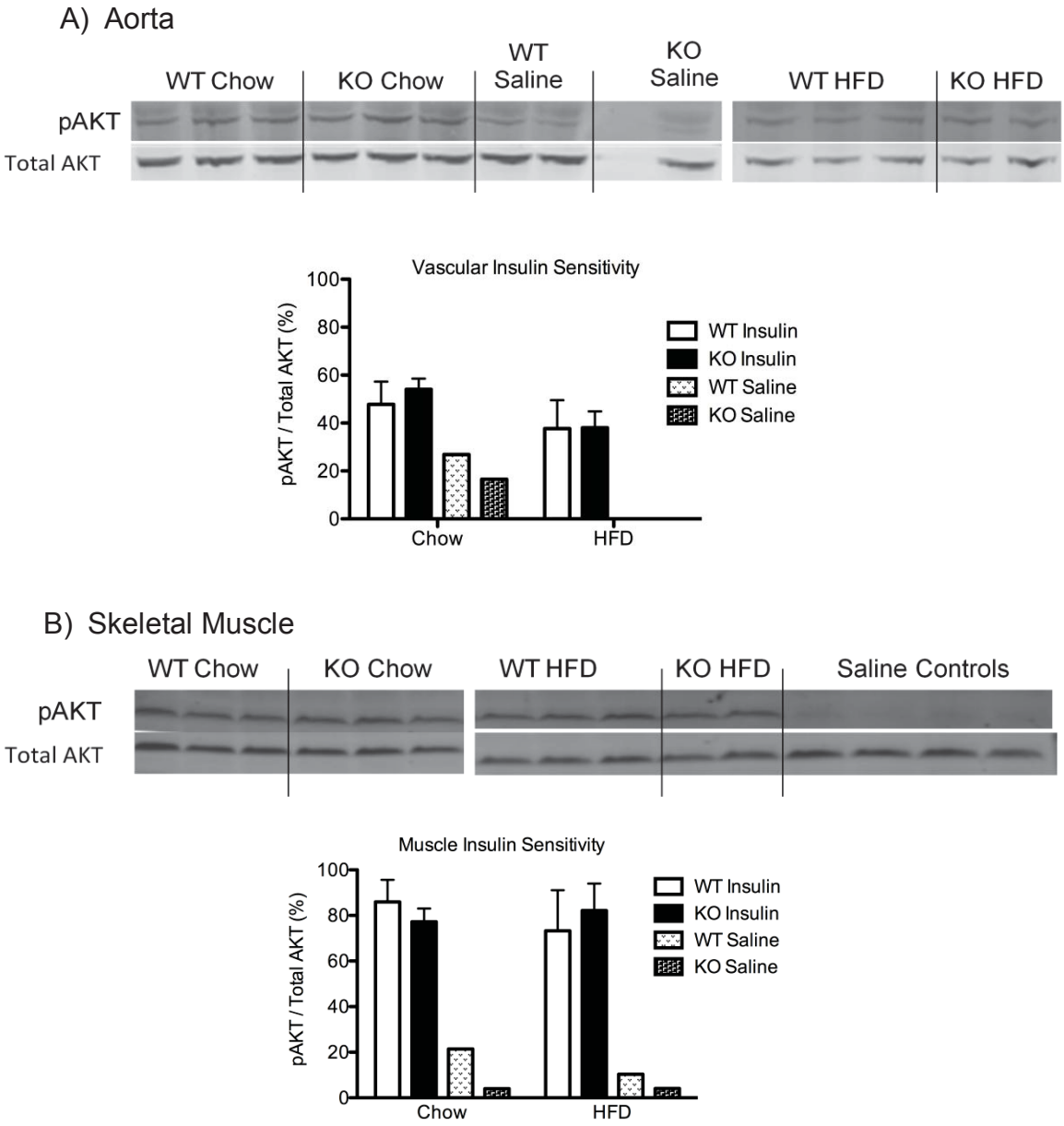

Figure 3.8. Insulin sensitivity of aortic (A) and skeletal muscle (B) tissues after 8 weeks of high-fat or chow diet. Tissue lysates from animals stimulated with 60U/kg insulin or saline control were probed for phosphorylated AKT. Blots were stripped and probed for total AKT to which the quantity of pAKT was normalized. A representative blot (top) and the densitometry performed using Image J (bottom) are shown for each tissue (*n* = 2-8 per group).

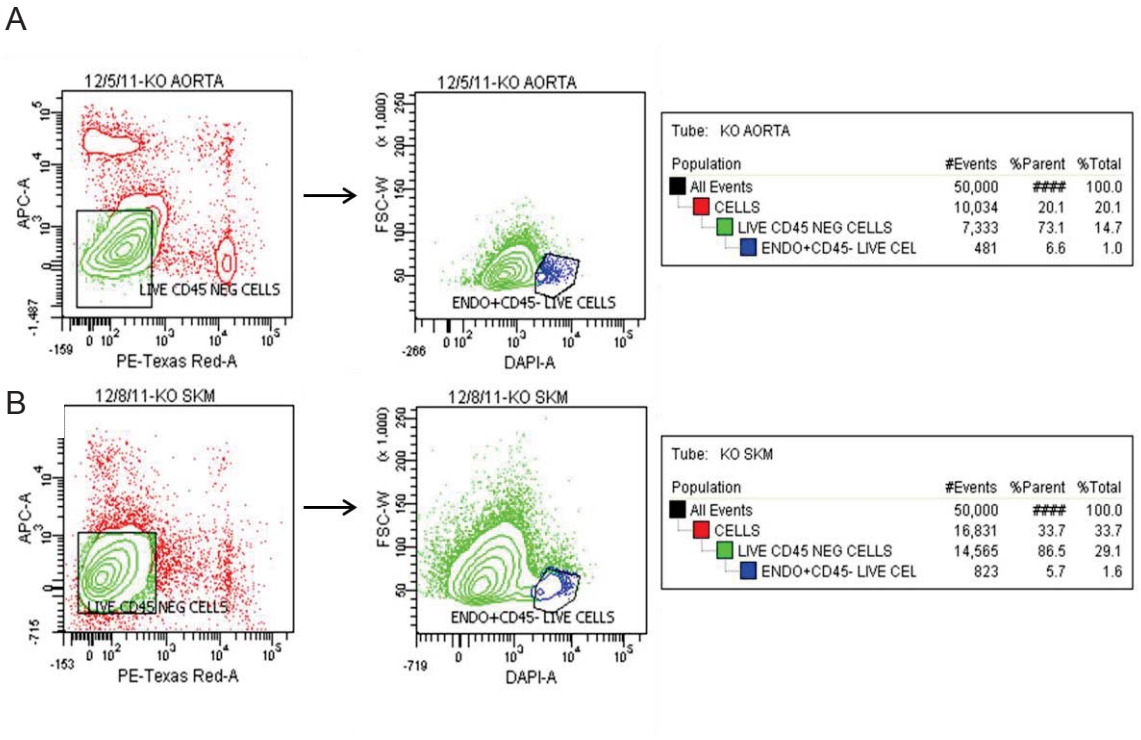

Figure 3.9 FACS isolation of Galectin-3(-/-) endothelium. (A) Collagenolytic digests of aortae (A) and leg muscle (B) of Galectin-3(-/-) and C57BL/6 mice were labeled with eFluor450-Endoglin and PE-CD45 and live/dead stain. Live, Endoglin^{+}/CD45^{-} cells were sorted directly into TRIzol reagent for subsequent gene expression analysis.

A

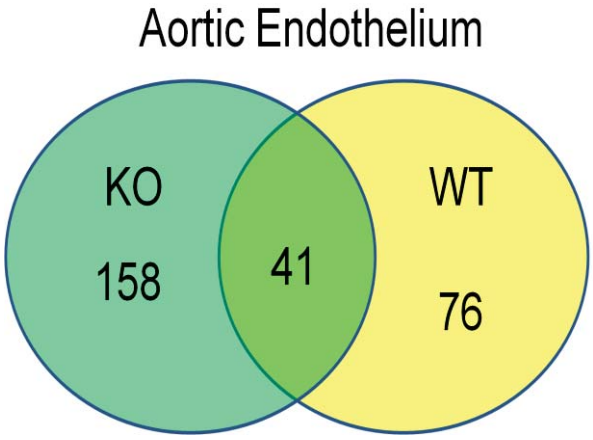

B

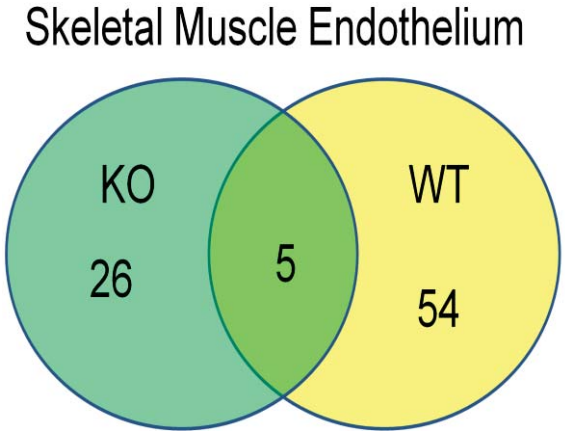

Figure 3.10. Number of commonly and differentially dysregulated transcripts in the endothelial response to diabetes exhibited by the KO and WT. Transcripts dysregulated >2 $\log_2$ [fold change] by HFD vs. chow diet in all 3 biologically replicate microarray experiments are shown for the aortic endothelium (A) and the skeletal muscle endothelium (B) of each strain.

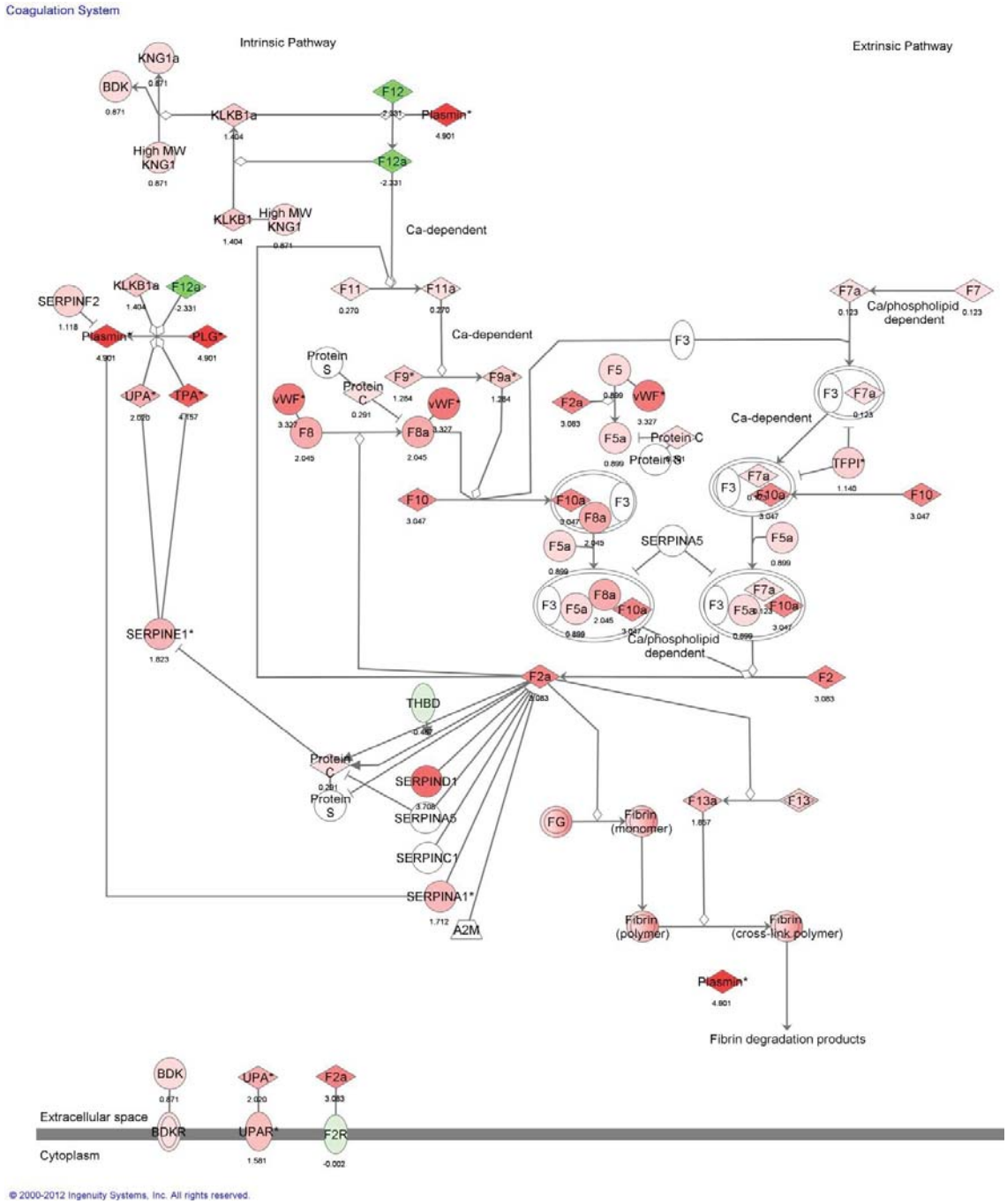

Figure 3.11. The Coagulation Cascade is highly upregulated in the aortic endothelium of diabetic KO mice compared to diabetic WT mice. Log_2[fold change] of KO HFD/WT HFD for all aortic transcripts of one experiment were uploaded into Ingenuity Pathway Analysis. The Coagulation Cascade was the most enriched canonical pathway in the aortic endothelium of knockout mice compared to WT mice.

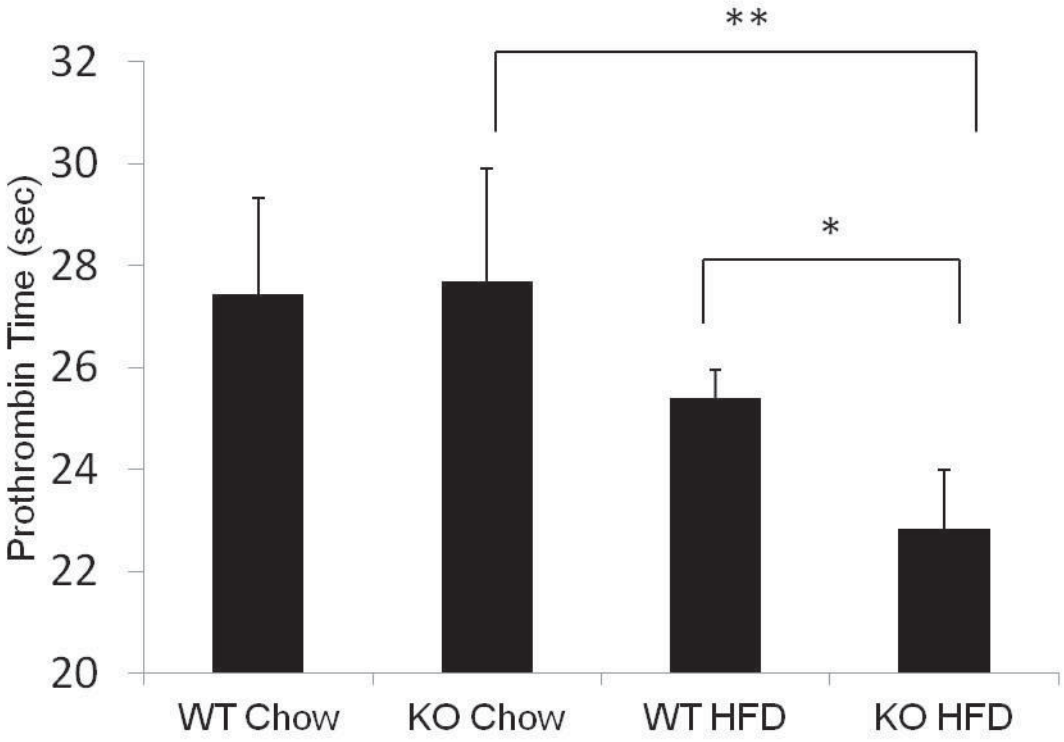

Figure 3.12. Activation of the extrinsic coagulation pathway in diabetic KO mice. Prothrombin time of citrate-anticoagulated plasma from WT and KO mice fed a high-fat or chow diet for 8 weeks was assessed by measuring the time to coagulation following the addition of a calcium thromboplastin reagent using a Diagnostica Stago Start 4 Hemostasis Analyzer. **P* <0.05; ***P* <0.01. *N* = 3 WT animals and *n* =4-5 KO animals.

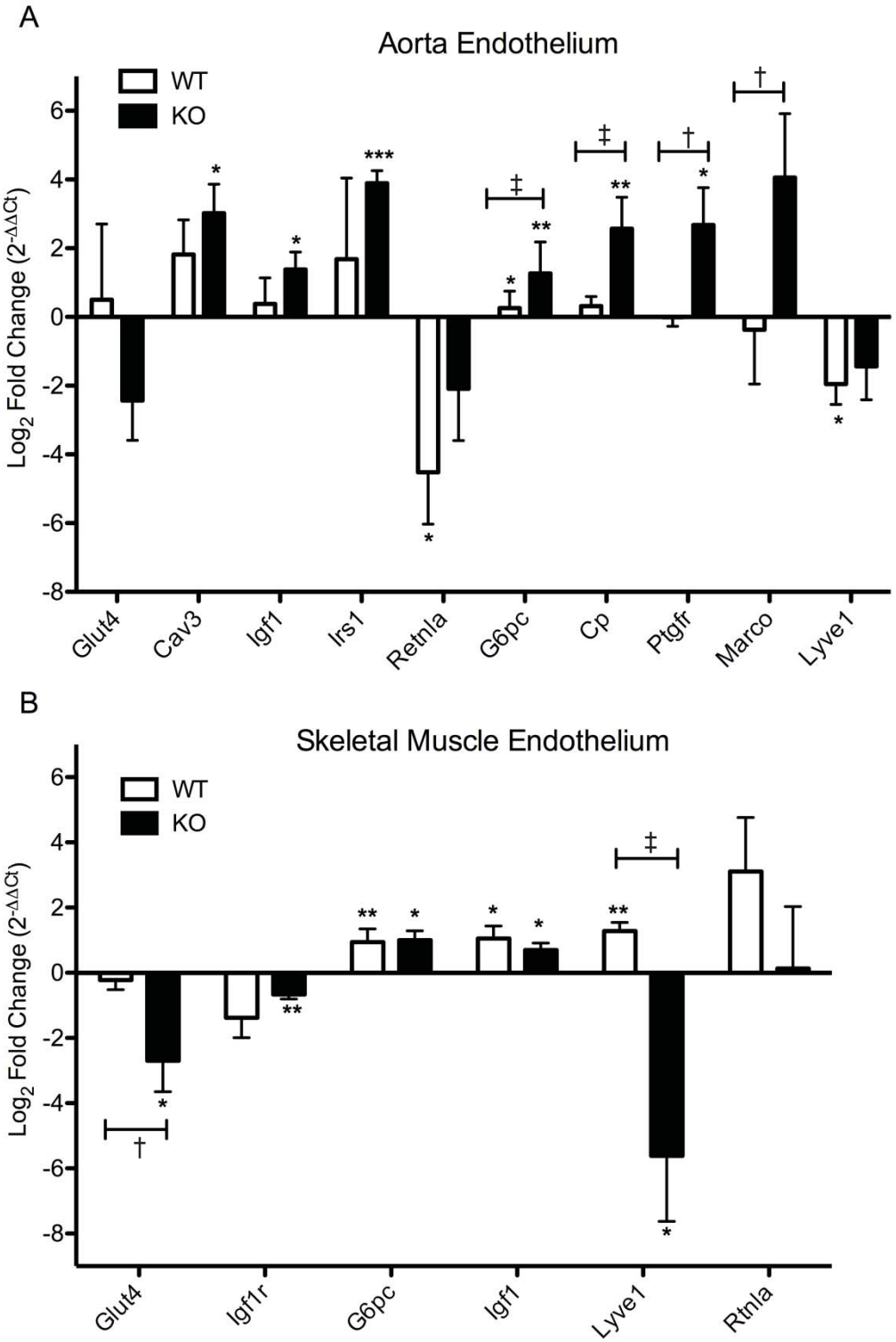

Figure 3.13. Log_2 fold change of endothelial transcripts dysregulated by high-fat diet vs. chow diet in the aortic endothelium (A) and skeletal muscle endothelium (B) of Galectin-3(-/-) and WT mice after 8 weeks of feeding as determined by qPCR.Data is presented as mean + SEM. *$P \leq$ 0.1 and **$P < 0.05$ vs. chow-fed controls; †$P \leq 0.1$ and ‡$P < 0.05$ vs. WT.

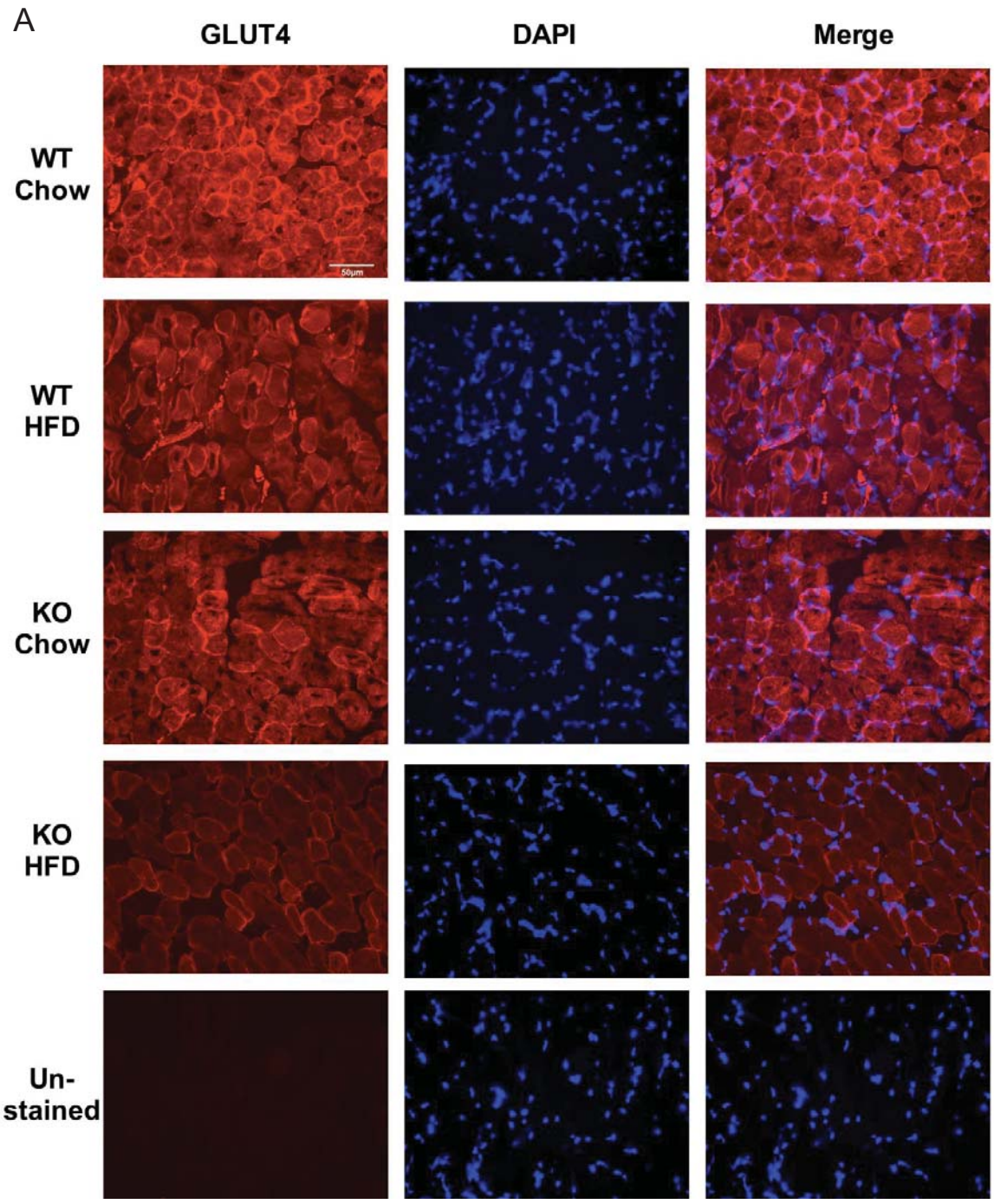
A
GLUT4
DAPI
Merge
WT Chow
WT HFD
KO Chow
KO HFD
Un-stained
50μm

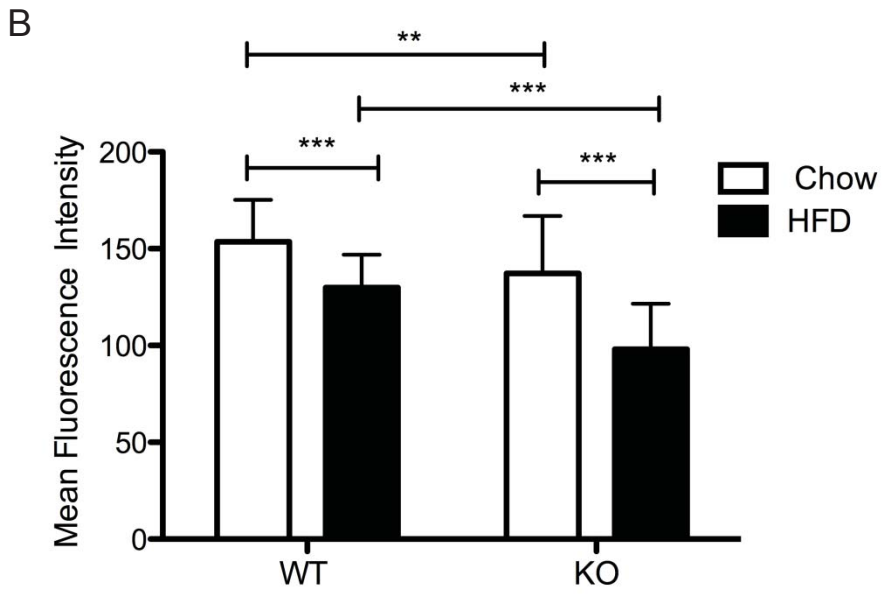

Figure 3.14. Immunofluorescence staining for GLUT4 in the skeletal muscle of WT and KO mice fed a high-fat or chow diet for 8 weeks. Ten micrometer, fresh-frozen sections were incubated overnight with rabbit anti-mouse GLUT4 antibody followed by incubation with an Alexa Fluor®568-conjugated goat anti-rabbit IgG secondary antibody followed by mounting in fluorescence mounting medium containing DAPI. (A) Representative images from 3 WT and 4 KO mice per group are shown at 40X magnification. Primary antibody was omitted from the unstained control. (B) Mean fluorescence intensity of 20 myofibers from 2 sections per animal was quantified using Image J. $^{**}P < 0.01$; $^{***}P < 0.001$.

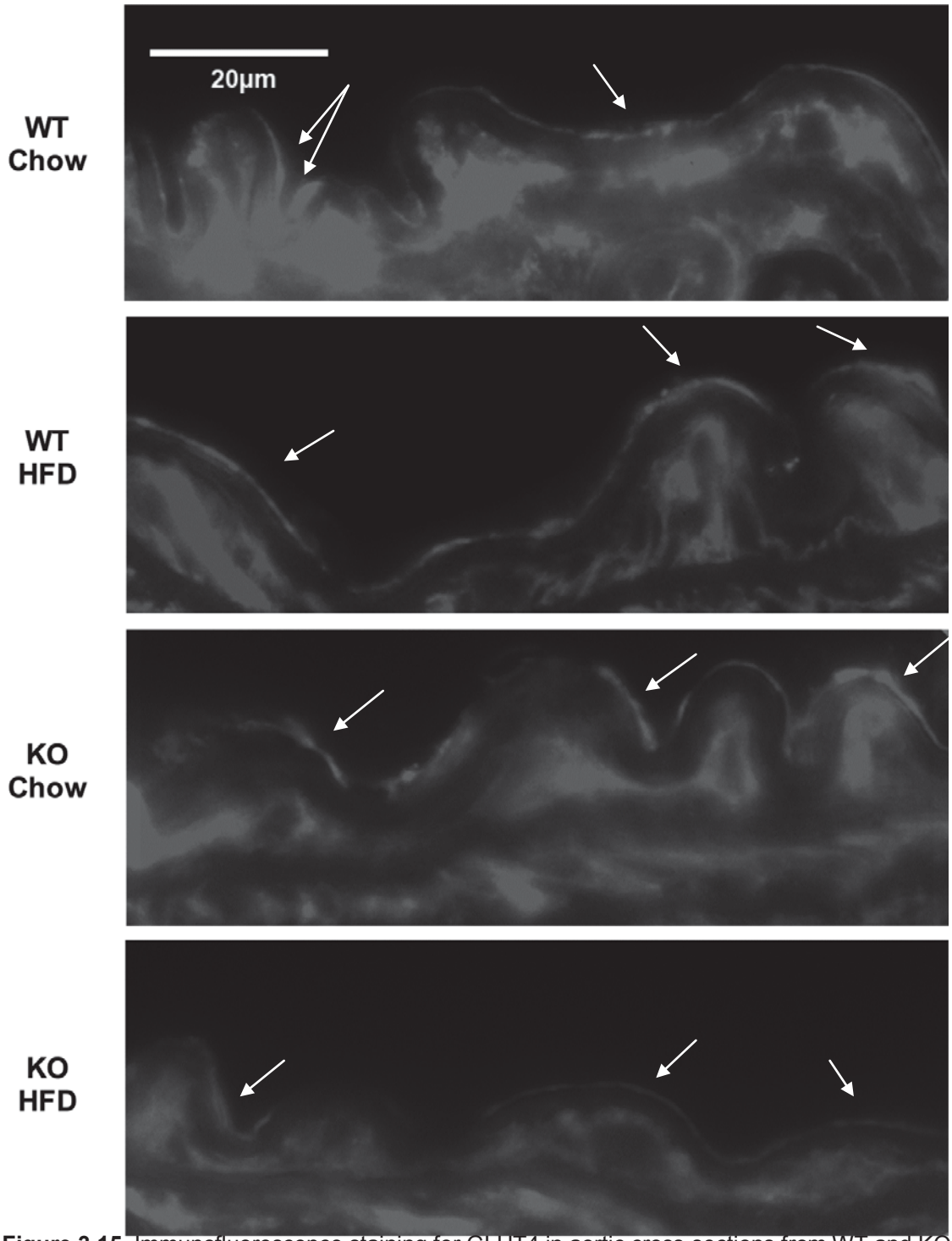

Figure 3.15. Immunofluorescence staining for GLUT4 in aortic cross-sections from WT and KO mice fed a high-fat or chow diet for 8 weeks. Ten micrometer, fresh-frozen sections were incubated overnight with rabbit anti-mouse GLUT4 antibody followed by incubation with an Alexa Fluor®568-conjugated goat anti-rabbit IgG. Representative images from 3 WT and 4 KO mice per group are shown at 100X magnification in grayscale. Arrows indicate areas of GLUT4 staining in the endothelial cell cytoplasm. No staining was observed in unstained controls where primary antibody was omitted (not shown).

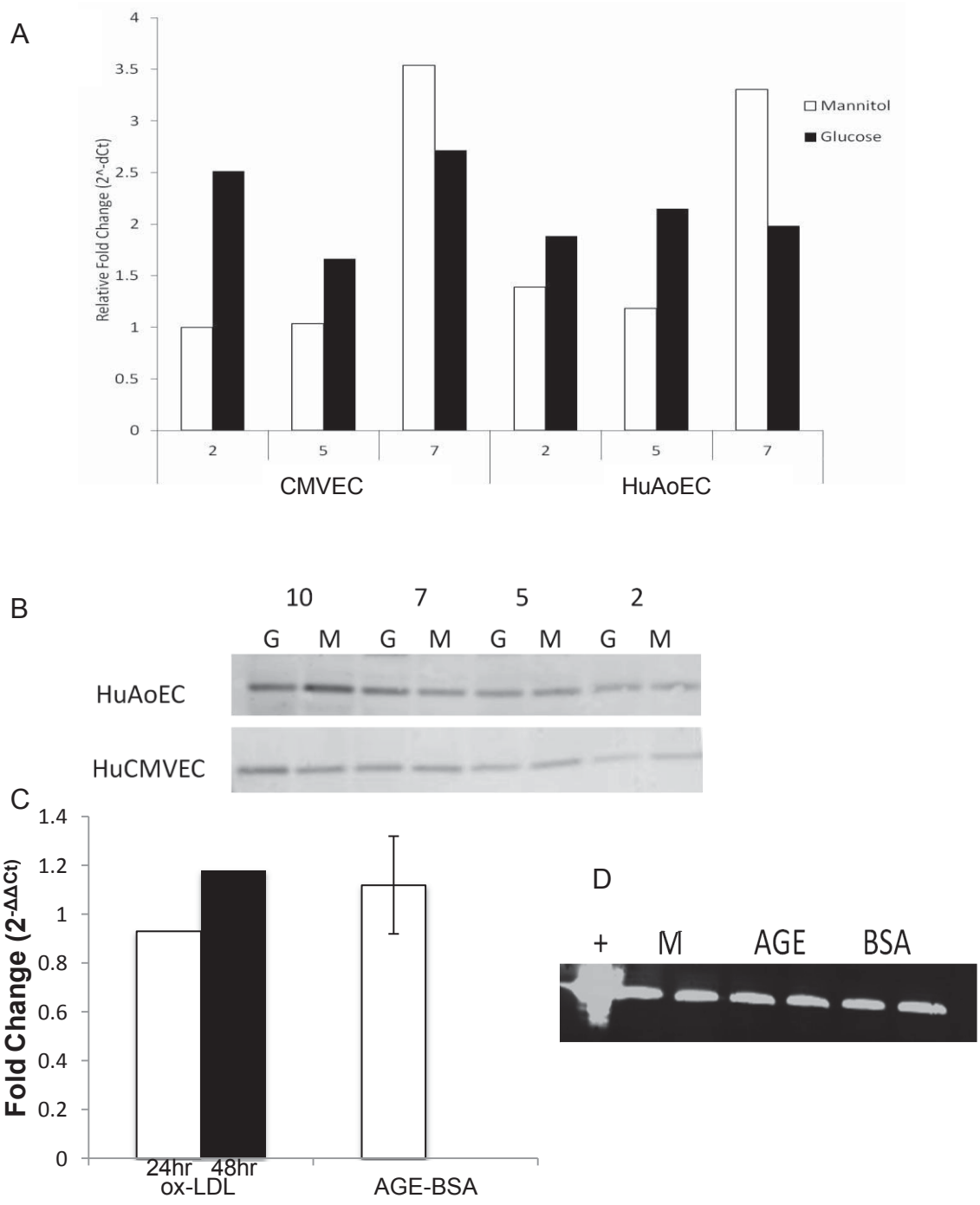

Figure 3.16. Galectin-3 mRNA and protein expression in cultured HuAoECs and CMVECs after treatment with isolated components of the diabetic milieu. HuAoECs and CMVECs were treated with 30mM glucose or 30mM mannitol for 2-10 days and galectin-3 mRNA (A) and protein (B) levels were assessed by real-time PCR and Western blotting, respectively. (C) *Lgals3* mRNA expression in HuAoECs following treatment with ox-LDL for 24 or 48 hrs or AGE-BSA for 4 days. Fold change is relative to media or BSA-treated control. (D) Intracellular LGALS3 protein in HuAoEC lysates following 4days of treatment with AGE-BSA, BSA alone, or media.

A

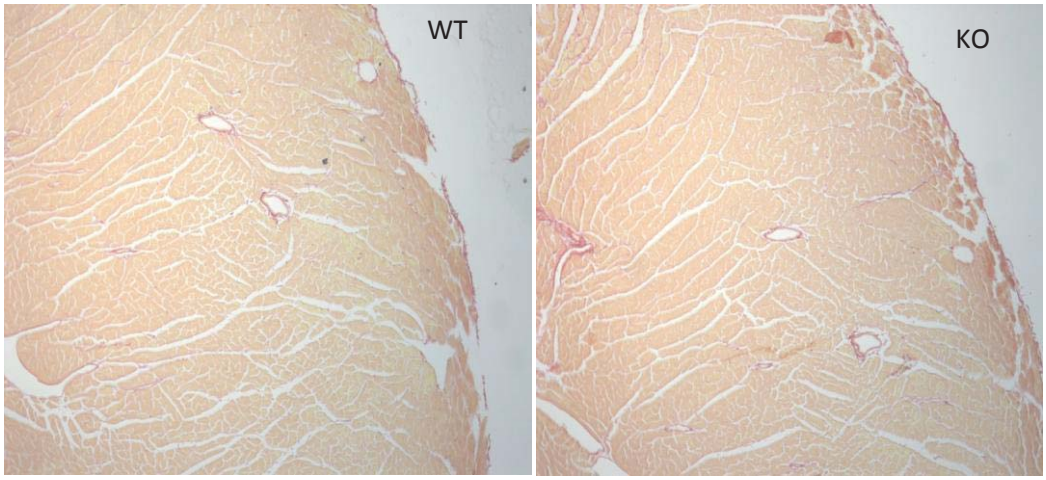

B

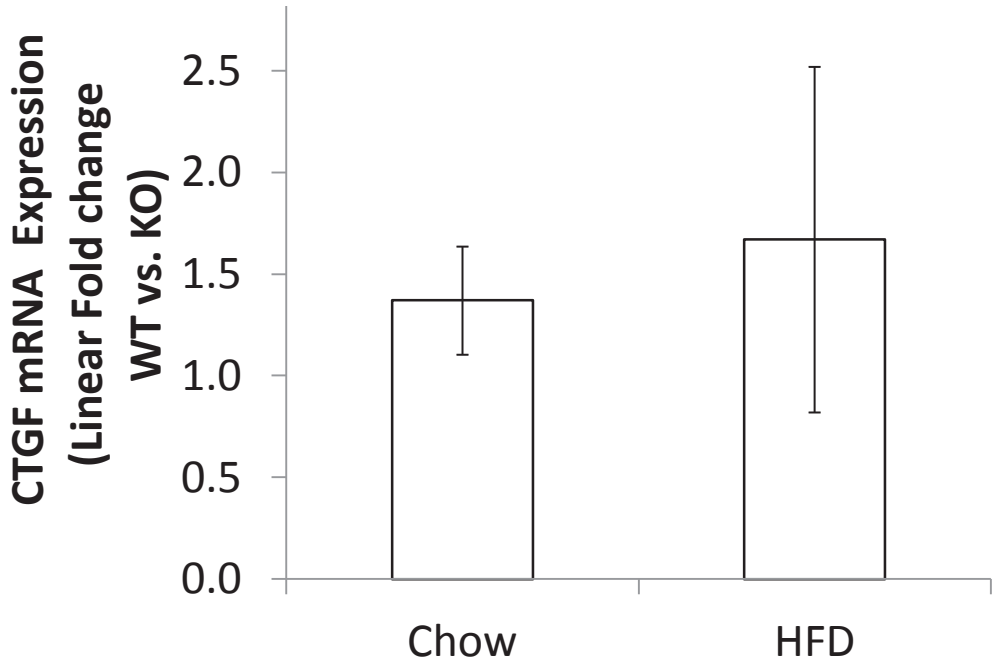

Figure 3.17. Fibrosis in KO and WT hearts after 8 weeks of HFD. (A) Heart sections were stained with picrosirius, which stains collagen red. (B) mRNA expression of *Ctgf* in the hearts assessed by real-time PCR.

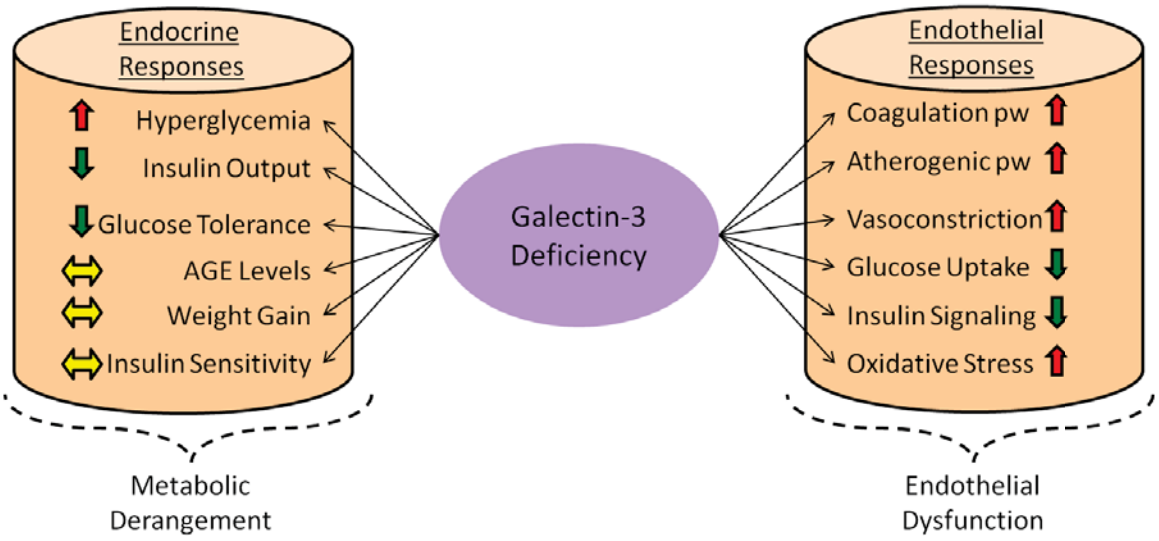

Figure 3.18. Summary of endocrine and endothelial responses of Galectin-3-deficient mice to a high-fat diet. Arrows indicate enhanced (red, up arrow), reduced (green, down arrow), or similar (yellow, horizontal arrow) response to a high-fat diet as compared to the response of wild-type mice.

Chapter 4: Conclusion

4.1 Project Overview and Significance

The overall goal of these studies was to gain an understanding of the molecular basis of the endothelial dysfunction associated with type 2 diabetes. Through our work, we have identified pathways and proteins that contribute to diabetic vasculopathy and promote adverse cardiovascular events. Chapter 2 describes the transcriptional changes occurring in the endothelium in response to a high-fat diet. Insights gained from these studies include the development of an endothelial isolation method, the identification of biomarkers for endothelial damage in diabetes, and the endothelial-specific upregulation of galectin-3 in diabetes.

4.1.1 Method for Isolating Pure Populations of Endothelial Cells

In order to accomplish these goals, we developed a murine model of type II diabetes in which a pure population of endothelial cells could be isolated by fluorescence-activated cell sorting. Chapter 2 describes the development of the Tie2-GFP diabetic model and the confirmation of endothelial identity of the sorted cells. For the experiments of Chapter 3, sorting based on endothelial-specific GFP expression was not possible, and therefore necessitated the development of another sorting method based on endoglin positive, CD45 negative expression. The techniques developed here will be useful for the study of endothelial cells in a variety of mouse models.

4.1.2 Biomarkers of Endothelial Damage in Diabetes

Transcriptional analyses of the aortic and skeletal muscle endothelium from mice fed a high-fat diet for 4, 6, or 8 weeks revealed the dysregulation of transcripts with roles in inflammation, vasoregulation, lipoxygenase activity, redox homeostasis, and binding of advanced glycation endproducts. Our findings implicate robust and consistent markers of endothelial dysfunction in diabetes that may be used as diagnostic biomarkers of the vascular complications of diabetes. The dysregulation of transcripts in both aortic and muscle endothelium indicate universal markers of endothelial dysfunction in diabetes. Galectin-3 is highly dysregulated in the macrovascular and microvascular endothelia of diabetic mice suggesting its use as a specific marker of endothelial damage, which is not presently available, and could be useful as a marker of early vascular pathology in a variety of diseases. Galectin-3 may be a measurable parameter for endothelial dysfunction that links molecular alterations in the endothelium to vascular pathology that has been long sought (Xu, 2009).

Furthermore, LGALS3 levels in the serum correlate with degree of insulin resistance and may serve to predict adverse events related to diabetes. Its levels may be used to monitor and diagnose the diabetic state as well as other conditions where increased levels of galectin-3 are observed (such as heart failure). Its value as a diagnostic marker for the cardiovascular complications of diabetes has prompted us to begin development of a ligand to measure LGALS3 levels in the blood. Current means to measure galectin-3 levels rely on antibody-based methods. We are working to develop a synthetic ligand based on the

binding specificity of LGALS3. Unlike antibodies, ligands are synthesized and may be lyophilized for long-term storage and stability thus offering a great improvement over traditional antibodies.

4.1.3 Endothelial-specific Expression of galectin-3

Galectin-3 mRNA is much more abundant in the aortic endothelium by 4 weeks of HFD and in the skeletal muscle endothelium by 6 weeks compared to chow-fed controls. The upregulation of LGALS3 protein was confirmed by immunofluorescent staining of sorted endothelial cells. Other studies have shown the upregulation of galectin-3 in whole aortic lysates from *db/db* mice and in atherosclerotic lesions where it localizes to macrophages (Nachtigal, 1998). Our data shows that galectin-3 is specifically upregulated in endothelial cells of diabetic mice and this has implications for the development of atherosclerosis. Preliminary studies of LGALS3 expression in peripheral blood mononuclear cells by flow cytometry shows a high level of expression, but the percentage of cells expressing LGALS3 is similar between HFD and chow-fed mice. In contrast, flow cytometry analysis of aortic endothelial cells derived from HFD and chow-fed mice revealed an increase in the expression of LGALS3 protein after high-fat feeding, although the change was not significant (39% vs. 28%, p=0.1, *n*=3). Due to the low number of GFP^+ events obtained from individual tissue suspensions, subsequent analyses of LGALS3 protein expression were performed by immunofluorescence staining of sorted endothelial cells. Immunofluorescence staining clearly shows increased LGALS3 expression in GFP^+ endothelial cells derived from HFD mice (Figure 2.8).

In Chapter 3, the role of galectin-3 in diabetic vasculopathy was examined by loss of function studies using the galectin-3(-/-) mouse. KO and wild-type mice were fed a high-fat diet and their endocrine and endothelial responses were assessed. Through these experiments, it was determined that galectin-3 plays a role in metabolic regulation and is protective against endothelial dysfunction in diabetes.

4.1.4 Galectin-3 Modulates Glucose Homeostasis

Chow-fed Galectin-3 knockout mice experience isolated hyperglycemia with no impairment in glucose or insulin tolerance as compared to wild-type mice. Upon high-fat feeding, a rapid increase in fasting glucose levels occurs without compensatory insulin output. In comparison, wild-type mice exhibit a gradual increase in fasting glucose levels and insulin levels. Diabetic KO mice display impaired glucose tolerance after a glucose challenge. Downregulation of *Glut4* mRNA in the endothelium and decreased abundance of GLUT4 protein in the aortic endothelium and skeletal muscle of KO mice after high-fat feeding suggest that LGALS3 may regulate glucose uptake. The decrease in GLUT4 may be responsible for the defective glucose metabolism of the KO, and suggests a role for galectin-3 in glucose homeostasis. Interestingly, these effects are independent of galectin-3's role in the uptake of advanced glycation endproducts as AGE levels are similar in WT and KO mice on either diet.

4.1.5 Galectin-3 is Protective against Endothelial Dysfunction in Diabetes

Transcriptional analysis of the endothelial response to diabetes in the KO revealed a greater response in the large vessel vasculature compared to WT. Differential dysregulation is observed for transcripts with roles in glucose uptake, insulin signaling, atherosclerosis, vasoregulation, and coagulation. A number of transcripts involved in cardiovascular development and function are dysregulated in the diabetic KO, further implicating galectin-3 in the vascular pathology of diabetes. Comparison of the endothelial transcriptome of diabetic KO and diabetic WT animals revealed the upregulation of the coagulation cascade in the galectin-3(-/-) animal (Fig. 3.11). As previously described, activation of the coagulation cascade plays a major role in the development of atherosclerosis where repeated cycles of plaque rupture and coagulation occur leading to thrombus formation. Physiological studies to assess the clotting time and activity of coagulation factors involved in the extrinsic coagulation pathways revealed differential coagulation activity in the plasma from KO and WT strains. The KO animal demonstrates enhanced activation of the coagulation cascade after 8 weeksof HFD, suggesting that galectin-3 protects against thrombosis and may have therapeutic value as an anti-clotting agent.

Taken together, our data indicates that galectin-3 upregulation is a protective mechanism against the endothelial dysfunction and metabolic derangement associated with diabetes. Therefore, it may be a useful therapy to prevent cardiovascular complications in diabetic patients. Future studies

involving the therapeutic administration of galectin-3 to wild-type mice on a high-fat diet may serve to ameliorate the adverse effects of diabetes. Assessment of endothelial dysfunction and metabolic characteristics associated with diabetes in these mice may shed light on the potential for galectin-3 as a therapeutic agent.

4.2 Future Studies

4.2.1 Protein Confirmation of Dysregulated Transcripts

The current study identifies many potential targets for galectin-3 modulation. However, transcriptional dysregulation does not automatically infer protein dysregulation. Post-translational modifications may lead to protein degradation or inactivation. Therefore, it is necessary to confirm our transcriptional findings at the protein level. Due to the limited number of endothelial cells obtained from tissues and limited quantity of protein, this is best accomplished by immunohistology of sorted endothelial cells (as shown for LGALS3 staining in Fig. 2.8) or by staining of tissue cross sections (as shown for GLUT4 in Fig. 3.15). We have confirmed the downregulation of GLUT4 protein in aortic and muscle sections from KO and WT animals on the HFD (Figs. 3.14 and 3.15). These sections may also be stained to confirm our transcriptional data at the protein level for other highly dysregulated and interesting transcripts such *as Marco* and *Adra2b.*

4.2.2 Examine the Effect of Galectin-3 Treatment on Endothelial Cell Function

In order to elucidate the effect of galectin-3 on endothelial cell function, gain of function and loss of function studies can be performed *in vitro.*

Preliminary gain of function studies have been performed by treating human aortic endothelial cells with human LGALS3 recombinant protein. Assessment of eNOS function in the presence and absence of galectin-3 has been attempted by measuring NO and cGMP production in cell culture supernatants. These studies are complicated by the very low levels of NO and cGMP produced and the short half-life of such molecules. Future attempts may include the use of more sensitive nitrite/nitrate assays, the measurement of radioactively labeled L-citrulline product, or the measurement of phosphorylated eNOS.

Previous studies have demonstrated the role of galectin-3 in cell-cell and cell-matrix adhesion. Because of the importance of maintaining the endothelial barrier in order to perform its function, we have assessed the effect of LGALS3 treatment on endothelial barrier function using the Electric Cell-substrate Impedance Sensing (ECIS) system. No differences were found between treated and non-treated cells. However, repeating these experiments with cells from the galectin-3 KO animal may show reduced barrier function compared to wild-type endothelial cells.

Vascular insulin resistance may also be assessed in culture by measuring the phosphorylation of AKT as previously shown in tissue lysates. Microarray data suggests that the galectin-3 KO also experiences oxidative stress, and this may be assessed in culture by measuring superoxide anion by the reduction of cytochrome *c* (Cosentino, 2008) or ROS generation by measuring DCF fluorescence (Wang, 2010). Also, in the future, it will be important to take a more in-depth look at the physiological effects of galectin-3 ablation on the vasculature.

For example, aortic vasomotor responses may be assessed by measuring vessel relaxation of aortic ring segments after treatment with vasodilators such as acetylcholine (Jiang, 2005).

4.2.3 Interrogation of the Downstream Pathways of Galectin-3

Candidate genes and pathways identified by our transcriptional data may be interrogated in culture by knockdown using short hairpin RNA constructs or the use of specific inhibitors. Lentiviral shRNA constructs directed against galectin-3 have been produced with the pGIPz system (Open Biosystems™) in our laboratory. Knockdown of galectin-3 in murine endothelial cells has been accomplished to about 50% of basal levels and this same approach may be used to knockdown the protein products of the dysregulated transcripts identified *in vivo*. These studies would help identify the downstream targets of galectin-3 and shed light on the pathways involving galectin-3.

4.2.4 Assess the Role of Galectin-3 in Fibrosis

Our studies indicate that galectin-3 modulates the expression of several components of the extracellular matrix in the endothelium. Other studies in Sprague-Dawley rats show that intrapericardial administration of galectin-3 increases LV collagen content and reduces cardiac output (Liu, 2008). However, no studies have been performed to assess the affect of galectin deletion on cardiac fibrosis in diabetes. We therefore sought to assess collagen deposition and the expression of a key pro-fibrotic gene, *Ctgf*, in the hearts of our diabetic KO and WT animals. Although no collagen deposition is visible in the hearts of diabetic KO or WT mice after 8 weeks of high-fat diet, there was a slight increase

in *Ctgf* in the WT but not in the KO animal. Extending the duration of the high-fat diet or the use of transverse aortic constriction on diabetic animals to induce fibrosis may show a difference in collagen deposition in WT and KO animals. These studies will elucidate the role of galectin-3 in cardiac fibrosis and shed light on its potential as a therapeutic target.

4.2.5 Investigation of Mechanisms Leading to the Metabolic Perturbations in Galectin-3 Knockout Mice

Our data suggests that decreased expression of GLUT4 may reduce uptake of glucose by peripheral tissues and lead to the hyperglycemia and impaired glucose tolerance of the galectin-3(-/-) mouse. However, the physiological response to insulin challenge should be tested to confirm whether the KO has a defect in glucose uptake following insulin stimulation. This can be accomplished by performing an insulin tolerance test or a euglycemic-hyperinsulinemic clamp study.

Preliminary studies of insulin secretion also suggest that KO mice may have a defect in glucose sensing via GLUT2 and/or insulin production/secretion. As shown below, *Lgals3(-/-)* mice on a HFD exhibit defective insulin secretion in response to glucose challenge. However, further studies are needed to confirm whether the response of the diabetic KO differs significantly from WT diabetic mice. Defects in first or second phase insulin response may explain the hyperglycemia experienced by the galectin KO. If theses defects are observed, a closer look at the pancreas of the KO mice may reveal β cell dysfunction or low insulin content.

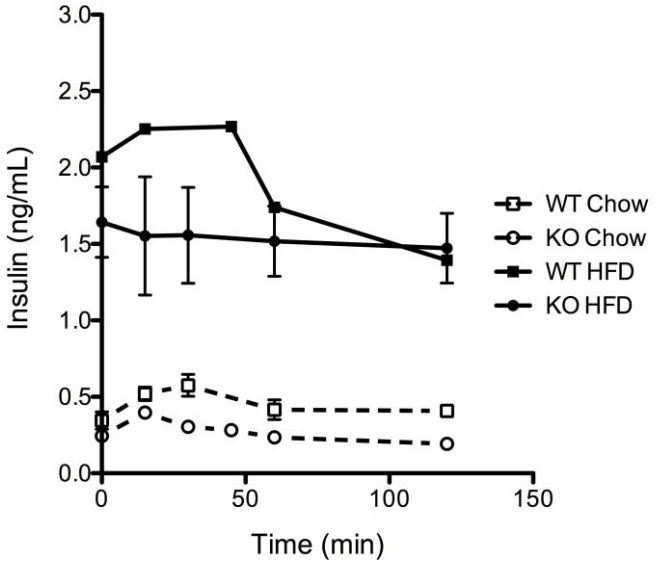

Figure 4.1. Glucose-stimulated insulin secretion in *Lgals3(-/-)* and wild-type mice after 8 weeks of chow or high-fat diet. Mice were fasted overnight and then injected intraperitoneally with glucose (1g/kg). Tail blood was collected into EDTA-coated tubes to separate plasma. Insulin levels in the plasma at the indicated timepoints after injection were measured by ELISA (Crystal Chem, cat. no. 90080). *N=3* for all groups except WT HFD where *n*=2.

Another possible cause of the hyperglycemia observed in the galectin KO is hepatic insulin resistance. When glucose levels are high, released insulin acts on the liver to inhibit pathways leading to gluconeogenesis and glycogenolysis. If the KO is experiencing hepatic insulin resistance, these pathways will not be inhibited, thus leading to the release of glucose into the bloodstream. Insulin sensitivity in the liver may be assessed by AKT phosphorylation after insulin challenge. Further studies are needed to verify hepatic insulin resistance or a defect in insulin production and secretion in diabetic KO mice.

4.3 Conclusions

Diabetes is characterized by hyperglycemia, hyperinsulinemia, inflammation, obesity, and an altered lipid profile. These factors directly impinge on the endothelium resulting in impaired vasomotor responses and the upregulation of pro-atherogenic mechanisms. Impaired endothelial function precedes diabetes and contributes to the development of insulin resistance and cardiovascular complications. Our *in vivo* assessment of the endothelial transcriptional response to diabetes provides a part of the molecular basis for the vascular pathology observed in diabetes. We have identified the dysregulation of novel transcripts with previously unrecognized roles in the endothelial dysfunction of diabetes, which may serve as diagnostic biomarkers for diabetic vasculopathy. One of these highly dysregulated transcripts, galectin-3, was further investigated for its role in the endothelial dysfunction associated with diabetes. Galectin-3 protein expression is upregulated in the endothelium of diabetic mice as well as in their serum, suggesting its utility as a biomarker for vascular pathology. Using the galectin-3 knockout mouse, we were able to deduce a protective role for galectin-3 in maintaining glucose homeostasis and endothelial function in the diabetic state. Differential dysregulation of transcripts involved in inflammation, vasoconstriction, coagulation, oxidant stress, glucose uptake, and insulin signaling is observed in the diabetic KO compared to WT mice. Further studies are needed to elucidate the exact mechanisms by which galectin-3 regulates glucose levels and preserves endothelial function in diabetes.

Appendix

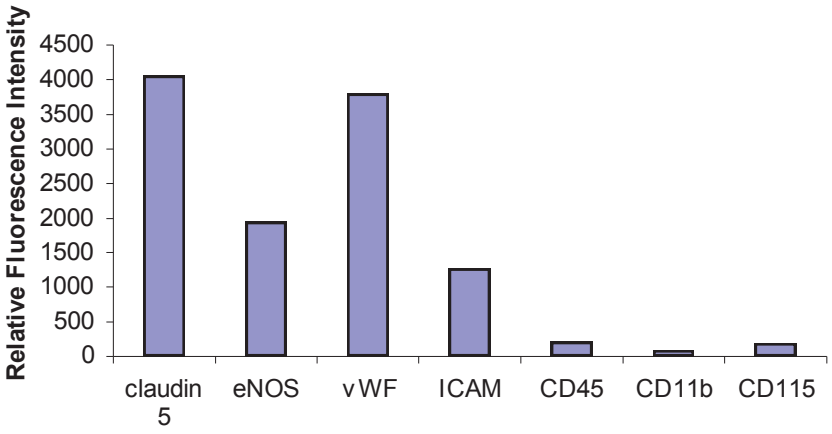

Figure A1. Relative fluorescent intensity of selected endothelial and leukocyte transcripts. The Cy-3-labeled mRNA transcripts were hybridized to the microarray oligo probes overnight. The microarray was scanned at 550nm and total fluorescent intensity emitted at 570nm was calculated using Genepix software. Endothelial transcripts include claudin-5, eNOS, vWF, and ICAM. Monocyte transcripts include CD45, CD11b, and CD115.

Table A1. Sequences of primers used for the real-time PCR experiments of Chapter 2 and the resulting amplified products. Following RT-PCR, amplicons were purified and sequenced by a 3730 DNA Analyzer (ABI). BLAST was used to confirm alignment of amplicon and transcript sequences.

Transcript	RefSeq ID	Forward / Reverse Primers	Amplicon Sequence
Lgals3	NM_ 010705	CAACAGGAGAGTCATTGTGTGTAA TTCAACCAGGACTTGTATTTTGAAT	GGCTGTATACTGGGGAA GGAGAAGACAGTCAGC CTTCCCCTTTGAGATGG AAAACCATTCAAAATACA AGTCCTGGTTGAAA
Ccl8	NM_ 021443	TGCTTTCATGTACTAAAGCTGAAGA CTACACAGAGAGACATACCCTGCTT	TAGGTGCTGAAGCTACG AGAGATCAACAATATCC AGTGCCCCATGGAAGCT GTGGTTTTCCAGACCAA GCAGGGTATGTCTCTCT GTGTAGA
Ccl9	NM_ 011338	CATTCTTACAACTGCTCTTGGAATC ACTGAATCCGTGAGTTATAGGACAG	TGCGATCCTGCACAGAG ACAAAGAAGCCAGAGCA GTCTGAAGGCACAGCAA GGGCTTGAAATTGAAAT GTTTCACATGGGCTTTC AAGACTCTTCAGATTGC TGCCTGTCCTATAACTC ACGGATTCAGTCG
Ftl1	NM_ 010240	ATCTCAAGATGAATGGGGTAAAAC CTCCTTATCCAGATAGTGGCTTTC	CGCTGCGGAGCTGCCTT GGCATGGAGAGAACCT GAATCAGGCCCTCTTGG ATCTGCATGCCCTGGGT TCTGCCCGCGCGGACC CTCATCTCTGTGACTTC CTGGAAAGCCACTATCT GGATAAGGAGA
Alox5ap	NM_ 009663	GTACCTGTTTGTGAGGCAAAAATAC AAGAAGAAGATGAGGTAATGGTTGA	TGTCGGCTCTGGAGAGA GACTCAGAGCACCCCTG GCTACATCTTCGGCAAG CGGATCATCCTGTTCCT GTTCCTCATGTCCTTCG CCGGGATACTCAACCAT TACCTCATCTTCTTCTTC G
Cyclo A	NM_ 008907	CAAAGTTCCAAAGACAGCAGAAAAC GGCACATGAATCCTGGAATAATTC	ATCTTGATATGGAGAGA AGGATTGGCTATAAGGG TCCTCCTTTCACAGAATT ATTCCAGGATTCATGTG CC

Table A2. Sequences of primers used for the real-time PCR described in Chapter 3.

Gene	Forward / Reverse Primers
Lgals3	TTT TCG CTT AAC GAT GCC TTA G GTA GGC CCC AGG ATA AGC AG
Igf1	AGG AGA CTG GAG ATG TAC TGT GC CTT CGT TTT CTT GTT TGT CGA TAG
G6pc	GGG TCT TCC TCT TAG CAC ATT TC AGC AGT CAA CCC ATA AAA GCT AAG
Igf1r	GGA TGG TGT CTT CAC TAC TCA TTC T ATG ACG AAA CGA AGA ACT TGC T
Lyve1	AAA CAG AAG CAT TTG TTG CAA GT CTT CAC ATA CCT TTT CAC GTA GCA
Retnla	AAG ACT ACA ACT TGT TCC CTT CTC A TTC GTT ACA GTG GAG GGA TAG TTA G
Cp	GTT CTA CTT GTT TCC CAC AGT GTT T GGA GTG CAT CTT ATT AGA CTC CTG A
Cav3	GGC TTT GCG TTC ACA TGT ACT GCA GTT AAA ACC CTT TAT TGC AG
Glut4	GGC ATC AAT GCT GTT TTC TAC TAT T TCT ACT AAG AGC ACC GAG ACC AAC
Irs1	ACA GCA GAA TGA AGA CCT AAA TGA C GTA CCA TCT ACT GAA GAG GAA GAC G
Marco	GGG ATG AAA GGG TCT TCT GG GTC CCC CAC TCA TTG TTA TAG TAA A
Ptgfr	GTT CAG AAG CCA GCA GCA TAG ACT GGG GAA TTA TTT CCA TTT ATT G
Cyclo A	CAAAGTTCCAAAGACAGCAGAAAAC GGCACATGAATCCTGGAATAATTC

References

Abdul-Ghani, M. A., Jenkinson, C. P., Richardson, D. K., Tripathy, D., & DeFronzo, R. A. (2006). Insulin secretion and action in subjects with impaired fasting glucose and impaired glucose tolerance: results from the Veterans Administration Genetic Epidemiology Study. *Diabetes, 55*(5), 1430-1435.

Abel, E. D. (2005). Myocardial insulin resistance and cardiac complications of diabetes. *Curr Drug Targets Immune Endocr Metabol Disord, 5*(2), 219-226.

Ahmad, N., Gabius, H. J., Andre, S., Kaltner, H., Sabesan, S., Roy, R., et al. (2004). Galectin-3 precipitates as a pentamer with synthetic multivalent carbohydrates and forms heterogeneous cross-linked complexes. *J Biol Chem, 279*(12), 10841-10847.

Ahmed, A. M. (2002). Deficiencies of history taking among medical students. *Saudi Med J, 23*(8), 991-994.

Akagiri, S., Naito, Y., Ichikawa, H., Mizushima, K., Takagi, T., Handa, O., et al. (2008). A Mouse Model of Metabolic Syndrome; Increase in Visceral Adipose Tissue Precedes the Development of Fatty Liver and Insulin Resistance in High-Fat Diet-Fed Male KK/Ta Mice. *J Clin Biochem Nutr, 42*(2), 150-157.

Alessi, M. C., & Juhan-Vague, I. (2008). Metabolic syndrome, haemostasis and thrombosis. *Thromb Haemost, 99*(6), 995-1000.

Alp, N. J., Mussa, S., Khoo, J., Cai, S., Guzik, T., Jefferson, A., et al. (2003). Tetrahydrobiopterin-dependent preservation of nitric oxide-mediated endothelial function in diabetes by targeted transgenic GTP-cyclohydrolase I overexpression. *J Clin Invest, 112*(5), 725-735.

Alzahrani, S. H., & Ajjan, R. A. (2010). Coagulation and fibrinolysis in diabetes. *Diab Vasc Dis Res, 7*(4), 260-273.

American Diabetes Association (2003): Report of the expert committee on the diagnosis and classification of diabetes mellitus. *Diabetes Care, 26 Suppl 1*, S5-20.

Andrades, M. E., Lorenzi, R., Berger, M., Guimaraes, J. A., Moreira, J. C., & Dal-Pizzol, F. (2009). Glycolaldehyde induces fibrinogen post-translational modification, delay in clotting and resistance to enzymatic digestion. *Chem Biol Interact, 180*(3), 478-484.

Annex, B. H., Denning, S. M., Channon, K. M., Sketch, M. H., Jr., Stack, R. S., Morrissey, J. H., et al. (1995). Differential expression of tissue factor protein in

directional atherectomy specimens from patients with stable and unstable coronary syndromes. *Circulation, 91*(3), 619-622.

Avogaro, A., de Kreutzenberg, S. V., & Fadini, G. (2008). Endothelial dysfunction: causes and consequences in patients with diabetes mellitus. *Diabetes Res Clin Pract, 82 Suppl 2*, S94-S101.

Bakker, W., Eringa, E. C., Sipkema, P., & van Hinsbergh, V. W. (2009). Endothelial dysfunction and diabetes: roles of hyperglycemia, impaired insulin signaling and obesity. *Cell Tissue Res, 335*(1), 165-189.

Banerji, S., Ni, J., Wang, S. X., Clasper, S., Su, J., Tammi, R., et al. (1999). LYVE-1, a new homologue of the CD44 glycoprotein, is a lymph-specific receptor for hyaluronan. *J Cell Biol, 144*(4), 789-801.

Barazzoni, R., Kiwanuka, E., Zanetti, M., Cristini, M., Vettore, M., & Tessari, P. (2003). Insulin acutely increases fibrinogen production in individuals with type 2 diabetes but not in individuals without diabetes. *Diabetes, 52*(7), 1851-1856.

Barondes, S. H., Cooper, D. N., Gitt, M. A., & Leffler, H. (1994). Galectins. Structure and function of a large family of animal lectins. *J Biol Chem, 269*(33), 20807-20810.

Bassi, R., Trevisani, A., Tezza, S., Ben Nasr, M., Gatti, F., Vergani, A., et al. (2012). Regenerative therapies for diabetic microangiopathy. *Exp Diabetes Res, 2012*, 916560.

Befroy, D. E., Petersen, K. F., Dufour, S., Mason, G. F., de Graaf, R. A., Rothman, D. L., et al. (2007). Impaired mitochondrial substrate oxidation in muscle of insulin-resistant offspring of type 2 diabetic patients. *Diabetes, 56*(5), 1376-1381.

Belfrage, P., Fredrikson, G., Olsson, H., & Stralfors, P. (1982). Hormonal regulation of adipose tissue lipolysis by reversible phosphorylation of hormone-sensitive lipase. *Prog Clin Biol Res, 102 Pt C*, 213-223.

Berglund, E. D., Li, C. Y., Poffenberger, G., Ayala, J. E., Fueger, P. T., Willis, S. E., et al. (2008). Glucose metabolism in vivo in four commonly used inbred mouse strains. *Diabetes, 57*(7), 1790-1799.

Blair, A., Shaul, P. W., Yuhanna, I. S., Conrad, P. A., & Smart, E. J. (1999). Oxidized low density lipoprotein displaces endothelial nitric-oxide synthase (eNOS) from plasmalemmal caveolae and impairs eNOS activation. *J Biol Chem, 274*(45), 32512-32519.

Bleich, D., Chen, S., Zipser, B., Sun, D., Funk, C. D., & Nadler, J. L. (1999). Resistance to type 1 diabetes induction in 12-lipoxygenase knockout mice. *J Clin Invest, 103*(10), 1431-1436.

Boden, G., Vaidyula, V. R., Homko, C., Cheung, P., & Rao, A. K. (2007). Circulating tissue factor procoagulant activity and thrombin generation in patients with type 2 diabetes: effects of insulin and glucose. *J Clin Endocrinol Metab, 92*(11), 4352-4358.

Boden, J., Wei, J., McNamara, G., Layman, H., Abdulreda, M., Andreopolous, F., et al. (2012). Whole-mount imaging of the mouse hindlimb vasculature using the lipophilic carbocyanine dye DiI. *Biotechniques, 0*(0), 1-4.

Bristow, A.F., R.E. Das, and D.R. Bangham. (1988). World Health Organization International Standards for highly purified human, porcine and bovine insulins. *J Biol Stand* 16:165-178.

Brownlee, M. (2001). Biochemistry and molecular cell biology of diabetic complications. *Nature, 414*(6865), 813-820.

Bruno, G., Cavallo-Perin, P., Bargero, G., Borra, M., D'Errico, N., & Pagano, G. (1996). Association of fibrinogen with glycemic control and albumin excretion rate in patients with non-insulin-dependent diabetes mellitus. *Ann Intern Med, 125*(8), 653-657.

Burton, A. (1954). Relation of Structure to Function of the Tissues of the Wall of Blood Vessels. *Physiological Reviews, 34*(4), 23.

Buse, J. B., Ginsberg, H. N., Bakris, G. L., Clark, N. G., Costa, F., Eckel, R., et al. (2007). Primary prevention of cardiovascular diseases in people with diabetes mellitus: a scientific statement from the American Heart Association and the American Diabetes Association. *Diabetes Care, 30*(1), 162-172.

Cade, W. (2008). Diabetes-Related Microvascular and Macrovascular Diseases in the Physical Therapy Setting. *Physical Therapy, 88*(11), 1322-1335.

Calvier, L., Miana, M., Reboul, P., Cachofeiro, V., Martinez-Martinez, E., de Boer, R. A., et al. Galectin-3 mediates aldosterone-induced vascular fibrosis. *Arterioscler Thromb Vasc Biol, 33*(1), 67-75.

Canning, P., Glenn, J. V., Hsu, D. K., Liu, F. T., Gardiner, T. A., & Stitt, A. W. (2007). Inhibition of advanced glycation and absence of galectin-3 prevent blood-retinal barrier dysfunction during short-term diabetes. *Exp Diabetes Res, 2007*, 51837.

Cefalu, W. T., Schneider, D. J., Carlson, H. E., Migdal, P., Gan Lim, L., Izon, M. P., et al. (2002). Effect of combination glipizide GITS/metformin on fibrinolytic and metabolic parameters in poorly controlled type 2 diabetic subjects. *Diabetes Care, 25*(12), 2123-2128.

Centers for Disease Control and Prevention. (2011). *National diabetes fact sheet: national estimates and general information on diabetes and prediabetes in the*

United States, 2011. Atlanta, GA: U.S. Department of Health and Human Services, Centers for Disease Control and Prevention.

Ceriello, A., Esposito, K., Ihnat, M., Zhang, J., & Giugliano, D. (2009). Simultaneous control of hyperglycemia and oxidative stress normalizes enhanced thrombin generation in type 1 diabetes. *J Thromb Haemost, 7*(7), 1228-1230.

Ceriello, A., Mercuri, F., Fabbro, D., Giacomello, R., Stel, G., Taboga, C., et al. (1998). Effect of intensive glycaemic control on fibrinogen plasma concentrations in patients with Type II diabetes mellitus. Relation with beta-fibrinogen genotype. *Diabetologia, 41*(11), 1270-1273.

Ceylan-Isik, A. F., Wu, S., Li, Q., Li, S. Y., & Ren, J. (2006). High-dose benfotiamine rescues cardiomyocyte contractile dysfunction in streptozotocin-induced diabetes mellitus. *J Appl Physiol, 100*(1), 150-156.

Chen, Q., Kim, E. E., Elio, K., Zambrano, C., Krass, S., Teng, J. C., et al. The role of tetrahydrobiopterin and dihydrobiopterin in ischemia/reperfusion injury when given at reperfusion. *Adv Pharmacol Sci, 2010*, 963914.

Chiu, D. S., Oram, J. F., LeBoeuf, R. C., Alpers, C. E., & O'Brien, K. D. (1997). High-density lipoprotein-binding protein (HBP)/vigilin is expressed in human atherosclerotic lesions and colocalizes with apolipoprotein E. *Arterioscler Thromb Vasc Biol, 17*(11), 2350-2358.

Chiu, J. J., Chen, L. J., Lee, P. L., Lee, C. I., Lo, L. W., Usami, S., et al. (2003). Shear stress inhibits adhesion molecule expression in vascular endothelial cells induced by coculture with smooth muscle cells. *Blood, 101*(7), 2667-2674.

Clifford, P. S., & Hellsten, Y. (2004). Vasodilatory mechanisms in contracting skeletal muscle. *J Appl Physiol, 97*(1), 393-403.

Colgan, S. M., & Austin, R. C. (2007). Homocysteinylation of Metallothionein Impairs Intracellular Redox Homeostasis: The Enemy Within! *Arterioscler Thromb Vasc Biol, 27*(1), 8-11.

Cosentino, F., Hurlimann, D., Delli Gatti, C., Chenevard, R., Blau, N., Alp, N. J., et al. (2008). Chronic treatment with tetrahydrobiopterin reverses endothelial dysfunction and oxidative stress in hypercholesterolaemia. *Heart, 94*(4), 487-492.

Cybulsky, M. I., & Gimbrone, M. A., Jr. (1991). Endothelial expression of a mononuclear leukocyte adhesion molecule during atherogenesis. *Science, 251*(4995), 788-791.

Cyrus, T., Pratico, D., Zhao, L., Witztum, J. L., Rader, D. J., Rokach, J., et al. (2001). Absence of 12/15-lipoxygenase expression decreases lipid peroxidation and

atherogenesis in apolipoprotein e-deficient mice. *Circulation, 103*(18), 2277-2282.

Dandona, P., & Aljada, A. (2004). Endothelial dysfunction in patients with type 2 diabetes and the effects of thiazolidinedione antidiabetic agents. *J Diabetes Complications, 18*(2), 91-102.

Darrow, A. L., Shohet, R. V., & Maresh, J. G. (2011). Transcriptional analysis of the endothelial response to diabetes reveals a role for galectin-3. *Physiol Genomics, 43*(20), 1144-1152.

Davidoff, A. J. (2006). Convergence of glucose- and fatty acid-induced abnormal myocardial excitation-contraction coupling and insulin signalling. *Clin Exp Pharmacol Physiol, 33*(1-2), 152-158.

Davidson, P. J., Li, S. Y., Lohse, A. G., Vandergaast, R., Verde, E., Pearson, A., et al. (2006). Transport of galectin-3 between the nucleus and cytoplasm. I. Conditions and signals for nuclear import. *Glycobiology, 16*(7), 602-611.

Davis, B., Dei Cas, A., Long, D. A., White, K. E., Hayward, A., Ku, C. H., et al. (2007). Podocyte-specific expression of angiopoietin-2 causes proteinuria and apoptosis of glomerular endothelia. *J Am Soc Nephrol, 18*(8), 2320-2329.

de Boer, R. A., Lok, D. J., Jaarsma, T., van der Meer, P., Voors, A. A., Hillege, H. L., et al. (2011). Predictive value of plasma galectin-3 levels in heart failure with reduced and preserved ejection fraction. *Ann Med, 43*(1), 60-68.

de Boer, R. A., Yu, L., & van Veldhuisen, D. J. (2010). Galectin-3 in cardiac remodeling and heart failure. *Curr Heart Fail Rep, 7*(1), 1-8.

Degenhardt, T. P., Alderson, N. L., Arrington, D. D., Beattie, R. J., Basgen, J. M., Steffes, M. W., et al. (2002). Pyridoxamine inhibits early renal disease and dyslipidemia in the streptozotocin-diabetic rat. *Kidney Int, 61*(3), 939-950.

DeVerse, J. S., Bailey, K. A., Jackson, K. N., & Passerini, A. G. (2012). Shear stress modulates RAGE-mediated inflammation in a model of diabetes-induced metabolic stress. *Am J Physiol Heart Circ Physiol, 302*(12), H2498-2508.

Dollery, C. T., Friedman, L. A., Hensby, C. N., Kohner, E., Lewis, P. J., Porta, M., et al. (1979). Circulating prostacyclin may be reduced in diabetes. *Lancet, 2*(8156-8157), 1365.

Dong, Z. M., Chapman, S. M., Brown, A. A., Frenette, P. S., Hynes, R. O., & Wagner, D. D. (1998). The combined role of P- and E-selectins in atherosclerosis. *J Clin Invest, 102*(1), 145-152.

Dumic, J., Dabelic, S., & Flogel, M. (2006). Galectin-3: an open-ended story. *Biochim Biophys Acta, 1760*(4), 616-635. Images reprinted with permission from Elsevier.

Dunn, E. J., Philippou, H., Ariens, R. A., & Grant, P. J. (2006). Molecular mechanisms involved in the resistance of fibrin to clot lysis by plasmin in subjects with type 2 diabetes mellitus. *Diabetologia, 49*(5), 1071-1080.

Dunne, M. J., Cosgrove, K. E., Shepherd, R. M., & Ammala, C. (1999). Potassium Channels, Sulphonylurea Receptors and Control of Insulin Release. *Trends Endocrinol Metab, 10*(4), 146-152. Image reprinted with permission from Elsevier.

Elola, M. T., Wolfenstein-Todel, C., Troncoso, M. F., Vasta, G. R., & Rabinovich, G. A. (2007). Galectins: matricellular glycan-binding proteins linking cell adhesion, migration, and survival. *Cell Mol Life Sci, 64*(13), 1679-1700.

Evans, J. F., Ferguson, A. D., Mosley, R. T., & Hutchinson, J. H. (2008). What's all the FLAP about?: 5-lipoxygenase-activating protein inhibitors for inflammatory diseases. *Trends in Pharmacological Sciences, 29*(2), 72-78.

Fang, Z. Y., Prins, J. B., & Marwick, T. H. (2004). Diabetic cardiomyopathy: evidence, mechanisms, and therapeutic implications. *Endocr Rev, 25*(4), 543-567.

Flatt, J. P. (1987). Dietary fat, carbohydrate balance, and weight maintenance: effects of exercise. *Am J Clin Nutr, 45*(1 Suppl), 296-306.

Fonsatti, E., & Maio, M. (2004). Highlights on endoglin (CD105): from basic findings towards clinical applications in human cancer. *J Transl Med, 2*(1), 18.

Forbes, J. M., Soldatos, G., & Thomas, M. C. (2005). Below the radar: advanced glycation end products that detour "around the side". Is HbA1c not an accurate enough predictor of long term progression and glycaemic control in diabetes? *Clin Biochem Rev, 26*(4), 123-134.

Fowler, M. J. (2008). Microvascular and Macrovascular Complications of Diabetes. *Clinical Diabetes, 26*(2), 77-82.

Francis, S. H., Busch, J. L., Corbin, J. D., & Sibley, D. (2010). cGMP-dependent protein kinases and cGMP phosphodiesterases in nitric oxide and cGMP action. *Pharmacol Rev, 62*(3), 525-563.

Frigeri, L. G., Zuberi, R. I., & Liu, F. T. (1993). Epsilon BP, a beta-galactoside-binding animal lectin, recognizes IgE receptor (Fc epsilon RI) and activates mast cells. *Biochemistry, 32*(30), 7644-7649.

Frustaci, A., Kajstura, J., Chimenti, C., Jakoniuk, I., Leri, A., Maseri, A., et al. (2000). Myocardial cell death in human diabetes. *Circ Res, 87*(12), 1123-1132.

Fukushi, J., Makagiansar, I. T., & Stallcup, W. B. (2004). NG2 proteoglycan promotes endothelial cell motility and angiogenesis via engagement of galectin-3 and alpha3beta1 integrin. *Mol Biol Cell, 15*(8), 3580-3590.

Funk, S. D., Yurdagul, A., Jr., & Orr, A. W. (2012). Hyperglycemia and endothelial dysfunction in atherosclerosis: lessons from type 1 diabetes. *Int J Vasc Med, 2012*, 569654.

Gebel, E. Diabetes by the numbers. *Diabetes Forecast, 65*(11), 42-46.

George, J., Afek, A., Shaish, A., Levkovitz, H., Bloom, N., Cyrus, T., et al. (2001). 12/15-Lipoxygenase gene disruption attenuates atherogenesis in LDL receptor-deficient mice. *Circulation, 104*(14), 1646-1650.

Gil, C. D., La, M., Perretti, M., & Oliani, S. M. (2006). Interaction of human neutrophils with endothelial cells regulates the expression of endogenous proteins annexin 1, galectin-1 and galectin-3. *Cell Biol Int, 30*(4), 338-344.

Glass, C. K., & Witztum, J. L. (2001). Atherosclerosis. the road ahead. *Cell, 104*(4), 503-516.

Gleissner, C. A., Galkina, E., Nadler, J. L., & Ley, K. (2007). Mechanisms by which diabetes increases cardiovascular disease. *Drug Discov Today Dis Mech, 4*(3), 131-140.

Glinsky, V. V., Kiriakova, G., Glinskii, O. V., Mossine, V. V., Mawhinney, T. P., Turk, J. R., et al. (2009). Synthetic galectin-3 inhibitor increases metastatic cancer cell sensitivity to taxol-induced apoptosis in vitro and in vivo. *Neoplasia, 11*(9), 901-909.

Gong, H. C., Honjo, Y., Nangia-Makker, P., Hogan, V., Mazurak, N., Bresalier, R. S., et al. (1999). The NH2 terminus of galectin-3 governs cellular compartmentalization and functions in cancer cells. *Cancer Res, 59*(24), 6239-6245.

Gregg, E. W., Sorlie, P., Paulose-Ram, R., Gu, Q., Eberhardt, M. S., Wolz, M., et al. (2004). Prevalence of lower-extremity disease in the US adult population >=40 years of age with and without diabetes: 1999-2000 national health and nutrition examination survey. *Diabetes Care, 27*(7), 1591-1597.

Gresele, P., Guglielmini, G., De Angelis, M., Ciferri, S., Ciofetta, M., Falcinelli, E., et al. (2003). Acute, short-term hyperglycemia enhances shear stress-induced platelet activation in patients with type II diabetes mellitus. *J Am Coll Cardiol, 41*(6), 1013-1020.

Gross, J. L., de Azevedo, M. J., Silveiro, S. P., Canani, L. H., Caramori, M. L., & Zelmanovitz, T. (2005). Diabetic nephropathy: diagnosis, prevention, and treatment. *Diabetes Care, 28*(1), 164-176.

Guay, V., Lamarche, B., Charest, A., Tremblay, A. J., & Couture, P. (2012). Effect of short-term low- and high-fat diets on low-density lipoprotein particle size in normolipidemic subjects. *Metabolism, 61*(1), 76-83.

Guerci, B., Bohme, P., Kearney-Schwartz, A., Zannad, F., & Drouin, P. (2001). Endothelial dysfunction and type 2 diabetes. Part 2: altered endothelial function and the effects of treatments in type 2 diabetes mellitus. *Diabetes Metab, 27*(4 Pt 1), 436-447.

Guerci, B., Kearney-Schwartz, A., Bohme, P., Zannad, F., & Drouin, P. (2001). Endothelial dysfunction and type 2 diabetes. Part 1: physiology and methods for exploring the endothelial function. *Diabetes Metab, 27*(4 Pt 1), 425-434.

Hadi, H. A., & Suwaidi, J. A. (2007). Endothelial dysfunction in diabetes mellitus. *Vasc Health Risk Manag, 3*(6), 853-876.

Hafer-Macko, C. E., Ivey, F. M., Sorkin, J. D., & Macko, R. F. (2007). Microvascular tissue plasminogen activator is reduced in diabetic neuropathy. *Neurology, 69*(3), 268-274.

Haffner, S. M., Lehto, S., Ronnemaa, T., Pyorala, K., & Laakso, M. (1998). Mortality from coronary heart disease in subjects with type 2 diabetes and in nondiabetic subjects with and without prior myocardial infarction. *N Engl J Med, 339*(4), 229-234.

Haller, H., Drab, M., & Luft, F. C. (1996). The role of hyperglycemia and hyperinsulinemia in the pathogenesis of diabetic angiopathy. *Clin Nephrol, 46*(4), 246-255.

Haluzik, M., Colombo, C., Gavrilova, O., Chua, S., Wolf, N., Chen, M., et al. (2004). Genetic background (C57BL/6J versus FVB/N) strongly influences the severity of diabetes and insulin resistance in ob/ob mice. *Endocrinology, 145*(7), 3258-3264.

Harrington, L. S., Findlay, G. M., & Lamb, R. F. (2005). Restraining PI3K: mTOR signalling goes back to the membrane. *Trends Biochem Sci, 30*(1), 35-42.

Hashimoto, T., Kihara, M., Imai, N., Yoshida, S., Shimoyamada, H., Yasuzaki, H., et al. (2007). Requirement of apelin-apelin receptor system for oxidative stress-linked atherosclerosis. *Am J Pathol, 171*(5), 1705-1712.

Henderson, N. C., Mackinnon, A. C., Farnworth, S. L., Poirier, F., Russo, F. P., Iredale, J. P., et al. (2006). Galectin-3 regulates myofibroblast activation and hepatic fibrosis. *Proc Natl Acad Sci U S A, 103*(13), 5060-5065.

Heywood, D. M., Mansfield, M. W., & Grant, P. J. (1996). Factor VII gene polymorphisms, factor VII:C levels and features of insulin resistance in non-insulin-dependent diabetes mellitus. *Thromb Haemost, 75*(3), 401-406.

Hiden, U., Maier, A., Bilban, M., Ghaffari-Tabrizi, N., Wadsack, C., Lang, I., et al. (2006). Insulin control of placental gene expression shifts from mother to foetus over the course of pregnancy. *Diabetologia, 49*(1), 123-131.

Hinsdale, M. E., Sullivan, P. M., Mezdour, H., & Maeda, N. (2002). ApoB-48 and apoB-100 differentially influence the expression of type-III hyperlipoproteinemia in APOE*2 mice. *J Lipid Res, 43*(9), 1520-1528.

Ho, M., Yang, E., Matcuk, G., Deng, D., Sampas, N., Tsalenko, A., et al. (2003). Identification of endothelial cell genes by combined database mining and microarray analysis. *Physiol. Genomics, 13*(3), 249-262.

Hsieh, S. H., Ying, N. W., Wu, M. H., Chiang, W. F., Hsu, C. L., Wong, T. Y., et al. (2008). Galectin-1, a novel ligand of neuropilin-1, activates VEGFR-2 signaling and modulates the migration of vascular endothelial cells. *Oncogene, 27*(26), 3746-3753.

Hsueh, W., Abel, E. D., Breslow, J. L., Maeda, N., Davis, R. C., Fisher, E. A., et al. (2007). Recipes for creating animal models of diabetic cardiovascular disease. *Circ Res, 100*(10), 1415-1427.

Huang, A., Yang, Y. M., Feher, A., Bagi, Z., Kaley, G., & Sun, D. (2012). Exacerbation of endothelial dysfunction during the progression of diabetes: role of oxidative stress. *Am J Physiol Regul Integr Comp Physiol, 302*(6), R674-681.

Huang da, W., Sherman, B. T., & Lempicki, R. A. (2009a). Bioinformatics enrichment tools: paths toward the comprehensive functional analysis of large gene lists. *Nucleic Acids Res, 37*(1), 1-13.

Huang da, W., Sherman, B. T., & Lempicki, R. A. (2009b). Systematic and integrative analysis of large gene lists using DAVID bioinformatics resources. *Nat Protoc, 4*(1), 44-57.

Hughes, R. C. (2001). Galectins as modulators of cell adhesion. *Biochimie, 83*(7), 667-676.

Iacobini, C., Menini, S., Ricci, C., Scipioni, A., Sansoni, V., Cordone, S., et al. (2009). Accelerated lipid-induced atherogenesis in galectin-3-deficient mice: role of lipoxidation via receptor-mediated mechanisms. *Arterioscler Thromb Vasc Biol, 29*(6), 831-836.

Ieronimakis, N., Balasundaram, G., & Reyes, M. (2008). Direct isolation, culture and transplant of mouse skeletal muscle derived endothelial cells with angiogenic potential. *PLoS One, 3*(3), e0001753.

Ikegami, H., Fujisawa, T., & Ogihara, T. (2004). Mouse models of type 1 and type 2 diabetes derived from the same closed colony: genetic susceptibility shared between two types of diabetes. *ILAR J, 45*(3), 268-277.

Inoguchi, T., Li, P., Umeda, F., Yu, H. Y., Kakimoto, M., Imamura, M., et al. (2000). High glucose level and free fatty acid stimulate reactive oxygen species production through protein kinase C--dependent activation of NAD(P)H oxidase in cultured vascular cells. *Diabetes, 49*(11), 1939-1945.

Ishizuka, T., Kawakami, M., Hidaka, T., Matsuki, Y., Takamizawa, M., Suzuki, K., et al. (1998). Stimulation with thromboxane A2 (TXA2) receptor agonist enhances ICAM-1, VCAM-1 or ELAM-1 expression by human vascular endothelial cells. *Clin Exp Immunol, 112*(3), 464-470.

Ito, S., Naito, M., Kobayashi, Y., Takatsuka, H., Jiang, S., Usuda, H., et al. (1999). Roles of a macrophage receptor with collagenous structure (MARCO) in host defense and heterogeneity of splenic marginal zone macrophages. *Arch Histol Cytol, 62*(1), 83-95.

Iurisci, I., Tinari, N., Natoli, C., Angelucci, D., Cianchetti, E., & Iacobelli, S. (2000). Concentrations of galectin-3 in the sera of normal controls and cancer patients. *Clin Cancer Res, 6*(4), 1389-1393.

Jang, M. K., Choi, M. S., & Park, Y. B. (1999). Regulation of ferritin light chain gene expression by oxidized low-density lipoproteins in human monocytic THP-1 cells. *Biochem Biophys Res Commun, 265*(2), 577-583.

Jansson, P. A., Pellme, F., Hammarstedt, A., Sandqvist, M., Brekke, H., Caidahl, K., et al. (2003). A novel cellular marker of insulin resistance and early atherosclerosis in humans is related to impaired fat cell differentiation and low adiponectin. *FASEB J, 17*(11), 1434-1440.

Jawien, J., Gajda, M., Rudling, M., Mateuszuk, L., Olszanecki, R., Guzik, T. J., et al. (2006). Inhibition of five lipoxygenase activating protein (FLAP) by MK-886 decreases atherosclerosis in apoE/LDLR-double knockout mice. *European Journal of Clinical Investigation, 36*(3), 141-146.

Jiang, X., Yang, F., Tan, H., Liao, D., Bryan, R. M., Jr., Randhawa, J. K., et al. (2005). Hyperhomocystinemia impairs endothelial function and eNOS activity via PKC activation. *Arterioscler Thromb Vasc Biol, 25*(12), 2515-2521.

Johnson, K. D., Glinskii, O. V., Mossine, V. V., Turk, J. R., Mawhinney, T. P., Anthony, D. C., et al. (2007). Galectin-3 as a potential therapeutic target in tumors arising from malignant endothelia. *Neoplasia, 9*(8), 662-670.

Johnson, M., Harrison, H. E., Raftery, A. T., & Elder, J. B. (1979). Vascular prostacyclin may be reduced in diabetes in man. *Lancet, 1*(8111), 325-326.

Johnston-Cox, H., Koupenova, M., Yang, D., Corkey, B., Gokce, N., Farb, M. G., et al. (2012). The A2b adenosine receptor modulates glucose homeostasis and obesity. *PLoS One, 7*(7), e40584.

Kadrofske, M. M., Openo, K. P., & Wang, J. L. (1998). The human LGALS3 (galectin-3) gene: determination of the gene structure and functional characterization of the promoter. *Arch Biochem Biophys, 349*(1), 7-20. Image reprinted with permission from Elsevier.

Kamm, K. E., & Stull, J. T. (1985). The function of myosin and myosin light chain kinase phosphorylation in smooth muscle. *Annu Rev Pharmacol Toxicol, 25*, 593-620.

Kanda, H., Tateya, S., Tamori, Y., Kotani, K., Hiasa, K., Kitazawa, R., et al. (2006). MCP-1 contributes to macrophage infiltration into adipose tissue, insulin resistance, and hepatic steatosis in obesity. *J Clin Invest, 116*(6), 1494-1505.

Karalliedde, J., & Gnudi, L. (2011). Endothelial factors and diabetic nephropathy. *Diabetes Care, 34 Suppl 2*, S291-296.

Karpen, C. W., Pritchard, K. A., Jr., Merola, A. J., & Panganamala, R. V. (1982). Alterations of the prostacyclin-thromboxane ratio in streptozotocin induced diabetic rats. *Prostaglandins Leukot Med, 8*(2), 93-103.

Kelley, D. E., He, J., Menshikova, E. V., & Ritov, V. B. (2002). Dysfunction of mitochondria in human skeletal muscle in type 2 diabetes. *Diabetes, 51*(10), 2944-2950.

Khaldoyanidi, S. K., Glinsky, V. V., Sikora, L., Glinskii, A. B., Mossine, V. V., Quinn, T. P., et al. (2003). MDA-MB-435 human breast carcinoma cell homo- and heterotypic adhesion under flow conditions is mediated in part by Thomsen-Friedenreich antigen-galectin-3 interactions. *J Biol Chem, 278*(6), 4127-4134.

Khan, S. S., Solomon, M. A., & McCoy, J. P., Jr. (2005). Detection of circulating endothelial cells and endothelial progenitor cells by flow cytometry. *Cytometry B Clin Cytom, 64*(1), 1-8.

Kim, F., Pham, M., Luttrell, I., Bannerman, D. D., Tupper, J., Thaler, J., et al. (2007). Toll-like receptor-4 mediates vascular inflammation and insulin resistance in diet-induced obesity. *Circ Res, 100*(11), 1589-1596.

Kim, F., Pham, M., Maloney, E., Rizzo, N. O., Morton, G. J., Wisse, B. E., et al. (2008). Vascular Inflammation, Insulin Resistance, and Reduced Nitric Oxide Production Precede the Onset of Peripheral Insulin Resistance. *Arterioscler Thromb Vasc Biol, 28*(11), 1982-1988.

King, K. M., & Rubin, G. (2003). A history of diabetes: from antiquity to discovering insulin. *Br J Nurs, 12*(18), 1091-1095.

Klein, R. L., Hunter, S. J., Jenkins, A. J., Zheng, D., Semler, A. J., Clore, J., et al. (2003). Fibrinogen is a marker for nephropathy and peripheral vascular disease in type 1 diabetes: studies of plasma fibrinogen and fibrinogen gene polymorphism in the DCCT/EDIC cohort. *Diabetes Care, 26*(5), 1439-1448.

Kraus, W. E., Houmard, J. A., Duscha, B. D., Knetzger, K. J., Wharton, M. B., McCartney, J. S., et al. (2002). Effects of the amount and intensity of exercise on plasma lipoproteins. *N Engl J Med, 347*(19), 1483-1492.

Krishnan, V., Bane, S. M., Kawle, P. D., Naresh, K. N., & Kalraiya, R. D. (2005). Altered melanoma cell surface glycosylation mediates organ specific adhesion and metastasis via lectin receptors on the lung vascular endothelium. *Clin Exp Metastasis, 22*(1), 11-24.

Kuhn, H., Heydeck, D., Hugou, I., & Gniwotta, C. (1997). In vivo action of 15-lipoxygenase in early stages of human atherogenesis. *J Clin Invest, 99*(5), 888-893.

Kuklinski, S., & Probstmeier, R. (1998). Homophilic binding properties of galectin-3: involvement of the carbohydrate recognition domain. *J Neurochem, 70*(2), 814-823.

Laios, K., Karamanou, M., Saridaki, Z., & Androutsos, G. (2012). Aretaeus of Cappadocia and the first description of diabetes. *Hormones (Athens), 11*(1), 109-113.

Lakshminrusimha, S., Porta, N. F., Farrow, K. N., Chen, B., Gugino, S. F., Kumar, V. H., et al. (2009). Milrinone enhances relaxation to prostacyclin and iloprost in pulmonary arteries isolated from lambs with persistent pulmonary hypertension of the newborn. *Pediatr Crit Care Med, 10*(1), 106-112.

Lee, M. R., Li, L., & Kitazawa, T. (1997). Cyclic GMP causes Ca2+ desensitization in vascular smooth muscle by activating the myosin light chain phosphatase. *J Biol Chem, 272*(8), 5063-5068.

Ley, K., Laudanna, C., Cybulsky, M. I., & Nourshargh, S. (2007). Getting to the site of inflammation: the leukocyte adhesion cascade updated. *Nat Rev Immunol, 7*(9), 678-689.

Li, J., Wang, Q., Chai, W., Chen, M. H., Liu, Z., & Shi, W. (2011). Hyperglycemia in apolipoprotein E-deficient mouse strains with different atherosclerosis susceptibility. *Cardiovasc Diabetol, 10*, 117.

Li, L., Naples, M., Song, H., Yuan, R., Ye, F., Shafi, S., et al. (2007). LCAT-null mice develop improved hepatic insulin sensitivity through altered regulation of transcription factors and suppressors of cytokine signaling. *Am J Physiol Endocrinol Metab, 293*(2), E587-594.

Li, S. Y., Davidson, P. J., Lin, N. Y., Patterson, R. J., Wang, J. L., & Arnoys, E. J. (2006). Transport of galectin-3 between the nucleus and cytoplasm. II. Identification of the signal for nuclear export. *Glycobiology, 16*(7), 612-622.

Lim, S. C., Caballero, A. E., Smakowski, P., LoGerfo, F. W., Horton, E. S., & Veves, A. (1999). Soluble intercellular adhesion molecule, vascular cell adhesion molecule, and impaired microvascular reactivity are early markers of vasculopathy in type 2 diabetic individuals without microalbuminuria. *Diabetes Care, 22*(11), 1865-1870.

Limbourg, A., Korff, T., Napp, L. C., Schaper, W., Drexler, H., & Limbourg, F. P. (2009). Evaluation of postnatal arteriogenesis and angiogenesis in a mouse model of hind-limb ischemia. *Nat Protoc, 4*(12), 1737-1746. Image reprinted by permission from Macmillan Publishers Ltd.

Liu, H. Y., Huang, Z. L., Yang, G. H., Lu, W. Q., & Yu, N. R. (2008). Inhibitory effect of modified citrus pectin on liver metastases in a mouse colon cancer model. *World J Gastroenterol, 14*(48), 7386-7391.

Liu, J. T., Song, E., Xu, A., Berger, T., Mak, T. W., Tse, H. F., et al. (2012). Lipocalin-2 deficiency prevents endothelial dysfunction associated with dietary obesity: role of cytochrome P450 2C inhibition. *Br J Pharmacol, 165*(2), 520-531.

Liu, X., Feng, Q., Chen, Y., Zuo, J., Gupta, N., Chang, Y., et al. (2009). Proteomics-Based Identification of Differentially-Expressed Proteins Including Galectin-1 in the Blood Plasma of Type 2 Diabetic Patients. *J Proteome Res*.

Liu, Y. H., D'Ambrosio, M., Liao, T. D., Peng, H., Rhaleb, N. E., Sharma, U., et al. (2009). N-acetyl-seryl-aspartyl-lysyl-proline prevents cardiac remodeling and dysfunction induced by galectin-3, a mammalian adhesion/growth-regulatory lectin. *Am J Physiol Heart Circ Physiol, 296*(2), H404-412.

Lorenzi, M. (2007). The Polyol Pathway as a Mechanism for Diabetic Retinopathy: Attractive, Elusive, and Resilient. *Experimental Diabetes Research, 2007*.

Lotan, R., Belloni, P. N., Tressler, R. J., Lotan, D., Xu, X. C., & Nicolson, G. L. (1994). Expression of galectins on microvessel endothelial cells and their involvement in tumour cell adhesion. *Glycoconj J, 11*(5), 462-468.

Lukyanov, P., Furtak, V., & Ochieng, J. (2005). Galectin-3 interacts with membrane lipids and penetrates the lipid bilayer. *Biochem Biophys Res Commun, 338*(2), 1031-1036.

Luu, N. T., Rahman, M., Stone, P. C., Rainger, G. E., & Nash, G. B. (2010). Responses of endothelial cells from different vessels to inflammatory cytokines and shear stress: evidence for the pliability of endothelial phenotype. *J Vasc Res, 47*(5), 451-461.

Mackinnon, A. C., Liu, X., Hadoke, P. W., Miller, M. R., Newby, D. E., & Sethi, T. (2013). Inhibition of galectin-3 reduces atherosclerosis in apolipoprotein E-deficient mice. *Glycobiology*.

Makino, H., Okada, S., Nagumo, A., Sugisawa, T., Miyamoto, Y., Kishimoto, I., et al. (2009). Decreased circulating CD34+ cells are associated with progression of diabetic nephropathy. *Diabet Med, 26*(2), 171-173.

Malik, R. A., Tesfaye, S., Thompson, S. D., Veves, A., Sharma, A. K., Boulton, A. J., et al. (1993). Endoneurial localisation of microvascular damage in human diabetic neuropathy. *Diabetologia, 36*(5), 454-459.

Manduteanu, I., Voinea, M., Serban, G., & Simionescu, M. (1999). High glucose induces enhanced monocyte adhesion to valvular endothelial cells via a mechanism involving ICAM-1, VCAM-1 and CD18. *Endothelium, 6*(4), 315-324.

Mangalmurti, N. S., Chatterjee, S., Cheng, G., Andersen, E., Mohammed, A., Siegel, D. L., et al. (2012). Advanced glycation end products on stored red blood cells increase endothelial reactive oxygen species generation through interaction with receptor for advanced glycation end products. *Transfusion, 50*(11), 2353-2361.

Marelli-Berg, F. M., Peek, E., Lidington, E. A., Stauss, H. J., & Lechler, R. I. (2000). Isolation of endothelial cells from murine tissue. *J Immunol Methods, 244*(1-2), 205-215.

Maresh, J. G., & Shohet, R. V. (2008). In vivo endothelial gene regulation in diabetes. *Cardiovasc Diabetol, 7*, 8.

Maresh, J. G., Xu, H., Jiang, N., & Shohet, R. V. (2004). In vivo transcriptional response of cardiac endothelium to lipopolysaccharide. *Arterioscler Thromb Vasc Biol, 24*(10), 1836-1841.

Martini, F., Nath, J. (2009). *Fundamentals of Anatomy & Physiology* (8 ed.): Pearson Education, Inc.

Marx, N., Walcher, D., Raichle, C., Aleksic, M., Bach, H., Grub, M., et al. (2004). C-peptide colocalizes with macrophages in early arteriosclerotic lesions of diabetic subjects and induces monocyte chemotaxis in vitro. *Arterioscler Thromb Vasc Biol, 24*(3), 540-545.

Masri, B., Morin, N., Cornu, M., Knibiehler, B., & Audigier, Y. (2004). Apelin (65-77) activates p70 S6 kinase and is mitogenic for umbilical endothelial cells. *FASEB J, 18*(15), 1909-1911.

Massa, S. M., Cooper, D. N., Leffler, H., & Barondes, S. H. (1993). L-29, an endogenous lectin, binds to glycoconjugate ligands with positive cooperativity. *Biochemistry, 32*(1), 260-267.

Mastej, K., & Adamiec, R. (2006). [Role of polymorphonuclear leukocytes in development vascular complications in diabetes]. *Pol Merkur Lekarski, 20*(115), 36-40.

Mazurek, N., Conklin, J., Byrd, J. C., Raz, A., & Bresalier, R. S. (2000). Phosphorylation of the beta-galactoside-binding protein galectin-3 modulates binding to its ligands. *J Biol Chem, 275*(46), 36311-36315.

McGettrick, H. M., Smith, E., Filer, A., Kissane, S., Salmon, M., Buckley, C. D., et al. (2009). Fibroblasts from different sites may promote or inhibit recruitment of flowing lymphocytes by endothelial cells. *Eur J Immunol, 39*(1), 113-125.

McQueen, A. P., Zhang, D., Hu, P., Swenson, L., Yang, Y., Zaha, V. G., et al. (2005). Contractile dysfunction in hypertrophied hearts with deficient insulin receptor signaling: possible role of reduced capillary density. *J Mol Cell Cardiol, 39*(6), 882-892.

Mehul, B., Bawumia, S., Martin, S. R., & Hughes, R. C. (1994). Structure of baby hamster kidney carbohydrate-binding protein CBP30, an S-type animal lectin. *J Biol Chem, 269*(27), 18250-18258.

Meininger, C. J., Cai, S., Parker, J. L., Channon, K. M., Kelly, K. A., Becker, E. J., et al. (2004). GTP cyclohydrolase I gene transfer reverses tetrahydrobiopterin deficiency and increases nitric oxide synthesis in endothelial cells and isolated vessels from diabetic rats. *FASEB J, 18*(15), 1900-1902.

Mensah-Brown, E. P., Al Rabesi, Z., Shahin, A., Al Shamsi, M., Arsenijevic, N., Hsu, D. K., et al. (2009). Targeted disruption of the galectin-3 gene results in decreased susceptibility to multiple low dose streptozotocin-induced diabetes in mice. *Clin Immunol, 130*(1), 83-88.

Meyrelles, S. S., Peotta, V. A., Pereira, T. M., & Vasquez, E. C. (2011). Endothelial dysfunction in the apolipoprotein E-deficient mouse: insights into the influence of diet, gender and aging. *Lipids Health Dis, 10*, 211.

Miinea, C. P., Sano, H., Kane, S., Sano, E., Fukuda, M., Peranen, J., et al. (2005). AS160, the Akt substrate regulating GLUT4 translocation, has a functional Rab GTPase-activating protein domain. *Biochem J, 391*(Pt 1), 87-93.

Mink, S. N., Kasian, K., Santos Martinez, L. E., Jacobs, H., Bose, R., Cheng, Z. Q., et al. (2008). Lysozyme, a mediator of sepsis that produces vasodilation by hydrogen peroxide signaling in an arterial preparation. *Am J Physiol Heart Circ Physiol, 294*(4), H1724-1735.

Mokuda, O., Sakamoto, Y., Ikeda, T., & Mashiba, H. (1990). Effects of anoxia and low free fatty acid on myocardial energy metabolism in streptozotocin-diabetic rats. *Ann Nutr Metab, 34*(5), 259-265.

Moutsatsos, I. K., Davis, J. M., & Wang, J. L. (1986). Endogenous lectins from cultured cells: subcellular localization of carbohydrate-binding protein 35 in 3T3 fibroblasts. *J Cell Biol, 102*(2), 477-483.

Moutsatsos, I. K., Wade, M., Schindler, M., & Wang, J. L. (1987). Endogenous lectins from cultured cells: nuclear localization of carbohydrate-binding protein 35 in proliferating 3T3 fibroblasts. *Proc Natl Acad Sci U S A, 84*(18), 6452-6456.

Mzhavia, N., Yu, S., Ikeda, S., Chu, T. T., Goldberg, I., & Dansky, H. M. (2008). Neuronatin: a new inflammation gene expressed on the aortic endothelium of diabetic mice. *Diabetes, 57*(10), 2774-2783.

Nachtigal, M., Al-Assaad, Z., Mayer, E. P., Kim, K., & Monsigny, M. (1998). Galectin-3 expression in human atherosclerotic lesions. *Am J Pathol, 152*(5), 1199-1208.

Nagai, R., Unno, Y., Hayashi, M. C., Masuda, S., Hayase, F., Kinae, N., et al. (2002). Peroxynitrite induces formation of N(epsilon)-(carboxymethyl) lysine by the cleavage of Amadori product and generation of glucosone and glyoxal from glucose: novel pathways for protein modification by peroxynitrite. *Diabetes, 51*(9), 2833-2839.

Nakagawa, T., Kosugi, T., Haneda, M., Rivard, C. J., & Long, D. A. (2009). Abnormal angiogenesis in diabetic nephropathy. *Diabetes, 58*(7), 1471-1478.

Nangia-Makker, P., Hogan, V., Honjo, Y., Baccarini, S., Tait, L., Bresalier, R., et al. (2002). Inhibition of human cancer cell growth and metastasis in nude mice by oral intake of modified citrus pectin. *J Natl Cancer Inst, 94*(24), 1854-1862.

Natarajan, R., & Nadler, J. L. (2004). Lipid inflammatory mediators in diabetic vascular disease. *Arterioscler Thromb Vasc Biol, 24*(9), 1542-1548.

Nathan, D. M., Kuenen, J., Borg, R., Zheng, H., Schoenfeld, D., & Heine, R. J. (2008). Translating the A1C assay into estimated average glucose values. *Diabetes Care, 31*(8), 1473-1478.

Nathan, D. M., Turgeon, H., & Regan, S. (2007). Relationship between glycated haemoglobin levels and mean glucose levels over time. *Diabetologia, 50*(11), 2239-2244.

Nomiyama, T., Igarashi, Y., Taka, H., Mineki, R., Uchida, T., Ogihara, T., et al. (2004). Reduction of insulin-stimulated glucose uptake by peroxynitrite is concurrent with tyrosine nitration of insulin receptor substrate-1. *Biochem Biophys Res Commun, 320*(3), 639-647.

Norata, G. D., Ongari, M., Uboldi, P., Pellegatta, F., & Catapano, A. L. (2005). Liver X receptor and retinoic X receptor agonists modulate the expression of genes involved in lipid metabolism in human endothelial cells. *Int J Mol Med, 16*(4), 717-722.

Nunoda, S., Genda, A., Sugihara, N., Nakayama, A., Mizuno, S., & Takeda, R. (1985). Quantitative approach to the histopathology of the biopsied right ventricular myocardium in patients with diabetes mellitus. *Heart Vessels, 1*(1), 43-47.

Ochieng, J., Platt, D., Tait, L., Hogan, V., Raz, T., Carmi, P., et al. (1993). Structure-function relationship of a recombinant human galactoside-binding protein. *Biochemistry, 32*(16), 4455-4460.

Oda, Y., Leffler, H., Sakakura, Y., Kasai, K., & Barondes, S. H. (1991). Human breast carcinoma cDNA encoding a galactoside-binding lectin homologous to mouse Mac-2 antigen. *Gene, 99*(2), 279-283.

Okamoto, Y., Kihara, S., Ouchi, N., Nishida, M., Arita, Y., Kumada, M., et al. (2002). Adiponectin reduces atherosclerosis in apolipoprotein E-deficient mice. *Circulation, 106*(22), 2767-2770.

Olokoba, A. B., Obateru, O. A., & Olokoba, L. B. (2012). Type 2 diabetes mellitus: a review of current trends. *Oman Med J, 27*(4), 269-273.

Orr, A. W., Sanders, J. M., Bevard, M., Coleman, E., Sarembock, I. J., & Schwartz, M. A. (2005). The subendothelial extracellular matrix modulates NF-kappaB activation by flow: a potential role in atherosclerosis. *J Cell Biol, 169*(1), 191-202.

Ouchi, N., Kihara, S., Arita, Y., Maeda, K., Kuriyama, H., Okamoto, Y., et al. (1999). Novel modulator for endothelial adhesion molecules: adipocyte-derived plasma protein adiponectin. *Circulation, 100*(25), 2473-2476.

Paces-Fessy, M., Boucher, D., Petit, E., Paute-Briand, S., & Blanchet-Tournier, M. F. (2004). The negative regulator of Gli, Suppressor of fused (Sufu), interacts with SAP18, Galectin3 and other nuclear proteins. *Biochem J, 378*(Pt 2), 353-362.

Pacher, P., & Szabo, C. (2006). Role of peroxynitrite in the pathogenesis of cardiovascular complications of diabetes. *Curr Opin Pharmacol, 6*(2), 136-141.

Papaspyridonos, M., McNeill, E., de Bono, J. P., Smith, A., Burnand, K. G., Channon, K. M., et al. (2008). Galectin-3 is an amplifier of inflammation in atherosclerotic

plaque progression through macrophage activation and monocyte chemoattraction. *Arterioscler Thromb Vasc Biol, 28*(3), 433-440.

Patti, M. E., Butte, A. J., Crunkhorn, S., Cusi, K., Berria, R., Kashyap, S., et al. (2003). Coordinated reduction of genes of oxidative metabolism in humans with insulin resistance and diabetes: Potential role of PGC1 and NRF1. *Proc Natl Acad Sci U S A, 100*(14), 8466-8471.

Perez-Gutierrez, R. M., & Damian-Guzman, M. (2012). Meliacinolin: a potent alpha-glucosidase and alpha-amylase inhibitor isolated from Azadirachta indica leaves and in vivo antidiabetic property in streptozotocin-nicotinamide-induced type 2 diabetes in mice. *Biol Pharm Bull, 35*(9), 1516-1524.

Petro, A. E., Cotter, J., Cooper, D. A., Peters, J. C., Surwit, S. J., & Surwit, R. S. (2004). Fat, carbohydrate, and calories in the development of diabetes and obesity in the C57BL/6J mouse. *Metabolism, 53*(4), 454-457.

Pieters, M., van Zyl, D. G., Rheeder, P., Jerling, J. C., Loots du, T., van der Westhuizen, F. H., et al. (2007). Glycation of fibrinogen in uncontrolled diabetic patients and the effects of glycaemic control on fibrinogen glycation. *Thromb Res, 120*(3), 439-446.

Pober, J. S., & Sessa, W. C. (2007). Evolving functions of endothelial cells in inflammation. *Nat Rev Immunol, 7*(10), 803-815.

Potenza, M. A., Gagliardi, S., Nacci, C., Carratu, M. R., & Montagnani, M. (2009). Endothelial dysfunction in diabetes: from mechanisms to therapeutic targets. *Curr Med Chem, 16*(1), 94-112.

Pricci, F., Leto, G., Amadio, L., Iacobini, C., Romeo, G., Cordone, S., et al. (2000). Role of galectin-3 as a receptor for advanced glycosylation end products. *Kidney Int Suppl, 77*, S31-39.

Prompers, L., Schaper, N., Apelqvist, J., Edmonds, M., Jude, E., Mauricio, D., et al. (2008). Prediction of outcome in individuals with diabetic foot ulcers: focus on the differences between individuals with and without peripheral arterial disease. The EURODIALE Study. *Diabetologia, 51*(5), 747-755.

Pugliese, G., Pricci, F., Iacobini, C., Leto, G., Amadio, L., Barsotti, P., et al. (2001). Accelerated diabetic glomerulopathy in galectin-3/AGE receptor 3 knockout mice. *FASEB J, 15*(13), 2471-2479.

Pugliese, G., Pricci, F., Leto, G., Amadio, L., Iacobini, C., Romeo, G., et al. (2000). The diabetic milieu modulates the advanced glycation end product-receptor complex in the mesangium by inducing or upregulating galectin-3 expression. *Diabetes, 49*(7), 1249-1257.

Rask-Madsen, C., & King, G. L. (2005). Proatherosclerotic mechanisms involving protein kinase C in diabetes and insulin resistance. *Arterioscler Thromb Vasc Biol, 25*(3), 487-496.

Rodriguez-Feo, J. A., Pasterkamp, G. (2007). Trends in Vascular Biology; Functional Restoration of Damaged Endothelium. *Current Pharmaceutical Design, 13*(17), 1723-1725.

Rosenberg, I. M., Iyer, R., Cherayil, B., Chiodino, C., & Pillai, S. (1993). Structure of the murine Mac-2 gene. Splice variants encode proteins lacking functional signal peptides. *J Biol Chem, 268*(17), 12393-12400.

Ruiter, M. S., van Golde, J. M., Schaper, N. C., Stehouwer, C. D., & Huijberts, M. S. (2010). Diabetes impairs arteriogenesis in the peripheral circulation: review of molecular mechanisms. *Clin Sci (Lond), 119*(6), 225-238.

Sahli, D., Eriksson, J. W., Boman, K., & Svensson, M. K. (2009). Tissue plasminogen activator (tPA) activity is a novel and early marker of asymptomatic LEAD in type 2 diabetes. *Thromb Res, 123*(5), 701-706.

Saint-Lu, N., Oortwijn, B. D., Pegon, J. N., Odouard, S., Christophe, O. D., de Groot, P. G., et al. Identification of galectin-1 and galectin-3 as novel partners for von Willebrand factor. *Arterioscler Thromb Vasc Biol, 32*(4), 894-901.

Sandoo, A., Carroll, D., Metsios, G. S., Kitas, G. D., & Veldhuijzen van Zanten, J. J. (2011). The association between microvascular and macrovascular endothelial function in patients with rheumatoid arthritis: a cross-sectional study. *Arthritis Res Ther, 13*(3), R99.

Sano, H., Hsu, D. K., Yu, L., Apgar, J. R., Kuwabara, I., Yamanaka, T., et al. (2000). Human galectin-3 is a novel chemoattractant for monocytes and macrophages. *J Immunol, 165*(4), 2156-2164.

Santaguida PL, B. C., Hunt D, Morrison K, Gerstein H, Raina P, Booker L, Yazdi H. (2005). Diagnosis, Prognosis, and Treatment of Impaired Glucose Tolerance and Impaired Fasting Glucose. Summary, Evidence Report/Technology Assessment no. 128. Prepared by the McMaster Evidence-based Practice Center. Agency for Healthcare Research and Quality. Accessible at www.ahrq.gov.

Santhanam, A. V., d'Uscio, L. V., Smith, L. A., & Katusic, Z. S. (2012). Uncoupling of eNOS causes superoxide anion production and impairs NO signaling in the cerebral microvessels of hph-1 mice. *J Neurochem, 122*(6), 1211-1218.

Sato, S., & Hughes, R. C. (1992). Binding specificity of a baby hamster kidney lectin for H type I and II chains, polylactosamine glycans, and appropriately glycosylated forms of laminin and fibronectin. *J Biol Chem, 267*(10), 6983-6990.

Schlaeger, T. M., Bartunkova, S., Lawitts, J. A., Teichmann, G., Risau, W., Deutsch, U., et al. (1997). Uniform vascular-endothelial-cell-specific gene expression in both embryonic and adult transgenic mice. *Proc Natl Acad Sci U S A, 94*(7), 3058-3063.

Schneider, C.A., Rasband, W.S., Eliceiri, K.W. (2012).NIH Image to ImageJ: 25 years of image analysis. Nature Methods 9, 671-675.

Sears, D. D., Miles, P. D., Chapman, J., Ofrecio, J. M., Almazan, F., Thapar, D., et al. (2009). 12/15-lipoxygenase is required for the early onset of high fat diet-induced adipose tissue inflammation and insulin resistance in mice. *PLoS One, 4*(9), e7250.

Seetharaman, J., Kanigsberg, A., Slaaby, R., Leffler, H., Barondes, S. H., & Rini, J. M. (1998). X-ray crystal structure of the human galectin-3 carbohydrate recognition domain at 2.1-A resolution. *J Biol Chem, 273*(21), 13047-13052.

Seki, N., Hashimoto, N., Sano, H., Horiuchi, S., Yagui, K., Makino, H., et al. (2003). Mechanisms involved in the stimulatory effect of advanced glycation end products on growth of rat aortic smooth muscle cells. *Metabolism, 52*(12), 1558-1563.

Seljeflot, I., Larsen, J. R., Dahl-Jorgensen, K., Hanssen, K. F., & Arnesen, H. (2006). Fibrinolytic activity is highly influenced by long-term glycemic control in Type 1 diabetic patients. *J Thromb Haemost, 4*(3), 686-688.

Shahab, A. (2006). Why does diabetes mellitus increase the risk of cardiovascular disease? *Acta Med Indones, 38*(1), 33-41.

Sharma, S., Sun, X., Kumar, S., Rafikov, R., Aramburo, A., Kalkan, G., et al. (2012). Preserving mitochondrial function prevents the proteasomal degradation of GTP cyclohydrolase I. *Free Radic Biol Med, 53*(2), 216-229.

Shimura, T., Takenaka, Y., Fukumori, T., Tsutsumi, S., Okada, K., Hogan, V., et al. (2005). Implication of galectin-3 in Wnt signaling. *Cancer Res, 65*(9), 3535-3537.

Song, J., Oh, J. Y., Sung, Y. A., Pak, Y. K., Park, K. S., & Lee, H. K. (2001). Peripheral blood mitochondrial DNA content is related to insulin sensitivity in offspring of type 2 diabetic patients. *Diabetes Care, 24*(5), 865-869.

Song, P., Wu, Y., Xu, J., Xie, Z., Dong, Y., Zhang, M., et al. (2007). Reactive nitrogen species induced by hyperglycemia suppresses Akt signaling and triggers apoptosis by upregulating phosphatase PTEN (phosphatase and tensin homologue deleted on chromosome 10) in an LKB1-dependent manner. *Circulation, 116*(14), 1585-1595.

Song, X., Kusakari, Y., Xiao, C. Y., Kinsella, S. D., Rosenberg, M. A., Scherrer-Crosbie, M., et al. mTOR attenuates the inflammatory response in cardiomyocytes and prevents cardiac dysfunction in pathological hypertrophy. *Am J Physiol Cell Physiol, 299*(6), C1256-1266.

Stegenga, M. E., van der Crabben, S. N., Dessing, M. C., Pater, J. M., van den Pangaart, P. S., de Vos, A. F., et al. (2008). Effect of acute hyperglycaemia and/or hyperinsulinaemia on proinflammatory gene expression, cytokine production and neutrophil function in humans. *Diabet Med, 25*(2), 157-164.

Stitt, A. W., He, C., & Vlassara, H. (1999). Characterization of the Advanced Glycation End-Product Receptor Complex in Human Vascular Endothelial Cells. *Biochemical and Biophysical Research Communications, 256*(3), 549-556.

Stitt, A. W., McGoldrick, C., Rice-McCaldin, A., McCance, D. R., Glenn, J. V., Hsu, D. K., et al. (2005). Impaired Retinal Angiogenesis in Diabetes: Role of Advanced Glycation End Products and Galectin-3. *Diabetes, 54*(3), 785-794.

Struyf, S., Proost, P., Vandercappellen, J., Dempe, S., Noyens, B., Nelissen, S., et al. (2009). Synergistic up-regulation of MCP-2/CCL8 activity is counteracted by chemokine cleavage, limiting its inflammatory and anti-tumoral effects. *Eur J Immunol*.

Stumvoll, M., Goldstein, B. J., & van Haeften, T. W. (2005). Type 2 diabetes: principles of pathogenesis and therapy. *Lancet, 365*(9467), 1333-1346. Image reprinted from *The Lancet* with permission from Elsevier.

Surwit, R. S., Feinglos, M. N., Rodin, J., Sutherland, A., Petro, A. E., Opara, E. C., et al. (1995). Differential effects of fat and sucrose on the development of obesity and diabetes in C57BL/6J and A/J mice. *Metabolism, 44*(5), 645-651.

Surwit, R. S., Kuhn, C. M., Cochrane, C., McCubbin, J. A., & Feinglos, M. N. (1988). Diet-induced type II diabetes in C57BL/6J mice. *Diabetes, 37*(9), 1163-1167.

Tabibiazar, R., Wagner, R. A., Deng, A., Tsao, P. S., & Quertermous, T. (2006). Proteomic profiles of serum inflammatory markers accurately predict atherosclerosis in mice. *Physiol. Genomics, 25*(2), 194-202.

Tahara, A., Kurosaki, E., Yokono, M., Yamajuku, D., Kihara, R., Hayashizaki, Y., et al. (2012). Antidiabetic effects of SGLT2-selective inhibitor ipragliflozin in streptozotocin-nicotinamide-induced mildly diabetic mice. *J Pharmacol Sci, 120*(1), 36-44.

Takenaka, Y., Fukumori, T., Yoshii, T., Oka, N., Inohara, H., Kim, H. R., et al. (2004). Nuclear export of phosphorylated galectin-3 regulates its antiapoptotic activity in response to chemotherapeutic drugs. *Mol Cell Biol, 24*(10), 4395-4406.

Tatemoto, K., Takayama, K., Zou, M. X., Kumaki, I., Zhang, W., Kumano, K., et al. (2001). The novel peptide apelin lowers blood pressure via a nitric oxide-dependent mechanism. *Regul Pept, 99*(2-3), 87-92.

Tenenbaum, A., Motro, M., Fisman, E. Z., Schwammenthal, E., Adler, Y., Goldenberg, I., et al. (2004). Peroxisome proliferator-activated receptor ligand bezafibrate for prevention of type 2 diabetes mellitus in patients with coronary artery disease. *Circulation, 109*(18), 2197-2202.

Tessari, P., Kiwanuka, E., Millioni, R., Vettore, M., Puricelli, L., Zanetti, M., et al. (2006). Albumin and fibrinogen synthesis and insulin effect in type 2 diabetic patients with normoalbuminuria. *Diabetes Care, 29*(2), 323-328.

Thiel, G., Al Sarraj, J., & Stefano, L. (2005). cAMP response element binding protein (CREB) activates transcription via two distinct genetic elements of the human glucose-6-phosphatase gene. *BMC Mol Biol, 6*, 2.

Tian, R., & Abel, E. D. (2001). Responses of GLUT4-deficient hearts to ischemia underscore the importance of glycolysis. *Circulation, 103*(24), 2961-2966.

Tripathy, D., Aljada, A., & Dandona, P. (2003). Free fatty acids (FFA) and endothelial dysfunction; role of increased oxidative stress and inflammation. --to: Steinberg et al. (2002) Vascular function, insulin resistance and fatty acids. *Diabetologia, 46*(2), 300-301.

Uittenbogaard, A., Shaul, P. W., Yuhanna, I. S., Blair, A., & Smart, E. J. (2000). High density lipoprotein prevents oxidized low density lipoprotein-induced inhibition of endothelial nitric-oxide synthase localization and activation in caveolae. *J Biol Chem, 275*(15), 11278-11283.

Umemoto, K., Leffler, H., Venot, A., Valafar, H., & Prestegard, J. H. (2003). Conformational differences in liganded and unliganded states of Galectin-3. *Biochemistry, 42*(13), 3688-3695.

UniProt Consortium. Reorganizing the protein space at the Universal Protein Resource (UniProt). (2012). *Nucleic Acids Res, 40*(Database issue), D71-75.

Vaidyula, V. R., Rao, A. K., Mozzoli, M., Homko, C., Cheung, P., & Boden, G. (2006). Effects of hyperglycemia and hyperinsulinemia on circulating tissue factor procoagulant activity and platelet CD40 ligand. *Diabetes, 55*(1), 202-208.

Venneri, M. A., De Palma, M., Ponzoni, M., Pucci, F., Scielzo, C., Zonari, E., et al. (2007). Identification of proangiogenic TIE2-expressing monocytes (TEMs) in human peripheral blood and cancer. *Blood, 109*(12), 5276-5285.

Verrier, E., Wang, L., Wadham, C., Albanese, N., Hahn, C., Gamble, J. R., et al. (2004). PPARgamma agonists ameliorate endothelial cell activation via inhibition of

diacylglycerol-protein kinase C signaling pathway: role of diacylglycerol kinase. *Circ Res, 94*(11), 1515-1522.

Vessieres, E., Freidja, M. L., Loufrani, L., Fassot, C., & Henrion, D. (2012). Flow (shear stress)-mediated remodeling of resistance arteries in diabetes. *Vascul Pharmacol, 57*(5-6), 173-178.

Vikramadithyan, R. K., Hu, Y., Noh, H. L., Liang, C. P., Hallam, K., Tall, A. R., et al. (2005). Human aldose reductase expression accelerates diabetic atherosclerosis in transgenic mice. *J Clin Invest, 115*(9), 2434-2443.

Vinik, A. I., Maser, R. E., Mitchell, B. D., & Freeman, R. (2003). Diabetic autonomic neuropathy. *Diabetes Care, 26*(5), 1553-1579.

Walcher, D., Babiak, C., Poletek, P., Rosenkranz, S., Bach, H., Betz, S., et al. (2006). C-Peptide induces vascular smooth muscle cell proliferation: involvement of SRC-kinase, phosphatidylinositol 3-kinase, and extracellular signal-regulated kinase 1/2. *Circ Res, 99*(11), 1181-1187.

Wang, G. F., Wu, S. Y., Xu, W., Jin, H., Zhu, Z. G., Li, Z. H., et al. (2010). Geniposide inhibits high glucose-induced cell adhesion through the NF-kappaB signaling pathway in human umbilical vein endothelial cells. *Acta Pharmacol Sin, 31*(8), 953-962.

Wang, L., Miller, C., Swarthout, R. F., Rao, M., Mackman, N., & Taubman, M. B. (2009). Vascular smooth muscle-derived tissue factor is critical for arterial thrombosis after ferric chloride-induced injury. *Blood, 113*(3), 705-713.

Waterston, R. H., Lindblad-Toh, K., Birney, E., Rogers, J., Abril, J. F., Agarwal, P., et al. (2002). Initial sequencing and comparative analysis of the mouse genome. *Nature, 420*(6915), 520-562.

Way, K. J., Isshiki, K., Suzuma, K., Yokota, T., Zvagelsky, D., Schoen, F. J., et al. (2002). Expression of connective tissue growth factor is increased in injured myocardium associated with protein kinase C beta2 activation and diabetes. *Diabetes, 51*(9), 2709-2718.

Weber, M., Sporrer, D., Weigert, J., Wanninger, J., Neumeier, M., Wurm, S., et al. (2009). Adiponectin downregulates galectin-3 whose cellular form is elevated whereas its soluble form is reduced in type 2 diabetic monocytes. *FEBS Lett, 583*(22), 3718-3724.

Weigert, J., Neumeier, M., Wanninger, J., Bauer, S., Farkas, S., Scherer, M. N., et al. (2010). Serum galectin-3 is elevated in obesity and negatively correlates with glycosylated hemoglobin in type 2 diabetes. *J Clin Endocrinol Metab, 95*(3), 1404-1411.

Wendt, T., Harja, E., Bucciarelli, L., Qu, W., Lu, Y., Rong, L. L., et al. (2006). RAGE modulates vascular inflammation and atherosclerosis in a murine model of type 2 diabetes. *Atherosclerosis, 185*(1), 70-77.

Wiernsperger, N., & Rapin, J. R. (2012). Microvascular diseases: is a new era coming? *Cardiovasc Hematol Agents Med Chem, 10*(2), 167-183.

Win, M. T., Yamamoto, Y., Munesue, S., Saito, H., Han, D., Motoyoshi, S., et al. (2012). Regulation of RAGE for attenuating progression of diabetic vascular complications. *Exp Diabetes Res, 2012*, 894605.

Woo, H. J., Lotz, M. M., Jung, J. U., & Mercurio, A. M. (1991). Carbohydrate-binding protein 35 (Mac-2), a laminin-binding lectin, forms functional dimers using cysteine 186. *J Biol Chem, 266*(28), 18419-18422.

World Health Organization (2006): *Definition and Diagnosis of Diabetes Mellitus and Intermediate Hyperglycemia*. (Report of a WHO/IDF consultation). Geneva: World Health Organization.

World Health Organization (2011)*: Use of Glycated Haemoglobin (Hb1Ac) in the diagnosis of Diabetes Mellitus*. (Abbreviated report of a WHO consultation). Geneva: World Health Organization WHO/NMH/CHP/CPM/11.1.

Wu, X., Somlyo, A. V., & Somlyo, A. P. (1996). Cyclic GMP-dependent stimulation reverses G-protein-coupled inhibition of smooth muscle myosin light chain phosphate. *Biochem Biophys Res Commun, 220*(3), 658-663.

Xu, J., & Zou, M. H. (2009). Molecular insights and therapeutic targets for diabetic endothelial dysfunction. *Circulation, 120*(13), 1266-1286.

Yamada, Y., Doi, T., Hamakubo, T., & Kodama, T. (1998). Scavenger receptor family proteins: roles for atherosclerosis, host defence and disorders of the central nervous system. *Cell Mol Life Sci, 54*(7), 628-640.

Yancey, P. G., Ding, Y., Fan, D., Blakemore, J. L., Zhang, Y., Ding, L., et al. (2011). Low-density lipoprotein receptor-related protein 1 prevents early atherosclerosis by limiting lesional apoptosis and inflammatory Ly-6Chigh monocytosis: evidence that the effects are not apolipoprotein E dependent. *Circulation, 124*(4), 454-464.

Yang, R. Y., Hsu, D. K., & Liu, F. T. (1996). Expression of galectin-3 modulates T-cell growth and apoptosis. *Proc Natl Acad Sci U S A, 93*(13), 6737-6742.

Zhang, J., Wu, Y., Zhang, Y., Leroith, D., Bernlohr, D. A., & Chen, X. (2008). The role of lipocalin 2 in the regulation of inflammation in adipocytes and macrophages. *Mol Endocrinol, 22*(6), 1416-1426.

Zhang, M., Dong, Y., Xu, J., Xie, Z., Wu, Y., Song, P., et al. (2008). Thromboxane receptor activates the AMP-activated protein kinase in vascular smooth muscle cells via hydrogen peroxide. *Circ Res, 102*(3), 328-337.

Zheng, F., Cai, W., Mitsuhashi, T., & Vlassara, H. (2001). Lysozyme enhances renal excretion of advanced glycation endproducts in vivo and suppresses adverse age-mediated cellular effects in vitro: a potential AGE sequestration therapy for diabetic nephropathy? *Mol Med, 7*(11), 737-747.

Zhou, J., Deo, B. K., Hosoya, K., Terasaki, T., Obrosova, I. G., Brosius, F. C., 3rd, et al. (2005). Increased JNK phosphorylation and oxidative stress in response to increased glucose flux through increased GLUT1 expression in rat retinal endothelial cells. *Invest Ophthalmol Vis Sci, 46*(9), 3403-3410.

Zhu, W., Sano, H., Nagai, R., Fukuhara, K., Miyazaki, A., & Horiuchi, S. (2001). The role of galectin-3 in endocytosis of advanced glycation end products and modified low density lipoproteins. *Biochem Biophys Res Commun, 280*(4), 1183-1188.

Zieman, S. J., & Kass, D. A. (2004). Advanced glycation endproduct crosslinking in the cardiovascular system: potential therapeutic target for cardiovascular disease. *Drugs, 64*(5), 459-470.

Zou, M. H., Cohen, R., & Ullrich, V. (2004). Peroxynitrite and vascular endothelial dysfunction in diabetes mellitus. *Endothelium, 11*(2), 89-97.

Zou, M. H., Shi, C., & Cohen, R. A. (2002). Oxidation of the zinc-thiolate complex and uncoupling of endothelial nitric oxide synthase by peroxynitrite. *J Clin Invest, 109*(6), 817-826.